University of Alberta

The Glacial and Relative Sea Level History of Southern Banks Island, NT, Canada

By

Jessica Megan Vaughan

A thesis submitted to the Faculty of Graduate Studies and Research

in partial fulfillment of the requirements for the degree of

Doctor of Philosophy

Department of Earth and Atmospheric Sciences

Spring 2014
Edmonton, Alberta

A mosaic of earthen hues

Lacquered in emerald green waters

Textured by wind

This pristine chapel floor

Laid out by time

And the dexterous hands of stone skippers

Attests to a slow history

Older than words

Older than deeds themselves

For my wonderful family and friends who have shown unconditional

love and support.

ABSTRACT

The mapping and dating of surficial glacial landforms and sediments across southern Banks Island document glaciation by the northwest Laurentide Ice Sheet (LIS) during the last glacial maximum. Geomorphic landforms confirm the operation of an ice stream at least 1000 m thick in Amundsen Gulf that was coalescent with thin, cold-based ice crossing the island's interior, both advancing offshore onto the polar continental shelf. Raised marine shorelines across western and southern Banks Island are barren, recording early withdrawal of the Amundsen Gulf Ice Stream *prior to* the resubmergence of Bering Strait and the re-entry of Pacific molluscs ~13,750 cal yr BP. This withdrawal resulted in a loss of ~60,000 km^2 of ice –triggering drawdown from the primary northwest LIS divide and instigating changes in subsequent ice flow. The Jesse moraine belt on eastern Banks Island records a lateglacial stillstand and/or readvance of Laurentide ice in Prince of Wales Strait (13,750 – 12,750 cal yr BP). Fossiliferous raised marine sediments that onlap the Jesse moraine belt constrain final deglaciation to ~12,600 cal yr BP, a minimum age for the breakup of the Amundsen Gulf Ice Stream.

The investigation of a 30 m thick and 6 km wide stratigraphic sequence at Worth Point, southwest Banks Island, identifies an advance of the ancestral LIS during the Mid-Pleistocene (*sensu lato*), substantially diversifying the glacial record on Banks Island. Glacial ice emplaced during this advance has persisted through at least two glacial-interglacial cycles, demonstrating the resilience of circumpolar permafrost. Pervasive deformation of the stratigraphic sequence also

records a detailed history of glaciotectonism in proglacial and subglacial settings that can result from interactions between cold-based ice and permafrost terrain. This newly recognized history rejects the long-established paleoenvironmental model of Worth Point that assumed a simple ‘layer-cake’ stratigraphy.

ACKNOWLEDGEMENTS

I wish to acknowledge a Natural Sciences and Engineering Research Council (NSERC) Northern Chair and Discovery Grant awarded to Dr. John England, which primarily funded this PhD. Additional funding was provided by a Circumpolar-Boreal Alberta Research (CBAR) Grant awarded by the Canadian Circumpolar Institute (CCI) and logistical support in the remote Canadian Arctic was provided by the Polar Continental Shelf Program (PCSP).

I would like to thank my supervisory committee members Dr John England, Dr Duane Froese, Dr Octavian Catuneanu, Dr Richard Waller and Dr Ray LeBlanc for their interest and constructive feedback. In particular, I wish to highlight the friendship, guidance, and unrelenting optimism of my supervisor Dr John England, who always believed in me. The encouragement and wisdom of both John and his wife Catherine not only shaped my academic career, but also allowed me to fulfill many rewarding aspects of my personal life.

During three field seasons on Banks Island I was fortunate enough to have the assistance of Maija Raudsepp (Co-founder of 'Shanty Camp'), Emily Moss ('Mrs Waddles'), Roy Coulthard ('Melancholy Merlot'), Aaron Nasogaluak, Kyle Wolki, Jonathon Doupé and Dave Evans. These field seasons introduced me to a silent landscape of unimaginable beauty that formed a spectacular playground for exploring, reflecting and discovering.

Throughout the rest of my time at the University of Alberta I enjoyed the insight and company of Tom Lakeman, Chantel Nixon, Mark Furze and Anna Pienkowski who took me under their wings in 2007. John Postma, Faye Wyatt, Kurt Borth, Ben Gready, Steve Mamet, Mei Mei Chong and countless other friends are also acknowledged for sharing their energy, laughter, and delicious biscuits with me.

I wish to thank my 'Yukon Family' in Whitehorse, who welcomed me into their home with open arms and taught me to always take life with a pinch of salt. Ross and Finn, you'll always be 'my boys'. My best friend and partner Sean Prokopiw deserves a humungous pat on the back for supporting me throughout the final stages of this PhD. His ability to cheer me up with a cup of tea and tangential story, usually about birds, were greatly appreciated during moments of thesis madness. Finally, I wish to thank my wonderful parents, Glyn and Wendy. Their unconditional support and encouragement made this PhD possible, and their rambunctious energy and contagious sense of humour always served to remind me of the importance of enjoying life to its fullest. Cheers Mum and Dad – I love you!

LIST OF CONTENTS

LIST OF TABLES

CHAPTER 2

LIST OF FIGURES

CHAPTER 1

CHAPTER 2

CHAPTER 3

CHAPTER 4

CHAPTER ONE

INTRODUCTION

1. SCOPE

The Quaternary (last 2.6 million years) evolution of the Arctic is still poorly documented, including the growth and decay of continental ice sheets and permafrost, the emergence and submergence of the Bering Land Bridge, and the sedimentary history of the Arctic Ocean. During periods of glaciation, ice sheets inundated circumpolar landmasses and advanced onto and beyond the polar continental shelf, entering the Arctic Ocean as expansive ice shelves (e.g. Vogt et al., 1994; Polyak et al., 2001, 2007; Kristoffersen et al., 2004; Jakobsson et al., 2005, 2008, in press; Engels et al., 2008; Fig. 1.1). Across northernmost North America this ice cover included the Laurentide Ice Sheet (LIS), Innuitian Ice Sheet (IIS), and Cordilleran Ice Sheet during the last glacial maximum (LGM; Prest, 1969; Dyke and Prest, 1987; Clague, 1989; Blake, 1970; 1992; England, 1999; Dyke et al., 2002; England et al., 2006). These ice sheets impacted many aspects of oceanographic, climatic, and terrestrial environmental change and their size and chronology still constitute the primary input for modelling modern global sea level change. Hence, clarifying the configuration, dynamics and chronology of past ice sheets and relative sea level change remains a compelling objective to Quaternary geology that engages a diverse array of disciplines.

This dissertation was designed to provide new insights into the glacial and relative sea level history of the northwest Laurentide Ice Sheet across southern Banks Island in the western Canadian Arctic Archipelago (CAA). Recent

geomorphic mapping and seismic surveys across the western CAA have documented the coalescence of the northwest sector of the LIS and the lowland sector of the IIS, which collectively discharged multiple ice streams into the Arctic Ocean (Blasco et al., 1990, 2005; Stokes et al., 2005, 2006, 2009; England et al., 2009; Lakeman and England, 2012, 2013; MacLean et al., 2012; Batchelor et al., in press; Nixon et al., in press). High-resolution geophysical surveys of the Arctic Ocean seabed distal to the western CAA have documented deep-draft scouring by former ice shelves or icebergs to depths >1000 m, placing important requirements on the thickness of the exported ice reaching these sites (Polyak et al., 2001, 2007; Engels et al., 2008; England et al., 2009; Scott et al., 2009; Stein et al., 2010; Jakobsson et al., 2010; MacLean et al., 2012; Dove et al., in press). Recent reconstructions supporting expansive LGM ice sheets in the western CAA are consistent with this deep scouring and fundamentally revise earlier reports of an ice-free biologic refugium throughout Banks Island that persisted for more than half a century (Hobbs, 1945; Jenness, 1952; Wilson et al., 1958; Fyles, 1962; Prest, 1969; French, 1972; Vincent, 1982, 1983, 1984, 1990; Harrington, 2005).

The current study investigates the glacial and relative sea level history recorded by surface and subsurface deposits on southern Banks Island (Fig. 1.2). This study tests an earlier regional synthesis of the Quaternary geology of Banks Island that reported a series of three successively less extensive glaciations spanning the Pleistocene (>780 – 80 ka BP; Vincent, 1982, 1983, 1984; Vincent et al., 1983, 1984). The limit of each glaciation was ascribed to lithologically distinct till sheets that were presumed to increase in age westward across the

island, terminating against a 'never glaciated' Tertiary peneplain on the northwest corner (Fig. 1.3; Vincent, 1982, 1983). Each proposed glaciation was also assigned a suite of corresponding moraines, proglacial lakes, and bracketing sediments of a preglacial transgression and a deglacial transgression (Fig. 1.3; Vincent, 1982, 1983). According to this model, Banks Island remained ice-free during the LGM, contacted only by an ice shelf on the northeast coast (Hodgson and Vincent, 1982). Notable deglacial transgressions associated with this glacial record include the Big Sea, following an intermediate glaciation, that purportedly inundated Banks Island up to 285 m asl prior to its forced (glacioisostatic) regression (Vincent, 1982, 1983). Subsequent deglacial transgressions were predominantly restricted to below 30 m asl and were presumed to record limited glacial unloading (Vincent, 1982, 1983). Despite identifying multiple marine transgressions associated with the removal of ice sheets that had previously crossed the marine channels of the western CAA en route to Banks Island, shells (ice-transported or within raised marine deposits) were not widely reported or dated by Vincent (1982, 1983). Consequently, the proposed sequence of glacial events for Banks Island remained poorly constrained, contrasting with reconstructions of other Laurentide and Innuitian margins where the dating of fossiliferous raised marine shorelines had proven to be the gold standard (e.g. Blake 1970). The surficial glacial model of Vincent (1982, 1983) was substantially elaborated through the investigation of coastal sections up to 50 m thick across Banks Island (Vincent, 1990). These investigations documented apparently *in situ* depositional sequences of glacial, nonglacial, and interglacial

deposits that were interpreted to record at least eight glaciations and five interglaciations extending back over one million years (Vincent, 1990; Barendregt et al., 1998). This stratigraphic model constituted the most detailed record of Neogene and Quaternary events in Arctic Canada outside of the Yukon Territory, and was correlated with widespread glacial records including those derived from Arctic Ocean sediment cores over 1000 km away (Vincent, 1982, 1990; Clark et al., 1984; Barendregt et al., 1998).

Chronological and stratigraphical limitations of this former Quaternary glacial model have been increasingly identified (Vincent, 1982, 1983, 1984, 1990; Barendregt et al., 1998). An ice-free LGM on Banks Island has been refuted by seismic surveys of M'Clure Strait and Amundsen Gulf as well as satellite imagery of glacial landforms adjacent to them that document their occupation by thick ice streams (Blasco et al., 1990, 2005; Stokes et al., 2005, 2006, 2009). Pervasive coverage by Laurentide ice during the LGM has been demonstrated by dates on ice-transported shells (constraining the age of ice advance) and on widespread deglacial marine limits (constraining the age of ice retreat) spanning southern Melville Island to central Banks Island (England et al., 2009; Lakeman and England, 2012, 2013). This fieldwork also documents the advance of the northwest LIS beyond the west coast of Banks Island and onto the polar continental shelf. Field mapping further demonstrates that erratics transported from Mainland Canada by the northwest LIS were deposited across northern Banks Island and southern Melville Island by an ice stream at least 635 m thick in M'Clure Strait (England et al., 2009). Widespread dates on deglacial shorelines

throughout M'Clure Strait record rapid retreat of this ice stream from western Banks Island and Melville Island southeastward to Victoria Island (300 km) at ~13,500 cal yr BP (England et al., 2009). Resulting differential emergence records a prominent rise in deglacial shorelines towards a former divide on or close to Victoria Island, likely the formerly identified M'Clintock Ice Divide (Dyke and Prest, 1987; England et al. 2009). Coastal moraine belts spanning eastern Banks Island demonstrate that this rapid retreat was followed by at least two late glacial readvances on or adjacent to eastern Banks Island, occasioned by renewed ice dispersal from an ice divide over the Shaler Mountains on northwest Victoria Island (Hodgson and Vincent 1982; Stokes et al., 2009; Lakeman and England, 2012, 2013). In addition to fundamental revisions of the surficial history of Banks Island, the elaborate subsurface record has been challenged on eastern Banks Island. Here, a stratigraphic section formerly purported to preserve glaciogenic units deposited by four separate ice sheets (Vincent, 1982, 1893) has been shown to record sedimentation by just two – one during the Early Pleistocene (>780 ka) and one during the LGM (Lakeman, 2012). Widespread observations of glaciotectonized stratigraphic sequences that were formerly proposed to have been *in situ* (Evans et al., in press) further undermine the previous subsurface record (Vincent, 1990; Barendregt et al., 1998).

2. STUDY AREA

Banks Island (70,000 km^2), western CAA, is a low-lying polar desert bordering the polar continental shelf and surrounded by the inter-island channels of Amundsen Gulf, M'Clure Strait, and Prince of Wales Strait (Fig. 1.2). Southern

Banks Island is topographically diverse, but includes the Durham Heights plateau (<730 m asl) on southeast Banks Island (Fig. 1.4a), an expansive outwash plain descending westwards to the Beaufort Sea (Fig. 1.4b), and multiple moraine belts and kettled lowlands fringing the south coast (Fig. 1.4c). The pre-Quaternary geology comprises Proterozoic volcanics of the Glenelg Fm, Devonian carbonates of the Weatherall and Parry Fms, Cretaceous sandstones and shales of the Isachsen, Christopher and Kanguk Fms, and Paleocene-Eocene sandstones and shales of the Eureka Sound Fm (Fig. 1.2; Thorsteinsson and Tozer, 1970; Miall, 1976, 1979; Fyles, 1990; Trettin, 1991). This bedrock has been capped by fluvial sand and gravel of the Mid-Miocene Ballast Brook Fm and Pliocene Beaufort Fm, which were deposited on a contiguous coastal plain prograding toward the polar continental shelf (Fig. 1.2; Fyles, 1990; Trettin, 1991; Fyles et al, 1994). Subsequent tectonic rifting and Quaternary ice advances have produced and deepened the inter-island channels of the CAA (Kerr, 1980; England, 1987).

3. OBJECTIVES AND METHODOLOGY

This dissertation has four primary objectives. The first objective is to determine the timing, extent, and nature of glaciation across southern Banks Island. This objective has been achieved through air photograph interpretation of the island's south coast followed by three field seasons (2008-2010) of mapping Quaternary landforms and sediments. Chronological control utilized accelerator mass spectrometer (AMS) radiocarbon dating of shells transported by the former LIS, supplemented by Uranium-Lead (U-Pb) zircon dating of far-travelled erratics and optically stimulated luminescence (OSL) dating of raised marine deposits.

This research was designed to contribute new insights into several themes including the flux of ice and debris delivered by the Amundsen Gulf Ice Stream to the Arctic Ocean and the stability of marine-terminating margins in the northwest LIS. The second, related objective of this dissertation is to document the nature and chronology of postglacial relative sea level change across southern Banks Island, from the Beaufort Sea to Prince of Wales Strait. This objective was achieved through widespread surveying of raised marine shorelines and AMS radiocarbon dating of shell-bearing raised marine deposits. This research ties the magnitude and pattern of postglacial sea level adjustments to the style of ice retreat in Amundsen Gulf and Prince of Wales Strait, and tests the previous proposal that all raised marine shorelines across southern Banks Island relate to the removal of ice sheets during multiple, pre-LGM glaciations (Vincent, 1982, 1983).

The third objective of this dissertation is to determine the long-term glacial history (pre-LGM) of Banks Island through the investigation of the subsurface record at Worth Point (30 m thick and 6 km wide), southwest Banks Island. The former stratigraphic model of Worth Point documented a sequence of undisturbed, horizontally-bedded Quaternary units, including the type-site for an organically rich, preglacial interval (Worth Point Fm; Vincent, 1990; Barendregt et al., 1998). Research at Worth Point (this study) documented a pervasively glaciotectonized stratigraphy that prompted a new research objective: to determine the relationship between the glaciotectonized architecture at Worth Point and former ice sheet-permafrost interactions. This objective was achieved through comprehensive

section logging combined with structural and sedimentological analyses. Clast form, macrofabric, and thin section analyses were undertaken to discriminate between former depositional/deformational styles and environments, and OSL dating was utilized to provide chronological control. This research was designed to provide new insights into the nature of glaciotectonism by cold-based ice, including the process-form relationships of hill-hole pairs and the deformation of diverse permafrozen lithologic units in both proglacial and subglacial settings. The fourth, related objective of this dissertation is to assess the implications of a revised long-term glacial record (determined through objective 3) at Worth Point, southwest Banks Island, for former stratigraphic correlations and for the history of the ancestral LIS. This research was designed to address a major gap in our knowledge of Quaternary events (the ancestral activity of the LIS) and ultimately raises new questions concerning the Quaternary evolution of circumpolar ice sheets and their impact upon the sedimentary history of the Arctic Ocean.

4. STRUCTURE OF DISSERTATION

This dissertation is written in paper format and is divided into three independent, yet complementary chapters following this introduction. A final chapter (Chapter 5) reviews the salient contributions of the three primary papers and provides suggestions for future research arising from these results.

Chapter 2, *The glacial and relative sea level history of southern Banks Island, NT, Canada: new insights into the configuration and dynamics of the northwest Laurentide Ice Sheet*. A version of this chapter co-authored with J. England will be submitted to Quaternary Research. This paper investigates the surficial glacial

landforms and sediments of southern Banks Island, addressing objectives 1 and 2 (above). Three research questions are addressed: 1) What is the configuration, style, and chronology of ice advance along Amundsen Gulf and across southern Banks Island?; 2) What is the chronology and style of ice retreat along Amundsen Gulf and across southern Banks Island?, and; 3) What is the pattern and chronology of relative sea level change and how does it reflect the paleotopography of former ice loads?.

Chapter 3, *Glaciotectonic deformation and reinterpretation of the Worth Point stratigraphic sequence: Banks Island, NT, Canada.* A version of this chapter co-authored with J. England and D.J.A Evans has been accepted by Quaternary Science Reviews and is currently in press. This chapter presents a detailed investigation of glaciotectonism by cold-based ice in permafrost terrain addressing objective 3 (above). Objectives are: 1) Describe the geomorphology, stratigraphy, sedimentology, glaciotectonic architecture and deformation structures at Worth Point; 2) Reconstruct the glacial stress regimes responsible for glaciotectonism and differentiate between deformation in proglacial, ice-marginal and subglacial environments; 3) Determine the number of glaciotectonic events responsible for deformation at Worth Point and their relative and absolute chronology, and; 4) Determine the role of permafrost in facilitating glaciotectonism and influencing the style and magnitude of deformation.

Chapter 4, *A revised Pleistocene glacial history for Banks Island, NT: insights from the polydeformed Worth Point stratigraphic sequence.* A version of this chapter co-authored with J. England will be submitted to Quaternary Science

Reviews. This paper explores the wider implications of a revised glaciotectonic model at Worth Point (presented in Chapter 3) for former paleoenvironmental correlations and for the history of the ancestral northwest LIS, addressing objective 4 (above). Objectives are: 1) Discuss new stratigraphic evidence debunking the former detailed record of Neogene and Quaternary change and present a revised long-term record of glaciation for Banks Island, and; 2) Assess the implications of a Mid-Pleistocene glaciation on southern Banks Island for reconstructions of circumpolar ice sheets and the Pleistocene history of the Arctic Ocean.

5. RATIONALE

Reconstructing the dynamics of former glaciation provides a plethora of relevant analogues that help to elucidate the behavior of contemporary ice sheets (e.g. Weertman, 1975; Hollin and Barry, 1979; Oppenheimer, 1998). Notably, during the LGM the western CAA was subsumed by a dynamic ice sheet complex with widespread marine-terminating margins and large ice streams in the inter-island channels – a configuration comparable with present day ice sheets in Greenland and Antarctica (Stokes et al., 2005, 2006, 2009; England et al., 2009; Lakeman and England, 2012, 2013). Clarifying the nature of former glaciation in the western CAA, in particular the role of marine-terminating margins in occasioning ice sheet collapse, can inform our understanding of how current ice sheets may respond (rate and magnitude) to ongoing climate amelioration and eustatic sea level rise (Conway et al., 2002; Peltier, 2002; Howat et al., 2007; Serreze et al., 2007; Bamber et al., 2009). Determining paleoglaciological changes

that triggered abrupt paleoclimatic and paleoceanographic change, such as the Younger Dryas cold reversal, are also instructive for elucidating potentially catastrophic thresholds in ice sheet stability (Dansgaard et al., 1993; Broecker et al., 2010).

Reconstructing postglacial relative sea level change provides new data that constrain geophysical models characterizing the properties and behaviour of the lithosphere and asthenosphere (e.g. Peltier et al., 1978; Peltier and Drummond, 2008). Such models are important for predicting future glacioisostatic readjustments that influence observed rates of relative sea level change – including at far field sites (peripheries of former ice sheets) such as Banks Island where ongoing submergence is impacting coastal communities (Peltier, 1998). Furthermore, postglacial relative sea level histories provide an insight into the complex interplay between the timing of deglaciation, glacioisostatic rebound, and eustatic sea level rise – ultimately informing our knowledge of deglacial dynamics and the intriguing positive feedbacks between ice sheet retreat and sea level change (Andrews, 1970; Peltier, 2002; Peltier and Drummond, 2008).

Understanding the interaction between cold-based ice and permafrost terrain provides an insight into a glaciological scenario that characterizes vast areas of modern ice sheets but remains poorly understood – contrasting with our extensive knowledge of glaciological processes beneath warm-based ice sheets (e.g. Boulton, 1972; Engelhardt et al., 1978; Iverson et al., 1995; Tulaczk et al., 1998). The highly dynamic nature of ice-bed coupling beneath cold-based ice, including its potential to impart deep-seated glaciotectonic deformation, demonstrates that

subzero temperatures at the ice-bed interface do not preclude the active generation of proglacial and subglacial landforms (Waller et al., 2012). These findings bear upon our understanding of how cold-based ice has modified the landscape of formerly glaciated regions, including areas in the mid-latitudes that are beyond the limit of current permafrost.

Documenting Quaternary Arctic paleoenvironments provides a framework that serves to identify long-term trends in high-latitude environmental change. These trends include former patterns of flora/fauna, timescales and frequency of glacial-interglacial events, and climatic forcing responsible for temporary ice sheet growth and wastage such as 'polar amplification' or a split jet stream advecting moisture into high latitudes (e.g. Holland and Bitz, 2003; Bromwich et al., 2004; Serreze and Barry, 2011). This long-term framework not only bears upon the evolution of circumpolar landscapes, but also serves to place modern environmental change in a meaningful long-term perspective.

6. REFERENCES

Andews, J.T. 1970. A Geomorphological Study of Post-glacial Uplift with Particular Reference to Arctic Canada. Institute of British Geographers, Alden Press, Oxford.

Bamber , J., Riccardo, E.M.R., Vermeersen, B.L.A., LeBrocq, A.M. 2009. Reassessment of the potential sea-level rise from a collapse of the West Antarctic Ice Sheet. Science. 324, 901-903.

Barendregt, R.W., Vincent, J-S., Irving, E., Baker, J. 1998. Magnetostratigraphy of Quaternary and Late Tertiary sediments on Banks Island, Canadian Arctic Archipelago. Canadian Journal of Earth Sciences. 35, 147-161.

Batchelor, C.L., Dowdeswell, J.A., Pietras, J.T. Evidence for multiple Quaternary ice advances and fan development from the Amundsen Gulf cross-shelf trough and slope, Canadian Beaufort Sea Margin. Marine and Petroleum Geology. In press.

Blake, W. Jr. 1970. Studies of glacial history in Arctic Canada. Canadian Journal of Earth Sciences. 7, 634-664.

Blake, W. Jr. 1992. Holocene emergence at Cape Herschel, east-central Ellesmere Island, Arctic Canada: implications for ice sheet configuration. Canadian Journal of Earth Sciences. 29, 1958-1980.

Blasco, S. M., Fortin, G., Hill, P.R., O'Connor, M.J., and Brigham- Grette, J. 1990. The late Neogene and Quaternary stratigraphy of the Canadian Beaufort continental shelf. In: Grantz, A., Johnson, L., Sweeney, J. F. (Eds). The Arctic

Ocean Region. The Geology of North America. Geological Society of America, Boulder, Colorado. 491–502.

Blasco, S.M., Bennett, R., Hughes-Clarke, J., Bartlett, J., Shearer, J.M. 2005. 3-D Multibeam Mapping Reveals Geological Processes Associated With Fluted Seabed, Slump Feature, Pockmarks, Mud Volcanoes and Deep Water Ice Scours in the Beaufort Sea–Amundsen Gulf. Geological Association of Canada – Mineralogical Association of Canada.

Boulton, G.S. 1972. The role of thermal regime in glacial sedimentation. In: Price, R.J., Sugden, D.E. (Eds.). Polar Geomorphology. London. 4, 1-19.

Broecker, W.S., Denton, G.H., Edwards, R.L., Cheng, H., Alley, R.B., Putnam, A.E. 2010. Putting the Younger Dryas cold event in context. Quaternary Science Reviews. 29, 1078-1081.

Bromwich, D.H., Toracinta, E.R., Wei, H., Oglesby, R.J., Fastook, J.L., Hughes, T.J. 2004. Polar MM5 Simulations of the Winter Climate of the Laurentide Ice Sheet at the LGM. Journal of Climate. 17, 3415-3433.

Clague, J.J. 1989. Quaternary geology of the Canadian Cordillera. In: Fulton, R.J. (Ed.). Quaternary Geology of Canada and Greenland. Geology of Canada Series. 1, 17-96.

Clark, D.L., Vincent, J-S., Jones, G.A., Morris, W.A. 1984. Correlation of marine and continental glacial and interglacial events, Arctic Ocean and Banks Island. Nature. 311, 147-149.

Conway, H., Cantania, G., Raymond, C.F., Gades, A.M., Scambos, T.A., Engelhardt, H. 2002. Switch of flow direction in an Antarctic ice stream. Nature. 419, 465-467.

Dansgaard, W., Johnsen, S.J., Clausen, H.B., Dahl-Jensen, D., Gundestrup, N.S., Hammer, C.U., Hvidberg, C.S., Steffensen, J.P., Sveinbjornsdottir, A.E., Jouzel, J., Bond, G. 1993. Evidence for general instability of past climate from a 250-kyr ice-core record. Nature. 364, 218-220.

Dove, D., Polyak, L., Coakley, B. Widespread multi-source glacial erosion on the Chukchi margin, Arctic Ocean. Quaternary Science Reviews. In press.

Dyke, A. S., Prest, V. K. 1987. Late Wisconsinan and Holocene history of the Laurentide Ice Sheet. Géographie physique et Quaternaire. 41, 237-263.

Dyke, A. S. Andrews, J. T. A., Clark, P. U., England, J. H., Miller, G. H., Shaw, J., & Veillette, J. J. 2002. The Laurentide and Innuitian ice sheets during the Last Glacial Maximum. Quaternary Science Reviews. 21, 9-31.

Engelhardt, H.F., Harrison, W.D., Kamb, B. 1978. Basal sliding and conditions at the glacier bed as revealed by bore-hole photography. Journal Of Glaciology. 20, 469-508.

Engels, J.L., Edwards, M.H., Polyak, L., Johnson, P.D. 2008. Seafloor evidence for ice shelf flow across the Alaska-Beaufort margin of the Arctic Ocean. Earth Surface Processes and Landforms. 33, 1047-1063.

England, J. 1999. Coalescent Greenland and Innuitian ice during the last glacial maximum: revising the Quaternary of the Canadian High Arctic. Quaternary Science Reviews. 18, 421-456.

England, J., Atkinson, N., Bednarski, J., Dyke, A. S., Hodgson, D. A., O'Cofaigh C. 2006. The Innuitian Ice Sheet: configuration, dynamics and chronology. Quaternary Science Reviews. 25, 689-703.

England, J.H., Furze, M.F.A., Doupe, J.P. 2009. Revision of the NW Laurentide Ice Sheet: implications for the paleoclimate, the northeast extremity of Beringia, and Arctic Ocean sedimentation. Quaternary Science Reviews. 28, 1573-1596.

Evans, D.J.A., England, J.H., LaFarge. C., Coulthard, R., Lakeman, T. Quaternary geology of the Duck Hawk Bluffs, southwest Banks Island, Arctic Canada: a re-investigation of a critical terrestrial type locality for glacial and interglacial events around the Arctic Ocean. Quaternary Science Reviews. In press.

French, H.M. 1972. The proglacial drainage of northwest Banks Island. The Musk-Ox. 10, 26-31.

Fyles, J.G. 1962. Physiography. In: Thorsteinsson R., Tozer, E.T. (Eds.). Banks, Victoria, and Steffansson Island, Arctic Archipelago. Geological Survey of Canada. Memoir 330, 8-17.

Fyles, J.G. 1990. Beaufort Formation (Late Tertiary) as seen from Prince Patrick Island, Arctic Canada. Arctic. 43, 393-403.

Fyles, J.G., Hills, L.V., Matthews, J.V., Barendregt, R., Baker, J., Irving, E., Jetté, H. 1994. Ballast Brook and Beaufort Formations (Late Tertiary) on northern Banks Island, Arctic Canada. Quaternary International. 22-23, 141-171.

Harrington, C. R. 2005. The eastern limit of Beringia: mammoth remains from Banks and Melville islands, Northwest Territories. Arctic. 58, 361-369.

Hobbs, W.H. 1945. The boundary of the latest glaciation in Arctic Canada. Science. 101, 549-551.

Holland, M.M., Bitz, C.M. 2003. Polar amplification of climate change in coupled models. Climate Dynamics. 21, 221-232.

Hollin, J.T., Barry, R.G. 1979. Empirical and theoretical evidence concerning the response of the Earth's ice and snow cover to a global temperature increase. Environmental International. 2, 437-444.

Howat, I., Joughin, I., Scambos, T. 2007. Rapid changes in ice discharge from Greenland outlet glaciers. Science. 315, 1559-1561.

Iverson, N.R., Hanson, B., Hooke, R.L.B., Jansson, P. 1995. Flow mechanism of glaciers on soft beds. Science. 267, 80-81.

Jakobsson, M., Gardner, J.V., Vogt, P., Mayer, L.A., Armstrong, A., Backman, J., Brennan, R., Calder, B., Hall, J.K., Kraft, B. 2005. Multibeam bathymetric and sediment profiler evidence for ice grounding on the Chukchi Borderland, Arctic Ocean. Quaternary Research. 63, 150-160.

Jakobsson, M., Polyak, L., Edwards, M., Klemen, J., Coakley, B. 2008. Glacial geomorphology of the Central Arctic Ocean: the Chukchi Borderland and the Lominosov Ridge. Earth Surface Processes and Landforms. 33, 526-545.

Jakobsson, M., Nilsson, J., O'Regan, M., Backman, J., Löwemark, L., Dowdeswell, J.A., Mayer, L., Polyak, L., Colleoni, F., Anderson, L., Björk, G., Darby, D., Eriksson, B., Hanslik, D., Hell, B., Marcussen, C., Sellén, E., Wallin,

Å. 2010. An Arctic Ocean ice shelf during MIS 6 constrained by new geophysical and geological data. Quaternary Science Reviews. 29, 3505-3517.

Jakobsson, M., Andreassen, K., Bjarnadóttir, L.R., Dove, D., Dowdeswell, J.A., England, J.H., Funder, S., Hogan, K., Ingólfsson, O., Jennings, A., Krog-Larsen, N., Kirchner, N., Landvik, J.Y., Mayer, L., Moller, P., Niessen, F., Nilsson, J., O'Regan, M., Polyak, L., Petersen, N.N., Stein, R. Arctic Ocean Glacial History. Quaternary Science Reviews. In press.

Jenness, J.L. 1952. Problem of glaciation in the western islands of Arctic Canada. Bulletin of Geological Society of America. 63, 939-952.

Kerr, J.W. 1980. Structural framework for the Lancaster aulacogen, Arctic Canada. Geological Survey of Canada Bulletin. 319.

Kristoffersen, Y., Sorokin, M.Y., Jokat, W., Svendsen, O. 2004. A submarine fan in the Amundsen Basin, Arctic Ocean. Marine Geology. 204, 317-324.

Lakeman, T.R. 2012. Revision of the Early Quaternary stratigraphy at Morgan Bluffs, Banks Island, western Canadian Arctic. PhD Thesis, University of Alberta, Edmonton, Canada.

Lakeman, T.R., England, J.H. 2012. Paleoglaciological insights from the age and morphology of the Jesse moraine belt, western Canadian Arctic. Quaternary Science Reviews. 47, 82-100.

Lakeman, T.R., England, J.H. 2013. Late Wisconsinan glaciation and postglacial relative sea level change on western Banks Island, Canadian Arctic Archipelago. Quaternary Research. 80, 99-112.

MacLean, B., Blasco, S., Bennett, R., Lakeman, T., Hughes-Clarke, J., Kuus, P., Patton, E. 2012. Marine evidence for a glacial ice stream in Amundsen Gulf, Canadian Arctic Archipelago. 42nd Annual Arctic Workshop abstract, March 7th-9th, University of Colorado, US.

Miall, A.D. 1976. Proterozoic and Paleozoic geology of Banks Island, Arctic Canada. Geological Survey of Canada Bulletin, 258.

Miall, A. D. 1979. Mesozoic and Tertiary geology of Banks Island, Arctic Canada: the history of an unstable craton margin. Geological Survey of Canada Memoir, 387: 235

Nixon, C.F., England, J.H., Lajeunesse, P., Hanson, M.A. Deciphering patterns of postglacial sea level at the junction of the Laurentide and Innuitian Ice Sheets, western Canadian Arctic. Quaternary Science Reviews. In press.

Oppenheimer, M. 1998. Gobal warming and the stability of the West Antarctic Ice Sheet. Nature. 393, 325-332.

Peltier, W.R. 1998. Postglacial variations in the level of the sea. Implications for climate dynamcis and solid-earth geophysics. Reviews of Geophysics. 36, 603-689.

Peltier, W.R. 2002. On eustatic sea level history: Last Glacial Maximum to Holocene. Quaternary Science Reviews. 21, 377-396.

Peltier, W.R., Farrell, W.E., Clark, J.A. 1978. Glacial isostasy and relative sea level: a global finite element model. Tectonophysics. 50, 81-110.

Peltier, W.R., Drummond, R. 2008. Theoretical stratification of the lithosphere: a direct inference based upon the geodetically observed pattern of the

glacial isostatic adjustment of the North American continent. Geophysical Research Letters. 35.

Polyak, L., Edwards, M.H., Coakley, B.J., Jakobsson, M. 2001. Ice shelves in the Pleistocene Arctic Ocean inferred from glaciogenic deep-sea bedforms. Nature. 410, 453-547.

Polyak, L., Darby, D., Bischof, J., Jakobsson, M. 2007. Stratigraphic constraints on Late Pleistocene glacial erosion and deglaciation of the Chukchi margin, Arctic Ocean. Quaternary Research. 67, 234-245.

Prest, V.K., 1969. Retreat of Wisconsinan and Recent ice in North America. Geological Survey of Canada. Map 1257A, scale 1:5,000,000.

Scott, D.B., Schell, T., St-Onge, G., Rochon, A., Blasco, S. 2009. Foraminiferal assemblage changes over the last 15,000 years on the Mackenzie Beaufort Sea Slope and Amundsen Gulf, Canada: Implications for past sea ice conditions. Paleoceanography. 24, 1-20.

Serreze, M.C., Barry, R.G. 2011. Processes and impacts of Arctic Amplification: A research synthesis. Global and Planetary Change. 77, 85-96.

Serreze, M.C., Barrett, A.P., Slater, A.G., Steele, M., Zhang, J., Trenberth, K.E. 2007. The large-scale energy budget of the Arctic. Journal of Geophysical Research. 112.

Stein, R., Matthiessen, J., Niessen, F., Krylov, R., Nam, S., Bazhenova, E. 2010. Towards a better litho-stratigraphy and reconstruction of Quaternary palaeoenvironment in the Amerasian Basin (Arctic Ocean). Polarforschung. 79, 97-121.

Stokes, C.R., Clark, C.D., Darby, D.A., Hodgson, D.A. 2005. Late Pleistocene ice export events into the Arctic Ocean from the M'Clure Strait Ice Stream, Canadian Arctic Archipelago. Global and Planetary Change. 49, 139–162.

Stokes, C.R., Clark, C., Winsborrow, M. 2006. Subglacial bedform evidence for a major paleo-ice stream in Amundsen Gulf and its retreat phases, Canadian Arctic Archipelago. Journal of Quaternary Science. 21, 300–412.

Stokes, C.R., Clark, C.D., Storrar, R. 2009. Major changes in ice stream dynamics during deglaciation of the north-western margin of the Laurentide Ice Sheet. Quaternary Science Reviews. 28, 721-738.

Thorsteinsson, R., Tozer, E.T. 1970. Geology of the Arctic Archipelago. In: Geology and economic minerals of Canada. Geological Survey of Canada, Economic Geology Report. 1, 547–590.

Trettin, H.P. (Ed.). 1991. Geology of the Innuitian Orogen and Arctic Platform of Canada and Greenland. Geology of Canada 3. Geological Survey of Canada, Ottawa.

Tsytovich, N.A. (Ed.). 1975. The mechanics of frozen ground. McGraw-Hill, New York.

Tulaczyk, S., Kamb, B., Scherer, R.P., Engelhardt, H.F. 1998. Sedimentary processes at the base of a West Antarctic ice stream: constraints from textural and compositional properties of subglacial debris. Journal of Sedimentary Research. 68, 487-496.

Vincent, J-S. 1982. The Quaternary History of Banks Island, Northwest Territories, Canada. Geographie Physique et Quaternaire. 36, 209-232.

Vincent, J-S. 1983. La geologie du quaternaire et la geomorphologie de L'ile Banks, arctique Canadien. In: Commission Geologique du Canada Memoir 405.

Vincent, J-S. 1984. Quaternary stratigraphy of the western Canadian Arctic Archipelago. In: Fulton, R.J. (Ed.). Quaternary Stratigraphy of Canada – A Canadian Contribution to IGCP Project 24. Geological Survey of Canada. 87-100.

Vincent, J-S. 1990. Late Tertiary and Early Pleistocene Deposits and History of Banks Island, southwestern Canadian Arctic Archipelago. Arctic. 43, 339-363.

Vogt, P.R., Crane, K., Sundvor, E. 1994. Deep Pleistocene iceberg ploughmarks on the Yermak Plateau: sidescan and 3.5 kHz evidence for thick calving fronts and a possible marine ice sheet in the Arctic Ocean. Geology. 22, 403-406.

Waller, R.I., Murton, J., Whiteman, C. 2009. Geological evidence for subglacial deformation of Pleistocene permafrost. Proceedings of the Geologists Association. 120, 155-162.

Waller, R.I., Murton, J.B., Kristensen, L. 2012. Glacier-permafrost interactions: Processes, products and glaciological implications. Sedimentary Geology. 255-256, 1-28.

Weertman, J. 1975. Stability of Antarctic Ice. Nature. 253, 159.

Wilson, J.T., Falconer, G., Mathews, W.H., Presk, V.K. 1958. Glacial Map of Canada. Geological Association of Canada, scale 1:5,000,000.

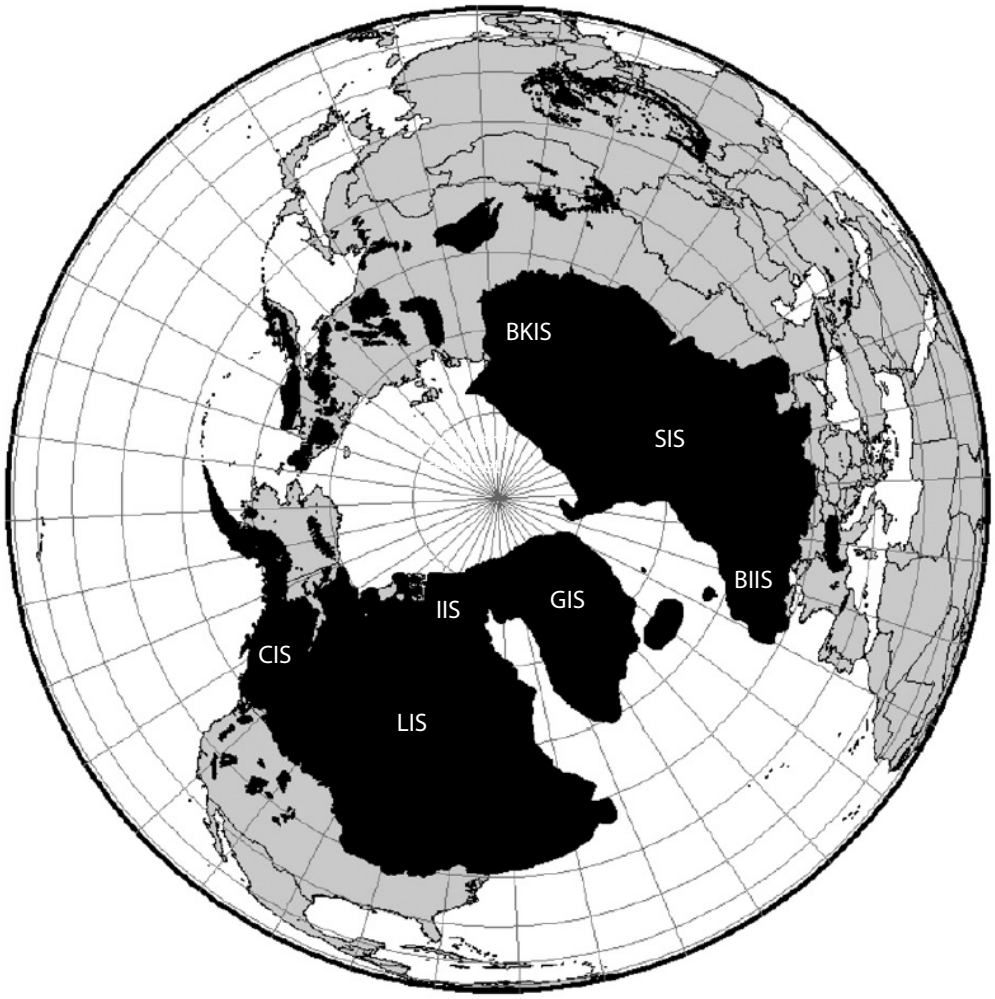

Fig. 1.1. Extent of northern hemisphere ice sheets during their Pleistocene maximum. Major ice sheets include: CIS = Cordilleran Ice Sheet, LIS = Laurentide Ice Sheet, IIS = Innuitian Ice Sheet, GIS = Greenland Ice Sheet, BIIS = British-Irish Ice Sheet, SIS = Scandinavian Ice Sheet, and BKIS = Barents-Kara Ice Sheet. From Ehlers and Gibbard (2007).

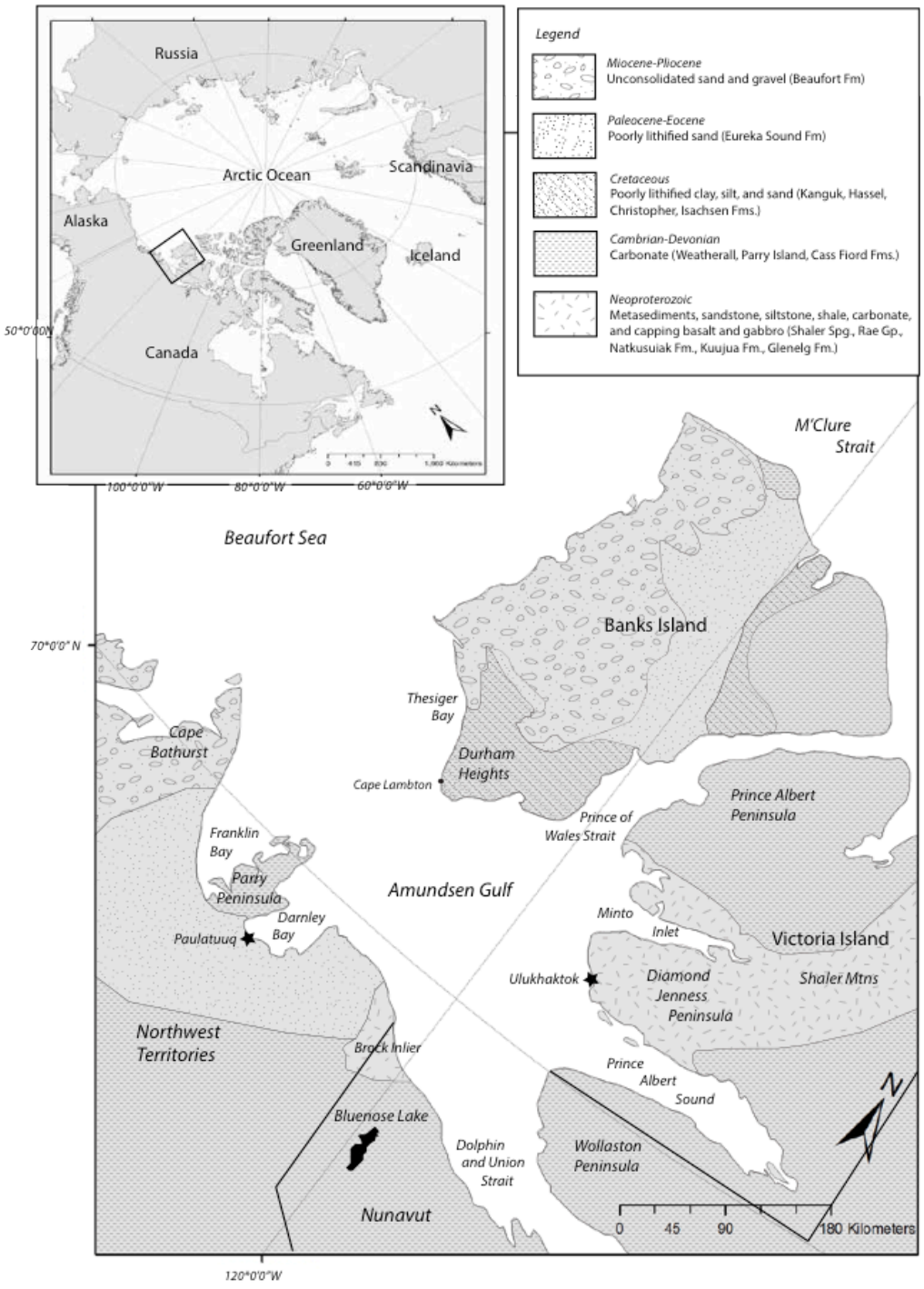

Fig. 1.2. Location map of Banks Island including major place names and generalized bedrock geology.

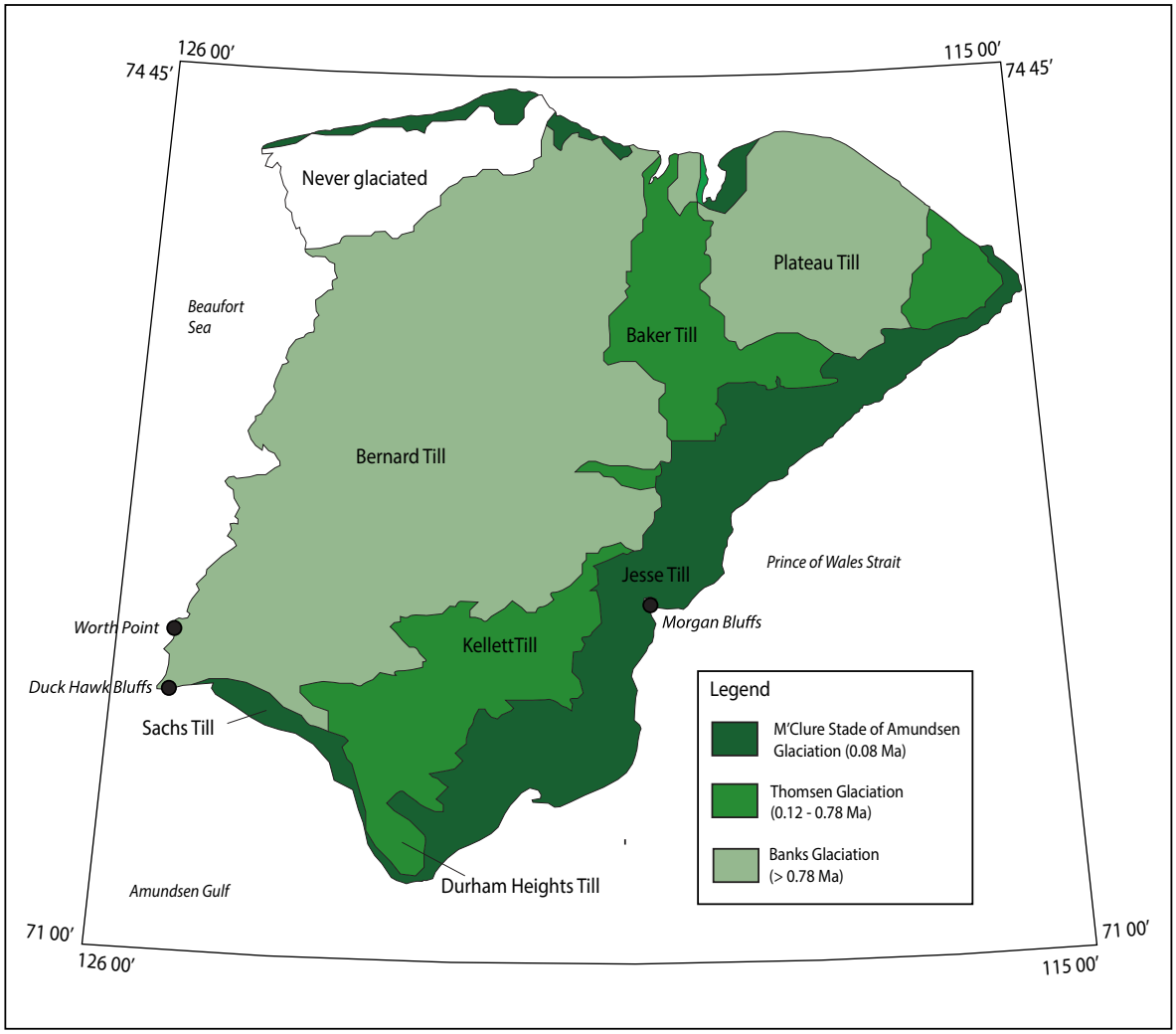

Fig. 1.3. Map of Banks Island showing the glacial limits of Vincent (1982). Note the never-glaciated landscape in the far northwest corner of Banks Island and the increasing age of till sheets with distance westward across the island. Major stratigraphic sections central to the former Quaternary glacial model are also indentified, including Worth Point on southwest Banks Island.

Fig. 1.4a

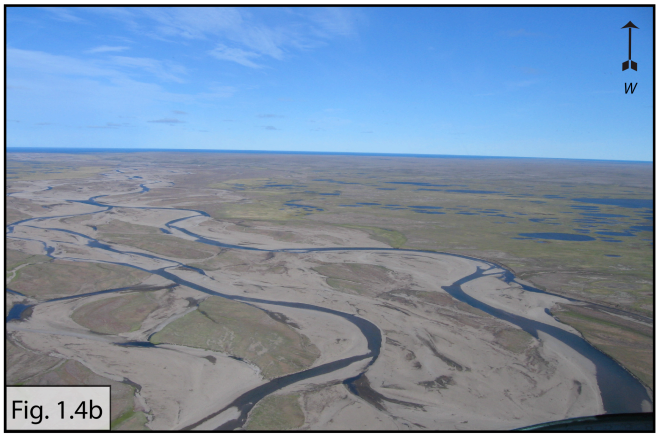

Fig. 1.4b

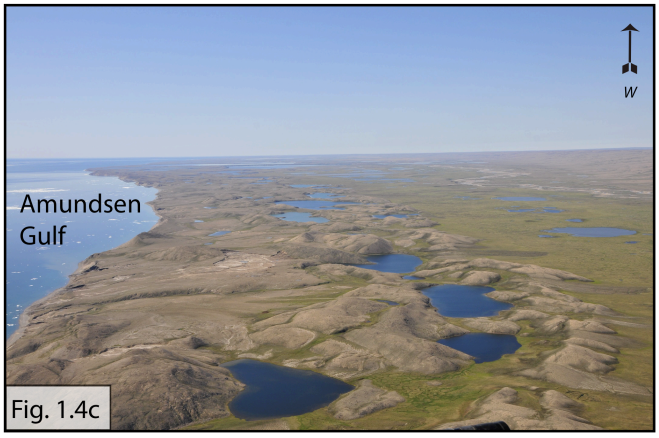

Fig. 1.4c

(Previous page)

Fig. 1.4a. Photograph looking east across the Durham Heights (< 730 m asl) adjacent to Amundsen Gulf, southeast Banks Island. Note gabbro-diabase sills of the Glenelg Fm that outcrop as horizontal bands.

Fig. 1.4b. Photograph looking towards the Beaufort Sea (west) across the westward descending outwash plain that characterizes much of the interior of southern Banks Island.

Fig. 1.4c. Photograph looking west across coast-parallel moraines fringing the south coast of Banks Island, adjacent to Amundsen Gulf.

CHAPTER 2

THE GLACIAL AND RELATIVE SEA LEVEL HISTORY OF SOUTHERN BANKS ISLAND, NT, CANADA: NEW INSIGHTS INTO THE CHRONOLOGY AND DYNAMICS OF THE NORTHWEST LAURENTIDE ICE SHEET

1. INTRODUCTION

Banks Island is located in the western Canadian Arctic Archipelago (CAA; Fig 2.1), where the northwestern Laurentide Ice Sheet (LIS) and southwestern Innuitian Ice Sheet (IIS) coalesced during the Last Glacial Maximum (LGM; England et al., 2009; Lakeman and England, 2012, 2013; Nixon et al., in press). This reconstruction includes former ice streams in the inter-island channels of M'Clure Strait and Amundsen Gulf, encircling Banks Island. These ice streams are proposed to have advanced onto the polar continental shelf, evacuating ice and sediment into the Arctic Ocean where thick ice shelves and/or 'paleocrystic' sea ice existed (Blasco et al., 1990, 2005; Stokes et al., 2005, 2006, 2009; Bradley and England, 2008; England et al., 2009; MacLean et al., 2012: Batchelor et al., in press). Furthermore, scouring by so-called 'enigmatic ice sheets' to depths of 450 m on the Arctic Ocean seabed, distal to the western CAA, are consistent with an extensive northwest LIS during the LGM and place new constraints on the thickness of evacuated ice required to reach such depths (Polyak et al., 2001, 2007; Engels et al., 2008; Jakobsson et al., 2010, in press; Dove et al., in press). Ice sheet mass loss by calving from M'Clure

Strait, Amundsen Gulf, and other marine-terminating margins has been identified as the primary mechanism for rapid deglaciation of the western CAA (Stokes et al., 2005, 2006, 2009; England et al., 2009; Lakeman and England, 2012). The western CAA, and notably the northwest LIS, serve as important analogues for the potential instability of marine-margins of the modern West Antarctic Ice Sheet - long identified as a margin vulnerable to catastrophic calving due to rapid outflow and thinning and/or eustatic sea level rise (e.g. Weertman, 1975; Hollin and Barry, 1979; Oppenheimer, 1998; Vaughan and Arthern, 2007). Constraining the dynamics that occasioned and controlled deglaciation of the western CAA, therefore, can inform our understanding of future ice sheet behaviour and its impact on relative sea level rise.

The focus of this study is southern Banks Island, where glacial landforms and sediments have been recognized for over half a century (Hobbs, 1945; Jenness, 1952; Fyles, 1962; Prest, 1969; French, 1972; Vincent, 1982, 1983; Dyke, 1986; Dyke and Prest, 1987; Dyke et al., 2002, 2003; Harrington, 2005). Prior to this study, the most systematic and widely adopted glacial reconstruction of Banks Island proposed a series of three pre-Late Wisconsinan glaciations extending from >780,000 to 80,000 yr BP that were expressed at the surface by lithologically distinct till sheets (Fig. 2.2a; Vincent, 1982, 1983, 1984; Vincent et al., 1983, 1984). However, a paucity of chronological control on these proposed glaciations (their sediments, associated relative sea levels, and interglaciations) left many aspects of this reconstruction unresolved (Vincent, 1982, 1983, 1984).

The reinvestigation of the Quaternary geology of central and northern Banks Island have recently demonstrated that the northwest LIS inundated the entire landscape during the Late Wisconsinan, extending an unknown distance onto the polar continental shelf (England et al., 2009; Lakeman and England, 2012, 2013). Newly recognized geomorphic landforms record the former confluence of thin, largely cold-based ice occupying most of the interior of Banks Island with an ice stream at least 635 m thick in M'Clure Strait (England et al., 2009; Lakeman and England, 2012, 2013). Furthermore, over 100 new radiocarbon dates broadly encompassing the Bølling-Allerød chronozone constrain a rapid, regional retreat of the northwest LIS throughout M'Clure Strait southeastward to Victoria Island. This was followed by at least two late glacial readvances on or adjacent to eastern Banks Island (Hodgson and Vincent 1982; England et al., 2009; Lakeman and England, 2012, 2013).

1.1. OBJECTIVES AND METHODS

The objectives of this study are to test the revised glacial model of Banks Island (England et al., 2009; Lakeman and England, 2012, 2013) by investigating the surficial geomorphology of southern Banks Island, which has not been revisited since the early survey of Vincent (1982, 1983, 1984). Three research questions are addressed: 1) What is the configuration, style, and chronology of ice advance along Amundsen Gulf and across southern Banks Island?; 2) What is the chronology and style of ice retreat along Amundsen Gulf and across southern Banks Island?; and 3) What is the pattern and chronology of relative sea level change and how does it reflect the paleotopography of former ice loads?

Addressing these questions also tests the hypothesis that an ice stream occupied Amundsen Gulf during the LGM (Blasco et al., 1990; 2005; Stokes et al., 2005, 2006, 2009; MacLean et al., 2012) and that the northwest LIS subsumed the southern interior of Banks Island and advanced onto the polar continental shelf (England et al., 2009; Lakeman and England, 2012, 2013).

The foundation of this study is based on widespread aerial photograph interpretation to identify Quaternary landforms and sediments (both terrestrial and marine) and to select key sites for fieldwork undertaken from 2008 – 2010. Field surveys extended from the southeast coast facing Prince of Wales Strait to the southwest coast facing the polar continental shelf, and extended up to 100 km inland (to the north). A chronology was primarily established utilizing accelerator mass spectrometry (AMS) radiocarbon dating of marine shells (ice-transported and in growth position) analysed at the KECK Carbon Cycle Accelerator Mass Spectrometry Laboratory, University of California. AMS radiocarbon dates on shells were then calibrated using Calib V.6.1 and the Marine 09 calibration curve (Reimer et al., 2009) with the application of a ΔR value of 335±85 (Coulthard et al., 2010). Unfossiliferous marine sediments were dated using the single-aliquot regenerative approach for optically stimulated luminescence (OSL) dating (Murray and Wintle, 2000) at the Sheffield Centre for International Drylands Research Luminescence Laboratory, UK. Additional efforts were made to determine the provenance of Shield erratics from mainland Canada in accordance with Doornbos et al (2009), and include both geochemical fingerprinting and Uranium-Lead (U-Pb) laser ablation dating conducted in the Heaman Laboratory,

Earth and Atmospheric Sciences, University of Alberta. The geographic locations of all samples collected and dated in this study are shown on Fig. 2.3.

1.2. BACKGROUND

Earlier surveys addressing the glacial history of Banks Island identified primary geomorphic and stratigraphic features including ice-marginal lakes (Hobbs, 1945), till (Washburn, 1947), meltwater channels (Jenness, 1952), and organic sediments of possible interglacial age (Craig and Fyles, 1960; Kuc, 1974). Fyles (1962) recognized an old (pre-Wisconsinan) fluvial landscape covering most of the island that was trimmed along the south and east coasts by a prominent moraine belt that he ascribed to the onshore advance of the Late Wisconsinan LIS – a margin adopted in later regional compilations of ice sheet limits (Prest, 1969).

The first systematic glacial survey of Banks Island, both surface and subsurface, significantly elaborated upon earlier observations (e.g. Fyles, 1962) and outlined a series of three progressively less extensive continental glaciations spanning > 780,000 to 80,000 yr BP (Fig. 2.2a; Vincent, 1982, 1983, 1984; Vincent et al., 1983, 1984). The limit of each glaciation was ascribed to lithologically distinct till sheets that were presumed to increase in age westward across the island, terminating against an ostensibly 'never glaciated' Late Tertiary fluvial landscape occupying northwest Banks Island (Fig. 2.2a; Vincent, 1982, 1983). Furthermore, each proposed glaciation was assigned a suite of corresponding moraines, proglacial lakes, and bracketing sediments of a preglacial transgression (recording ice advance) and a deglacial transgression to

postglacial forced regression (recording ice retreat; Fig. 2.2b; Vincent, 1982, 1983). With limited absolute dating control, the relative ages of geomorphic landforms were based on textural and morphological differences, whereas raised marine shorelines and sediments were distinguished by presumed crustal unloading amounts (Vincent, 1982, 1983). Notably, this glacial model reassigned the Late Wisconsinan LIS limit of Fyles (1962, along the east coast of the island) to an Early Wisconsinan margin, placing the Late Wisconsinan limit on Victoria Island (farther east, Fig. 2.2a; Vincent, 1982, 1983). This surficial model of multiple glaciations was subsequently used as a framework to interpret diverse subsurface stratigraphic units exposed in ~50 m thick coastal sections around Banks Island, ultimately prompting the identification of up to eight continental glaciations and five interglaciations spanning over one million years (Vincent, 1990; Barendregt et al, 1998).

Chronologic, startigraphic and glacioisostatic limitations to the original Banks Island model (Vincent, 1982, 1983, 1984, 1990; Vincent et al., 1983, 1984) have been increasingly identified. Chronologic limitations include the paucity of reported and dated shells, especially within widespread deposits along the north and east coasts. This paucity contrasts with other areas of the CAA, where the radicarbon dating of fossilferous shorelines is the hallmark of glacial reconstructions (e.g. Blake, 1970; Dyke and Prest, 1987; Dyke et al., 2002; England et al., 2006). Stratigraphic problems pertain to reinterpretations of coastal sections where glaciotectonism fundamentally contradicts earlier assumptions of non-deformed sedimentary sequences (Lakeman, 2012; Evans et al., in press;

Vaughan et al., in press). Glacioisostatic limitations include the lack of evidence for multiple raised marine shorelines that were attributed to the proposed model of multiple glaciations (Vincent 1982, 1983). This is particularly problematic for the 'Big Sea' following the Thomsen Glaciation (pre-Sangamonian) whose published isobases reach 215 m asl along with others drawn on the same shoreline. Indeed all of the isobases shown by Vincent (1983) converge with those as low as 90 m asl (Vincent 1983), contravening the fact that contours cannot cross and suggesting that they are probably unrelated to an actual shoreline (e.g. to the Big Sea) vs. bedrock outcrops such as the mapped interior limit of the Beaufort Fm (England et al. 2009).

Dyke (1986) was the first to challenge the established Banks Island model, rejecting the interpretation that an 88 m shoreline on northeast Banks Island dated to an Early Wisconsinan highstand (younger than the proposed Big Sea), because it contains shells in growth position dated to ~10,600 ^{14}C yr BP (Vincent, 1982, 1983; Hodgson and Vincent, 1984). Like later reinterpretations of the Banks Island model (England et al., 2009; Lakeman and England 2013) the 88 m shoreline was reinterpreted by Dyke to record Late Wisconsinan marine limit, thereby recording far greater glacial unloading than previously recognized (Vincent 1982, 1983). Consequently, the Late Wisconsinan ice margin was reverted back to the original limit of Fyles (1962) and adopted in subsequent regional reconstructions (Dyke, 1986; Dyke and Prest, 1987; Dyke et al., 2002; Dyke et al., 2003). Moreover, basal dates obtained from lake sediments occupying till sheets ascribed to all three, pre-Late Wisconsinan glaciations (Vincent, 1982,

1983) date between ~10,600 and ~9000 ^{14}C yr BP (Gajewski et al., 2000). These dates are consistent with a pervasive late Wisconsinan ice cover across Banks Island, though this interpetation was suprisingly never proposed by Gajewski et al. (2000), nor entertained by Vincent (1982, 1983) whose widely dated peat deposits across the island also produced early Holocene ages.

The current consensus following a resurvey of central and northern Banks Island supports the complete coverage of Banks Island by the northwest LIS during the LGM, amalgamating the deposition of the formerly proposed till sheets (Vincent, 1982, 1983) into a single, Late Wisconsinan glaciation (England et al., 2009; Lakeman and England, 2012, 2013). Notably, the formerly proposed till sheets, reported to be 'lithologically distinct' (Vincent 1982, 1983), have boundaries that are now recognized to coincide with the contact separating different bedrock (England et al., 2009). Similarly, fine-grained deposits formerly assigned to multiple preglacial and postglacial seas have been shown to coincide with deposits ranging from Creatceous bedrock to Late Wisconsinan glaciolacustrine and/or marine silt (England et al., 2009; Lakeman and England, 2012). These resurveys also identify previously unreported, shell-bearing marine limit deltas and geomorphic landforms that mark the Late Wisconsinan limit as designated by Fyles (1962) - albeit this is now recognized to be a late glacial stillstand and/or readvance between 13,750 and 12,750 cal yr BP (Lakeman and England, 2012). Collectively, this evidence for an expansive northwest LIS on Banks Island is in agreement with satellite mapping that records ice sheet bedforms produced across the western CAA during the LGM and subsequent

stages of deglaciation (Stokes et al., 2005, 2006, 2009; Nixon et al., in press). This reconstruction is also consistent with extensive ice on the mainland south of Amundsen Gulf, where Laurentide ice terminated west of the Mackenzie Delta (Mackay, 1959; Murton et al., 1997; Fritz et al., 2012) and in the Mackenzie Mountains and Peel Plateau impounding Glacial Lake Old Crow (Hughes, 1972; Morlan et al., 1990; Duk-Rodkin and Hughes, 1991; Zazula et al., 2004; Kennedy et al., 2010).

1.3. REGIONAL SETTING

Southern Banks Island (~ 20,000 km^2) encompasses a topographically diverse region bound by the Beaufort Sea to the west, Amundsen Gulf to the south, and Prince of Wales Strait to the east. The interior comprises a gently sloping outwash plain inset by prominent east-west trending river valleys that descend towards the Beaufort Sea. Two coastal moraines – the Sachs Moraine and Sand Hills Moraine belt - trim the interior along the south-central coast and are separated by kettled lowlands. The Jesse moraine belt trims the east coast and contacts the outwash plain descending to the west. The dominant bedrock comprises sand and silt of the Cretaceous Christopher Fm and Hassel Fm and sand and gravel of the Pliocene Beaufort Fm (Fig 2.1). On far southeast Banks Island, the Durham Heights form a distinct topographic high (up to 730 m asl) composed of Proterozoic gabbro-diabase sills of the Glenelg Fm, overlain by Early Cretaceous Christopher and Hassel Fms and fragmented pockets of dissected Pliocene Beaufort Fm.

2. RESULTS: SURFICIAL OBSERVATIONS

The surficial geomorphology of southern Banks Island is strongly overprinted by the most recent record of glacial retreat. Consequently, geomorphic observations are presented in chronologic order of ice retreat, proceeding from southwest to southeast Banks Island, followed by observations of raised marine landforms and sediments. The collection site of all samples dated on southern Banks Island are shown in Fig. 2.3, and the primary glacial geomorphology within the entire study area is shown in Fig. 2.4.

2.1. GLACIAL GEOMORPHOLOGY

2.1.1. Lower Kellett Valley

On the far southwest tip of Banks Island, prominent moraines and ice-marginal meltwater channels deposited sub-parallel to the west coast (Beaufort Sea) impinge ~2 km inland and span a distance of ~7 km from Kellett Point to the eastern end of Duck Hawk Bluffs (Fig. 2.5). The orientation of the moraines combined with their limited inland extent are interpreted to record deposition by trunk ice or an ice stream flowing westward in Amundsen Gulf. These moraines are contacted to the north by a separate set of arcuate moraines and ice-marginal meltwater channels that delineate a coalescent ice lobe in the Kellett Valley (Fig. 2.5). The advance of this ice lobe offshore onto the polar continental shelf is recorded by subglacial till that caps a coastal stratigraphic section and displays an E-W oriented macrofabric (Worth Point, ~25 km north of Kellett Point, Fig. 2.2a; Vaughan et al., in press). On the west coast of southern Banks Island, meltwater channels grade to a gravelly marine limit beach that rises progressively northward

from 11 m asl to 15 m asl, over a distance of ~40 km (Fig. 2.4). An accordant marine limit beach contacted by similarly configured meltwater channels is recorded farther north (Lakeman and England, 2013) – supporting the sequential retreat of a contiguous ice margin from western Banks Island.

2.1.2. Sachs Moraine

Along south-central Banks Island, the westward-descending Sachs Moraine parallels the coast for >100 km, trimming the interior plateau up to 15 km inland (Figs. 2.5 and 2.6). Previously, the Sachs Moraine was interpreted to mark either the Early Wisconsinan (Vincent, 1982) or Late Wisconsinan ice limit (Fig. 2.2b; Hodgson et al., 1984; Dyke, 1986; Dyke and Prest, 1987). At its eastern end, the Sachs moraine impinges 6 km inland, abutting Raddi Lake and extending into the Masik River valley (Figs. 2.4 and 2.6). The elevation of the moraine (310 m asl) combined with the depth of Amundsen Gulf (400 m) requires an ice thickness of 710 m, far in excess of what would be necessary for the ice to be grounded vs. floating. In contrast, if the trunk ice had been floating, the Sachs Moraine should have had a freeboard of only 40 m asl (consistent with the channel depth of 400 m) and a near-horizontal gradient (~0.1/km), that incorporates the regional glacioisostatic delevelling following deglaciation. At its western end, the moraine passes offshore 3 km before the southwest tip of Banks Island, recording a gradient of ~3 m/km that reflects the paleotopography of the trunk ice or ice stream responsible for its deposition.

The central and eastern parts of the Sachs Moraine include multiple ridges of thrust and deformed till that trim the interior plateau (Figs. 2.5 and 2.6).

Coastward of these moraines, till is up to 6 m thick, fossiliferous, and lithologically distinct from till farther inland. Notably, the Sachs Moraine is composed of a silty-clay matrix with abundant mafic erratics, including boulders < 5 m^3 and smaller granite and quartzite boulders. Distal to the Sachs Moraine, till is spatially discontinuous and unfossiliferous, composed of a sandy matrix with abundant quartzite erratics and rare mafic and granite erratics. Ice-transported shells within the Sachs Moraine till include two unidentified shell fragments that dated 41,931 ± 481 cal yr BP (UCI-54177, Table 2.1), and 44,469 ± 893 cal yr BP (UCI-54187, Table 2.1) and one fragment of *Astarte borealis* that dated 24,383 ± 355 cal yr BP (UCI-89674, Table 2.1). The youngest finite date (~24,00 cal yr BP) currently provides the best maximum age for deposition of the Sachs Moraine.

The western end of the Sachs Moraine is composed of stacked rafts of sand and gravel, interpreted to have been derived from glaciofluvial outwash (Fig. 2.7a). Each raft displays an undisturbed sequence of planar-bedded gravel (rounded and commonly striated) interbedded with planar cross-bedded sand containing reworked *A. borealis.* These shells dated 43,797 ± 778 cal yr BP (UCI-54186, Table 2.1), 46,564 ± 2366 cal yr BP (UCI-55263, Table 2.1), and 46,867 ± 1383 cal yr BP (UCI-54181, Table 2.1). Although these dates are toward the upper limit of accurate radiocarbon dating (e.g. Walker, 2005), the similarity of shell dates collected from the Sachs Moraine may record an early marine isotope stage (MIS) 3 age redeposited by Late Wisconsinan ice. The absence of internal deformation within the stacked rafts suggest that they were frozen during

deformation, and the lack of a capping diamicton suggests that they were thrust ice-marginally without being subsequently overridden.

Beyond the western edge of the Sachs Moraine, outwash can be traced distally for ~300 m where coastal exposures record aggradation of at least 12 m (Fig. 2.7b). The outwash coarsens upwards and grades conformably into 8 m of massive, mass flow diamictons yielding mafic erratics < 0.5 m^3. The entire sequence of coarsening-upwards outwash and mass flow diamictons is interpreted to represent subaqueous deposition from an advancing glacier margin into a glacioisostatically raised sea, likely in the form of an aggrading outwash fan. The outwash fan terminates at a prominent marine limit bench (20 m asl; section 2.2.2) that can be traced eastward towards south-central Banks Island for several kilometres (Fig. 2.7c).

Within the major east-west trending valleys of southwest Banks Island, lobate ice-marginal meltwater channels and localized glaciotectonized bedrock display a convex down-valley pattern outlining former tongues of Laurentide ice (Fig. 2.4). Subdued medial moraines, often associated with kettle lakes and kame terraces, demarcate interlobate contacts on the low divides separating these shallow valleys. These divides also served to separate divergent meltwater channels evident on aerial photographs (Fig. 2.4). These landforms indicate that the interior Laurentide margin was thin and digitate, but nevertheless extended offshore onto the polar continental shelf. During deglaciation, it is apparent that the thin, westward flowing ice lobes became confined by the local topography, despite its subdued relief (< 50 m). The latest, proglacial meltwater channels

emanating from the western margin of the Sachs Moraine drain freely into the lower Kellett Valley (Figs. 2.4 and 2.5). Because interior ice does not deflect these channels, it is inferred that the lower Kellett Valley became ice-free while marine ice (in Amundsen Gulf) remained onshore at the Sachs Moraine.

Fifteen kilometres to the east of Kellett Point (Fig. 2.4) proglacial meltwater channels emanating from the Sachs Moraine are deflected westward, presumably by a cold-based ice lobe occupying the Kellett Valley (Figs. 2.4 and 2.5). This deflection continues for ~15 km, indicating that ice in the lower Kellett Valley retreated eastward in contact with marine trunk ice, which remained onshore, close to its maximum position. Eastward of this deflection pattern (~30 km east of Kellett Point), proglacial channels no longer emanate inland from the Sachs Moraine (Fig. 2.6) but rather are replaced by those formed along the Kellett valley lobe. This change in meltwater channel configuration, reflecting only interior Laurentide ice, indicates that the marine trunk ice had now moved offshore from the Sachs Moraine. Despite their initial separation, it is clear that terrestrial and marine deglaciation of southern Banks Island was synchronous.

Ice-marginal meltwater channels routed westward from the Sachs Moraine (abutting Raddi Lake) grade into multiple outwash fans that are associated with paleo-shorelines up to 120 m asl perched on the valley walls (Fig. 2.6). These shorelines record impoundment of an ice-dammed lake, herein termed ‘Glacial lake Raddi’, when trunk ice occupied its onshore position at the Sachs Moraine. Glacial Lake Raddi was originally identified by Vincent (1982), though attributed to an Early Wisconsinan ice margin.

Nested recessional moraines and sub-horizontal kame terraces on the proximal (seaward) side of the Sachs Moraine are interpreted to record the progressive thinning and lowering of marine trunk ice from its maximum position (Fig. 2.6). Linear, sharp-crested moraines in the Mary Sachs Valley record minor stillstands and/or readvances of the marine trunk ice as it continued its overall, seaward withdrawal. Most notably, Angus Moraine (Fig. 2.5) is an exceptionally linear moraine composed of cobble-rich diamicton overlying buried ice that was previously identified as glacial (Worsley, 1999). A comparably linear and sharp-crested ice-cored moraine is located at the eastern end of the Mary Sachs Valley (Fig. 2.6). Because of their ice-cores, both moraines may represent localized controlled moraine deposition by a cold-based margin.

Overlying these recessional moraines and kame terraces are previously unidentified sequences of glaciolacustrine silt that reach 76 to 84 m asl (Figs. 2.7d and 2.7e) that are accordant with a series of shorelines trimming the interior plateau (Fig. 2.7f). The silt and accordant shorelines record an ice-dammed lake in Mary Sachs Valley, herein termed 'Glacial Lake Mary Sachs', impounded between trunk ice in Amundsen Gulf and the Sachs Moraine (Fig. 2.8). Below Raddi Lake at the eastern end of the Mary Sachs Valley, an outwash fan at 80 m asl records the westward drainage of Glacial Lake Raddi into Glacial Lake Mary Sachs (Fig. 2.6). The lower elevation of the outwash fan (4 m below the upper limit of glaciolacustrine silt) indicates that Glacial Lake Mary Sachs had lowered prior to westward drainage of Glacial Lake Raddi. This lowering was most likely governed by the opening of temporary outlets as trunk ice oscillated against the

Sachs Moraine. These oscillations would have also controlled the timing and routing of drainage from Glacial Lake Raddi. The elevation of glaciolacustrine silt in the Mary Sachs Valley requires that trunk ice impounding Glacial Lake Mary Sachs was at least 486 m thick offshore, assuming a depth in the marine channel of 400 m. Had trunk ice withdrawn from southern Banks Island as a floating ice shelf, hydraulic connection between the ocean and what would have been an interior epishelf lake (England et al. 2009), would have permitted brackish marine sediments to aggrade to the deglacial marine limit of ~20 m asl (section 2.2.2.).

2.1.3. Sand Hills Moraine

A subsequent stillstand and/or readvance of trunk ice in Amundsen Gulf is required to deposit the Sand Hills Moraine belt that fringes the eastern end of the Mary Sachs Valley (Fig. 2.6). The moraine is approximately 25 km long, 2 km wide, and up to 150 m high. The belt comprises three linear rows of sharp-crested, coast-parallel moraines separated by discontinuous fragments of smaller, linear moraines (Fig. 2.7g). Bracketing the western margin are subdued fragments of linear moraines associated with hummocky deposits, kettle lakes, and widespread retrogressive thaw flow slides (Fig. 2.6). These thaw flow slides expose foliated, debris-rich ice containing striated clasts that require a glacial origin (French and Harry, 1990). Currently, the ice cores are capped by patchy debris up to 1 m thick (less than the depth of the modern active layer), permitting rapid melting and extensive sediment reworking. Retrogressive thaw flow slides on the Sand Hills Moraine belt also expose foliated, debris-rich ice coring the moraines that are indicative of a glacial origin (Fig. 2.7h). In contrast to the hummocky terrain, ice-

cores on the Sand Hills Moraine belt are capped by continuous debris up to 6 m thick, enclosing them within permafrost that ensures preservation of their structural rigidity and linearity. It follows that wherever thaw flow slides can expose more ice, this linearity will be erased until the Sand Hills Moraine belt resembles the adjacent hummocky topography to the west, as recognized for similar ice-cored moraines on Victoria Island (Dyke and Savelle, 2000).

Debris cover on the Sand Hills Moraine belt is composed of a wide variety of proglacial sediments, including glaciofluvial sand and gravel, deformation till, and glaciolacustrine silt and clay. The internal architecture of the moraines commonly comprises stacked slabs of these proglacial sediments, overlying buried, foliated glacial ice. The simplest explanation of this internal architecture, combined with the structural linearity of the moraines, is the concentration of debris due to compressive flow at the frozen trunk ice margin (Evans, 2009). Such compression is invoked here to explain the thrust and stacked debris-rich subglacial ice, including proglacial sediments frozen to the bed, producing englacial, transverse debris septa (Evans, 2009). Debris septa would be subject to differential ablation at the snout surface, resulting in upstanding debris ridges that would continue to become detached from the frozen snout as ablation continued, eventually producing linear ice-cored controlled moraines (Evans, 2009).

The Sand Hills Moraine belt comprises three prominent rows of controlled moraine, and therefore three debris septa. The distance from the most proximal to the most distal row is less than 2 km, indicating that the polythermal margin and zone of compression was narrow – though an unknown volume of sediment may

have been lost to erosion along this submerging coastline. This narrow ice margin may also reflect a short-lived readvance and rapid moraine-building.–Indeed, moraines capped by glaciofluvial sand and gravel juxtaposed with moraines capped by till containing large erratics are indicative of rapid deformation of proglacial sediments (no sorting/reworking) and the overriding of some previously thrust debris septa, possibly by an oscillatory ice margin (Evans, 2009). In addition to polythermal bed conditions, glacial advance across fine-grained sediments flooring Glacial Lake Mary Sachs may have acted as a décollement surface that facilitated deformation in the overlying and rapidly aggrading proglacial sediments (Mathews and Mackay, 1960).

Multiple debris flows descend from the distal side of the Sand Hills Moraine belt and coalesce to form < 400 m wide fans in the Mary Sachs Valley (Fig. 2.7i). The Mary Sachs River has truncated the distal margins of these fans exposing 3 – 5 beds of massive to crudely bedded gravel (2.5 m thick) that display scour-and-fill structures and fine upwards into laminated sand and silt (Fig. 2.7j). The development of multiple, coalescent debris flows during construction of the Sand Hills Moraine belt is interpreted to record the mass wastage of debris-rich ice that would have been delivered to the polythermal ice margin via thrusting.

Strikingly linear meltwater channels and perched kame terraces occupying parallel troughs within the Sand Hills Moraine belt are interpreted to record channelled outwash enclosed by thrust sheets at the ice margin (Fig. 2.7g). Raised lacustrine shorelines also trim these nested moraines. Outwash channels from these lakes incise several moraines and extend to gravel outwash fans entering the

Mary Sachs Valley (Fig. 2.7k). The outwash fans aggrade to ~53 m asl and are accordant with the uppermost limit of lacustrine shorelines trimming distal moraines (facing the Mary Sachs Valley; Fig. 2.7l). Abundant mafic-dominated clasts (< 10 cm^2) mantling the Mary Sachs Valley also reach 50 m asl (Fig. 2.7m). These landforms and sediments (at ~53 m asl) are ~30 m above marine limit (20 m asl; section 2.2.2) and ~30 m below glaciolacustrine silts and shorelines trimming the interior plateau (up to 84 m asl; section 2.1.2), thereby recording deposition into a lower lake that likely represents a later stage of Glacial Lake Mary Sachs (Fig. 2.8). Consequently, the mafic-dominated clasts mantling the Mary Sachs Valley are interpreted as ice-rafted dropstones delivered into Glacial Lake Mary Sachs by icebergs calving from the trunk ice snout.

The ice sheet configuration required to impound Glacial Lake Mary Sachs during deposition of the Sand Hills Moraine belt remains speculative (Fig. 2.8). However, based on a lack of cross-cutting landforms on the Sachs Moraine, it is unlikely that the ice lobe occupying Kellett Valley advanced downslope to block the western end of the Mary Sachs Valley. Rather, it is more likely that trunk ice readvanced inland, west of the Sand Hills Moraine belt, where it would have abutted the interior plateau. Because the Sand Hills Moraine belt would have blocked southward drainage, it is probable that final drainage was routed westward towards present day Sachs Harbour (Figs. 2.5 and 2.8). During this event, high volumes of meltwater and sediment would have been exported into western Amundsen Gulf, across the kettled, fan-shaped plain that today covers ~ 450 km^2 and extends as a conspicuous lowland westward from the Mary Sachs

Valley (Fig. 2.7n). The surface of the plain has been reworked into extensive networks of sand dunes that mask the underlying sediment (Good and Bryant, 1985). However, limited subsurface exposures indicate that the apex comprises horizontally bedded glaciofluvial sand and gravel that grade distally to gently dipping sandy beds (French et al., 1982). The outermost edge of the plain is trimmed by horizontally bedded sand. These sediments are interpreted to be topsets and foresets deposited into a shallow marine embayment marking deglacial marine limit (20 m asl; section 2.2.2.). Detrital organics collected from sand and peat immediately overlying the outwash fan yield radiocarbon dates of ~10,600 and ~8400 ^{14}C yr BP, providing a minimum limiting age for Late Wisconsinan Laurentide retreat (Pissart et al., 1977).

2.1.4. Upper Kellett Valley

Following the drainage of Glacial Lake Mary Sachs and abandonment of the Sand Hills Moraine belt, cold-based interior ice retreated eastward, demarcated by former ice lobes in the Kellett and Masik valleys (Fig. 2.4). Within the Kellett valley, arcuate thrust-block moraines associated with kettle lakes and ice-marginal meltwater channels record former ice margins (Fig. 2.4). The most widespread thrust-block moraines occur at the boundary between the Beaufort Fm (west) and the Kanguk Fm (east), formerly interpreted to mark the limit of the Mid-Pleistocene Thomsen Glaciation (Figs 2.2b and 2.9; Vincent, 1982). Here, a transition from permeable to non-permeable substrate likely promoted the build up of hydraulic pressures in permafrozen sediments during temporary stillstand or localized readvance, facilitating displacement and thrusting along a décollement

plane (Mathews and Mackay, 1960). The resulting thrust-block moraines comprise three prominent arcuate thrust blocks inset by a series of smaller, imbricated thrust blocks with intervening depressions (Fig. 2.9; Evans and England, 1991). Lakes occupying depressions on the proximal side of several thrust blocks likely mark localized source basins from which the blocks originated (Fig. 2.9; Aber, 1985). Thrust blocks are composed entirely of stacked rafts of Kanguk Fm with no associated glaciogenic deposits, suggesting that they were thrust proglacially by a cold-based ice margin (Fig. 2.9; Evans and England, 1991).

2.1.5. Masik Valley and Durham Heights

Previous interpretations recognized an ice-dammed lake up to 230 m deep in the Masik Valley and adjoining valleys of the Durham Heights, purportedly impounded by an Early Wisconsinan ice lobe retreating offshore (Vincent, 1982). However, no landforms or sediments indicative of such a glaciolacustrine environment were observed in the Masik Valley or neighbouring valleys. Instead, kame terraces and nested recessional moraines oriented down-valley record the sequential retreat of an ice lobe *inland* (northeast) within the Masik Valley, opposite to previous interpretations (Fig. 2.4; Vincent, 1982, 1983). Prior to inland retreat, this ice lobe must have been confluent with trunk ice that advanced into the lower Masik Valley, as recorded by lithologically distinct till associated with the eastern extension of the Sachs Moraine (Fig. 2.4). The absence of lacustrine sediments in the Masik Valley suggests that meltwater drained freely

from the retreating Masik Valley ice lobe to Amundsen Gulf, as attested by its marine limit delta (section 2.2.2.).

On the south coast of Banks Island mafic erratics (< 5 m^3) are scattered along the Sachs Moraine at elevations up to 300 m asl and across the Durham Heights at elevations up to 730 m asl (Fig. 2.10a). Geochemical analyses of 8 sampled mafic erratics indicate that they match the geochemical fingerprint of the Franklin dyke swarm that outcrops nearby on southeast Banks Island and adjacent Victoria Island to the east (Harlan et al., 2003). One erratic (BCO9-5; Table 2.2) yielded four zircon crystals (>30 μm) that were suitable for U-Pb laser ablation dating in the Heaman Laboratory, University of Alberta. Resultant U-Pb dates ranged from 670 to 725 Ma (with a one sigma average of 706 ± 25 Ma), encompassing the Franklin dyke swarm formation age of 720 Ma. The Franklin dyke swarm is geographically wide-ranging, and includes the Coronation Sills and Brock Inlier south of Banks Island on the Canadian mainland, and the Minto Inlier on Victoria Island to the east (Harlan et al., 2003). Based on the size of the mafic erratics (< 5 m^3; Fig. 2.10a), their comparatively high copper concentrations, and a substantial area of outcrop required to supply such widespread erratics, a simple flow path would identify Victoria Island as the most likely provenance. Paleozoic carbonates and Precambrian granites (Fig. 2.10b; J. England, pers comm. 2012) also mantle the Durham Heights, supporting dispersal from Cambrian-Devonian bedrock on Victoria Island and from the Precambrian Shield, mainland Canada, respectively. The elevation of mafic, carbonate, and granite erratics (up to 730 m asl) – delivered by trunk ice in Amundsen Gulf –

indicates that trunk ice must have been at least 1000 m thick, accounting for depths in the marine channel of ~400 m. Glacially-smoothed coastal outcrops of the Glenelg Fm (Figs. 2.10c and 2.10d) displaying widespread striae (oriented east-west), document the passage of this thick, warm-based trunk ice.

East of the Masik valley, nested ice-marginal meltwater channels and small recessional moraines in the valleys of the Durham Heights indicate that smaller ice lobes withdrew radially inland, likely towards plateau ice caps that have since disappeared (Fig. 2.4). Along the coast, cliffs (< 730 m high) preserve sub-horizontal, ice-marginal meltwater channels that record a progressively thinning margin that must have remained cold-based (locally) to support a perched drainage across this slope (Fig. 2.4). A period of restabilization is inferred at the narrowest part of Amundsen Gulf that separates Cape Lambton on the southeast coast of Banks Island from Parry Peninsula on the mainland (Fig. 2.1). At this proposed pinning point, westward-dipping, gravel foreset beds (50 m thick) onlap the coast and extend laterally for ~2 km. The abundance of these foreset beds supports a stillstand, whereas the elevation of the foresets (~25 m above regional marine limit; section 2.2.2.) support progradation into a proglacial lake impounded by a grounded marine margin.

2.1.6. Jesse moraine belt

The glacial geomorphology in the uppermost reaches of the Kellett and Masik rivers is distinguished by widespread linear moraines and ice-marginal meltwater channels within a major moraine belt that extends up to 50 km inland (Fig. 2.4.). The equivalent moraine belt has been recognized farther north, both on

the east coast of Banks Island and on the opposite coast of Victoria Island, where it has been collectively named the Jesse moraine belt (13,750 – 12,750 cal yr BP; Lakeman and England, 2012).

Bordering southern Prince of Wales Strait, the Jesse moraine belt is comprised of two parts: 1) a higher, inland part that overtops the island's drainage divide (400 m asl) and extends 50 km west from Prince of Wales Strait; and 2) a lower, coastal part east of the island's drainage divide, on slopes descending to Prince of Wales Strait. Overall, the limit of the Jesse moraine belt is digitate and constrained by topography. For example, moraines extend westward up to 30 km into the Nelson River Valley but terminate well below the Durham Heights directly to the south (Fig 2.4). The moraine belt contrasts markedly with terrain to the west (distal), where sinuous proglacial meltwater channels form an expansive outwash plain descending to the Beaufort Sea (Figs. 2.4 and 2.11).

The inland part of the Jesse moraine belt is characterized by interconnected chains of kettle lakes and fragmented kame terraces that occur in association with linear moraines dissected by ice-marginal meltwater channels (Fig. 2.4). North of the Nelson River and up to 6 km inland (Fig. 2.4), the internal architecture of linear moraines is comprised of thrust slabs of unconsolidated Cretaceous bedrock and glaciogenic deposits (till, glaciofluvial sand and gravel, and localized glaciolacustrine silt). Numerous retrogressive thaw flow slides expose buried ice intercalated with the thrust bedrock and glaciogenic deposits (Fig. 2.12a). The ice is foliated, debris-rich, and contains striated clasts supporting a glacial origin. The simplest interpretation of this stratigraphic architecture, along

with the linear geomorphology of the moraines, is that they are controlled moraines (Evans, 2009) deposited by a polythermal ice margin, as inferred for the Sand Hills Moraine belt. Ice-marginal meltwater channels and kame terraces are interpreted to record the routing of outwash between former debris septa at the ice sheet terminus. The advance upslope from Prince of Wales Strait to the inland plateau also would have promoted compression and thrusting within the cold-based margin followed by the stacking of debris septa (Benn and Evans, 2010).

North of the upper Masik Valley, linear moraines within the upper, inland part of the Jesse moraine belt transition into hummocky terrain associated with large kettle lakes (Fig. 2.4, inland of Cardwell Brook). If large areas of the inland plateau are also cored by glacial ice – like the linear moraines above – then this hummocky and kettled topography likely reflects terrain with a debris cover thinner than the modern active layer, leading to widespread thermokarst, as proposed for the Sand Hills Moraine belt (Dyke and Savelle, 2000).

Elsewhere on the inland plateau, till can be up to 5 m thick, highly polygonated, and occasionally fluted. The flutings are oriented east-west, perpendicular to the coast, and cluster where the bedrock is predominantly Kanguk Fm that also contributes to the composition of the overlying till. For example, till overlying Kanguk Fm is distinctly more clay-rich, whereas till overlying Christopher and Hassel Fms (sand and silt) is more sand-rich. Till within the entire Jesse moraine belt contains a high percentage of Paleozoic carbonates entrained by Laurentide ice on Victoria Island to the east.

The second part of the Jesse moraine belt, comprising a coastal plain sloping toward Prince of Wales Strait, displays a different geomorphic signature than the inland plateau. Here, the cliffed coastline is dissected by several valleys oriented perpendicular to the coast, including the Cardwell, Treadwell, and Schuyter Point valleys (Fig. 2.11). Lobate thrust-block moraines and ice-marginal meltwater channels at the heads of these valleys are interpreted to document thinning cold-based trunk ice from Prince of Wales Strait that retreated downslope to form topographically constrained ice lobes (Fig. 2.11). Of particular note are thick sequences of glaciolacustrine silt perched against valley walls up to 150 m asl. These lacustrine deposits mark former ice-dammed lakes impounded by grounded trunk ice retreating downslope into the Strait. At numerous sites (above 50 m asl), the glaciolacustrine deposits have been thrust into ice-marginal moraines. Closer to the coast, kame terraces recording later proglacial lakes display lobate configurations, occasionally becoming discontinuous and conical (Figs. 2.13b and 2.12). Ice-marginal meltwater channels are closely associated with these lobate kames and often terminate at the apexes of small kame deltas (Fig. 2.12). These nested deglacial landforms record the final stages of retreat by grounded ice as it thinned, stagnated, and became destabilized upon entering Prince of Wales Strait.

Prominent flutings composed of clast-poor till span an area ~5 km wide and reach 15 km into the lower De Salis River Valley (Fig. 2.14). The flutings record onshore ice flow from Prince of Wales Strait by a topographically confined

tongue of trunk ice (confined below 50 m asl) that terminated at a series of arcuate, broad-crested push moraines (Fig 2.14).

Elsewhere, ice-shelf moraines commonly trim the coastal plain adjacent to Prince of Wales Strait. At Schuyter Point (Fig. 2.11), nested ice-shelf moraines at 39 m asl occur just below marine limit (40 m asl) and merge with lower, fossiliferous shorelines that mark the relative sea level (37 m asl) in which the ice shelves floated (Fig. 2.11). The ice-shelf moraines flanking the south end of Prince of Wales Strait (Banks Island coast) are oriented NE-SW and display broad crests composed of well-sorted sand and pebble-granules displaying load structures indicative of subaqueous deposition (Fig. 2.12c). Ice-shelf moraines in the lower Treadwell Valley and south of De Salis Bay also occur below marine limit, recording the grounding of ice shelves abutting the coastline either during initial deglaciation or during a later readvance when relative sea level had fallen below marine limit.

Three fragments of *A. borealis* collected from till on the coastal plain (above marine limit) dated 27,258 ± 381 cal yr BP (UCI-55265, Table 2.3), 33,540 ± 457 cal yr BP (UCI-89673; Table 2.3) and 38,709 ± 870 cal yr BP (UCI-89675; Table 2.3). Another fragment of *H. arctica* at the same site dated 43,566 ± 1067 cal yr BP (UCI-89677; Table 2.3). The youngest date (~27,000 cal yr BP) provides the best maximum age estimate for deposition of the Jesse moraine belt, whereas the ice shelf moraines, nested within this margin must be younger. Previously, the Jesse moraine belt was assigned to an Early Wisconsinan

glaciation (Fig. 2b; Vincent, 1982) but this must now be revised to the Late Wisconsinan based on the redeposition of shells dated to MIS 3.

2.2. RAISED MARINE LANDFORMS AND SEDIMENTS

2.2.1. Pre-Late Wisconsinan

Erosion of the west coast of Banks Island has exposed sequences of locally glaciotectonized sand and silt (up to 9 m thick) overlain by undisturbed gravel beaches (11-15 m asl). The overlying beaches can be traced back to a Late Wisconsinan ice margin and are interpreted to record deglacial marine limit. Two samples of glaciotectonized sand (2-3 m asl) were collected at Kellett Point, and an additional sample of apparently undisturbed sand (2-3 m asl) was collected at Worth Point for OSL dating (Fig. 2.4). The two samples at Kellett Point provide concordant OSL burial ages of 94 ± 4.6 ka BP and 94 ± 4.2 ka BP whereas the sample from Worth Point dated 98 ± 4.7 ka BP (Table 2.4). These OSL dates support a marine transgression during MIS 5, following the Sangamonian Interglacial (130 – 115 ka BP; Bradley, 1999). Glaciotectonism of MIS 5 marine sediments support a subsequent ice advance beyond southwest Banks Island and onto the polar continental shelf.

Raised shorelines, both beaches and less frequent ice-contact deltas, mark marine limit across southern Banks Island (Fig 2.4). At several sites, these shorelines are mantled, and immediately underlain by reworked (fragmented) shells. The shells predominantly belong to the species *A. borealis*, but include a diverse taxonomic assemblage unreported from deglacial beaches elsewhere in the western CAA (dominated almost exclusively by *H. arctica*). For example, at

Kellett Point, a discrete, fossiliferous bed immediately beneath the beach marking marine limit includes fragments of *A. borealis, Mya arenaria, Thyasira gouldi,* and *Portlandia arctica,* (Alec Aitken, pers. comm, 2009). This range of species likely reflects the admixing of shells entrained from surrounding marine channels by the advancing LIS prior to their redeposition on Banks Island. A fragment of *M. arenaria* from this discrete bed is at the uppermost limit of accurate radiocarbon dating and cannot be calibrated (UCI-54183; Table 2.1). However, reworked shells collected across western Banks Island by Lakeman and England (2013) and McNeely and Jorgensen (1992) date consistently to MIS 3, possibly recording redeposition by Late Wisconsinan ice.

2.2.2. Late Wisconsinan

Marine limit shorelines and beaches across southern Banks Island conform to a single gradient, rising progressively from the Beaufort Sea to Prince of Wales Strait (Fig. 2.4). The elevation of marine limit also rises northward along the southwest coast, from 11 m asl at Kellett Point to 15 m asl at Lennie River (across 40 km; Fig. 2.4). Marine limit is demarcated on the southwest coast by deglacial meltwater channels that terminate at a prominent, gravel beach barren of fossils. Interestingly, the lateral migration of the sandurs within the major east-west trending river valleys (former outwash channels) have eroded earlier outwash terraces (including marine limit) throughout the Holocene when these valleys were eventually incised below modern sea level as forced regression continued to an unspecified and undated lowstand offshore. Lateral erosion and downcutting is attributed to the large catchment areas of the outwash valleys, which supplied

vigorous braided streams until retreating Laurentide ice withdrew eastward across the island's drainage divide (the crest of the Jesse moraine belt) bordering Prince of Wales Strait (Fig. 2.4). Consequently, from initial deglaciation of the west coast until final deglaciation of the east coast outwash incised the landscape as net glacial emergence progressed. Based on the low marine limit around Kellett Point (11 m asl) it is inferred that relative sea level would have rapidly regressed offshore (within a few hundred years) given conservative estimates on the rate of initial emergence (≥3-5 m/100 years; Andrews 1970; Dyke and Peltier 2000). A similar conclusion has been reached concerning the deglacial and postglacial record of west-central Banks Island (Lakeman and England, 2013) and other areas of the western CAA (Nixon et al., in press). All of these areas are currently experiencing a prominent, modern transgression from the Holocene lowstand.

Marine limit displays a conspicuous eastward rise across southern Banks Island, from 11 m asl at Kellett Point to 26 m asl around the Durham Heights at the island's southeast corner (Fig. 2.4). At intermediate sites along the south-central coast of Banks Island, marine limit reaches ~20 m asl, marked by washing limits and graded outwash. For example, in the Atitok Valley (immediately east of the Masik Valley), marine limit is marked by a transition from prominently kettled outwash fans at 37 m asl to well-rounded and sorted littoral sand and gravel that form an accordant terrace at 24 m asl (T1 in Fig. 2.15). A series of lower terraces at 16 m asl, 13 m asl, and 9 m asl persevered in the lower Atitok and Masik valleys document the glacioisostatically-forced regression (Fig. 2.15). On the opposing (west) side of the lower Masik Valley, horizontal ice-shelf

moraines are sub-parallel to Amundsen Gulf with short flutings (< 2 km) extending beyond them below 10 m asl (Fig. 2.15). The flutings are interpreted to record scouring by icebergs calved from the ice shelf into a similar marine limit (24 m asl). Farther east, marine limit is marked by beaches fringing ~50 km of the Durham Heights at 24 – 26 m asl (Fig. 2.4). The uniformity of marine limit across ~50 km may record the persistence of an ice shelf in Amundsen Gulf that prevented rapid establishment of marine limit. Northward from the Durham Heights, along Prince of Wales Strait, marine limit rises progressively from 25 m asl to 40 m asl at Schuyter Point (north of Cape Treadwell; Fig. 2.4).

North of the Nelson River, the coastal plain contains the first occurrence of fossiliferous marine deposits in growth position noted across southern Banks Island, between this locality and Kellett Point (~200 km, Fig. 2.4). The marine deposits occur as beaches and ice-contact deltas on coastal interfluves or as flights of beaches within low-lying areas. Nineteen new samples of *H. arctica* and one new sample of *Cyrtodaria kurriana* were collected from these deposits across 200 km (Fig 2.3). All shell dates fall between 12,160 ± 260 cal yr BP (UCI-68629) and 12,770 ± 195 cal yr BP (UCI-68619; Table 2.5) and indicate that final deglaciation of the southeast coast was rapid, centred on 12,600 cal yr BP. This rapid ice retreat across 200 km likely records the destabilization of marine-based Laurentide ice that underwent a transition from a grounded to a floating margin within Prince of Wales Strait.

The presence versus absence of shell-bearing marine sediments on Banks Island displays a consistent pattern whereby shells are absent in relation to marine

limit across the entire western half of the island and only appear, perhaps initially following the establishment of marine limit (e.g. in Mercy Bay, north-central Banks Island; J. England, pers. comm, 2013) or in concert with it (Prince of Wales Strait; England et al., 2009; Lakeman and England, 2012). Throughout Banks Island, the oldest shells currently dated are ~ 13,750 cal yr BP (in Mercy Bay), and these are interpreted to record the re-entry of Pacific water and the first re-establishment of marine molluscs along the retreating margin of the northwest LIS (England and Furze 2008; England et al., 2009). Consequently, marine shells become progressively younger with distance eastwards from Mercy Bay, following the retreating Laurentide ice margin southwards to central Prince of Wales Strait where the youngest deglacial shells are ~12,600 cal yr BP (England et al., 2009; Lakeman and England, 2012; This study).

Differential emergence across northern Banks Island, based on the gradient of marine limit alone, reaches 49 m (England et al., 2009) – almost double the amount of 26 m reported here across southern Banks Island. Furthermore, marine limit on northeast Banks Island reaches 60 m asl, compared to just 26 m asl on southeast Banks Island. The greater total *and* differential emergence on northern Banks Island is most simply explained by thicker ice occupying M'Clure Strait during the last glaciation vs. that in Amundsen Gulf during the same interval. This is unsurprising given the available catchment area for M'Clure Strait, which extended into the central CAA where ice supply from the Keewatin ice dome could have been bolstered by dispersal from the lowland sector of the IIS to the north (England et al., 2006) as well as from a nearby

Laurentide ice divide over the Shaler Mountains on northwest Victoria Island (Hodgson, 1994; Stokes et al., 2009; Lakeman and England 2012). By contrast, the catchment area for Amundsen Gulf was likely more distant, presumably extending back into the Keewatin Ice Dome on the Canadian mainland (Stokes et al., 2005, 2006). Lower emergence on southern Banks Island may also reflect a shorter interval of ice cover compared to northern Banks Island.

2.2.3. Holocene

The postglacial relative sea level history of southern Banks Island is dominated by relative sea level rise. Submergence of Banks Island in response to eustatic sea level rise continues today, as documented by drowned tundra, beaches, spits, river valleys and kettle lakes that trim the coastline (Fig. 2.16). Dominating this trend is the collapse and migration of a glacial forebulge back towards the regional centre of glacial loading on the mainland (Dyke and Peltier, 2000). The current position of the forebulge coincides with the crest of the modern zero isobase; a theoretical line separating areas of net transgression from net regression (Walcott, 1970). Geophysical modelling places the zero isobase on Prince Albert Peninsula, Victoria Island, and in Viscount Melville Sound, east of Melville Island (Peltier, 2004). Recent observations of submergence across all of Melville Island confirm the migration of the zero isobase into Viscount Melville Sound (Lajeunesse and Hanson, 2008; Nixon et al., in press). The glacial and relative sea level history of Banks Island presented here demonstrates that the island is on the submerging side of the zero isobase, therefore precluding future glacioisostatic rebound (Dyke and Peltier, 2000).

3. REVISED GLACIAL MODEL

3.1. Advance

Evidence from southern Banks Island supports coalescent terrestrial and marine-based ice of the northwest LIS that subsumed the region and extended onto the polar continental shelf after ~24,000 cal yr BP. This supplants the previous model that had proposed island-wide, ice-free conditions during the LGM (Vincent, 1982, 1983, 1984). New fieldwork indicates that cold-based ice flowed westward across the interior while confluent marine-based ice occupied western Amundsen Gulf, likely as an ice stream (Blasco et al., 1990, 2005; Stokes et al., 2005, 2006, 2009). Mafic and carbonate erratics deposited at elevations up to 730 m asl on the Durham Heights indicate that the ice stream was at least 1 km thick in the lower reaches of Amundsen Gulf, reinforcing its extension to the continental shelf edge and providing new volumetric constraints on ice export from the northwest LIS (Jakobsson et al., in press). Geochemical analyses and U-Pb dating of mafic erratics on the Durham Heights support a trajectory for the Amundsen Gulf Ice Stream that flowed westward across the Minto Inlier on Victoria Island. This ice may have ben supplied from a local divide on Victoria Island and/or from the previously identified M'Clintock Ice Divide that ran north-south along M'Clintock Channel farther east (Fig. 2.17; Dyke and Prest, 1987). Widespread granite erratics mantling the Durham Heights also require dispersal from the more distant Precambrian Shield of mainland Canada, possibly prior to the entrainment of mafic erratics on Victoria Island by the Amundsen Gulf Ice Stream (Stokes et al., 2006). Once established, such a vigorous westward flow

would likely preclude granite-bearing Laurentide ice from reaching the Durham Heights. Elsewhere, the abundance of carbonate erratics within the Jesse moraine belt of eastern Banks Island supports renewed late-glacial ice flow from Victoria Island, occasioned by dispersal from an ice divide over the Shaler Mountains (Fig. 2.17; Stokes, 2005; Lakeman and England, 2012). Observations of widespread Neoproterozoic erratics across the northern Jesse moraine belt, which are similarly sourced from Victoria Island, provide further support for a Shaler Mountain ice divide (Lakeman and England, 2012).

3.2. Deglaciation

Geomorphic evidence (moraines, meltwater channels and a common marine limit) indicates that the retreat of both marine and terrestrial (interior) parts of the northwest LIS occurred in concert across western Banks Island, including the Laurentide margin farther north with which it was contiguous (England et al., 2009; Lakeman and England 2013). This initial retreat from western Banks Island, including Amundsen Gulf, occurred prior to the resubmergence of Bering Strait and the re-entry of Pacific molluscs ~13,750 cal yr BP (England and Furze, 2008; England et al., 2009). Ice sheet withdrawal across southern Banks Island can be subdivided into two phases that correspond to Laurentide retreat previously documented across central and northern Banks Island (Lakeman and England, 2012, 2013).

3.2.1 Beaufort Phase

The earliest Beaufort Phase (Lakeman and England, 2013) was characterized by the steady eastward retreat of the LIS as a thin, cold-based,

lobate margin topographically confined to major east-west river valleys (former outwash channels). Contemporaneous retreat of the Amundsen Gulf Ice Stream was interrupted by periodic onshore flow of this marine-based ice. For example, both the Sachs Moraine and later Sand Hills Moraine belt record readvances of the Amundsen Gulf Ice Stream (then more than 450 m thick) following earlier stabilization in Thesiger Bay (Fig. 2.6). Possible pinning between shallow continental shelves up to 200 m bsl between Thesiger Bay and Cape Bathhurst on the opposing Canadian mainland may have promoted a period of trunk ice stability there (Fig. 2.1). Withdrawal of trunk ice from the earlier Sachs Moraine resulted in the damming of Glacial Lake Mary Sachs (up to 86 m asl) and the westward drainage of Glacial Lake Raddi (up to 120 m asl; Fig. 2.8). The Sand Hills Moraine belt records a second, widespread resurgence of the marine-based ice that drove onshore depositing prominent controlled moraines in a subaqueous environment (a lower stage of Glacial Lake Mary Sachs). In the absence of any evident climatic forcing, this onshore advance is assumed to reflect a re-equilibration of ice flow and ice divides within a marine-based margin (Lakeman and England, 2012). A third period of temporary restabilization of the Amundsen Gulf ice is inferred from the thick gravel foreset beds aggraded to 50 m asl at Cape Lambton, below the Durham Heights (Fig. 2.1). Although shells within deglacial, raised marine beaches were unavailable to date ice retreat from the Banks Island coast of Amundsen Gulf, OSL dates on the opposing Canadian mainland indicate ice-free conditions on the Tuktoyaktuk coast by 14,000 – 16,000 cal yr BP (Murton et al., 2007). Assuming these ages also correspond to

the retreat of ice from the southeast coast of Banks Island, they would reinforce the interpretation that this deglacial sea was barren of fossils as it predated the resubmergence of Bering Strait (England and Furze 2008). Low rates of postglacial hemipelagic sedimentation in western Amundsen Gulf also support low productivity during initial marine incursion (Blasco et al., 2005).

Following the removal of trunk ice abutting the Durham Heights, two cold-based ice lobes retreated northward (inland) and eastward from the Kellett and Masik valleys, bordered above by small plateau ice caps occupying the Durham Heights. Similar eastward retreat characterized withdrawal of cold-based Laurentide ice from the Thomsen Valley on north-central Banks Island and from the eastern end of the M'Clure Strait Ice Stream (Lakeman and England, 2012). This deglacial phase, termed the 'Thomsen Phase', is constrained by deglacial marine shells at the head of Mercy Bay (~13,750 cal yr BP; England et al., 2009) and by shells underlying marine limit in the lower Thomsen Valley (~13,600 cal yr BP: Lakeman and England, 2012). The absence of shells in growth position from deglacial marine sediments across the entire south coast of Banks Island indicates that the Amundsen Gulf Ice Stream had broken-up entirely (adjacent to southern Banks Island) *prior* to the retreat of the M'Clure Strait Ice Stream to Mercy Bay. From Mercy Bay eastward, the raised deglacial shorelines are unfailingly fossiliferous (and younger than 13,500 cal yr BP; England et al., 2009), dismissing previous speculations for an earlier retreat of the M'Clure Strait Ice Stream (Stokes et al., 2009).

3.2.2. Prince of Wales Phase

The Prince of Wales Phase is distinguished by a regional stillstand and/or readvance of Laurentide ice resulting in deposition of the Jesse moraine belt (13,750 – 12,750 cal yr BP; Lakeman and England, 2012). Correlative deposits have been identified on central and northern Banks Island and on the Prince Albert Peninsula on the opposing coastline of Victoria Island (Lakeman and England, 2012). Collectively, the Jesse moraine belt outlines a former glacier occupying Prince Of Wales Strait that terminated in M'Clure Strait as a tidewater margin (Lakeman and England, 2012). The dynamics and glaciological implications of the moraine belt have been well characterized by Lakeman and England (2012), who emphasize its importance for signifying a regional expansion of warm-based thermal regimes in the western CAA in response to a reorganization of ice flow trajectories. This reorganization may have been triggered, in part, by ice sheet drawdown following the early deglaciation of western Amundsen Gulf.

On southern Banks Island, the Jesse moraine belt is similarly prominent, characterized by widespread controlled moraines on the inland plateau, augmented by upslope advance across the interior plateau north of the Durham heights. A high percentage of carbonate clasts within the Jesse moraine belt support renewed ice flow from a lateglacial ice divide over the Shaler Mountains (Lakeman and England, 2012). Strong onshore flow across southeastern Banks Island is recorded in the Nelson River Valley where the Jesse moraine belt extends 30 km inland, reaching ~400 m asl. This vigorous advance suggests that

the ice from Victoria Island was augmented by westward flow from the Amundsen Gulf Ice Stream, which had remained grounded in central Amundsen Gulf until ~12,600 cal yr BP. On the Canadian mainland, deposition of controlled moraine at Bluenose Lake records slow retreat of grounded ice in south-central Amundsen Gulf (Fig. 2.1; St-Onge and McMartin, 1995, 1999) that has been correlated provisionally with deposition of the Jesse moraine belt based on the overall continuity of the northwest LIS margin (Lakeman and England, 2012). Consequently, it is inferred that the Amundsen Gulf Ice Stream contributed to the Jesse moraine belt on southeast Banks Island as it also did for moraines around Bluenose Lake (east of the Brock Inlier) during this interval (Fig. 2.1). This retreating, marine-based ice stream would have been highly unstable, comprising a calving margin spanning the widest part of Amundsen Gulf (>200 km).

Across southeast Banks Island, glacial landforms document subsequent downslope wastage of digitate Laurentide ice confined to the main coastal valleys where arcuate moraines are prominent. Final ice retreat from southeast Banks Island involved the thinning of an oscillatory margin that deposited conical kames and kame terraces along the coast. A rapid transition from grounded to floating ice is recorded by horizontal ice-shelf moraines trimming the coastline below marine limit. Twenty new deglacial shell dates document the establishment of marine limit and the transition to nearby ice-shelves in southern Prince of Wales Strait ~12,600 cal yr BP. By comparison, deglaciation of northern Prince of Wales Strait (300 km farther north) occurred only shortly before this (~12,750 cal yr BP; Lakeman and England, 2012). Along the length of the Strait, error bars on

deglacial radiocarbon dates produce overlapping ages indicating that this rate of ice removal is unresolvable.

4. DISCUSSION

4.1. Configuration of the northwest Laurentide Ice Sheet during the last glacial maximum

New evidence for the advance of the northwest LIS beyond southern Banks Island and onto the polar continental shelf during the last glaciation is consistent with widespread reports for coalescent and pervasive Innuitian and Laurentide ice sheets occupying the western CAA during the LGM (Blake 1970; England et al., 2006, 2009; Stokes et al., 2005, 2006, 2009; Lakeman and England, 2012). Similarly, the northwest LIS also attained its maximum (all-time) limit farther south, entering the Richardson Mountains and Peel Plateau where it impounded Glacial Lake Old Crow in the Yukon interior, as well as subsuming the Mackenzie Delta and Yukon Coastal Plain (Mackay, 1959; Hughes, 1972; Morlan et al., 1990; Duk-Rodkin and Hughes, 1991; Murton et al., 1997; Dyke et al., 2002; Zazula et al., 2004; Bateman and Murton, 2006; Kennedy et al., 2010; Fritz et al., 2012). The vigorous export of thick Laurentide ice into the Arctic Ocean during the LGM is also supported by deep draft glaciogenic erosion on the floor of the Arctic Ocean (Polyak et al., 2001, 2007; Engels et al., 2008; Jakobsson et al., 2008, 2009, in press; Dove et al., 2013).

South of Banks Island, around the Mackenzie delta and southern Beaufort Sea, the last advance of the northwest LIS has been constrained to the Late

Wisconsinan, postdating 21,000 cal yr BP (Murton et al., 1997; Bateman and Murton, 2006; Murton et al., 2007), and possibly as late as ~16,200 cal yr BP (Fritz et al., 2012) to ~14,000 cal yr BP (Murton et al., 1997). Although the youngest limiting date for the latest passage of Laurentide ice across southern Banks Island is ~24,000 cal yr BP, it is likely that this advance occurred in concert with that on the adjacent mainland, as the northwest LIS would have been supplied by the same regional ice dispersal centre over Keewatin (Dyke and Prest, 1987; Tarasov and Peltier, 2004; Doornbos et al. 2009). This late advance of the northwest LIS contrasts with most of its other margins, which had already attained their maximum extent and were undergoing deglaciation by 19,000 cal yr BP (Clark et al., 2009). Asynchronous glacial advance may have been governed by moisture delivery, which increased after the LIS reached a critical size and diverted a northern branch of the jet stream to the High Arctic (Bromwich et al., 2004).

Widespread, coast-parallel striae and streamlined bedrock (Glenelg Fm) on southern Banks Island confirm the former presence of the Amundsen Gulf Ice Stream that reached at least 1000 m thick along the southern flank of the Durham Heights (Fig. 2.4). Up-ice (farther east), fast flow landforms mapped on Victoria Island and the opposing Canadian mainland (spanning 400 km from Coronation Gulf to Cape Bathurst) converge towards central Amundsen Gulf where megascale glacial lineations on the channel floor demonstrate that the ice stream was fed by a large catchment (Fyles, 1963; Blasco et al., 1990, 2005; Stokes et al., 2005, 2006, 2009). Furthermore, seismic analyses of western Amundsen Gulf

indicate that a series of stratigraphic units - interpreted as stacked till sheets - extend to the continental shelf edge and feed into a trough mouth fan containing a minimum of 10,000 km^3 of glaciogenic debris (Blasco et al., 1990, 2005; Batchelor et al., 2012, in press; MacLean et al., 2012). Transverse moraines superimposed over the stacked till sheets are interpreted to record deglacial back stepping of the marine-terminating margin (Lakeman et al., 2013). Evidence for iceberg keel scour-marks to depths of 350 – 450 m bsl on the seabed distal to Amundsen Gulf, notably on the Chukchi shelf and rise, as well as the Northwind Ridge, likely record primary mass loss through calving of deep draft icebergs from the Amundsen Gulf Ice Stream and other marine margins of the western CAA during retreat (Fig. 2.18; Polyak et al., 2001, 2007; Engels et al., 2008; Jakobsson et al., 2008, 2009, in press; Dove et al., 2013). Ice at least 1000 m thick in western Amundsen Gulf, reported here, provides an identifiable source for the erosive ice that scoured at least the Amerasian side of the Arctic Ocean (west of the Lomonosov Ridge).

4.2. Dynamics of the northwest Laurentide Ice Sheet during deglaciation

The early withdrawal of the Amundsen Gulf Ice Stream (14,000 – 15,000 cal yr BP) preceded retreat of the M'Clure Strait Ice Stream (~13,750 cal yr BP, England et al; 2009). This earlier retreat through Amundsen Gulf, from the continental shelf to southeast Banks Island, would have removed ~60,000 km^2 of ice – constituting the most significant mass loss from the northwest LIS prior to ~13,750 cal yr BP, when molluscs re-entered the western CAA via Bering Strait. Based on this chronology, the removal of Laurentide ice from Amundsen Gulf,

and possibly the retreat of its margin both to the north and south, approximates the timing of meltwater pulse 1A (MWP-1A) - the abrupt 20 m rise of global sea level over ~500 yrs, centred on 14,600 cal yr BP (Carson, 2009). Previous geophysical models addressing former ice sheet contributions to MWP-1A have predominantly identified the Antarctic Ice Sheet as the primary contributor to this sea level rise, though several reconstructions recognize that the LIS may have contributed 5-10 m (Tarasov and Pelier, 2006; Carlson, 2009). Retreat from western Amundsen Gulf now provides support for an LIS contribution, as does independent evidence for a freshwater spike in Arctic Ocean sediment cores during MWP-1A (Poore et al., 1999). Moreover, proceeding mass loss from western Amundsen Gulf would have triggered ice sheet drawdown from its dispersal centre and possibly contributed to its reconfiguration, involving either the M'Clintock Ice Divide on Victoria Island (Dyke and Prest, 1987) or a preceding LGM divide running east-west across Keewatin (Fig. 2.17; Tarasov and Peltier, 2004; Doornbos et al. 2009). Drawdown of ice into Amundsen Gulf from the Canadian mainland may also have reduced westward ice flow to the Yukon and Northwest Territories, facilitating the early withdrawal of ice recorded there (e.g. Murton et al., 1997; Zazula et al., 2009). The resultant thinning of the regional ice divide would likely have reduced westward dispersal both to the interior of Banks Island (where ice was thin and topographically confined), and to M'Clure Strait where subsequent deglaciation (~13,500 cal yr BP) was rapid (Fig. 2.17; Stokes et al., 2009; England et al., 2009; Lakeman and England 2012). Initial retreat of the northwest LIS involved removal primarily by calving of two

prominent ice streams in Amundsen Gulf and M'Clure Strait that gave way to ice shelves as thinning progressed in these deep channels. The ice and sediment volume from these former ice streams, up to 1 km thick, far exceeded the contribution made by the retreat of the much thinner, cold-based terrestrial ice that had crossed Banks Island previously. Consequently, the unconfined marine-terminating margins are inferred to have been the primary instigators of ice sheet disintegration in the western CAA.

New deglacial dates from southern Prince of Wales Strait indicate final ice retreat from Banks Island by ~12,600 cal ka BP (this paper). These dates can be compared to those from Diamond Jenness Peninsula and Wollaston Peninsula on the adjacent coast of southwest Victoria Island (Fig. 2.1; Dyke and Savelle, 2000; Dyke et al., 2003) that have been calibrated to 12,730 cal yr BP and 12,720 cal yr BP, respectively (Lakeman and England, 2012). These dates are concordant with a deglacial date from Darnley Bay, central Amundsen Gulf, on the Canadian mainland (Fig. 2.1; 12,770 cal yr BP; Lakeman and England, 2012; Dyke et al., 2003). The mean ages and standard errors on these deglacial dates provide ages that are statistically indistinguishable, supporting rapid (essentially instantaneous) ice evacuation from central and eastern Amundsen Gulf. This removal is also recorded in marine sediments flooring western Amundsen Gulf, where an abrupt spike in mean grain size, magnetic susceptibility, and inorganic carbon content has been dated between 12,620 cal yr BP and 12,655 cal yr BP (Scott et al., 2009). This large-scale break-up may have been in response to a global trigger, such as eustatic sea level rise or climatic amelioration throughout the proceeding Bølling-

Allerød chronozone (Alley, 2000; Peltier, 2002). Regardless, the isochronous removal of at least 45,000 km^2 of ice from central and eastern Amundsen Gulf would have triggered an equally abrupt adjustment throughout the remaining northwest LIS, leaving its land-based margins in a position to restabilize (Dyke and Savelle, 2000).

Widespread surveys of deglacial marine limit across the entire south coast of Banks Island, and northward up the west coast from Kellett Point (Fig. 2.4) are fully compatible with the previously published, island-wide gradient that show substantial glacial unloading, rising eastward, following retreat of a pervasive Late Wisconsinan LIS (England et al., 2009; Lakeman and England 2012, 2013). Despite low marine limit elevations across southwestern Banks Island (facing the Beaufort Sea; i.e., 11-15 m asl), this postglacial rebound includes a substantial (countering) eustatic rise of ≥80 m, which makes uplift along the former northwest LIS margin >90-120 m asl, comparable to the rebound along the northeast LIS margin on eastern Baffin Island (Dyke and Prest, 1987). Deglacial marine limits are barren throughout southern, western and northwestern Banks Island as ice retreat occurred in contact with a mollusc-free Arctic Ocean prior to the resubmergence of Bering Strait (~13,750 cal yr BP; England and Furze 2008). In these areas the re-entry of the fauna occurred after relative sea level regressed offshore en route to its Holocene lowstand. Across northeastern and eastern Banks Island, later deglaciation (~12,700 cal yr BP) combined with greater glacioisostatic unloading resulted in deglacial shorelines that had become both shell-bearing and elevated well above modern sea level (20-60 m asl). This

greater postglacial emergence towards the east records increasing proximity to the former dispersal centres for the western CAA located either in Keewatin (Dyke and Prest, 1987; Tarasov and Peltier 2004; Doornbos et al 2009) or on/adjacent to Victoria Island (Dyke and Prest 1987; Stokes et al., 2009; Lakeman and England, 2012). Notwithstanding the differential rebound across Banks Island, all areas are today are experiencing an ongoing marine transgression from their Holocene lowstand.

5. CONCLUSIONS

This study revises the long-standing, glacial history of southern Banks Island by documenting the advance of coalescent marine and terrestrial margins of the northwest LIS that subsumed the highest topography on the island (< 730 m asl) en route to the polar continental shelf during the LGM. New constraints are placed on the thickness of ice evacuated through western Amundsen Gulf that identify a source for deep-draft (>450 m thick) iceberg delivery to the Arctic Ocean where glaciogenic scouring of the seabed has been documented during the LGM (e.g. Polyak et al., 2001, 2007; Engels et al., 2008; Jakobsson et al., 2008, 2009, in press). Moreover, the analysis of marine limit gradients and the conspicuous absence of shells in growth position within all emergent marine deposits along the 200 km coastline of southern Banks Island require that the Amundsen Gulf Ice Stream retreated to southeast Banks Island prior to the re-entry of Pacific fauna ~13,750 cal yr BP. This retreat predated removal of the M'Clure Strait Ice Stream abutting northern Banks Island – contributing to an improved understanding of the paleotopography and deglacial dynamics of the

northwest LIS that warrants further assessment by glaciological modelling to assess its possible impacts on ice sheet reconfiguration. Observations pertaining to the style of ice withdrawal from Amundsen Gulf indicate that the grounded ice stream was characterized by at least two, separate onshore readvances, depositing the Sachs Moraine and later Sand Hills Moraine belt. The removal of approximately 60,000 km^2 of ice from western Amundsen Gulf constitutes the earliest large-scale retreat of the LIS that is chronologically aligned with MWP-1A, raising the possibility that this retreat contributed to it. Early retreat of the Amundsen Gulf Ice Stream would have also triggered drawdown from the primary northwest LIS divide, possibly instigating changes to its paleotopography and hence, subsequent ice-flow trajectories. This study also provides chronologic control for the abrupt and widespread deglaciation across southeast Banks Island and eastern Amundsen Gulf, (~12,600 cal yr BP) documenting the final collapse of the Amundsen Gulf Ice Stream (Dyke and Savelle, 2000; Dyke et al., 2003; Lakeman and England, 2012).

Collectively, this record highlights several new observations documenting: the extent and history of the northwest LIS in the western CAA, including its impact upon Arctic Ocean sedimentation and seafloor scouring; the deglacial dynamics of the northwest LIS that was dominated by marine-terminating margins that formed both ice streams and ice shelves; and the pattern of glacioisostatic crustal readjustments relevant to geophysical modelling throughout an area where postglacial emergence had been unrecognized. This revised glacial and relative sea level record represents the final contribution to an island-wide,

Quaternary survey previously reported for central and northern Banks Island (England et al., 2009; Lakeman and England, 2012). Collectively, these reconstructions fundamentally revise the formerly proposed model of multiple glaciations and sea level adjustments (Vincent, 1982, 1983).

6. REFERENCES

Aber, J.S. 1985. The nature of glaciotectonism. Geologie en Mijnbouw. 64, 389-395.

Alley, R. 2000. Ice-core evidence of abrupt climate changes. Proceedings of the National Academy of Sciences of the United States of America. 97, 1331-1334.

Andews, J.T. 1970 A Geomorphological Study of Post-glacial Uplift with Particular Reference to Arctic Canada. Institute of British Geographers, Alden Press, Oxford.

Bamber , J., Riccardo, E.M.R., Vermeersen, B.L.A., LeBrocq, A.M. 2009. Reassessment of the Potential seal-level rise from a collapse of the West Antarctic Ice Sheet. Science. 324, 901-903.

Barendregt, R.W., Vincent, J-S., Irving, E., Baker, J. 1998. Magnetostratigraphy of Quaternary and Late Tertiary sediments on Banks Island, Canadian Arctic Archipelago. Canadian Journal of Earth Sciences. 35, 147-161.

Batchelor, C.L., Dowdeswell, J.A., Pietras, J.T. Evidence for multiple Quaternary ice advances and fan development from the Amundsen Gulf cross-shelf trough and slope, Canadian Beaufort Sea Margin. Marine and Petroleum Geology. In press.

Bateman, M.D., Murton, J.B. 2006. The chronostratigraphy of Late Pleistocene glacial and periglacial aoelian activity in the Tuktoyaktuk coastlands, NWT, Canada. Quaternary Science Reviews. 25, 2552-2568.

Benn, D. I., Evans, D.J.A. 2010. Glaciers and Glaciation. Hodder Education, England.

Blake, W., Jr. 1970. Studies of glacial history in Arctic Canada. Canadian Journal of Earth Sciences. 7, 634-644.

Blasco, S. M., Fortin, G., Hill, P.R., O'Connor, M.J., and Brigham- Grette, J., 1990. The late Neogene and Quaternary stratigraphy of the Canadian Beaufort continental shelf, In The Arctic Ocean Region. The Geology of North America, Vol. L, Grantz, A., Johnson, L., Sweeney, J. F., (Eds): Geological Society of America: Boulder, Colorado. 491–502.

Blasco, S., Bartlett, J., Bennett, R., Hughes-Clark, J., Maclean, B., Scott, S., Sonnichsen, G. 2005. Northwest Passage marine sediments: a record of Quaternary history and climate change. Arctic Workshop abstract, March 9th-12th, University of Alberta, Edmonton, Canada.

Bradley, R.S. 1999. Paleoclimatology: Reconstructing climates of the Quaternary. Academic Press. Sandiego.

Bromwich, D.H., Toracinta, E.R., Wei, H., Oglesby, R.J., Fastook, J.L., Hughes, T.J. 2004. Polar MM5 Simulations of the Winter Climate of the Laurentide Ice Sheet at the LGM. Journal of Climate. 17, 3415-3433.

Clark, D.L., Vincent, J-S., Jones, G.A., Morris, W.A. 1984. Correlation of marine and continental glacial and interglacial events, Arctic Ocean and Banks Island. Nature. 311, 147-149.

Bradley, R.S., England, J.H. 2008. The Younger Dryas and the Sea of Ancient Ice. Quaternary Research. 70, 1-10.

Carlson, A.E. 2009. Geochemical constraints on the Laurentide Ice Sheet contribution to meltwater pulse 1A. Quaternary Science Reviews. 28, 1625-1630.

Clark, P.U., Dyke, A.S., Shakun, J.D., Carlson, A.E., Clark, J., Wohlfarth, B., Mitrovica, J.X., Hostetler, S.W., McCabe, A.M. 2009. The Last Glacial Maximum. Science. 325, 710, 714.

Coulthard, R.D., Furze, M.F.A., Pienkiwski, A.J., Nixon, F.C., England, J.H. 2010. New marine ΔR values for Arctic Canada. Quaternary Geochronology. 5, 419-434.

Craig, B.G., Fyles, J.G. 1960. Pleistocene geology of Arctic Canada. Geological Survey of Canada. Paper 60-10.

Darby, D.A., Bischof, J.F., Speilhagen, R.F., Marshall, S.A., Herman, S.W. 2002. Arctic ice export events and their potential impact on global climate during the late Pleistocene. Paleoceanography. 17, 1-17.

Doornbos, C., Heaman,L., Doupé, J. P., England, J. H., Simonetti, A. and Lajeunesse. P. 2009. The first integrated use of *in growth position* U-Pb geochronology and geochemical analyses to determine long-distance transport of erratics, from mainland Canada to the western Canadian Arctic Archipelago. Canadian Journal of Earth Sciences. 46, 101-122.

Dove, D., Polyak, L., Coakley, B. Widespread, multi-source glacial erosion on the Chukchi margin of the Arctic Ocean. Quaternary Science Reviews. In press.

Duk-Rodkin, A. and Hughes, O. L. 1991. Age relationships of Laurentide and montane glaciations, Mackenzie Mountains, Northwest Territories. Géographie physique et Quaternaire. 45, 79-90.

Dyke, A.S. 1986. A reinterpretation of glacial and marine limits around the northwestern Laurentide Ice Sheet. Canadian Journal of Earth Sciences. 24, 591-601.

Dyke, A.S. 2004. An outline of the deglaciation of North America with emphasis on central and northern Canada. In: Ehlers, J., Gibbard, P.L (Eds), Quaternary Glaciations, Extent and Chronology. Part II. North America. Developments in Quaternary Science, vol 2b. Elsevier, Amsterdam.

Dyke, A. S. and Prest, V. K. 1987. Late Wisconsisnan and Holocene history of the Laurentide Ice Sheet. Géographie physique et Quaternaire. 41, 237-263.

Dyke, A.S., Savelle, J.M. 2000. Major end moraines of Younger Dryas age on Wollaston Peninsula, Victoria Island, Canadian Arctic: implications for paleoclimate and for formation of hummocky moraine. Canadian Journal of Earth Sciences. 37, 601-619.

Dyke, A.S., Peltier, W.R. 2000. Forms, response times and variability of relative sea-level curves, glaciated North America. Geomorphology. 32, 315-333.

Dyke, A. S. Andrews, J. T. A., Clark, P. U., England, J. H., Miller, G. H., Shaw, J., & Veillette, J. J. 2002. The Laurentide and Innuitian ice sheets during the Last Glacial Maximum. Quaternary Science Reviews. 21, 9-31.

Dyke, A.S., Moore, A., Robertson, L. 2003. Deglciation of North America. In: Geological Survey of Canada, Open File 1574.

England, J.H., Atkinson, H., Bednarski, J., Dykes, A.S., Hodgson, D.A., O Cofaigh, C. 2006. The Innuitian Ice Sheet: configuration, dynamics and chronology. Quaternary Science Reviews. 28, 1573-1596.

England, J.H., Furze, M.F.A. 2008. New evidence from the western Canadian Arctic Archipelago for the resubmergence of Bering Strait. Quaternary Research. 70, 60-67.

England, J.H., Furze, M.F.A., Doupe, J.P. 2009. Revision of the NW Laurentide Ice Sheet: implications for the paleoclimate, the northeast extremity of Beringia, and Arctic Ocean sedimentation. Quaternary Science Reviews. 28, 1573-1596.

Engels, J.L., Edwards, M.H., Polyak, L., Johnson, P.D. 2008. Seafloor evidence for ice shelf flow across the Alaska-Beaufort margin of the Arctic Ocean. Earth Srface Porcesses and Landforms. 33, 1047-1063.

Evans, D.J.A. 2009. Controlled moraines: origins, characteristics and paleoglaciological implications. Quaternary Science Reviews. 28, 183-208.

Evans, D.J.A., England, J. 1991. Canadian landform examples 19, high arctic thrust block moraines. Canadian Geographer. 35, 93-97.

Evans, D.J.A., England, J.H., LaFarge. C., Coulthard, R., Lakeman, T. Quaternary geology of the Duck Hawk Bluffs, southwest Banks Island, Arctic Canada: a re-investigation of a critical terrestrial type locality for glacial and

interglacial events around the Arctic Ocean. Submitted to Quaternary Science Reviews.

French, H.M. 1972. The proglacial drainage of northwest Banks Island. The Musk-Ox. 10, 26-31.

French, H.M., Harry, D.G., Clark, M.J. 1982. Ground ice stratigraphy and late-Quaternary events, southwest Banks Island, Canadian Arctic. Climate and Permafrost. 81-90.

Fritz, M., Wetterich, S., Schirrmeister, L., Meyer, H., Lantuit, H., Preusser, F., Pollard, W.H. 2012. Eastern Beringia and beyond: Late Wisconsinan and Holocene landscape dynamics along the Yukon Coastal Plain, Canada. Palaeogeography, Palaeoclimatology, Palaeoecology. 319, 28-45.

Fyles, J.G. 1962. Phsiography. In: Thorsteinssonm R., Tozer, E.T. Banks, Victoria, and Steffansson Island, Arctic Archipelago. Geological Survey of Canada. Memoir 330, 8-17.

Gajewski, K., Mott, R. J., Ritchie, J. C. & Hadden, K. 2000. Holocene vegetation history of Banks Island, Northwest Territories, Canada. Canadian Journal of Botany. 78, 430-436.

Good, T.R., Bryant, I. D. 1985. Fuvio-aeolian sedimentation – An example from Banks Island, N.W.T., Canada. Geografiska Annaler. 67 A, 1-2.

Harlan, S.S., Heaman, L., LeCheminant, A.N., Premo, W.R. 2003. Gunbarrel Mafic Magmatic Event: A key 780 Ma marker for Rodinia Plate Reconstructions. Geology. 31, 1053-1056.

Harrington, C. R. 2005. The eastern limit of Beringia: mammoth remains from Banks and Melville islands, Northwest Territories. Arctic. 58, 361-369.

Hobbs, W.H. 1945. The boundary of the latest glaciation in Arctic Canada. Science. 101, 549-551.

Hodgson, D.A. 1994. Episodic ice streams and ice shelves during retreat of the northwesternmost sector of the Late Wisconsinan Laurentide Ice Sheet over the central Canadian Arctic Archipelago. Boreas. 23, 14-28.

Hodgson, D.A., Vincent, J-S. 1984. A 10,000 yr BP extensive ice shelf over Viscount Melville Sound, Arctic Canada. Quaternary Research. 22, 18-30.

Hodgson, D.A., Vincent, J.-S., Fyles, J.G., 1984. Quaternary geology of central Melville Island. In: Geological Survey of Canada, Paper 83–16.

Hollin, J.T., Barry, R.G. 1979. Emprical and theoretical evidence concerning the response of the Earth's ice and snow cover to a global temperature increase. Environmental International. 2, 437-444.

Hughes, O.L. 1972. Surficial geology of northern Yukon Territory and northwestern District of Mackenzie. Northwest Territories. Geological Survey of Canada. Paper 69-36, 11.

Jakobsson, M., Gardner, J.V., Vogt, P., Mayer, L.A., Armstrong, A., Backman, J., Brennan, R., Calder, B., Hall, J.K., Kraft, B. 2005. Multibeam bathymetric and sediment profiler evidence for ice grounding on the Chukchi Boderland, Arctic Ocean. Quaternary Research. 63, 150-160.

Jakobsson, M., Polyak, L., Edwards, M., Klemen, J., Coakley, B. 2008. Glacial geomorphology of the Central Arctic Ocean: the Chukchi Borderland and the Lominosov Ridge. Earth Surface Processes and Landforms. 33, 526-545.

Jakobsson, M., Nilsson, J., O'Regan, M., Backman, J., Löwemark, L., Dowdeswell, J.A., Mayer, L., Polyak, L., Colleoni, F., Anderson, L., Björk, G., Darby, D., Eriksson, B., Hanslik, D., Hell, B., Marcussen, C., Sellén, E., Wallin, Å. 2010. An Arctic Ocean ice shelf during MIS 6 constrained by new geophysical and geological data. Quaternary Science Reviews. 29, 3505-3517.

Jakobsson, M., Andreassen, K., Bjarnadóttir, L.R., Dove, D., Dowdeswell, J.A., England, J.H., Funder, S., Hogan, K., Ingólfsson, O., Jennings, A., Krog-Larsen, N., Kirchner, N., Landvik, J.Y., Mayer, L., Moller, P., Niessen, F., Nilsson, J., O'Regan, M., Polyak, L., Petersen, N.N., Stein, R. Arctic Ocean Glacial History. Article in press.

Jenness, J.L. 1952. Problem of glaciation in the western islands of Arctic Canada. Bulletin of Geological Society of America. 63, 939-952.

Kauffman, D.S., Ager, T.A., Anderson, P.M., Andrews, J.T., Bartlein, P.J., Brubaker, L.B., Coats, L.B., Cwynar, L.C., Duvall, M.L., Dyke, A.S., Edwards, M.E., Eisner, W.R., Gakewski, K., Gerisdottir, A., Hu, F.S., Jennings, A.E., Kaplan, M.R., Kerwin, M.W., Lozhkin, A.V., MacDonald, G.M., Miller, G.H., Mock, J.J., Oswald, W.W., Otto-Bleisner, B.L., Porinchu, D.F., Ruhland, K., Smol, J.P., Steig, E.J., Wolfe, B,B. 2004. Holocene thermal maximum in the western Arctic (0-180W). Quaternary Science Reviews. 23, 529-560.

Kennedy, K.E., Friese, D.G., Zazula, G.D., Lauriol, B. 2010. Last Glacial Maximum age for the northwest Laurentide maximum from the Eagle River spillway and delta complex, northern Yukon. Quaternary Science Reviews. 29, 1288-1300.

Kuc, M. 1974. The interglacial flora of Worth Point, western Banks Island. Report of activities, Part B, Geological Survey of Canada. Paper 74-1B, 227-231

Lakeman, T.R., England, J.H. 2012. Paleoglaciological insights from the age and morphology of the Jesse moraine belt, western Canadian Arctic. Quaternary Science Reviews. 47, 82-100.

Lakeman, T.R., England, J.H., 2013. Late Wisconsinan glaciation and postglacial relative sea level change on western Banks Island, Canadian Arctic Archipelago. Quaternary Research. 80, 99-112.

Lakeman, T.R., MacLean, B., Blasco, S., Bennett, R., Hughes Clarke, J.E. 2012. Chronology and dynamics of the Amundsen Gulf Ice Stream in Arctic Canada during the last glacial-interglacial transition. Abstract for the EGU General Assembly, Vienna, Austria.

MacAyeal, D.R. 1992. Irregular oscillations of the West Antarctic Ice Sheet. Nature. 359, 29-32.

Mackay, J.R. 1959. Glacier ice-thrust features of the Yukon Coast. Geographical Bulletin of Canada. 13, 5-21

MacLean, B., Blasco, S., Bennett, R., Lakeman, T., Hughes-Clarke, J., Kuus, P., Patton, E. 2012. Marine evidence for a glacial ice stream in Amundsen

Gulf, Canadian Arctic Archipelago. 42nd Annual Arctic Workshop abstract, March 7th-9th, University of Colorado, US.

Mathews, W.W., Mackay, J.R. 1960. Deformation of soils by glacier ice and influence of pore pressures and permafrost. Transactions of the Royal Society of Canada. 54, 27-36.

McMartin, I., Henderson, P. 2004. Evidence from Keewatin (Central Nunavut) for paleo-ice divide migration. Geographie et Quaternaire. 58, 163-186.

McNeely, R. 1989. Geological Survey of Canada Radiocarbon Dates XXVIII. Geological Survey of Canada Paper 88-7.

McNeely, R., Jorgensen, P.K. 1992. Geological Survey of Canada Radiocarbon Dates XXX. Geological Survey of Canada Paper 90-7.

Morlan, R.E., Nelson, D.E., Brown, T.A., Vogel, J.S., Southon, J.R. 1990. Accelerator mass spectrometry dates on bones from Old Crow, northern Yukon Territory. Canadian Journal of Archaeology. 14, 75-92.

Murray, A.S., Wintle, A.G. 2000. Luminescence dating of quartz using an improved single-aliquot regenerative-dose protocol. Radiation Measurements. 32, 57-73.

Murton, J.B., French, H.M., Lamothe, M. 1997. Late Wisconsinan erosion and eolian deposition, Summer Island area, Pleistocene Mackenzie Delta, Northwest Territories: optical dating and implications for glacial chronology. Canadian Journal of Earth Sciences. 34, 190-199.

Murton, J.B., Bateman, M.D. 2006. The chronostratigraphy of Late Pleistocene Glacial and Periglacial Aeolian Activity in the Tuktoyaktuk Coastlands, NWT, Canada. Quaternary Science Reviews. 25, 2552-2568.

Murton, J.B., Frechen, M., Maddy, D. 2007. Luminescence dating of mid- to Late-Wisconsinan aeolian sand as a constraint on the last advance of the Laurentide Ice Sheet across the Tuktoyaktuk Coastlands, western Arctic Canada. Canadian Journal of Earth Sciences. 44, 857-863.

Nixon, C.F., England, J.H., Lajeunesse, P., Hanson, M.A. Deciphering patterns of postglacial sea level at the junction of the Laurentide and Innuitian Ice Sheets, western Canadian Arctic. Quaternary Science Reviews. In press.

Oppenheimer, M. 1998. Gobal warming and the stability of the West Antarctic Ice Sheet. Nature. 393, 325-332.

Peltier, W.R. 2002. On eustatic sea level history: Last Glacial Maximum to Holocene. Quaternary Science Reviews. 21, 377-396.

Peltier, W.R. 2004. Global Glacial Isostasy and the Surface of the Ice-Age Earth: The ICE-5G (VM2) Model and GRACE. Annual Reviews of Earth and Planetary Sciences. 32, 111-149.

Pissart, A., Vincent, J-S., Edlend, S.A. 1977. Dépots et phénomènes éoliens sur L'ile de Banks, Territories du Nord-Ouest, Canada. Canadian Journal of Earth Sciences. 14, 2462-2480

Polyak, L., Edwards, M.H., Coackley, B.J., Jakobsson, M. 2001. Ice shelves in the Pleistocene Arctic Ocean inferred from glaciogenic deep-sea bedforms. Nature. 410, 453-547.

Polyak, L., Curry, W.B., Darby, D.A., Bischof, J., Cronin, T.M., 2004. Contrasting glacial/interglacial regimes in the western Arctic Ocean as exemplified by a sedimentary record from the Mendeleev Ridge. Palaeogeography Palaeoclimatology Palaeoecology. 203, 73-93.

Polyak, L., Darby, D., Bischof, J., Jakobsson, M. 2007. Stratigraphic constraints on Late Pleistocene glacial erosion and deglaciation of the Chukchi margin, Arctic Ocean. Quaternary Research. 67, 234-245.

Polyak, L., Bischof, J., Ortiz, J., Darby, D., Chappell, J., Xuan, C., Kaufman, D., Loylie, R., Schneider, D., Adler, R. 2009. Late Quaternary stratigraphy and sedimentation patterns in the western Arctic Ocean. Global Planetary Change. 68, 5-17.

Poore, R.Z., Ostermann, L., Curry, W.B., Phillips, R.L. 1999. Late Pleistocene and Holocene meltwater events in the western Arctic Ocean. Geology. 27, 759-762.

Prest, V.K., 1969. Retreat of Wisconsinan and Recent ice in North America. Geological Survey of Canada. Map 1257A, scale 1:5,000,000.

Raudsepp, M. 2009. Provenance of Mainland Erratics on S. Banks Island, NWT. BSc. Thesis. University of Alberta, Canada.

Reimer, P.J., Baillie, M.G.L., Bard, E., Bayliss, A., Beck, J.W., Blackwell, P.G., Bronk-Ramsey, C., Buck, C.E., Burr, G.S., Edwards, R.L., Friedrich, M., Grootes, P.M., Guilderson, T.P., Hajdas, I., Heaton, T.J., Hogg, A.G., Hughen, K.A., Kaiser, K.F., Kromer, B., McCormac, F.G., Manning, S., Reimer, R.W., Richards, D.A., Southon, J.R., Talamo, S., Turney, C.S.M., van der Plicht, J.,

Weyhenmeyer, C.E. 2009. IntCal09 and Marine09 radiocarbon age calibration curves, 0-50,000 years cal BP. Radiocarbon. 51, 1111-1150.

Scott, D.B., Schell, T., St-Onge, G., Rochon, A., Blasco, S. 2009. Foraminiferal assemblage changes over the last 15,000 years on the Mackenzie Beaufort Sea Slope and Amundsen Gulf, Canada: Implications for past sea ice conditions. Paleoceanography. 24, 1-20.

St-Onge, D.A., McMartin, I. 1995. Quaternary Geology of the Inman River Area, Northwest Territories. In: Geological Survey of Canada. Bulletin 446.

St-Onge, D.A., McMartin, I. 1999. La moraine du Lac Bluenose (Territories du nordouest), une moraine a noyau de glace de glacier. Geographie Physique et Quaternaire. 53, 287-295.

Stokes, C.R., Clark, C.D., Darby, D.A., Hodgson, D.A. 2005. Late Pleistocene ice export events into the Arctic Ocean from the M'Clure Strait Ice Stream, Canadian Arctic Archipelago. Global and Planetary Change. 49, 139–162.

Stokes, C.R., Clark, C., Winsborrow, M. 2006. Subglacial bedform evidence for a major palaeo-ice stream in Amundsen Gulf and its retreat phases, Canadian Arctic Archipelago. Journal of Quaternary Science. 21, 300–412.

Stokes, C.R., Clark, C.D., Storrar, R. 2009. Major changes in ice stream dynamics during deglaciation of the north-western margin of the Laurentide Ice Sheet. Quaternary Science Reviews. 28, 721-738.

Stokes, C.R., Tarasov, L. 2010. Ice Streaming in the Laurentide Ice Sheet: a first comparison between data-calibrated numerical model output and geophysical evidence. Geophysical Research Letters, 37.

Stokes, C.R., Tarasov, L., Dyke, A.S. 2012. Dynamics of the North American Ice Sheet Complex during its inception and build-up to the Last Glacial Maximum. Quaternary Science Reviews. 50, 86-104.

Tarasov, L., Peltier., R.W. 2004. A geophysically constrained large ensemble analysis of the deglacial history of the North American ice-sheet complex. Quaternary Science Reviews. 23, 359-388.

Tarasov, L., Peltier, R.W. 2006. A calibrated deglacial drainage chronology for the North American continent: evidence for an Arctic trigger for the Younger Dryas. Quaternary Science Reviews. 25, 659-668.

Vaughan, D.G., Arthern, R. 2007. Why is it hard to predict the future of ice sheets?. Science. 315, 1503-1504.

Vaughan, J.M, England, J.H, Evans, D.J.A. Glaciotectonic deformation and reinterpretation of the Worth Point stratigraphic sequence: Banks Island, NT, Canada. Submitted to Quaternary Science Reviews. In press.

Vincent, J-S. 1982. The Quaternary History of Banks Island, Northwest Territories, Canada. Geographie Physique et Quaternaire. 36, 209-232.

Vincent, J-S. 1983. La geologie du quaternaire et la geomorphologie de L'ile Banks, arctique Canadien. In: Commission Geologique du Canada Memoir 405.

Vincent, J-S. 1984. Quaternary stratigraphy of the western Canadian Arctic Archipelago. In: Fulton, R.J. (ed.), Quaternary Stratigraphy of Canada – A Canadian Contribution to IGCP Project 24. Geological Survey of Canada. 84-10, 87-100.

Vincent, J-S. 1990. Late Tertiary and Early Pleistocene Deposits and History of Banks Island, southwestern Canadian Arctic Archipelago. Arctic. 43, 339-363.

Vincent, J.S., Occhietti, S., Rutter, N., Lortie, G., Guilbault, J-P., De Boutray, B. 1983. The Late Tertiary-Quaternary record of the Duck Hawk Bluffs, Banks Island, Canadian Arctic Archipelago. Canadian Journal of Earth Science. 20, 1694-1712.

Vincent, J-S., Morris, W.A. & Occhietti, S. 1984. Glacial and non-glacial sediments of Matuyama paleomagnetic age on Banks Island, Canadian Arctic Archipelago. Geology. 12, 139-142.

Walker, M. 2005. Quaternary Dating Methods. John Wiley & Sons Ltd. Chichester.

Washburn, A.L. 1947. Reconnaissance geology of portions of Victoria Island and adjacent regions, Arctic Canada. Geological Society of America. Memoir 22, 142.

Weertman, J. 1975. Stability of Antarctic Ice. Nature. 253, 159.

Wilson, J.T., Falconer, G., Mathews, W.H., Presk, V.K. 1958. Glacial Map of Canada. Geological Association of Canada, scale 1:5,000,000.

Worsley, P. 1999. Context of relict Wisconsinan glacial ice at Angus Lake, SW Banks Island, western Canadian Arctic and stratigraphic implications. Boreas. 28, 543-550.

Zazula, G.D., Duk-Rodkin, A., Schweger, C.E., Morlan, R.E. 2004. Late Pleistocene chronology of glacial lake Old Crow and the northwest margin of the Laurentide Ice Sheet. In: Ehlers, J., Gibbard, P.I (Eds.), Quaternary Glaciations – Extent and Chronology, Part II. Elsevier, 347-362.

Zazula, G.D., MacKay, G., Andrews, T.D., Shapiro, B., Letts, B., Brock, F. 2009. A late Pleistocene steppe bison (*Bison priscus*) partial carcass from Tsiigehtchic, Northwest Territories, Canada. Quaternary Science Reviews. 28, 2734-2742.

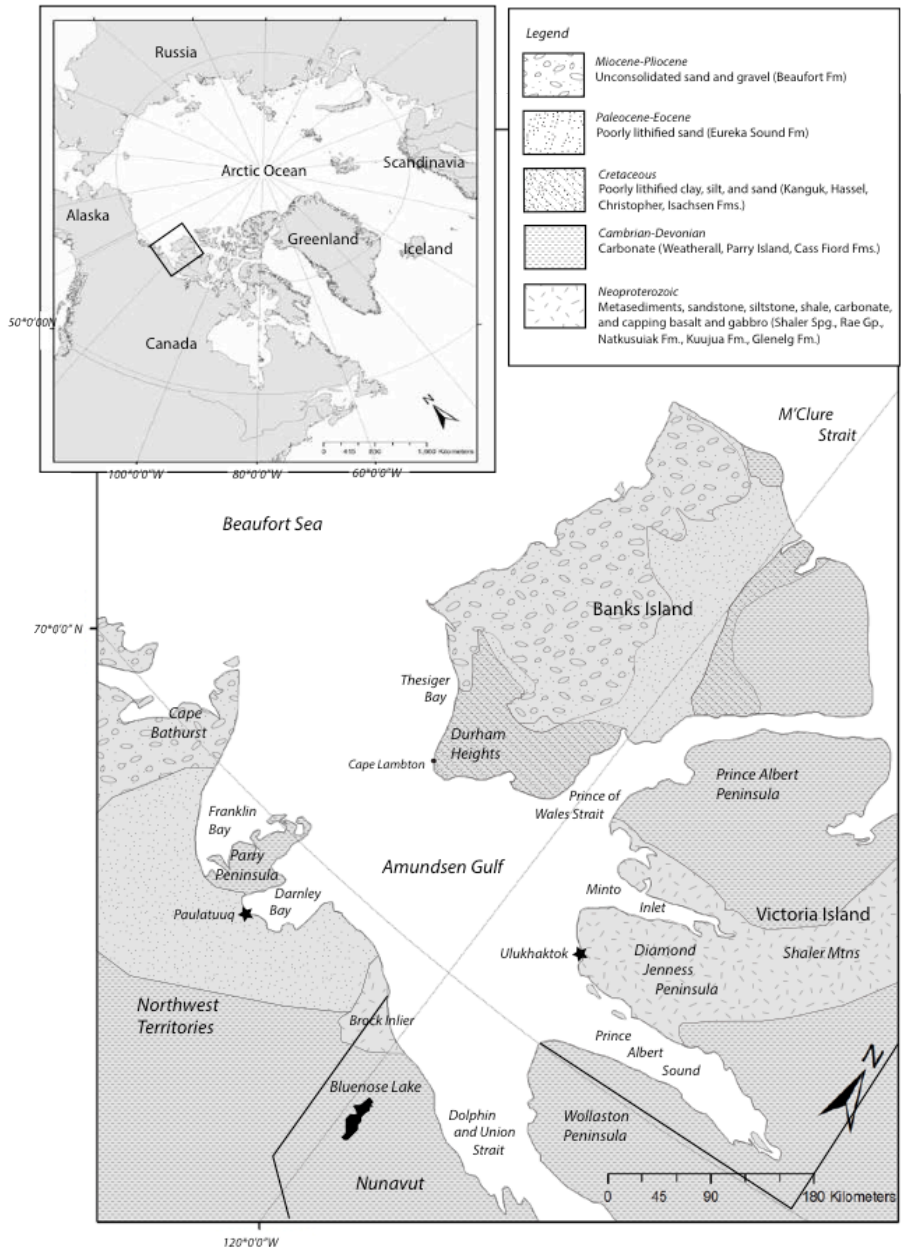

Fig 2.1. Map showing location of Banks Island in the western Canadian Arctic Archipelago including generalized bedrock geology and place names cited in text.

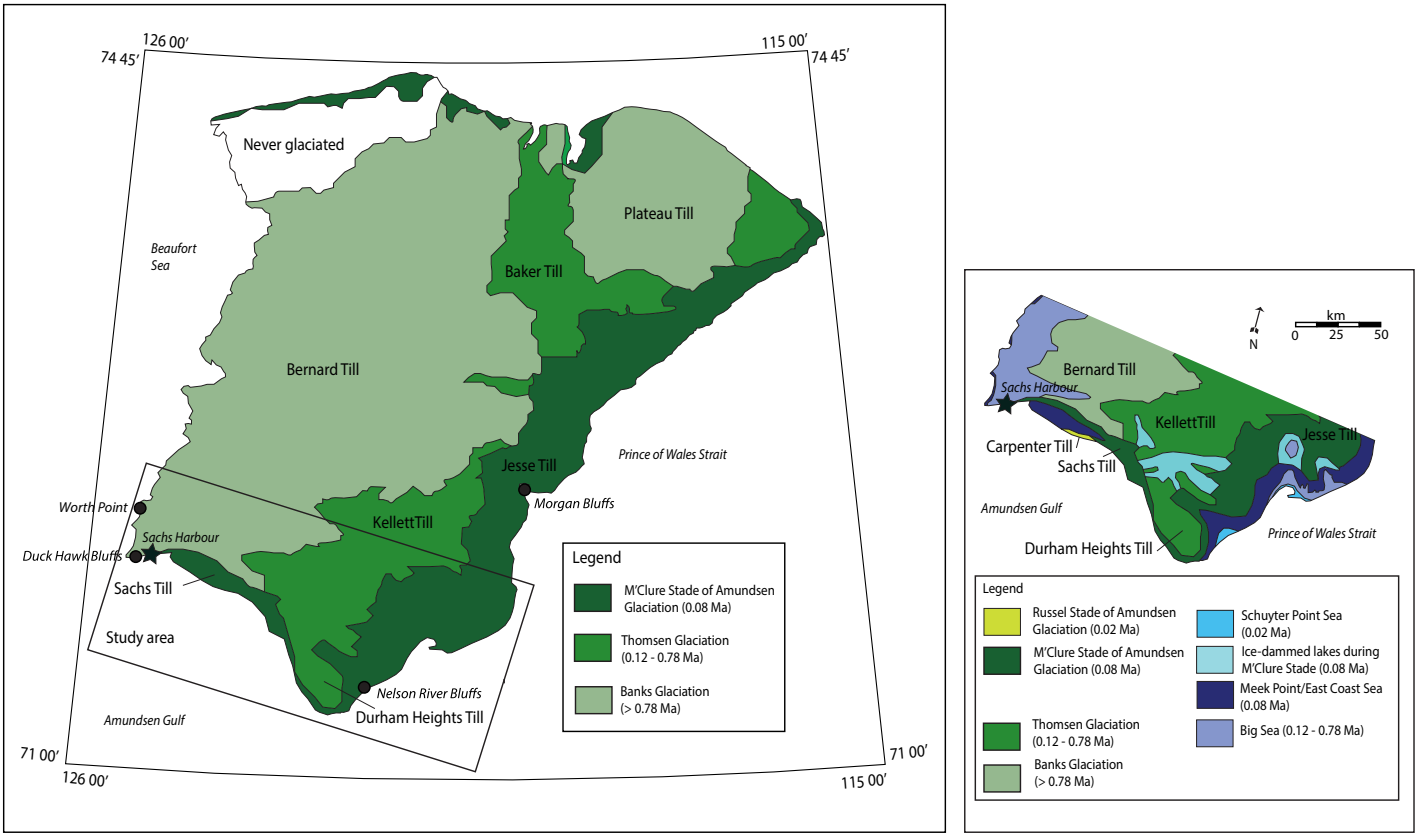

Fig. 2.2a (left) Map of Banks Island showing the three surficial till sheets of Vincent (1982, 1983). Note how the till sheets increase in age westward and terminate against a 'never glaciated' landscape on northwest Banks Island. The youngest till deposits (dark green) wrap around the south, east, and north coasts and purportedly record the maximum limit of Laurentide ice during the Early Wisconsinan.

Fig. 2.2b (right) Map of southern Banks Island showing primary glacial landforms and sediments of Vincent (1982). Note the numerous marine sediments (in purple and blue) associated with each purported glaciation (limits in green), and the large ice-dammed lakes (lightest blue) impounded by the Early Wisconsinan ice margin (dark green).

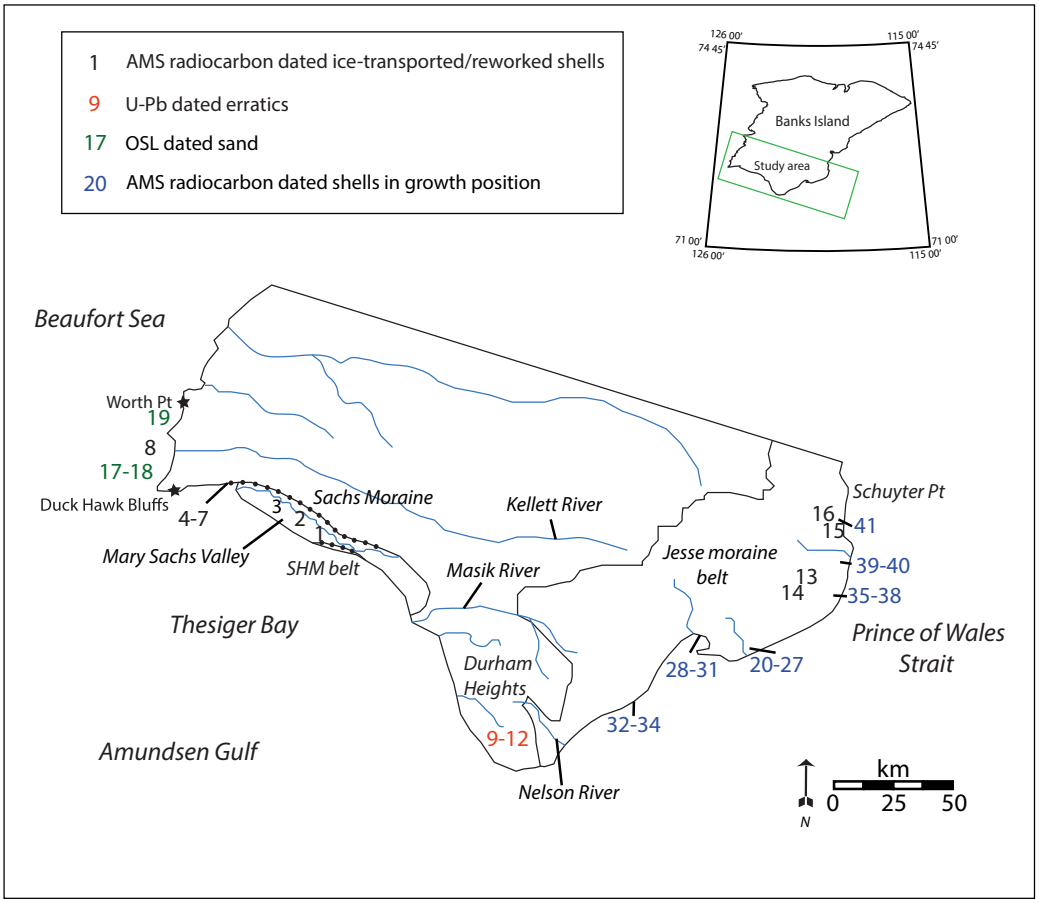

Fig 2.3. Map of southern Banks Island showing the collection site for each sample. Sample numbers are colour coded according to sample type and dating method. Each sample number corresponds to a separate date listed in Tables 2.1, 2.2, 2.3, 2.4, and 2.5. The Sachs Moraine, Sand Hills Moraine (SHM) belt, Jesse moraine belt and primary locations cited in text are shown.

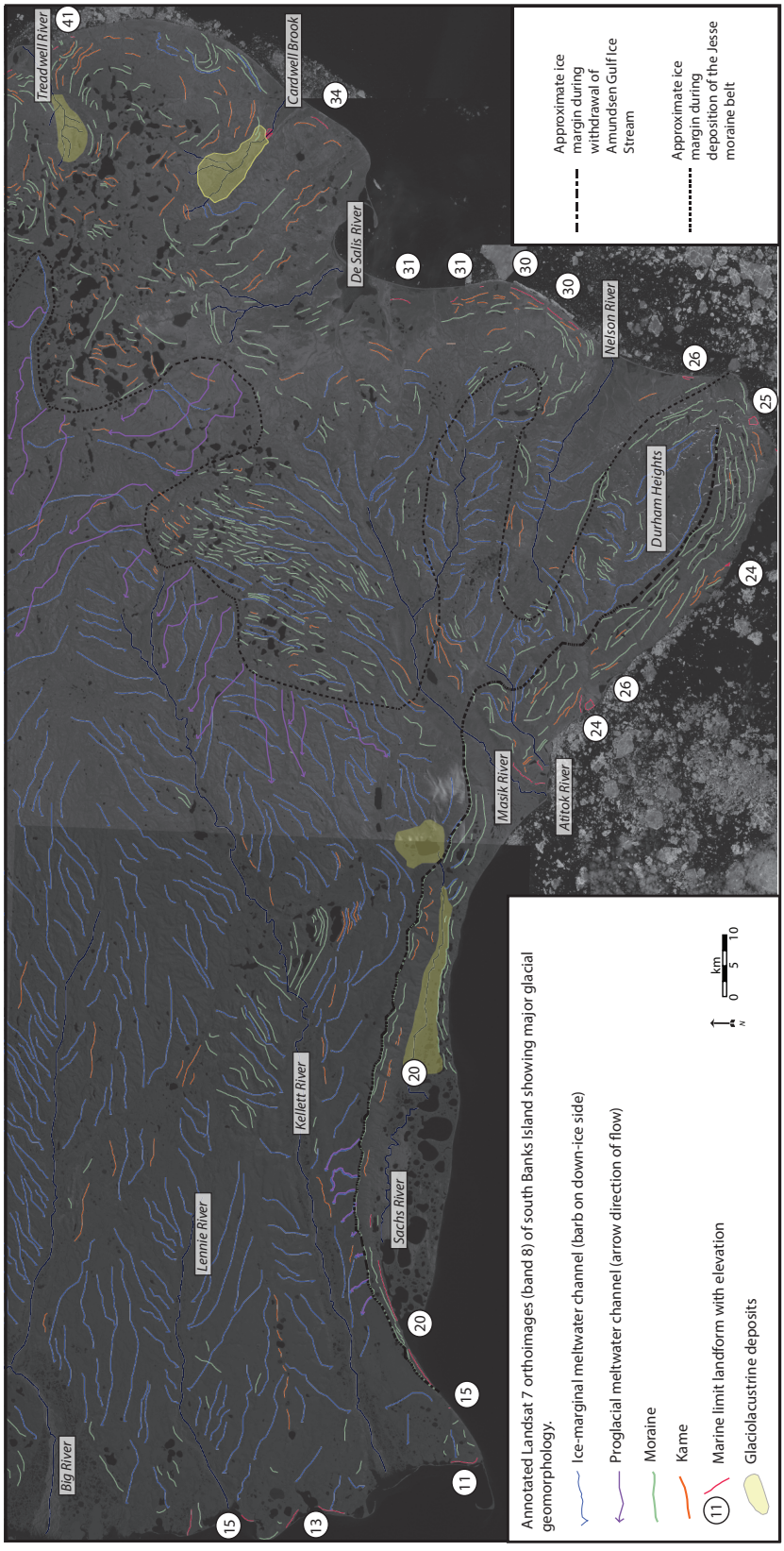
Treadwell River
Cardwell Brook
De Salis River
Nelson River
Durham Heights
Masik River
Atitok River
Kellett River
Lennie River
Sachs River
Big River
Approximate ice margin during withdrawal of Amundsen Gulf Ice Stream
Approximate ice margin during deposition of the Jesse moraine belt
Annotated Landsat 7 orthoimages (band 8) of south Banks Island showing major glacial geomorphology.
Ice-marginal meltwater channel (barb on down-ice side)
Proglacial meltwater channel (arrow direction of flow)
Moraine
Kame
Marine limit landform with elevation
Glaciolacustrine deposits
km
0
5
10
N

Fig. 2.4

Fig. 2.4 (previous page). Annotated Landsat 7 orthoimages (band 8) of southern Banks Island showing primary glacial geomorphology and marine limit elevations (m asl). Note approximate limits of trunk ice during deposition of the Sachs Moraine and Jesse moraine belt. Also note the kettles, linear moraines and kame terraces that characterize terrain coastward of these approximate ice limits, in contrast with the interior (distal to the limits) where ice retreat is primarily recorded by ice-marginal meltwater channels. Marine limit elevations can be seen to rise northward along the west coast (from 11 to 15 m asl), eastward along the south coast (from 11 to 25 m asl), and northward along the east coast (from 25 to 41 m asl), reflecting greater glacial unloading to the east and northeast where ice divides were located in Keewatin and on or adjacent to Victoria Island (Dyke and Prest, 1987; Hodgson, 1994; England et al., 2009; Lakeman and England, 2012).

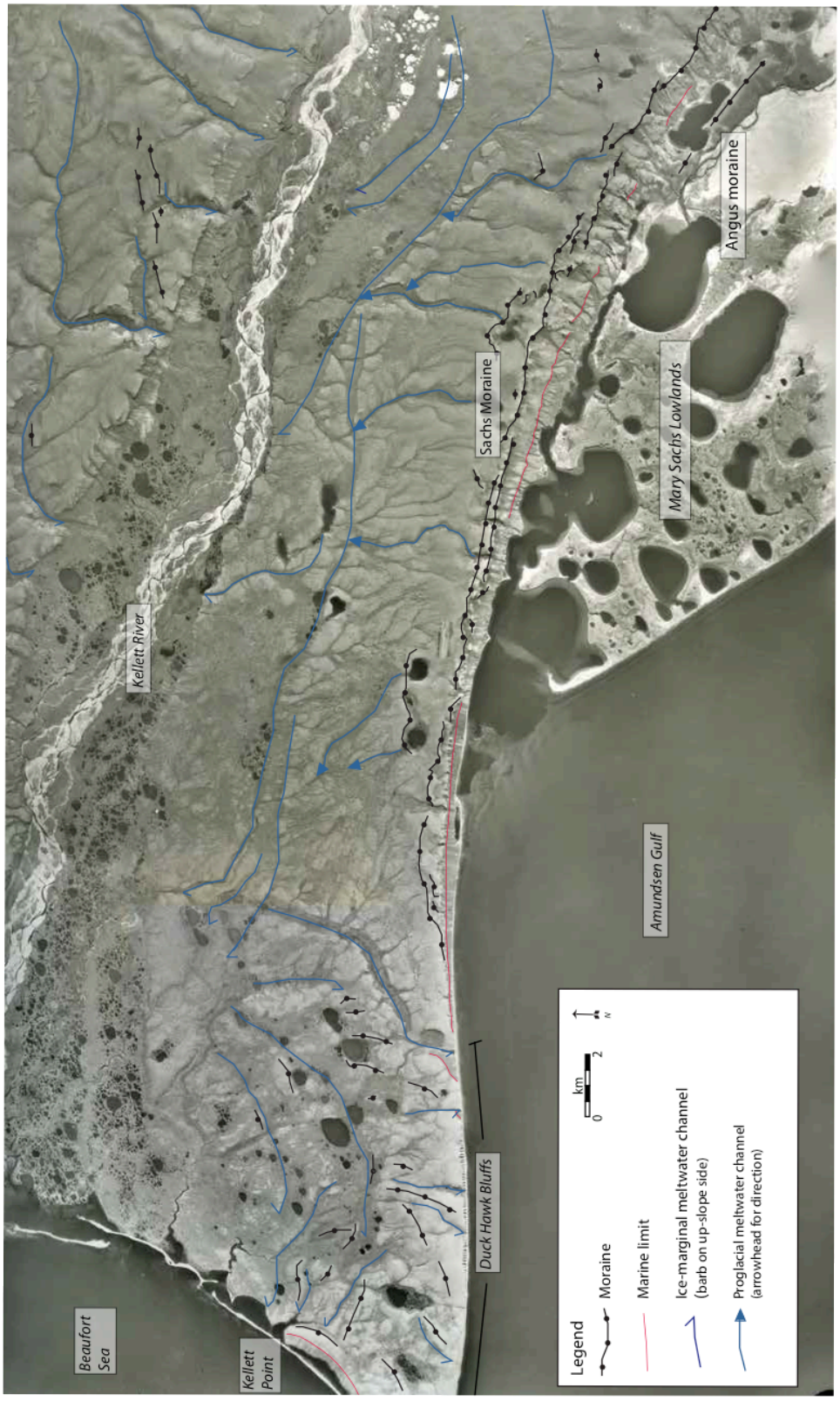
Beaufort Sea
Kellett Point
Duck Hawk Bluffs
Kellett River
Sachs Moraine
Mary Sachs Lowlands
Angus moraine
Amundsen Gulf
Legend
Moraine
Marine limit
Ice-marginal meltwater channel (barb on up-slope side)
Proglacial meltwater channel (arrowhead for direction)
km
0
2
N

Fig. 2.5.

Fig. 2.5. (previous page). Annotated photomosaic of aerial photographs showing primary glacial geomorphology on southwest Banks Island, including the western Sachs Moraine and lower Kellett River Valley. Moraines immediately north of Duck Hawk Bluffs are interlobate and record the coalescence of trunk ice in Amundsen Gulf and an ice lobe in the Kellett Valley. Note proglacial meltwater channels emanating from the crest of the Sachs Moraine into the lower Kellett Valley. The conspicuous Mary Sachs lowlands (bottom right of photo) are interpreted to record the westward drainage of a glacial lake over glacial ice. The continued melting of the buried glacial ice has produced thermokarst terrain.

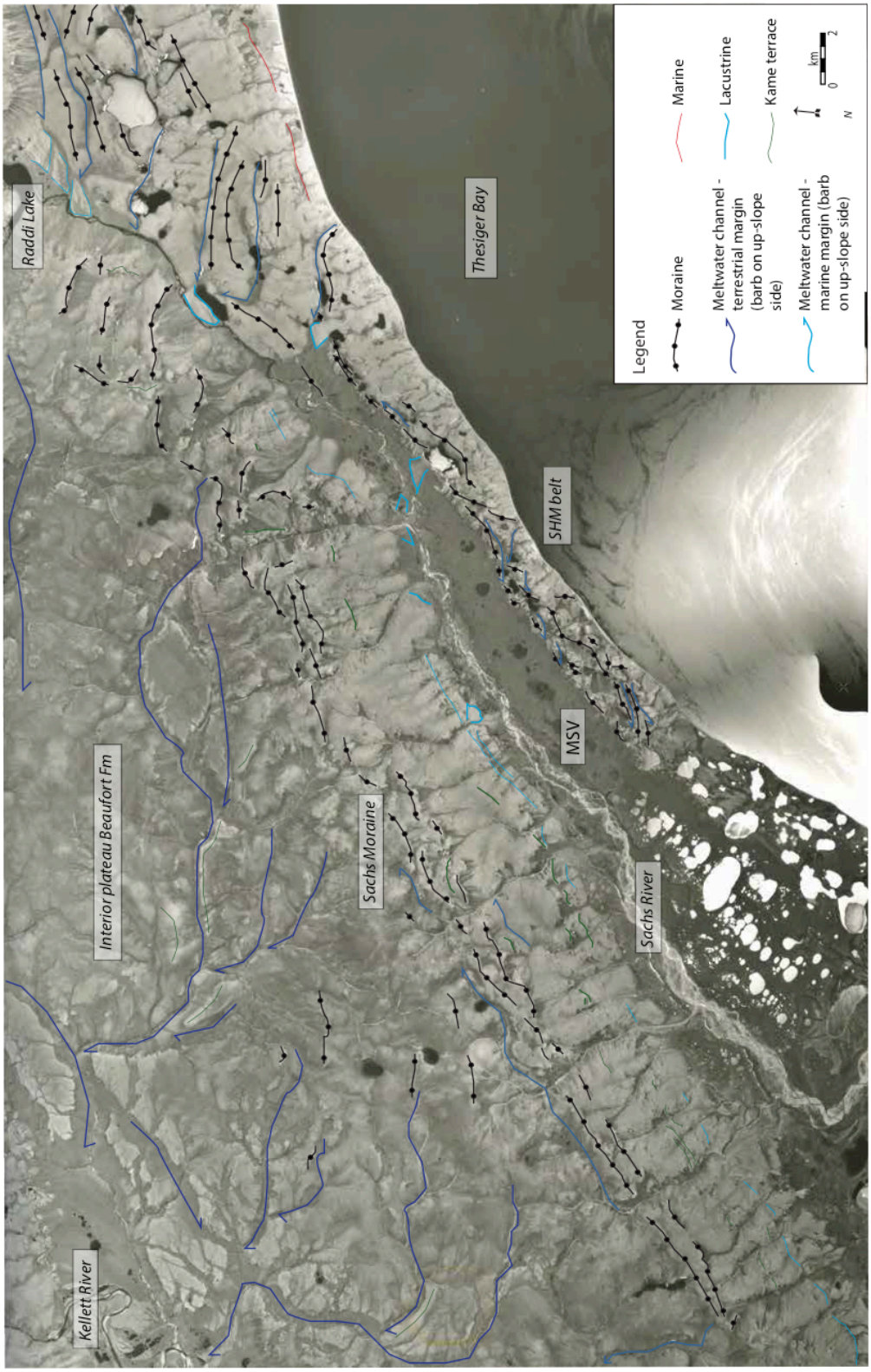
Raddi Lake
Thesiger Bay
SHM belt
MSV
Interior plateau Beaufort Fm
Sachs Moraine
Sachs River
Kellett River
Legend
Moraine
Marine
Meltwater channel - terrestrial margin (barb on up-slope side)
Lacustrine
Kame terrace
Meltwater channel - marine margin (barb on up-slope side)
km
0
2
N

Fig. 2.6.

Fig. 2.6. (previous page). Annotated photomosaic of aerial photographs showing primary glacial geomorphology on south-central Banks Island, including the Sachs Moraine and Sand Hills Moraine (SHM) belt. Note the sub-horizontal kame terraces perched against the coastward side of the Sachs Moraine recording progressive offshore retreat of trunk ice. Also note outwash fans (light blue) adjacent to (south of) Raddi Lake (120 m asl) and meltwater channel routed westward from Raddi Lake that terminates a lower outwash fan (80 m asl) at the eastern end of the Mary Sachs Valley (MSV). Outwash fans emanating into the Mary Sachs Valley from the Sand Hills Moraine belt (53 m asl) can also be observed. Distal to the Sachs Moraine (inland) ice-marginal meltwater channels record the eastward retreat of a cold-based ice lobe confined to the Kellett Valley.

Table 2.1. Radiocarbon dates for redeposited molluscs within or adjacent to the Sachs Moraine, south-central and southwest Banks Island. Dates provided by KECK Carbon Cycle Accelerator Mass Spectrometry Laboratory, University of California.

Sample Number	Lab Number	^{14}C age (yr BP)	Lab error	Calibrated age range (yr BP)	Dated material	Co-ordinates	Sample elev (m asl)
1	UCI-54177	38,290	310	41,450 – 42,412	Shell fragment	71.74165 N 124.04543 W	132
2	UCI-54187	41,750	460	43,576 – 45,361	Shell fragment	71.95957 N 124.67710 W	73
3	UCI-89674	21,020	70	24,028 – 24,738	*A. borealis* fragment	71.95267 N 124.83395 W	57
4	UCI-54186	40,910	420	43,019 – 44,574	*A. borealis* fragment	71.96888 N 125.48305 W	2
5	UCI-55263	43,760	1180	44,198 – 48,930	*A. borealis* fragment	71.96888 N 125.48305 W	2
6	UCI-54181	44,280	640	45,484 – 48,249	*A. borealis* fragment	71.96888 N 125.48305 W	3
7	UCI-54184	46,590	840	N/A*	*A. borealis* fragment	71.96888 N 125.48305 W	3
8	UCI-54183	47,400	930	N/A*	*M. arenaria* fragment	71.00333 N 125.72777 W	9

* Dates with N/A are beyond the range of radiocarbon calibration.

ΔR applied to pre-Holocene molluscs is not known with confidence as the regional oceanography remains poorly constrained for this time period (Coulthard et al., 2010).


E
Fig. 2.7a


Fig. 2.7b:

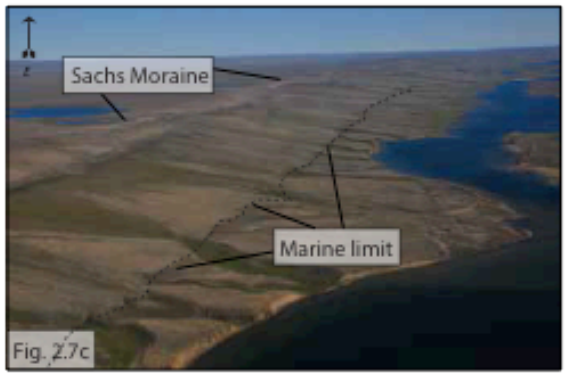
E
Sachs Moraine
Marine limit
Fig. 2.7c


N
Fig. 2.7d


N
Fig. 2.7e

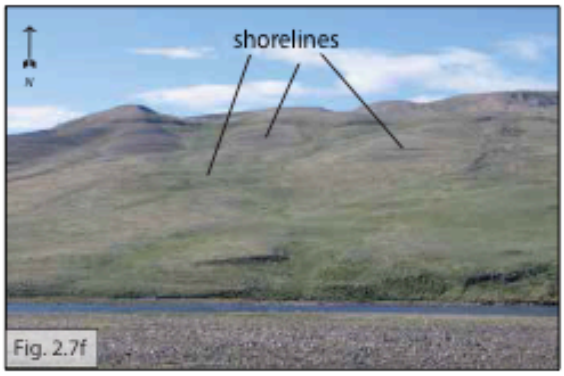
N
shorelines
Fig. 2.7f

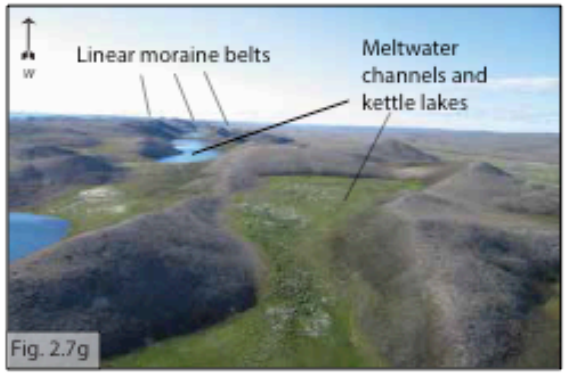
W
Linear moraine belts
Meltwater channels and kettle lakes
Fig. 2.7g

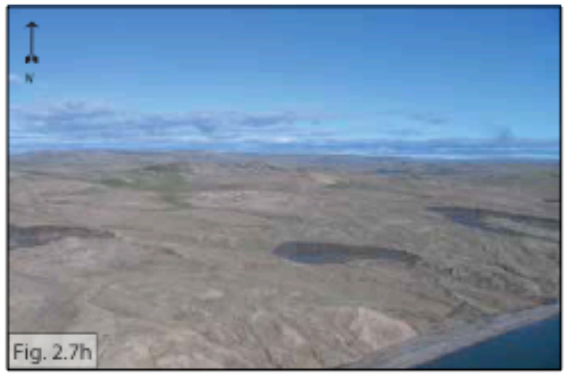
N
Fig. 2.7h

(previous page)

Fig. 2.7a. Photograph showing a thrust raft of glaciofluvial outwash that comprises the western end of the Sachs Moraine. The moraine was deposited during a deglacial readvance of trunk ice in Amundsen Gulf.

Fig. 2.7b. Photograph showing the lowermost 2-3 m of outwash immediately west of the Sachs Moraine. The outwash is interpreted to record subaqueous deposition into the deglacial sea from trunk ice in Amundsen Gulf.

Fig. 2.7c. Oblique photograph looking east across the Sachs Moraine. Note prominent marine limit bench coastward of the moraine. Photograph credit: J England, 2012.

Fig. 2.7d. Photograph showing glaciolacustrine silt perched against the interior plateau in the Mary Sachs Valley up to 86 m asl. The silt was deposited in Glacial Lake Mary Sachs, impounded between trunk ice in Amundsen Gulf and the Sachs Moraine.

Fig. 2.7e. Photograph showing close-up of glaciolacustrine silt in the Mary Sachs Valley.

Fig. 2.7f. Photograph looking north toward the crest of the Sachs Moraine. Note horizontal shorelines recording previous levels of ice-dammed Glacial Lake Mary Sachs.

Fig. 2.7g. Photograph looking west across the Sand Hills Moraine belt. Note the linearity of the moraines and intervening meltwater channels and kettle lakes. Moraine linearity is interpreted to reflect the preservation of debris septa imparted during controlled moraine deposition.

Fig. 2.7h. Photograph looking north toward to Sand Hills Moraine belt. Note retrogressive thaw flow slides that expose buried glacial ice. The linearity of the Sand Hills Moraine belt will be erased as ice cores (buried glacial ice) exposed by retrogressive thaw flow slides degrade

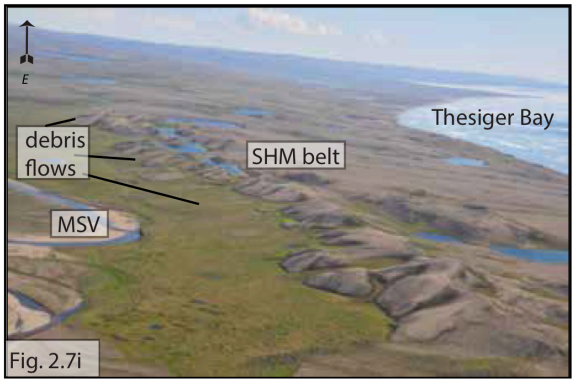
E
Thesiger Bay
debris flows
SHM belt
MSV
Fig. 2.7i


S
Fig. 2.7j

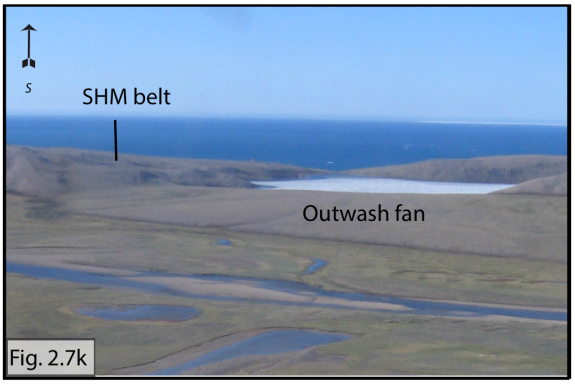
S
SHM belt
Outwash fan
Fig. 2.7k

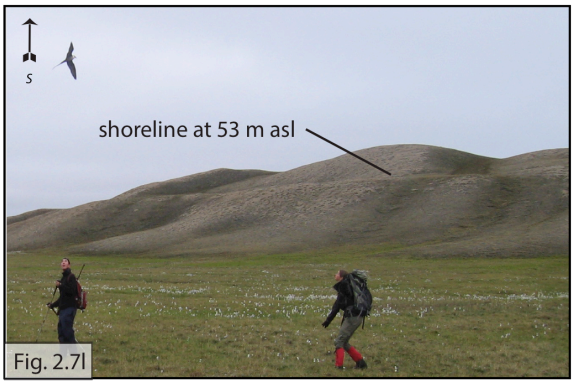
S
shoreline at 53 m asl
Fig. 2.7l


N
Fig. 2.7m

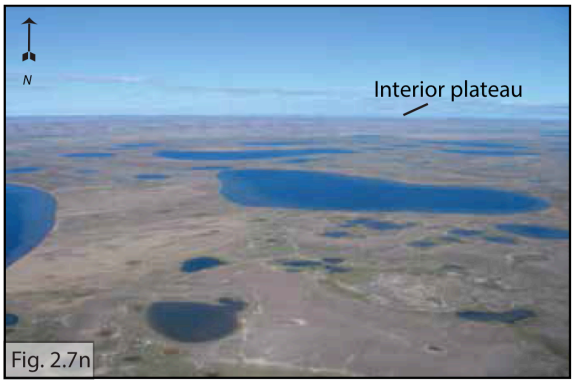
N
Interior plateau
Fig. 2.7n

(previous page).

Fig 2.7.i. Photograph looking east across the Sand Hills Moraine (SHM) belt and the Mary Sachs Valley (MSV). Note the debris flows emanating from the most distal moraines into the Mary Sachs Valley where they are truncated by the Mary Sachs River. Photograph credit: J England, 2012.

Fig. 2.7j. Photograph showing the stratigraphy of a debris flow. Inset photograph shows location of exposure cut by the Mary Sachs River.

Fig. 2.7k. Photograph looking south from the Mary Sachs Valley (MSV) toward Thesiger Bay (Amundsen Gulf). Note outwash fan (53 m asl) emanating from the most distal (inland) moraine into the Mary Sachs Valley at the bottom of photo. The outwash fan is ~30 m above marine limit and aggraded into a lower, later stage of Glacial Lake Mary Sachs.

Fig. 2.7l. Photograph showing a lake shoreline at 53 m asl trimming a distal moraine of the Sand Hills Moraine belt facing the Mary Sachs Valley. The shoreline is accordant with the outwash fan emanating from the Sand Hills Moraine belt (Fig. 2.7k) and similarly records a later stage of Glacial Lake Mary Sachs.

Fig. 2.7m. Photograph showing small, largely mafic clasts that mantle the Mary Sachs Valley up to 50 m asl.

Fig. 2.7n. Photograph looking north toward the interior plateau across the large kettled plain that extends westward from the Mary Sachs Valley. The plain is interpreted to record deglacial marine limit ~20 m asl.

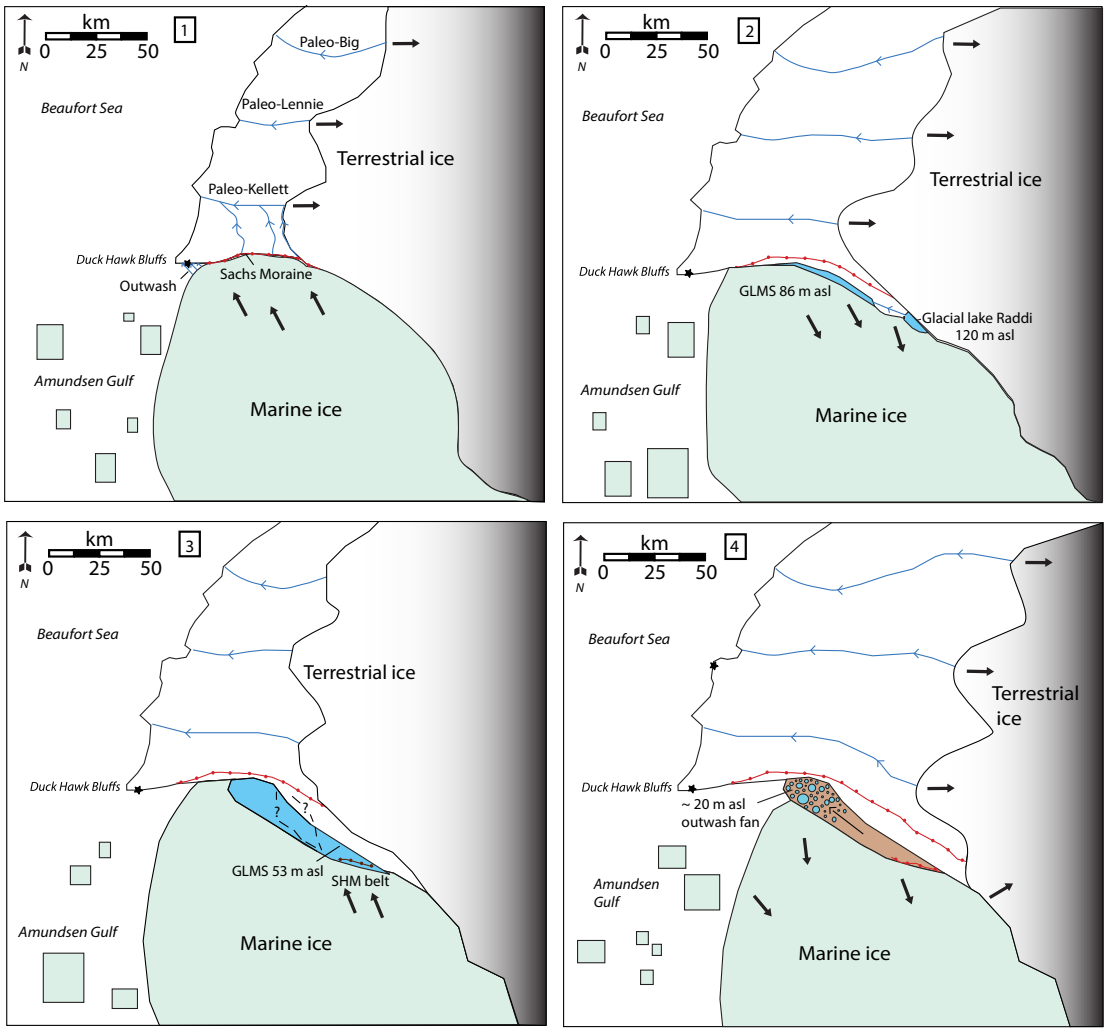
km
0 25 50
N
1
Paleo-Big
Paleo-Lennie
Terrestrial ice
Paleo-Kellett
Beaufort Sea
Duck Hawk Bluffs
Outwash
Sachs Moraine
Amundsen Gulf
Marine ice
2
GLMS 86 m asl
Glacial lake Raddi
120 m asl
3
GLMS 53 m asl
SHM belt
4
~ 20 m asl
outwash fan
Amundsen
Gulf

Fig. 2.8.

Fig. 2.8. (previous page). Simplified conceptual model of the evolution of Glacial Lake Mary Sachs (GLMS) and the Sand Hills Moraine (SHM) belt. Box 1 shows the approximate position of marine ice abutting the Sachs Moraine with a coalescent ice lobe in the lower Kellett Valley. Box 2 shows subsequent offshore retreat of marine ice from the Sachs Moraine and the damming of Glacial Lake Mary Sachs up to 86 m asl and Glacial Lake Raddi up to 120 m asl. Westward drainage of Glacial Lake Raddi into Glacial Lake Mary Sachs is also shown. Box 3 shows the approximate position of marine ice during a subsequent readvance that deposited the Sand Hills Moraine belt. A lowering of Glacial Lake Mary Sachs to 53 m asl is shown. Box 4 shows final withdrawal of marine ice from the Sand Hills Moraine belt and westward drainage of Glacial Lake Mary Sachs to produce a marine limit outwash fan at ~20 m asl.

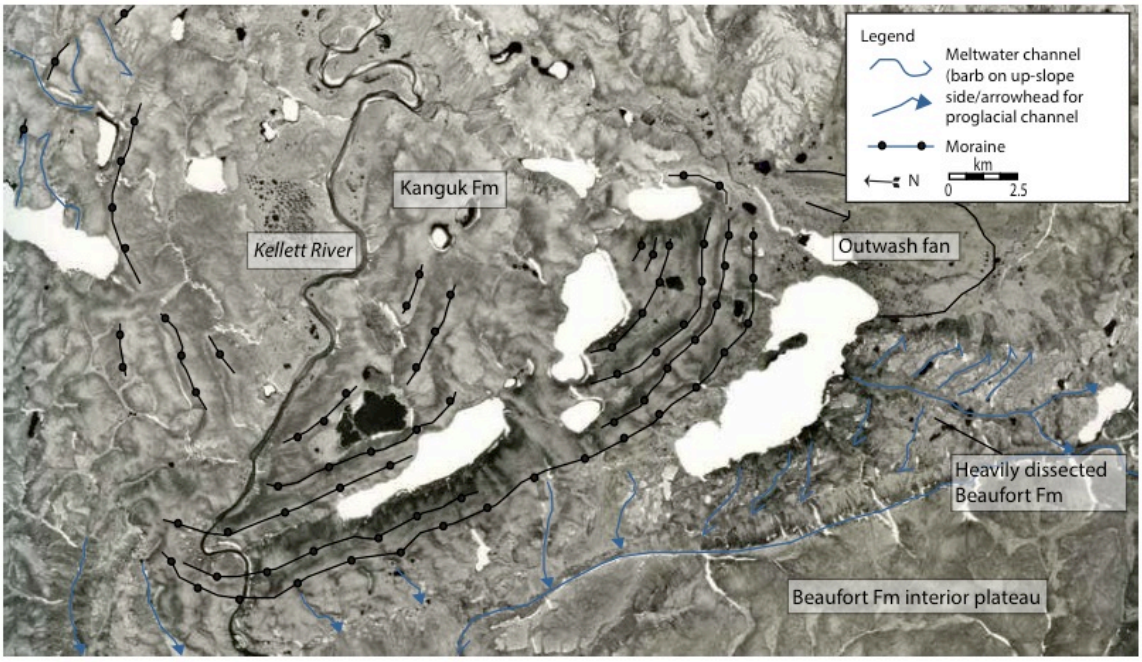

Fig. 2.9. Annotated aerial photograph showing the primary glacial geomorphology of the Kellett Valley thrust-block moraine. Note prominent thrust blocks (right) inset by a series of smaller thrust blocks (left). Also note the arcuate shape of the outermost thrust block, delineating a former ice lobe in the Kellett Valley.

Fig. 2.10a

Fig. 2.10b

Fig. 2.10c

Fig. 2.10d

(previous page)

Fig. 2.10a. Photograph of a Proterozoic mafic erratic on the Durham Heights.

Fig. 2.10b. View of Precambrian granite erratics mantling the Durham Heights, including close-up of granite erratics (inset). The granite erratics occur in association with Proterozoic mafic erratics and Cambrian-Devonian carbonate erratics. Photograph credit: J. England, 2012.

Fig. 2.10c. Photograph looking west along the coast of Amundsen Gulf adjacent to the Durham Heights. Widespread striated bedrock (Glenelg Fm) within ~2 km of the coast record an abrupt transition to warm-based trunk ice that on-lapped Banks Island from Amundsen Gulf.

Fig. 2.10d. Photograph looking west along the coast of Amundsen Gulf west of the Masik River. Note the east-west oriented striae on the Glenelg Fm outcrop (gabbro-diabase), recording the passage of warm-based trunk ice in Amundsen Gulf. Photograph credit: J England, 2012.

Table. 2.2. U-Pb dates obtained on zircon crystals from a mafic erratic sampled on the Durham Heights, southeast Banks Island. Dates provided by the Heaman Laboratory using the in-situ mass spectrometry laser ablation technique, Earth and Atmospheric Sciences, University of Alberta.

Sample Number	Laboratory Number	Pb-206/U-238 (Ma)	Location	Co-ordinates	Sample material
9	BCO9-5(1)	670	Durham Heights	71.19583 N 123.20888 W	Proterozoic mafic
10	BCO9-5(2)	707	Durham Heights	71.19583 N 123.20888 W	Proterozoic mafic
11	BCO9-5(3)	721	Durham Heights	71.19583 N 123.20888 W	Proterozoic mafic
12	BCO9-5(4)	725	Durham Heights	71.19583 N 123.20888 W	Proterozoic mafic


Legend
Moraine
Kame
Marine limit
Meltwater channel (barb on up-slope side or arrowhead for proglacial channel)
Approximate ice margin
km
0
4
N
Interfluve
Glaciolacustrine deposits
Ice shelf moraine
Outwash plain

Fig. 2.11.

Fig. 2.11. (Previous page). Annotated photomosaic of aerial photographs showing the characteristic glacial geomorphology of Schuyter Point, southeast Banks Island. Note the ice shelf moraines oriented NE-SW on the coast, the moraines at the head of Schuyter Valley that delineate a topographically constrained ice lobe, and the expansive outwash plain to the west. The prominent band of kettle lakes (immediately west of the lobate moraines) are interpreted to record the melting of buried glacial ice that has been exposed by retrogressive thaw flow slides.

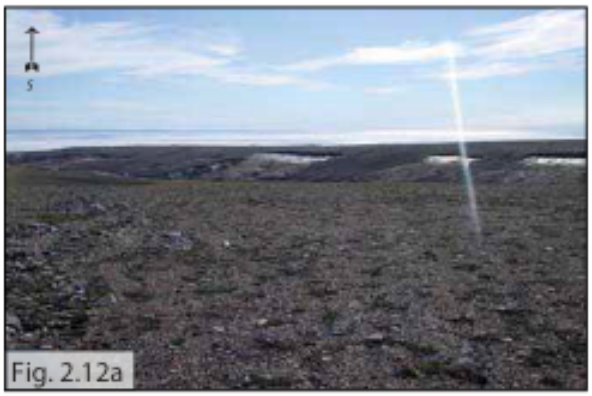

Fig. 2.12a. Photograph looking south along the margin of the inland plateau where the Jesse moraine belt terminates. Note retrogressive thaw flow slides that expose buried glacial ice.

Fig. 2.12b. Photograph looking north showing conical kames along the coastal plain where the Jesse moraine belt contacts Prince of Wales Strait.

Fig. 2.12c. Photograph looking north across the coastal plain at Schuyter Point, adjacent to Prince of Wales Strait. Note the broad-crested ice-shelf moraine (39 m asl) running from bottom right of the photograph (SE-NW).

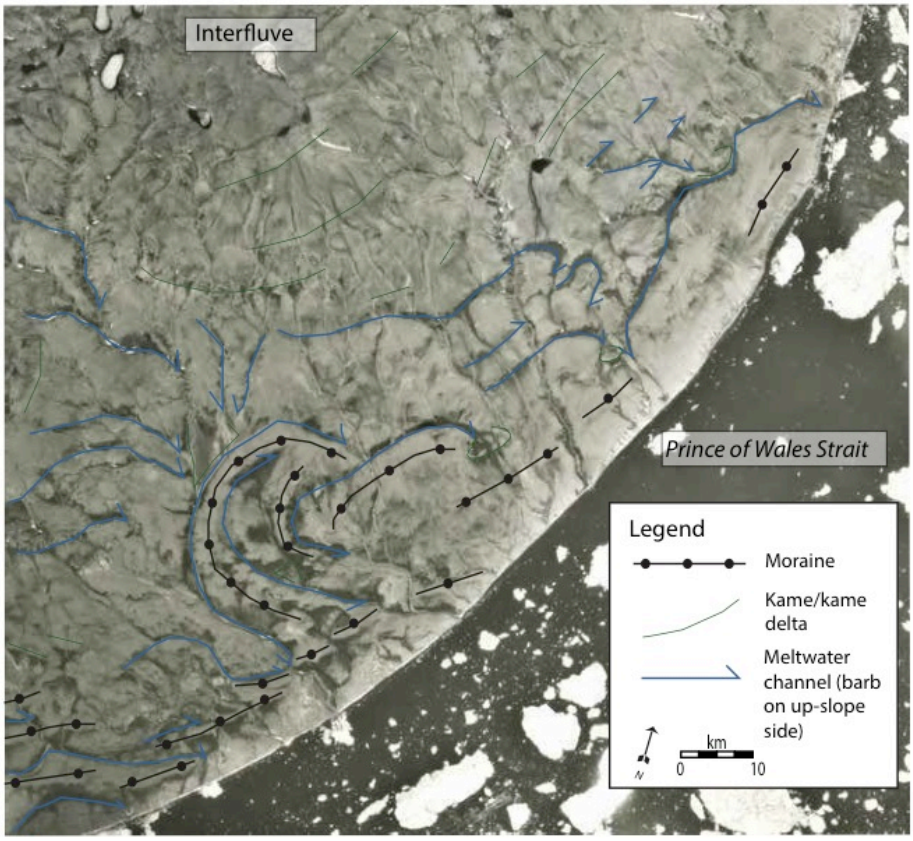

Fig. 2.13. Annotated aerial photograph showing the primary glacial geomorphology of the coastal plain of the Jesse moraine belt, south of Cape Treadwell. Note the convoluted moraines and ice-marginal meltwater channels that record the final stages of ice retreat into Prince of Wales Strait.

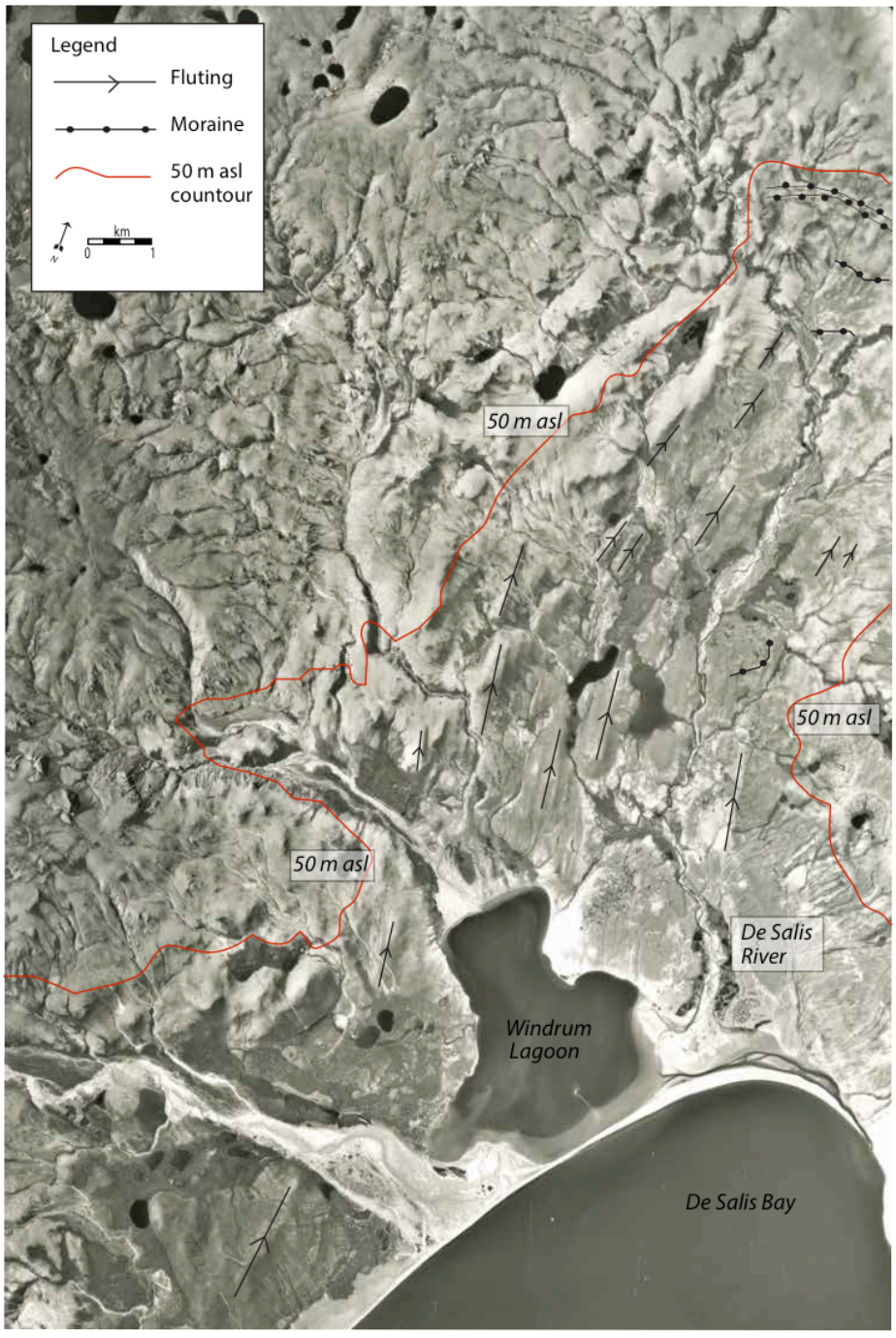

Fig. 2.14. Annotated aerial photograph showing the De Salis Bay flutings. Note how all flutings are confined below the 50 m contour and terminate at a series of push moraines (top right).

Table 2.3. Radiocarbon dates for redeposited molluscs within the Jesse moraine belt, southeast Banks Island. Dates provided by KECK Carbon Cycle Accelerator Mass Spectrometry Laboratory, University of California.

Sample Number	Lab Number	^{14}C age (yr BP)	Lab error	Calibrated age range (yr BP)	Dated material	Co-ordinates	Sample elev (m asl)
13	UCI-55265	23,710	160	26,877 – 27,638	*A. borealis* fragment	71.66823 N 120.42584 W	25
14	UCI-89673	30,140	200	33,083 – 33,996	*A. borealis* fragment	71.66823 N 120.42584 W	37
15	UCI-89675	34,940	330	37,839 – 39,579	*A. borealis* fragment	71.66823 N 120.42584 W	37
16	UCI-89677	40,520	660	42,499 – 44,633	*H. arctica* fragment	71.66823 N 120.42584 W	42

ΔR applied to pre-Holocene molluscs is not known with confidence as the regional oceanography remains poorly constrained for this time period (Coulthard et al., 2010).

Table 2.4. OSL dates for quartz using the single aliquot regenerative technique at the Sheffield Centre for International Drylands Research Luminescence Laboratory, UK. Samples collected from sand beds 2-3 m asl on southwest Banks Island.

Sample Number	Laboratory Number	Depth (cm)	De (gy)	Dose Rate ($\mu Gy/a^{-1}$)	Age (ka)	Co-ordinates
17	Shfd11045	200	103.2 ± 1.47	1122 ± 51	94 ± 4.6	71.00333 N
						125.727778 W
18	Shfd11046	200	83.7 ± 0.79	930 ± 40	94 ± 4.2	71.00333 N
						125.727778 W
19	Shfd11044	200	68.2 ± 1.58	714 ± 29	98 ± 4.7	71.066700 N
						125.717772 W

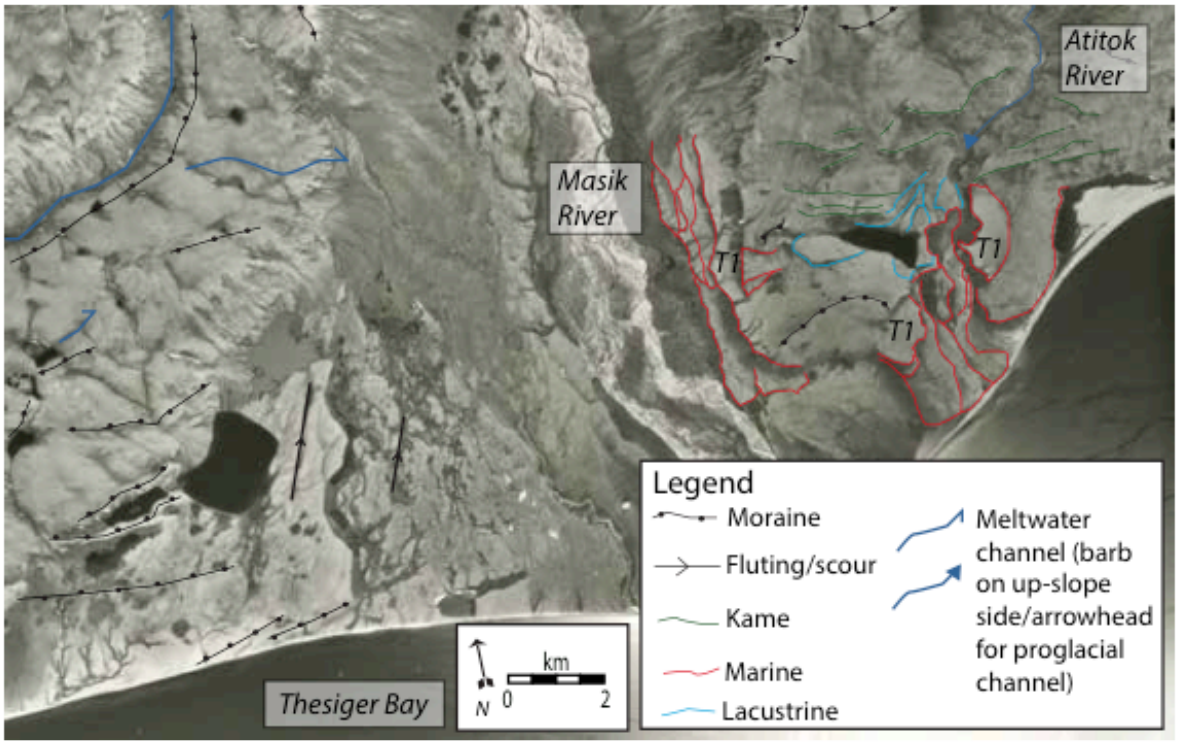

Fig. 2.15. Annotated aerial photograph showing the primary glacial geomorphology of the lower Masik Valley. Note the series of raised marine terraces (red) with T1 representing marine limit. Terraces above the marine beaches (green) are kames. Also note the ice shelf moraines sub-parallel to the coast (west of Masik River) fronted by flutings oriented northeast (inland).

Table 2.5. Radiocarbon dates for molluscs collected from raised marine beaches up to 33 m asl on eastern Banks Island (adjacent to Prince of Wales Strait). Dates provided by KECK Carbon Cycle Accelerator Mass Spectrometry Laboratory, University of California.

Sample Number	Lab Number	^{14}C age (yr BP)	Lab error	Calibrated age range (yr BP)	Dated material	Co-ordinates	Sample elev (m asl)
20	UCI-68613	11,205	20	12,066 – 12,592	*H. arctica*	71.41083 N 121.08638 W	31
21	UCI-68614	11,470	20	12,525 – 12,869	*H. arctica*	71.41083 N 121.08638 W	20
22	UCI-68615	11,615	25	12,583 – 12,969	*H. arctica*	71.41083 N 121.08638 W	33
23	UCI-68616	11,105	20	11,911 – 12,421	*C. kurriana*	71.41083 N 121.08638 W	31
24	UCI-68617	11,475	25	12,527 – 12,875	*H. arctica*	71.41083 N 121.08638 W	29
25	UCI-68618	11,640	20	12,600 – 12,977	*H arctica*	71.41083 N 121.08638 W	23
26	UCI-68619	11,610	20	12,579 – 12,968	*H. arctica*	71.41083 N 121.08638 W	23
27	UCI-68620	11,430	25	12,369 – 12,779	*H. arctica*	71.4136 N 121.81972 W	10
28	UCI-68621	11,485	25	12,535 – 12,881	*H. arctica*	71.4136 N 121.81972 W	12
29	UCI-68623	11,150	20	11,982 – 12,564	*H. arctica*	71.4136 N 121.81972 W	10
30	UCI-68624	11,275	20	12,179 – 12,634	*H. arctica*	71.4136 N 121.81972 W	20

31	UCI-68625	11,605	25	12,577 – 12,964	*H. arctica*	71.31805 N 122.02972 W	15
32	UCI-68627	11,385	25	12,334 – 12,737	*H. arctica*	71.31805 N 122.02972 W	15
33	UCI-68628	11,455	20	12,517 – 12,845	*H. arctica*	71.31805 N 122.02972 W	19
34	UCI-68629	11,100	20	11,900 – 12,420	*H. arctica*	71.40666 N 121.17638 W	13
35	UCI-68630	11,460	20	12,520 – 12,857	*H. arctica*	71.40666 N 121.17638 W	27
36	UCI-68631	11,595	25	12,576 – 12,949	*H. arctica*	71.40666 N 121.17638 W	25
37	UCI-68632	11,530	25	12,558 – 12,899	*H. arctica*	71.40666 N 121.17638 W	1
38	UCI-68633	11,415	25	12,359 – 12,761	*H. arctica*	71.42255 N 121.03444 W	14
39	UCI-68634	11,290	20	12,185 – 12,649	*H. arctica*	71.42255 N 121.03444 W	22
40	UCI-89672	11,550	25	12,566 – 12,909	*H. arctica*	71.46027 N 120.79527 W	10

Fig. 2.16. Photograph looking west across the submerged lower reaches of the modern Kellett River delta. Ongoing relative sea level rise from a Holocene lowstand is causing widespread relative sea level rise across all of Banks Island.

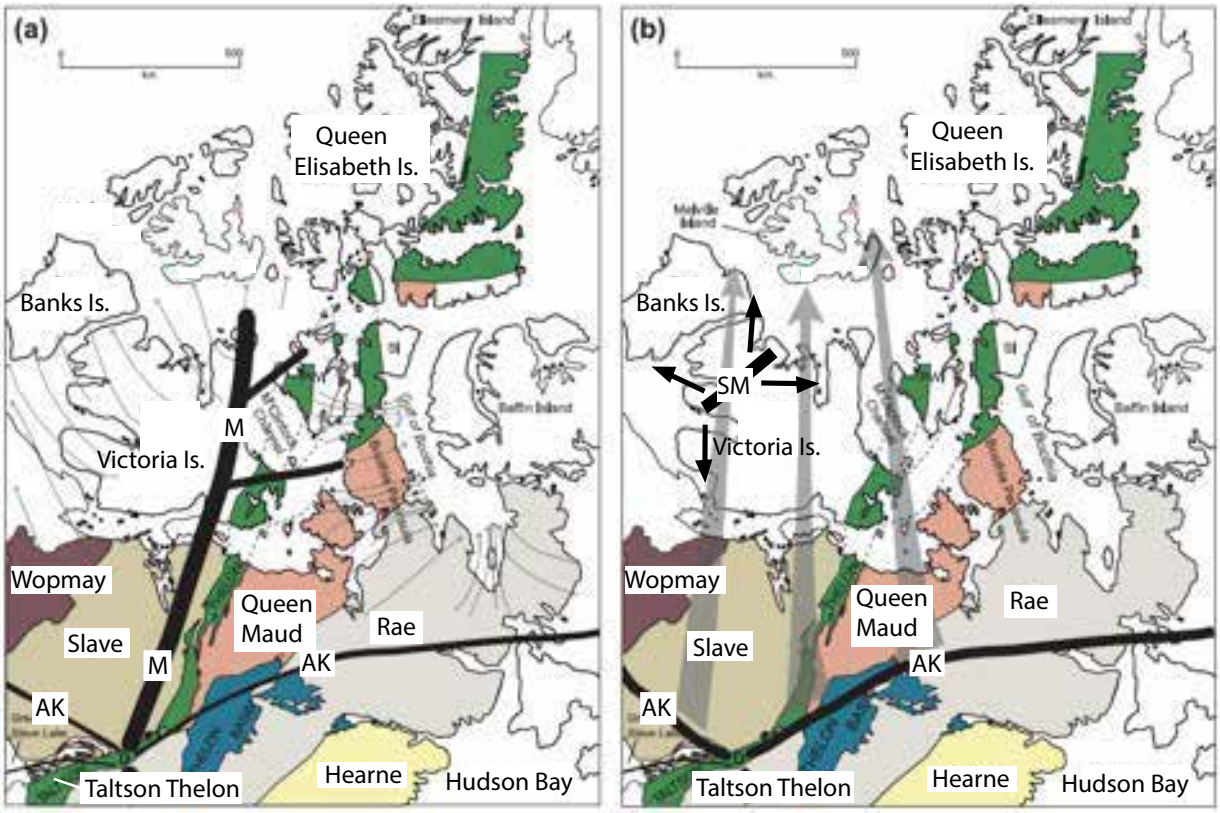

Fig. 2.17. Map based on Dyke and Prest (1987) by Doornbos et al (2009). The map on left (a) shows a dominant north-south trending M'Clintock Ice Divide (M) dispersing ice westward from Victoria Island to Banks Island. The map on right (b) shows the dominant east-west trending Ancrestral Keewatin Ice Divide (AK) dispersing ice northward and northwestward from the Canadian mainland to Banks Island. A lateglacial ice divide over the Shaler Mountains (SM) is also shown, dispersing ice westward to Banks Island via Prince of Wales Strait. Principal orogenic belts are identified.

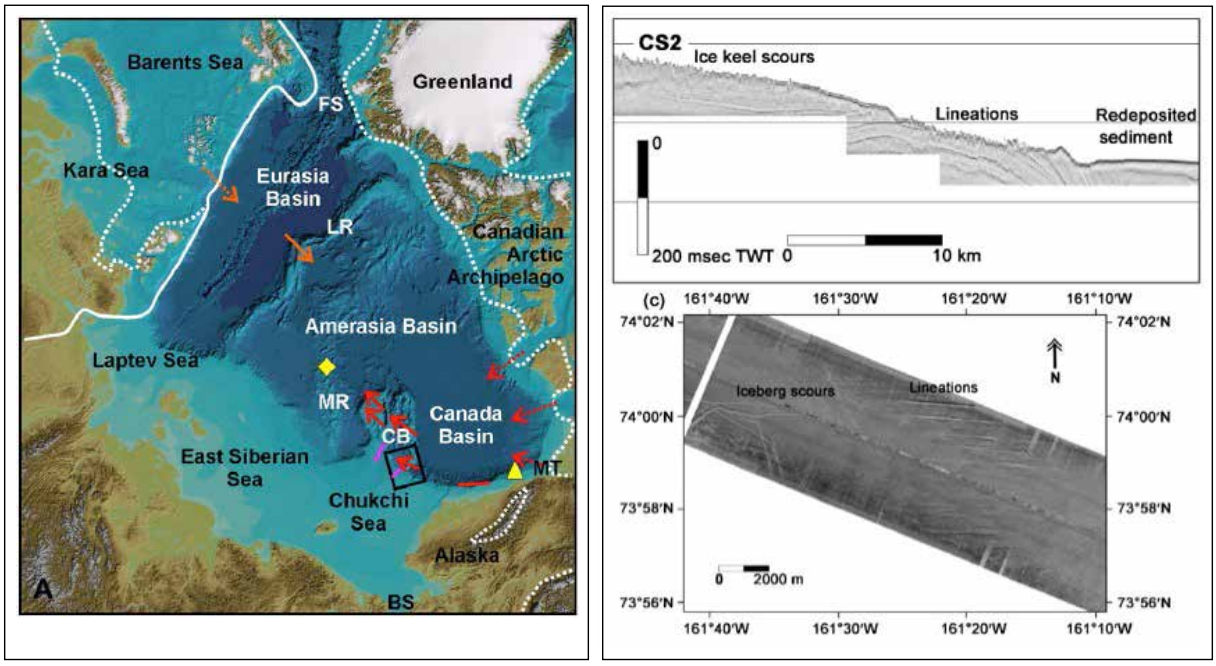

Fig. 2.18. Bathymetric map on left shows Arctic Ocean with mapped glaciogenic directional bedforms (solid bars/arrows) and suggested provenance (dotted arrows) from Polyak et al (2007). LR = Lominosov Ridge, MR = Mendeleev Ridge, CB = Chukchi Borderland, MT = Mackenzie Trough, FM = Fram Strait, BS = Bering Strait. White dashed line in western CAA is the ice sheet limit after Dyke et al (2002). Note the suggested Laurentide Ice Sheet provenance for glaciogenic features on the CB (including Northwind Ridge and Chukchi Plateau). Images on right, from Jakobsson et al (2008), show sidescan profile of glaciogenic bedforms (surface lineations) and iceberg scours on the Northwind Ridge (bottom left, *see* Canada Basin side of site CB on accompanying map). Chirp stratigraphic profile (top right) shows ice-keel scours in water depths up to 400 m and glacial lineations in depths up to 900 m (Jakobsson et al., 2008).

CHAPTER 3

GLACIOTECTONIC DEFORMATION AND REINTERPRETATION OF THE WORTH POINT STRATIGRAPHIC SEQUENCE: BANKS ISLAND, NT.

1. INTRODUCTION

Previous investigations of Neogene and Quaternary deposits preserved at the surface and within purportedly *in situ* subsurface sections across Banks Island proposed the lengthiest framework of environmental change in the Canadian Arctic Archipelago (CAA; Vincent, 1982, 1983, 1989, 1990; Vincent et al., 1983, 1984; Barendregt et al., 1998). The framework documented up to eight continental glaciations and five interglaciations associated with multiple marine transgression/regression cycles that span the entire Pleistocene (Vincent, 1990; Vincent et al., 1984; Barendregt et al., 1998). Stratigraphic units exposed at Worth Point, southwest Banks Island, form a critical type section reported to include a 'layer-cake' sequence of preglacial organics assigned to the Worth Point Fm, till from the earliest glaciation on Banks Island, and marine deposits from a glacioisostatically forced marine transgression during an intermediate glaciation (Vincent 1982, 1983, 1984, 1989, 1990, 1992; Vincent et al., 1984; Matthews et al., 1986; Barendregt et al., 1998). Magnetostratigraphic analyses of the Pleistocene units identified the Bruhnes-Matuyama magnetic reversal (0.78 Ma) at the contact between the Worth Point Fm and overlying till, forming an important marker horizon that permitted long-distance correlations between the Banks Island framework, magnetically constrained Arctic Ocean records, and

widespread North American Quaternary marine and terrestrial records (Clark et al., 1984; Barendregt et al., 1998; Darby, 2003; Ehlers and Gibbard, 2004; Ehlers et al., 2011). This chapter directly tests this elaborate and influential model.

Recently, the integrity of the Banks Island environmental framework has been challenged by a fundamental revision of the surficial geology of Banks Island (England et al., 2009; Lakeman and England, 2012, 2013; This thesis, Chapter 2). This research amalgamates all of the former multiple Quaternary till sheets (assigned to three glaciations, Vincent, 1982) into a single, island-wide Late Wisconsinan glaciation (England et al., 2009; Lakeman and England 2013; This thesis, Chapter 2). Consequently, this revised surficial model on Banks Island warrants the reinvestigation of the subsurface stratigraphy, whose events were assumed to mirror those of the previous, multiple glaciation model, including their proposed preglacial and postglacial seas and intervening interglacials.

New investigations of the stratigraphy at Worth Point indicate that the deposits are pervasively glaciotectonized, thereby contradicting the previously proposed 'layer-cake' stratigraphy and implicitly their former palaeoenvironmental interpretations. This chapter presents the sedimentology, structural geology and chronology of the Worth Point section and provides a revised architectural framework that constitutes the first detailed reconstruction of glaciotectonism on Banks Island, CAA (Figs. 3.1 and 3.2).

1. 1. OBJECTIVES AND METHODS

The objectives of this chapter are: 1) to describe the geomorphology, stratigraphy, sedimentology, glaciotectonic architecture and deformation

structures at Worth Point; 2) to reconstruct the glacial stress regimes responsible for glaciotectonism and to differentiate between deformation in proglacial, ice-marginal and subglacial environments; 3) to determine the number of glaciotectonic events responsible for deformation at Worth Point and their relative and absolute chronology, and; 4) to determine the role of permafrost in facilitating glaciotectonism and influencing the style and magnitude of deformation.

These objectives are achieved through a multidisciplinary approach combining geomorphology, stratigraphy, sedimentology and structural analyses. Separate lithologic units are identified and described according to grain size, sorting, depositional structures, deformation structures, inclusions, and degree of consolidation and lithification. The tectonostratigraphy of the bluffs is constructed based on lithostratigraphy, lithofacies boundaries, contacts and shear zones, the style of deformation (ductile or brittle) and the orientation of folds and faults. Specific attention is given to analyzing cross-cutting relationships and overprinted deformation structures in order to reconstruct the relative timing of tectonic events. The range of macro-scale deformation structures and their size, frequency and orientation are recorded. Four sections were selected to be logged in detail, each representative of a primary and diagnostic deformation style. Clast form and macrofabric analyses, as well as thin section analysis, were undertaken to discriminate between former depositional/deformational styles and environments. Absolute chronological control for the deposition of key glacial deposits was established through the employments of OSL dating (e.g. Wintle, 2010) and

relative chronological control was established through the analysis of cross-cutting and overprinted deformation structures.

1.2. REGIONAL SETTING

The coast of southwest Banks Island is subject to widespread slope failure and erosion due to ongoing submergence, enhanced coastal erosion as summer sea ice is reduced, and the melt-out of permafrost and buried glacial ice (Figs. 3.3a and 3.3b). The landscape is characterized by low arctic tundra inset by large river valleys draining westward to the Beaufort Sea across gently undulating terrain. Meltwater channels, small recessional moraines, and glaciotectonized landforms related to the former passage and wastage of Laurentide ice dominate the glacial geomorphology. Ice-pushed hills flanking the west coast of Banks Island are the most common glaciotectonic landforms, forming distinct topographic highs displaced by the westward flowing Laurentide Ice Sheet (LIS). The ice-pushed hill at Worth Point is mildly crescentic in shape with tectonized ridges forming the crest. The hill is associated with a similarly-sized depression directly inland (southeast) occupied by two lakes and adjacent tundra ponds, thought to mark the source depression (Fig. 3.2). Numerous coastal bluffs expose a detailed record of widely-correlated glacial and nonglacial Quaternary environments (Vincent, 1990; Barendregt et al., 1998).

2. RESULTS

Due to the detailed descriptions of complex lithofacies and deformation structures presented in the following section, important sedimentological and

stratigraphical interpretations are made throughout to aid the reader. The sedimentology of eight lithofacies identified in the Worth Point stratigraphic sequence are presented and interpreted first. Interpreted lithologic units are then placed into the broader context of the tectonic architecture at Worth Point. This architecture is subdivided into three major structural domains, A – C, from south to north. Each structural domain is presented and interpreted separately, with a representative section from each domain logged and described in detail to better characterize local deformation styles within dominant lithologic units. Finally, section-wide deformation structures are presented and interpreted in their spatial and stratigraphic context.

2.1. Sedimentology

Eight lithofacies are identified in the glaciotectonized Worth Point stratigraphic sequence. Original lithofacies thickness, geometry, and contacts remain unknown due to extensive deformation.

2.1.1. *Lithofacies 1: Laminated mudstone (Late Cretaceous Kanguk Formation – Kk Fm)*

LF 1 is the most exposed unit at Worth Point, extending below the base of the bluffs in many locations and occurring as stacked rafts > 30 m thick (Fig. 3.3c). It is composed of well-sorted, dark grey-brown clay displaying distinct bedding, presumably once horizontal. Individual laminae are < 1 cm thick, show little internal variation and contain no inclusions or lonestones. The unit reflects deposition in a stable, low-energy environment, most likely distal marine. LF 1 is interpreted to be distal marine mudstone of the Late Cretaceous Kanguk

Formation (Kk Fm). Comparable outcrops of mudstone assigned to the Kk Fm have been widely observed throughout the Canadian Arctic (Núñez-Betelu et al., 1994).

2.1.2. *Lithofacies 2: Cobble-gravel, sandstone and siltstone with compressed organics (Palaeocene-Eocene Eureka Sound Formation - ES Fm)*

LF 2 occurs as discrete rafts that are most common in the southern and central parts of the Worth Point stratigraphic sequence (Fig. 3.3d). It includes well-sorted, fining-upwards sequences of horizontally-bedded, quartzite-dominated cobble-gravel, imbricated granules-cobbles, cross-bedded granules and sand, silt, and flaser-bedded clay. The unit is semi-lithified to unlithified with compressed charcoal inclusions throughout. The most commonly exposed components of the fining-upwards sequence are cross-bedded silt and sand that have been stained green and red by presumed groundwater seepage. The sequence reflects deposition in a deltaic environment with channel, bar, overbank, and tidal deposits. LF 2 is interpreted to be the low-energy deltaic deposits of the Paleocene-Eocene Eureka Sound Formation (ES Fm). Comparable cyclic successions of sand, silt, shale and lignitic coal assigned to the ES Fm have been described on northern Banks Island and throughout the Canadian Arctic (Miall, 1976).

2.1.3. *Lithofacies 3: Sand and gravel with uncompressed logs and organics (Pliocene Beaufort Formation – Bft Fm)*

LF 3 occurs as discrete rafts and isolated pods, and has been commonly fluidized and remobilized throughout the Worth Point stratigraphic sequence (Fig.

3.3e). It includes unlithified, horizontally-bedded and occasionally cross-bedded, well-sorted sand and gravel, cross-bedded sand, and uncompressed and waterworn logs, peat mats and disseminated organics. The gravel clasts are very rounded (RWR = 68%; Fig 3.4, Sites 3 and 4), clast-supported, and dominated by quartzite, sandstone, and siltstone, with a noticeable lack of granite. Clast size is fairly consistent, with long-axes of 2.5 to 19 cm and a mode of 7 cm. Organics are unevenly dispersed throughout LF 3, but are locally concentrated, with peat mats extending laterally < 20 m and containing occasional whole logs. The clast-supported, occasionally cross-bedded nature of the sand and gravel suggesting deposition in a braided river channel, with cross-bedded sand recording bar deposition and localized concentrations of organics recording the build-up of overbank vegetation in former log jams and/or the establishment of vegetation in abandoned channels. LF 3 is assigned to the Pliocene Beaufort Formation (Bft Fm). The occurrence of unaltered wood (mostly conifers) and organics, associated with horizontally-bedded and cross-bedded sand and gravel are characteristic of the BFt Fm and are consistent with other exposures described across Banks Island (Fyles et al., 1994) and elsewhere in the CAA (Tozer, 1956; Craig and Fyles, 1960; Miall, 1979).

2.1.4. *Lithofacies 4: Crudely stratified mudstone with lonestones (glaciomarine diamict)*

LF 4 occurs as discrete rafts and is common in the central and northern section of the stratigraphic sequence (Fig. 3.3f). It comprises well-sorted, gray-brown clay that is compositionally similar to LF 1. However, LF 4 displays crude

bedding, presumably originally horizontal. Individual beds are ~ 10 cm thick and are visible only by a change in colour, not grain size. Small pebble-granule inclusions (< 5 cm) are dispersed throughout the unit and are largely composed of quartzite and sandstone with rare granite. Distinctly larger clasts (< 40 cm) are occasionally observed in the unit, and are commonly striated, associated with load structures, and composed of quartzite. To better differentiate between LF 1 and LF 4, electrical conductivity and pH analyses were undertaken on five samples of LF 1 and three samples of LF 4 from various locations along the bluffs. These analyses indicate that both units have similar pH values (LF 1 = 5.62 to 7.14 and LF 4 = 3.1 to 6.85). However, conductivity measurements indicate that LF 1 has consistently low conductivity values of 0.031 – 2.28 mS/cm whereas LF 4 has consistently higher values ranging from 10.3 – 16.8 mS/cm. The distinctly higher conductivity values for LF 4 may reflect enhanced porewater salinity as a result of more recent deposition (relative to LF 1) in a saline, marine environment. LF 4 is interpreted to be a glaciomarine diamict with striated dropstones, principally composed of reworked Kk Fm.

2.1.5. *Lithofacies 5: Unfossiliferous, coarse sand and gravel (glaciofluvial sand and gravel)*

LF 5 infills incised valleys that grade to below modern sea level in the northernmost section of the stratigraphic sequence (Fig. 3.3g). The valleys contain sub-horizontally (and occasionally horizontally) bedded sand and gravel that are both unlithified and unfossiliferous. The gravel is clast-supported and sub-rounded (RWR = 23%; Fig. 3.4, Sites 5 and 6), with 15% of clasts bearing striae.

The gravel is distinctly higher-caliber than in LF 3, with long-axes 10 – 35 cm with a mode of 22 cm. Dominant clast lithologies are quartzite, sandstone, and siltstone with occasional granite. Some small (< 20 cm) beds of sand-granules are interbedded with gravel and display crude cross-bedding. Two samples from the sand-granule interbeds were collected for optically stimulated luminescence (OSL) dating at the Sheffield Centre for International Drylands Research, University of Sheffield, UK. Minimum burial dates of 247±17 ka and 407±33 ka were obtained for the sand (quartz) grains using the single-aliquot regenerative technique. An age discrepancy of > 150 ka between the OSL dates necessitates that one must be incorrect, as discussed in Chapter 4. Regardless, both dates support aggradation of the sand and gravel during the Mid-Pleistocene (*sensu lato*). LF 5 is interpreted to be glaciofluvial sand and gravel, based largely on the coarse, striated nature of the gravel as well as the occurrence of erratic granite clasts.

2.1.6. *Lithofacies 6: Compact diamict (subglacial traction till)*

LF 6 occurs as fragmented pockets capping the central and northern parts of Worth Point (Fig. 3.3h). It includes a poorly-sorted, heterogeneous mix of clasts in a compacted silty-clay matrix. Clasts are mostly angular and sub-angular (RWR = 5%; Fig. 3.4, Sites 1 and 2), with 20% displaying striae. Dominant lithologies are quartzite, sandstone, and siltstone, with rare granite and gabbro clasts. A clast macrofabric reveals a distinct east-west orientation, with an S1 eigenvalue of 0.746 (Fig. 3.4, Site 2). LF 6 is interpreted as a subglacial traction

till (*sensu* Evans et al., 2006), due to its strong clast macrofabric, predominantly sub-angular clasts, far-travelled erratics and compaction.

2.1.7. *Lithofacies 7: Deformed and sheared heterogeneous diamict (glaciotectonite)*

LF 7 is only exposed at the former type-site of the Worth Point Fm, where it includes a sheared, deformed, faulted and reworked mélange of LFs 1, 3 and 4 (Fig. 3.3i). It is exceptionally heterogeneous, with attenuated pods of stiff, coarse-grained sand and gravel and semi-continuous mats of peat, wood, and disseminated organics derived from LF 3. This has been incorporated into a deformed clayey-silt matrix derived from LFs 1 and 4. LF 7 displays localized fluidization and remobilization of LF 3 and a distinct increase in crude sub-horizontal banding upsection. LF 7 is interpreted as a glaciotectonite.

2.1.8. *Lithofacies 8: Banded debris-rich ice and massive ice (buried glacial ice and intrasedimental ice)*

LF 8 is ubiquitous throughout the Worth Point section and comprises ice in two distinct forms: banded, debris-rich ice with striated clasts (Fig. 3.3j); and massive, clast-free ice (Fig. 3.3k). The banded, debris-rich ice is widespread in the southern and central parts of Worth Point where it occurs as isolated pods, rafts and larger tabular bodies (< 30 m^2) that form part of a thrust sequence with LFs 1, 2 and 3. Primary lithologies of debris within the ice are quartzite and sandstone derived from LF 2 and LF 3 as well as occasional ice-transported mafic and granite erratics. Debris within the ice ranges in size from mud to boulders (long-axes < 40 cm) and clasts commonly display striae. Individual bands of debris

range from 1 – 15 cm thickness. This ice is interpreted as buried glacial ice containing far-travelled erratics from at least southeast Banks Island as well as the Precambrian Shield on the Canadian mainland. The clast-free massive ice is also common throughout Worth Point where it tends to infill gaps and fault planes (usually < 1 m thick) rather than forming rafts and tabular bodies. This clast-free ice is interpreted to be non-glacial, epigenetic or syngenetic intrasedimental ice (Mackay, 1971, 1989).

These eight lithofacies collectively represent the primary stratigraphic units at Worth Point and are now presented in their tectonostratigraphic setting.

2.2. Tectonostratigraphy

The Worth Point stratigraphic sequence can be subdivided into three distinct structural domains (A-C) extending from south to north (Fig. 3.5). Each domain records a change in the intensity and style of deformation.

2.2.1. Domain A

Domain A forms the southernmost 2 km of Worth Point and is characterized by stacked, imbricated rafts of Kk Fm, ES Fm and Bft Fm (Fig. 3.5). Individual rafts tend to be composed of discrete bedrock units, suggesting that bedrock contacts acted as décollement planes. The imbricately stacked rafts are orientated towards 120° and are cross-cut toward the modern surface by bedrock rafts orientated towards 280°. The dominant dip direction towards 120° likely represents the primary direction of deformation, recording a SE-NW orientated stress field. Rafts demonstrating a cross-cutting dip direction towards 280° are interpreted to record the development of conjugate shears due to the

buildup of back stress. The dip of the thrust-faulted rafts progressively diminishes with elevation. For example, at the base of the bluffs, rafts dip at 50 - 80° whereas at the surface dips range from near horizontal to 30° (Fig. 3.5). The steeper thrust angles at the base of the cliff are attributed to the presence of permafrost (at least in patches) during deformation. Permafrost would have preserved the structural integrity of each unit, permitting strata to maintain a near-vertical orientation while withstanding compression and lateral compaction. Deformation becomes progressively more ductile towards Domain B (northward) where Kk Fm is the dominant lithofacies - indeed often the only material exposed for hundreds of meters.

Throughout Domain A, dense networks of faults dissect isoclinal and recumbent folds in the Kk Fm, creating rootless folds that often display drag structures (Figs. 3.6a and 3.6b). These folds are large-scale (amplitudes > 10 m) and likely evolved from symmetric gentle and open folds to asymmetric isoclinal and recumbent folds as glacially-imposed stresses increased. Several generations of folds can be observed, with a later set of tighter overturned folds cross-cutting a more open, rootless set. Disharmonic folds are widespread and indicate the onset of fold interference under a variable stress regime (Figs. 3.6c and 3.6d).

Throughout Domain A, the Kk Fm is heavily fragmented and dissected by a dense network of anastomosing jointing, essentially comprising a fault breccia (Fig. 3.3c). The distinct foliation developed during brecciation is superimposed on the bedding planes of the Kk Fm (see thin section analysis), often cross-cutting the primary bedding of the rafts but almost always paralleling the dip of the

thrust-faults bounding the raft. This indicates that the shear stress field responsible for brecciation was oriented in the same direction as the previous compressional stress regime responsible for the initial displacement of the bedrock raft. The fault systems may be contemporaneous, or the same faults may have been reactivated during subsequent shear deformation. Well-defined shear zones with measurable slickensides (Figs. 3.7a-3.7f) record displacement along shear planes, and indicate that the strata had significant sediment shear strength during deformation, likely reflecting the presence of permafrost.

The ES Fm forms part of the imbricate thrust sequence and is easily recognizable where it has been stained green and red by presumed groundwater seepage (Fig. 3.3d). Rafts of ES Fm display large-scale open folds that have been subsequently truncated by thrust-faults and reverse-faults (Fig. 3.8a). Elsewhere, clastic dykes are widespread throughout Domain A, testifying to the presence of liquid water and the patchy nature of permafrost (Figs. 3.8a–3.8c). The clastic dykes tend to comprise narrow branching networks of laminated massive sand and clay or large blow-out structures composed of coarse sand and gravel. In all cases, clastic dykes appear to have been injected into pre-existing faults and fractures, mostly along shear planes and thrusts. Because the material infilling the dykes is sourced from the host aquifer, it can be deduced that the coarse and permeable Bft Fm and ES Fm constituted the aquifers during glaciotectonism. The inclusion of cobbles, gravel, and occasional boulders (< 30 cm^2) within clastic dykes are testament to exceptionally high porewater pressures that fluidized the host aquifer (Rijsdijk et al., 1999).

Sheared and rotated blocks of glacial ice (< 10 m^2) occur throughout domain A. The ice is foliated with bands of debris that occasionally bear striated clasts (Fig. 3.3j). It is difficult to locate the precise contact with surrounding units as the debris within the ice is dominated by Kk Fm mud that is highly susceptible to ongoing failure during melt-out. Segregated ground ice lenses and sheets that parallel the bedding of the thrust and deformed strata are also widespread. Most of this ground ice clearly formed *in situ* prior to deformation; nonetheless, in some sections undisturbed ground ice has preferentially developed in faults and joints after deformation (Fig. 3.7b).

2.2.2. Sub-Domain A1

Sub-Domain A1 (Fig. 3.5) is located 1.2 km from the south end of Domain A where slumping has exposed an E-W orientated section (~10 m wide and ~6 m high) composed of stacked rafts of Bft Fm, ES Fm and Kk Fm (Fig. 3.9a). A raft of ES Fm dips at 25° towards 290° and is bounded by abrupt contacts with an overlying raft of Kk Fm and an underlying raft of Bft Fm, thereby forming an inverted sequence (i.e. the reverse order of original deposition). Because the displacement direction of the ES Fm raft is opposite to the main thrusting style observed in Domain A (orientated towards the southeast), it was likely back-thrust into position. The contact between the ES Fm and the overlying Kk Fm is characterized by numerous rip-up inclusions from the underlying ES Fm (Fig. 3.9b). Primary bedding structures within the ES Fm have been preserved, including flaser-bedded silt and clay overlain by compacted cobble-gravel, followed by cross-laminated sand and sand-pebbles. The excellent preservation of

fine bedding within the back thrust raft of ES Fm suggest that it must have been frozen, at least in patches, during emplacement (Figs. 3.9b and 3.9c). Several normal faults cross-cut the compacted cobble-gravel and indicate that brittle deformation occurred within the unit before failure was accommodated at the margins by back-thrusting. A change in the style of deformation is observed toward the base of the cobble-gravel. Here, gentle anticlinal and synclinal folds occur in the cobble-gravel, and sand intrusions with load structures penetrate upward into the flaser-bedded silt and clay. This change in deformation from brittle to ductile deformation toward the base of the ES Fm raft suggests that the lower part of the ES Fm raft remained unfrozen at the time of displacement, and continued to undergo ductile deformation while overlying coarser-grained sediments failed in a brittle manner.

Isolated bodies of debris-rich and foliated glacial ice form the contact between the raft of ES Fm and the underlying raft of Bft Fm (Fig. 3.9d). The ice appears to form broadly tabular rafts that consistently bracket rafts of ES Fm and Bft Fm. Because the glacial ice forms part of the thrust sequence, rather than cross-cutting the sequence, it is likely that it was emplaced contemporaneously.

2.2.3. Sub-Domain A2

Sub-Domain A2 is located at the very northern end of Domain A where a postglacial gully (Fig. 3.5) has exposed a section oriented E-W (~96 m wide and ~33 m high) composed of rafts of ES Fm, glaciomarine diamict and Kk Fm that pass distally (coastward) into folded Kk Fm (Fig. 3.10a). The most proximal (landward) units comprise a low-angle, thrust-faulted raft of ES Fm bracketed by

two rafts of Kk Fm (Fig. 3.10a). The rafts of ES Fm and Kk Fm dip at 10° orientated towards 120°, a direction that is consistent with the widespread southeast direction of thrust-faulted rafts throughout Domain A. This style of deformation presumably records a dominant compressional stress field generated by ice advancing from the source basin. Three imbricately stacked rafts of glaciomarine diamict, Kk Fm, and ES Fm truncate the low-angle, thrust-faulted rafts (Fig. 3.10b). The stacked rafts have been rotated into near vertical positions with dips of 75° - 85° orientated towards 280°. The high dip of the stacked rafts inclined away from the source basin, suggests that they have been back thrust into position, most likely in response to sustained lateral compaction and the buildup of back stress. Bracketing all the rafts in this proximal zone are intensely brecciated mélange zones displaying rip-ups that attest to a period of shear deformation (Figs. 3.7a, 3.7e and 3.7f). The base of deformation could not be observed due to a lack of exposure and likely extends below the gully bottom to a basal décollement.

The distal part of Sub-Domain A2 comprises Kk Fm displaying large-scale isoclinal folds fronted (coastward) by the core of a recumbent fold (Fig. 3.6c). The isoclinal folds have been compressed and subsequently thrust-faulted, leaving them rootless, with their original orientations indiscernible. The dissecting thrust-faults dip at ~ 45° orientated towards ~120° and were likely formed under the same stress regime as the low-angle, thrust-faulted rafts in the proximal zone of A2. The most distal part of A2 displays the core of a ~25 m long and ~30 m wide recumbent fold, with a plunge of ~20° orientated towards ~350°. The fold

displays no evidence of brittle deformation and records a period of continued ductile deformation by simple shear.

The magnitude and style of deformation changes clearly with distance along Sub-Domain A2, progressing from complex thrust-faulted rafts in the proximal zone (brittle deformation), to large-scale isoclinal folds dissected by thrust-faults in the central zone (ductile and brittle deformation), to large-scale recumbent folds in the distal zone (ductile deformation). This pattern of deformation, along with the general orientation of thrust-faults (toward the southeast), suggests that the section was initially deformed by a compressional stress regime imparted by an ice sheet advancing from the southeast. The development of intense shear zones and the onset of overfolding indicates that a later deformation event subsequently redeformed the section.

2.2.4. Domain B

Domain B forms 2.2 km of the central part of the Worth Point section and displays the greatest range of deformation (Fig. 3.5). This diversity is attributed to the presence of all eight lithofacies and hence their different responses to glacially-imposed stress, and to the strong overprinting of deformation structures generated by multiple intervals of overriding.

The southern and central parts of Domain B are characterized by thrust-faulted rafts of Kk Fm displaying convoluted, overturned folds that have a wide range of dip between 10-90° but a consistent orientation towards ~100°. These rafts of Kk Fm are intercalated with more localized thrust-faulted rafts of ES Fm that display a similarly wide range of dip between 10-90° also orientated towards

~100°. More gently dipping (0 - 45º) thrust-faulted rafts of glaciomarine diamict orientated towards ~130° are also common throughout Domain B. However, the glaciomarine rafts consistently cross-cut the thrust-faulted rafts of Kk Fm and ES Fm, requiring that they were emplaced during a later event. Nonetheless, the Kk Fm, ES Fm and glaciomarine diamict rafts have all been thrust-faulted into position by a compressional stress regime. Both the thrust-faulted rafts of Kk Fm and the cross-cutting thrust-faulted rafts of glaciomarine diamict have been subsequently dissected by dense networks of faults that commonly run perpendicular to southeast-dipping bedding planes and thrust-faults. The nature of faulting within the Kk Fm and glaciomarine diamict is so pervasive that the deformed units should be classified as breccias. Brecciation of the Kk Fm and glaciomarine diamict was likely contemporaneous, recording an even later deformation event. A lack of brecciation in the associated rafts of thrust-faulted ES Fm probably relates to the coarse-grained and permeable nature of this bedrock, which would have promoted lower porewater pressures and higher shear strengths. Bodies of debris-rich, buried glacial ice (< 20 m^2) are intercalated with thrust-faulted rafts of Kk Fm and ES Fm, and were presumably emplaced during initial compressional thrust-faulting. The buried glacial ice is not associated with a diamict, and was likely emplaced proglacially. Intrasedimental ice also commonly occupies thrust-faults, contacts between different lithologic units, and other easily exploitable spaces within the strata.

The central part of Domain B is capped by glaciofluvial sand and gravel and fragmented pockets of diamict (Fig. 3.5). The glaciofluvial sand and gravel

infill three shallow (< 5 m deep) and wide (~40 m wide) channels that incise the uppermost strata, including buried glacial ice. The gravel is coarse, poorly-sorted, and sub-horizontally bedded, with limited evidence for post-depositional deformation. Overlying the glaciofluvial sand and gravel with an angular unconformity are two pockets of consolidated diamict (~10 m wide and ~2 m high). The diamict is indurated and characterized by a sandy-silt matrix, highly angular to sub-angular clasts (RWR = 7%; Fig. 3.4, Site 1) including rare granites and is interpreted as a subglacial till.

The northern part of Domain B is characterized by a glaciotectonite (~20 m thick) comprising sheared rafts of Bft Fm, glaciomarine diamict and Kk Fm (B1). The Sub-Domain B1 outcrop exposing the glaciotectonite forms the most enigmatic site at Worth Point and is easily identifiable by logs and peat (sourced from the Bft Fm) eroding out of the bluffs (Figs. 3.11a and 3.11c). This thick organic unit was originally assumed to be *in situ* and proposed as the type section for the preglacial Worth Point Fm (Vincent 1982, 1983, 1984, 1989, 1990, 1992; Vincent et al., 1984; Matthews et al., 1986; Barendregt et al., 1998).

2.2.5. Sub-Domain B1

Sub-Domain B1 is located at the northern end of Domain B where a coastal section oriented N-S (~27 m high and ~20 m wide) exposes a diverse glaciotectonic sequence (Figs. 3.11a – 3.11c). The section has been dissected by a postglacial valley on its southern edge, which exposes an additional 5 m of the section, perpendicular to the coast (Fig. 3.11c). Here, the section is composed of a

sheared and deformed mélange of glaciomarine diamict, Kk Fm and Bft Fm that is interpreted to be a glaciotectonite.

A contiguous raft of Bft Fm forms the base of the section. Ongoing melt-out of ground ice in the overlying strata makes it impossible to determine the precise dip of the raft, but bedding within the raft dips 30° orientated towards 130°. Because the gravel is planar-bedded, this dip is considered to record the displacement of the raft itself. A thrust-faulted raft of glaciomarine diamict, displaying widespread evidence of shear, overlies the Bft Fm and forms the base of a thick glaciotectonite mélange (Fig. 3.11b). The glaciomarine raft contains isolated pods of Bft Fm that have been attenuated, rotated and sheared (Fig. 3.11d). Disharmonic anticlines and synclines with smaller-scale parasitic folds within the glaciomarine diamict have been cross-cut by thrust-faults and back thrusts. Clastic dykes infilled with wood fragments, peat, sand, and gravel sourced from the basal raft of Bft Fm have been injected upwards into the glaciomarine diamict and commonly exploit pre-existing shear planes and faults (Fig. 3.11d). Localized zones of massive Bft Fm sand and gravel within the glaciomarine diamict (sourced from the underlying Bft Fm) attest to the fluidization and remobilization of sediment during shearing. The basal raft of Bft Fm clearly formed an aquifer that expelled groundwater under high porewater pressures into the overlying strata.

Semi-coherent rafts of organic-rich beds sourced from the Bft Fm have been preserved within the overlying glaciotectonite. The lowermost organic raft is the most prominent and comprises water-worn but uncompressed logs and wood

(Figs. 3.11b and 3.11c). Two overlying rafts comprise laterally continuous peat mats that extend horizontally for ~20 m (Fig. 3.11b). Although organics have been sheared from the margins of the rafts and incorporated into the surrounding glaciotectonite, the lateral continuity of the rafts and the excellent preservation of organics within the rafts suggest that they were frozen during original transport and deposition. Although Bft Fm wood has not been observed *in situ* on southern Banks Island, the lake basins directly behind Worth Point are the most probable source for these organic rafts.

A raft of Kk Fm has been stacked above the uppermost organic raft and incorporated into the glaciotectonite mélange. The glaciotectonic sequence extending upward from the Kk Fm raft comprises sheared pods of glaciomarine diamict and Kk Fm with minor pods of sand and peat sourced from the underlying Bft Fm. The sequence distinctly lacks the widespread faults and clastic dykes observed down-section (Fig. 3.11d) and instead displays crude sub-horizontal banding that becomes increasingly more prominent with distance up-section (Figs. 3.11e and 3.11f). Where evidence of fluid injection is observed, it tends to be in the form of small blow-out structures infilled with coarse sand sourced from localized pods of Bft Fm. These smaller-scale blow-outs likely formed in response to ongoing shear deformation.

The conspicuous nature of the sediments eroding from the base of Sub-Domain B1 (i.e. whole logs and peat mats) create the impression of decreasing deformation up-section. At the base, a wide variety of lithologic units outcrop, including coarse sand, gravel and organics. These different lithologic units have

varying permeability and shear strength that would have responded differently to applied stress. Consequently, a complex mosaic of ductile deformation (in the fine-grained units) and brittle deformation (in the coarse-grained units) would likely have ensued. The sub-horizontal banding in the glaciotectonite farther up-section attests to high cumulative strain and a probable increase in the magnitude of deformation with elevation. This pattern of cumulative strain up-section has been proposed to characterize many subglacial shear environments (Banham 1977; Pedersen 1989; Hiemstra et al., 2007; Benn and Evans, 2010). The possible existence of 'warm' permafrost (close to its melt point) within a subglacial shear zone, may also explain the development of frozen, competent pods of 'hard-frozen' coarse-grained sediment observed within the weaker matrix of 'plastic-frozen' fine-grained sediment (Waller et al., 2011).

Finally, the glaciotectonite is capped by ~1 m of fining-upward sequences of pebble-granules, silt, and clay. This sequence is interpreted to record the deposition of mass flow deposits into standing water during deglaciation, when unconsolidated sediment was reworked and locally re-deposited in small ponds and basins. Collectively, Sub-Domain B1 comprises a basal raft of Bft Fm overlain by a thick glaciotectonite mélange displaying cumulative strain up-section, which in turn has been capped by mass flow deposits.

2.2.6. Domain C

Domain C forms the northernmost and least deformed part of the Worth Point section (1.8 km, Fig. 3.5). This domain is characterized by low-angle, thrust-faulted and back thrust rafts of Kk Fm, crosscut by thrust-faulted rafts of

glaciomarine diamict. Subsequently, narrow, V-shaped gullies have been incised into these units and then infilled with coarse glaciofluvial sand and gravel.

Thrust-faulted and back thrust rafts of Kk Fm both display low dips of 10-30°. However, back thrusted rafts are orientated towards 130°, as is common throughout Domains A and B, and thrust-faulted rafts are orientated towards 80-100°. Throughout Domain C the southeast-dipping back thrusts have been consistently cross-cut by the eastward-dipping thrust-faults, reflecting a subsequent E-W oriented stress field and deformation event. The low dip of both sets of thrusts suggest that Domain C did not experience strong compression or lateral compaction, but rather occupied a zone of unconstrained thrust propagation with reduced stress, presumably distal to the ice margin.

The rafts of Kk Fm display low-amplitude gentle to open overfolds and recumbent folds that are truncated by widely spaced (every > 30 m) low-angle faults. Localized shear zones exhibiting brecciation along fault planes become increasingly less common towards the northern part of Domain C. The thrust-faulted rafts of glaciomarine diamict orientated towards ~80°, cross-cut the back thrust rafts of Kk Fm dipping towards 130°, but appear to be consistently orientated in the same direction as the thrust-faulted rafts of Kk Fm. Nonetheless, the rafts of glaciomarine diamict display distinctly less ductile deformation than the rafts of Kk Fm. Furthermore, the glaciomarine rafts often cap the Kk Fm towards the top of the bluffs and have been thrust as coherent rafts along distinct eastward-dipping thrust-faults in several locations. Clearly the Kk Fm underwent initial ductile deformation followed by back thrusting imposed by a stress regime

oriented SE-NW. After the deposition of glaciomarine diamict a second, E-W orientated stress regime was responsible for thrust-faulting the glaciomarine diamict and some rafts of Kk Fm.

Three prominent V-shaped gullies and several smaller ones (see Figs. 3.12a and 3.12b) incise the Kk Fm and glaciomarine diamict. The gullies descend below the base of the bluffs and therefore grade to a former relative sea level below modern. The gullies are moderately deep (< 30 m) compared to their width (~100 m) and are separated by narrow, angular interfluves of Kk Fm (< 10 m). Laterally continuous, sub-horizontally (and occasionally horizontally) bedded glaciofluvial sand and gravel infill the gullies and are in turn unconformably overlain by fragmented pockets of compact diamict and fining-upward sequences of sand, silt and laminated clay. This infill is interpreted to record a subsequent marine transgression and/or an abundant sediment supply, possibly from a nearby ice margin.

2.2.7. Sub-Domain C1

Sub-Domain C1 constitutes the northernmost end of Domain C and has a fully exposed section (~29 m high and ~200 m wide) through one of these gullies (Fig. 3.5). Here, the infilling gravel is mostly sub-rounded with a minor fraction of sub-angular clasts bearing striations and boulders < 40 cm^2. The clasts are dominantly quartzites sourced from Victoria Island to the east and occasional granites sourced from mainland Canada to the southeast (Figs. 3.12a and 3.12b). The presence of granites, along with the coarse and unfossiliferous nature of the gravel, distinguishes the glaciofluvial gravel from the preglacial Bft Fm. Two

samples from separate beds of sand interbedded with the gravel provide minimum OSL burial ages of 247±17 ka and 407±33 ka (Sheffield Centre for International Drylands Research, UK, 2012). This constrains the glaciofluvial aggradation to the Mid-Pleistocene (*sensu lato*), as well as the presumed marine transgression required to facilitate their aggradation. The gravel appears undisturbed across tens of meters (laterally and vertically) making it difficult to determine if the bedding dip of ~15° towards 080° records minor thrusting as coherent rafts or its original depositional slope (i.e. delta foresets prograding offshore). Nonetheless, the dip direction of the gravel is consistent with the orientation of the second set of thrust-faults observed in the Kk Fm as well as to the glaciomarine diamict throughout Domain C. This suggests that the gravel, glaciomarine diamict, and thrust-faulted Kk Fm were deformed by the same glaciotectonic event following glaciofluvial aggradation.

A clast-supported diamict (Fig. 3.3h) overlies the glaciofluvial sand and gravel with an angular unconformity. The diamict has a compacted clay-silt matrix displaying a wide range of clast size and shape. Clasts within the diamict are faceted and striated, and a clast macrofabric displays an east-west orientation with an S1 eigenvalue of 0.746 (Fig. 3.4, Site 2). Based on its strong fabric, clast forms, and surface striae, the diamict is interpreted as a subglacial traction till. As such, the till provides direct evidence for the overidding of Worth Point by an ice sheet after a Mid-Pleistocene regression and transgression that incised and later infilled the incision of the V-shaped gullies plus at least one deformation event responsible for the folding and back-thrusting of the Kk Fm. Multiple sequences

of poorly sorted clasts and granules, fining-upward into sand, silt and laminated clay, overlie the till. The localized nature of the fining-upward sequences likely reflects the remobilization of unconsolidated glacial deposits and their re-deposition into small ponds and basins via mass flows.

2.3. Deformation styles and structures

At Worth Point, permafrost has preserved deformation styles and structures developed in a wide range of lithologic units, providing insights into lithologic-specific responses to glacially-imposed stress regimes (Aber, 1985). Coarse-grained units at Worth Point (Bft Fm, ES Fm, glaciofluvial sand and gravel) are characterized by brittle deformation. These lithologic units commonly form discrete bedrock rafts with well preserved internal bedding and depositional structures (e.g. Figs 3.7a, 3.9b-3.9c, 3.10a-3.10b). These coarse-grained sediments possess high shear strength during deformation due to high frozen porewater content, resulting in large-scale brittle failure along discrete planes of weakness. Coarse-grained sediment is expected to undergo brittle failure when grains are firmly cemented by pore ice, which occurs at temperatures of < -0.5°C in sand (Waller et al., 2012). The presence of permafrost at Worth Point would have helped to maintain temperatures below -0.5°C, thereby promoting continued large-scale brittle failure. Where coarse-grained sediment displays minor ductile deformation, it is closely associated with the pervasive deformation of the surrounding sediment, as observed within the glaciotectonite mélange at Sub-Domain B1 (Fig. 3.11d). This minor ductile deformation may relate to an increase in glacially-imposed stress and/or an increase in temperature (warming of

permafrost) towards the pressure-melting point. If temperatures did increase sufficiently, more porewater would be available to create a partially-frozen slurry of ice, water, and sediment. Clearly, increasing the volume of liquid water would reduce sediment shear strength (greater dilation) and promote ductile deformation (Twiss & Moores, 1992; Waller et al., 2012).

Fine-grained sediment deformation at Worth Point (Kk Fm and glaciomarine diamict) is characterized by complex, large-scale, pervasive folding (e.g. Figs. 3.6a-3.6b). Because permafrost is inferred to have existed at Worth Point, at least in patches, fine-grained sediment must have undergone ductile deformation at subzero temperatures. The direct juxtaposition of ductile deformation in fine-grained sediment, and brittle deformation in frozen, coarse-grained sediment (clearly displayed in Sub-Domain C1) supports the existence of 'warm permafrost' (Waller et al., 2009). Warm permafrost is characterized by temperatures below, but close to, the melt point that permits relatively high amounts of water to exist within fine-grained sediment, possibly down to -7°C in very fine-grained clays (Tsytovich, 1975; Waller et al., 2012). The existence of warm permafrost would explain the wide range of brittle and ductile deformation observed within different lithofacies at Worth Point.

No doubt, a wide range of interconnected factors influenced the style of deformation at Worth Point, and not all factors are lithologically-specific. The ratio of liquid to frozen porewater contained in sediment - controlling its shear strength - is a function of grain-size and temperature, but also a function of stress (Waller et al., 2012). These variables would have changed at Worth Point as

glaciers advanced and retreated across the permafrost terrain. For example, when ice initially advanced over Worth Point, permafrost likely would have been thick and continuous, promoting brittle deformation. However, as ice persisted at Worth Point, permafrost would have warmed from the bottom-up by geothermal heating (Dyke, 1993), favouring the addition of water as well as more ductile deformation (cf. Mooers 1990a, b; Waller et al., 2012). Therefore, the variable physical properties of the permafrozen sediment at Worth Point, and their consequent response to changeable glacial stress regimes, would have evolved over the course of multiple phases of glaciotectonism. This evolution would have resulted in the diverse spectrum of juxtaposed deformation described here.

Further insights into the dynamics and style of glaciotectonic deformation at Worth Point can be inferred from the analysis of macroscale structures such as shear zones, clastic dykes, and boudins. Shear zones are extensive, spanning a wide range of scales and a broad range of stratigraphic settings (Figs. 3.7a-3.7f). Shear zones are defined as 'planar zones of relatively intense deformation' that are characterized by brittle faulting and brecciation (Phillips et al., 2011). Brecciation attests to exceptionally high shear stress common to subglacial environments (Pedersen, 1980; McCarroll and Rijsdijk, 2003). The most complex shear zones have developed between sheared bedrock rafts of different lithologies. In these stratigraphic settings, sediment from the two rafts have been ripped-up, detached, and rotated in an inter-raft mélange (Figs. 3.7a, 3.7e and 3.7f). The edges of the sheared rafts often display pervasive brecciation and/or clast imbrication (Fig. 3.7d), likely recording deformation under a sustained shear

stress within a brittle subglacial shear zone (van der Wateren 1995; Eyles and Boyce 1998). Two thin-section samples of Kk Fm were collected from a brecciated surface displaying slickensides that dip 80˚ towards 180˚ (Fig. 3.13a). Analysis of the thin sections provides additional insight into the nature of microscale deformation at Worth Point and record the presence of two dominant fabrics (Figs. 3.13b and 3.13c). A primary fabric (S1) is crosscut, often at right angles, by a secondary fabric (S2). The secondary fabric displays small-scale faults that have displaced the primary fabric and in some areas completely overprinted the primary fabric with a dense network of foliations. Irregular open fissures are common and often develop where larger foliations intersect.

Clastic dykes result from hydrofracturing and are common within the glaciotectonized sequence at Worth Point (Figs. 3.8b-3.8d). This association is unsurprising given that: a) glaciotectonic environments are regions of high stresses that overpressurize water, and b) faulting and thrusting associated with glaciotectonic deformation provide escape routes for the overpressurized water and sediment (Rijsdijk et al., 1999; Le Heron and Etienne, 2005; Piotrowski, 2006; Phillips and Merritt, 2008; Van der Meer et al, 2009). At Worth Point, it is also possible that patchy permafrost - combined with impermeable strata such as Kk Fm and glaciomarine diamict - further enhanced hydrofracturing by forming aquicludes that confined water to aquifers. Eventually, the overpressurized water and sediment would have burst-out of these aquifers into surrounding strata, exploiting pre-existing faults and fractures. The pressures generated during the burst-out of overpressurized water and sediment would have been sufficient to

liquefy the host sediment, injecting it into the hydrofracture (cf. Le Heron and Etienne, 2005).

At Worth Point, two different types of clastic dykes are differentiated. The first comprises clastic dykes that have been injected along recognizable faults and shear planes (i.e. high strain zones). These dykes often narrow upwards and are infilled with coarse-grained sand and gravel sourced from the Bft Fm (figs. 3.8a and 3.8b). Such characteristics indicate that the dykes formed under high hydraulic pressure released in a single event, leading to the deposition of the coarse sand and gravel as a massive unit. Blocked subaerial escape routes (possibly due to the presence of ice) may have allowed hydraulic pressures to build to high levels, resulting in debris liquefaction and the entrainment of large cobbles within the escaping fluid from host aquifers. The narrowing-upward configuration of the dykes suggest that they were expelled upward into the strata from an underlying aquifer. Similar upward-filled clastic dykes have been described from a subglacially glaciotectonised stratigraphic sequence at Killiney Bay, Ireland (Rijsdijk et al., 1999). There, the host aquifer also comprised permeable coarse gravel that became hydraulically confined by an impermeable unit of overlying till. The resulting clastic dykes are up to 7 m long, frequently branch into complex geometries, and yet remain rooted in their source gravel aquifers (Rijsdijk et al., 1999). At Worth Point, the upward-filled, coarse-grained dykes occasionally crosscut one another (Fig. 3.8b). Such cross-cutting patterns record multi-phase hydrofracturing within the same water-escape route that follows major shear planes and fault surfaces. Comparable ‘high strain zones’ at

the contact between thrust-faulted rafts are known to have provided a focus for hydrofracturing during subglacial glaciotectonism at Clava, Scotland (Phillips and Merritt, 2008). Similarly, coarse-grained clastic dykes at Worth Point likely reflect hydrofracturing in a subglacial setting.

The second type of clastic dyke is closely associated with strata displaying evidence for compressional deformation. These dykes comprise finer branching networks of narrow (< 20 cm wide) channels infilled with laminated sand and clay (Fig. 3.8c). These laminated clastic dykes clearly record hydrofracturing under lower hydraulic pressure that permitted the sorting of grain size during settling and infilling (Van der Meer et al., 2009). These dykes are commonly injected along smaller faults and joints (mostly in the Kk Fm) and are often truncated by faults themselves. This second type of clastic dyke is considered to have developed in an ice-marginal setting when compressional stresses overpressurized aquifers, but the potential for fluid to escape to the surface, unimpeded by ice, resulted in lower hydraulic pressure.

Boudins are widespread deformation structures throughout Domain A. Here, they are composed of coarse-grained Bft Fm sand and gravel, and form streamlined inclusions within complexly deformed Kk Fm (Fig. 3.6d). The boudins consistently display attenuation in a sub-horizontal direction and have been transported within a plastic Kk Fm matrix. These orientated boudins support deformation within a ductile shear zone (cf. Benn and Evans 1996).

3. INTERPRETATION

The internal architecture of Worth Point accords with the surficial geomorphology comprising an ice-thrust hill < 50 m asl that steepens distally (coastward, Fig. 3.2). Subtle crescentic ridges forming the crest of the hill are assumed to reflect the position of prominent thrust rafts outcropping beneath the capping unit of subglacial till. Two lakes with a similar orientation to the hill are located directly inland and are interpreted to occupy the source depression from which the hill was derived (Fig. 3.2). Consequently, the landform is interpreted as a hill-hole pair and similar examples commonly flank the west coast of Banks Island farther north. Construction of the Worth Point hill-hole pair is attributed to the advance and overriding of southwest Banks Island by thin, cold-based ice margins emanating from divides to the southeast during the Mid-Pleistocene (*sensu lato*) and Late Wisconsinan (Lakeman and England, 2013). Geomorphic evidence, primarily the configuration of deglacial ice-marginal meltwater channels, indicates that Laurentide ice crossed the interior of Banks Island during the Late Wisconsinan, including the Kellett and Lennie River valleys surrounding Worth Point (Fig. 3.2; This thesis, Chapter 2). Of these, ice descending the Kellett River Valley, south of Worth Point, is considered the primary source for constructing the Worth Point hill-hole pair. Nonetheless, convergence of cold-based ice lobes from both the Kellett and Lennie River valleys likely contributed to multiple periods of glaciotectonism along the intervening coastline (Fig. 3.2). Although bathymetric profiles support westward ice flow through Amundsen Gulf (Blasco et al., 2005; MacLean et al., 2012), the passage of this trunk ice onto

Banks Island appears to have been limited to a prominent lateral moraine paralleling its south coast (< 1 km inland). Therefore, trunk ice in Amundsen Gulf is not invoked to explain glaciotectonism at Worth Point.

Permafrost at Worth Point, and along the west coast of Banks Island, undoubtedly augmented glaciotectonism. Although current permafrost on southwest Banks Island is continuous and likely > 750 m thick (Taylor et al., 1996), periods of permafrost degradation likely occurred in the past. For example, Worth Point is located on the Beaufort Sea coast where raised marine sediments OSL dated between 94 ± 4.2 ka and 118 ± 5.7 ka support a marine isotope stage (MIS) 5 transgression that would have degraded terrestrial permafrost thickness below ~11 m asl today (Lakeman and England, 2013; This thesis, Chapter 2). Earlier marine transgressions (to unspecified elevations) are also inferred at Worth Point based on the deposition of glaciomarine diamicts observed in Domains B and C, as well as the glaciofluvial aggradation observed in Domain C. The occurrence of thinner permafrost would have facilitated thrusting and deformation at Worth Point, like thrust-dominated landforms noted elsewhere throughout the Canadian High Arctic (Evans and England, 1991). In these cases, thrust-block moraines produced by late Holocene readvances are widespread on valley floors well below marine limit. Here, the reaggradation of permafrost is shallow (10's vs 100's of meters) due to the recent emergence of areas below ~40 m asl that favour surface décollement produced by widespread Neoglacial readvances (Evans and England, 1991). A similar relationship between degraded (thinner) permafrost and ice-thrusting would have characterized Worth Point

following earlier marine transgressions/regressions associated with ice advance and retreat. The close association between thrust-dominated landforms, such as thrust-block moraines and hill-hole pairs, and former areas of shallow modern permafrost at low elevations in the Canadian Arctic raises the likelihood that shallow permafrost is a primary condition for the initiation of thrusting (Evans and England, 1991; Boulton, 1999). A critical range of permafrost and glacier ice thicknesses may exist, within which deformation is promoted by effective ice-bed coupling, provided that suitable material for deformation is also present. Alternatively, others have proposed that glaciotectonic deformation and thrust mass construction is due to glacier surging (Sharp 1985, 1988; Croot 1988; Evans and Rea 1999, 2003; Evans et al. 2007). If so, former ice sheet surges may have been involved in the production of some Banks Island moraines regardless of accompanying permafrost characteristics (cf. Evans et al. 1999, 2008). Currently, the formation of the Worth Point hill-hole pair is attributed to thin, cold-based ice lobes that would have been unlikely to surge.

A bedrock boundary approximately 2 km east of Worth Point may have contributed to glaciotectonism because the source depression of the hill-hole pair coincides with the contact between Kk Fm to the west (coast) and Bft Fm to the east (inland). The coarse Bft Fm is permeable, and therefore during ice advance, expelled groundwater could drain freely through/beneath it towards the impermeable Kk Fm. Hence, when ice reached the fine-grained Kk Fm, increased groundwater drainage there would have raised porewater pressures and reduced its frictional strength, serving to initiate glaciotectonic deformation coastward of

this bedrock boundary. Furthermore, permafrost is inferred to have played a fundamental role in influencing the subsequent *style* of deformation at Worth Point. For example, it is thought that permafrost was locally warm and patchy, promoting hydrofracturing along with the development of contrasting deformation styles in coarse-grained (brittle) and fine-grained (ductile) lithofacies. Such permafrost characteristics have been inferred to explain similarly contrasting deformation observed in glaciotectonized stratigraphic sequences in the Mackenzie Delta to the south of Banks Island (Waller et al., 2012). As well, the wide range of lithologic units in the subsurface at Worth Point may have further enhanced deformation (Boulton, 1972). Contacts between lithologic units appear to have formed décollement planes along which displacement occurred more readily, promoting the formation of discrete bedrock rafts. Moreover, because the style and magnitude of deformation is directly related to the grain size, sorting, and cohesion of sediments, the wide range of lithofacies at Worth Point would have produced a range of deformation processes and structures. This diversity of structures was enhanced further by the strong overprinting and cross-cutting of multiple generations of deformation structures and styles throughout Domains A-C. Based on this overprinting, two distinct glaciotectonic events with multiple stress regimes have been identified. Key stratigraphic evidence to support each glaciotectonic event is presented below.

3.1. Relative chronology of glaciotectonism and relative sea level change

3.1.1. Glaciotectonic event 1

Throughout the Worth Point stratigraphic sequence (Domains A-C), the dominant orientation of thrust-faulted rafts is SE-NW. Therefore, it is assumed that the ice margin responsible for this deformation also advanced from the southeast, down the Kellett River (Fig. 3.2). The location of lakes and tundra ponds in a basin ~2 km to the southeast of the bluffs reinforces the interpretation that they mark the source depression from which the ice-pushed hill at Worth Point originated. If so, the bluffs provide an exposure at a right-angle to the thrust, with Domains A-C displaying a progressive proximal to distal deformation sequence (Fig 3.14, Box 8).

All Domains are dominated by thrust-faulting produced by compression, most likely generated ice-marginally, as manifested today across the northern part of the CAA (Evans and England, 1991; McCarroll and Rijsdijk, 2003). The dip and number of thrust-faulted rafts decrease northward (from Domain A–C) because the compression from the former ice margin also decreases in this direction (cf. Mulugeta and Koyi 1987). Accordingly, the most proximal area (Domain A) displays imbricately stacked rafts of thrust-faulted bedrock (nearly vertical). Towards the surface, these bedrock rafts have been truncated by more gently dipping back-thrust rafts. This back thrusting is well displayed in Sub-Domain A2 (Fig. 3.10b) where back-thrust rafts of ES Fm, Kk Fm and glaciomarine diamict truncate thrust-faulted bedrock. As the dip of thrust-faulted bedrock rafts decreases northward in Domain B, fold preservation increases.

Large-scale isoclinal folds with drag structures are widespread in Domain B, and likely evolved from open, symmetric folds that steepened and overturned in places, becoming unrooted during lateral compression. Domain C is the most distal and least deformed domain, displaying large, open, symmetric folds truncated by low angle thrust-faults and back thrusts. This pattern of thrust-faulting, back thrusting, and stacking in proximal, intermediate, and distal positions is typical of what is described as ice-marginal piggy-back thrusting (Rotnicki 1976). Piggy-back thrusting involves the development of new thrusts distal to previously active thrusts, resulting in the stacking of proximal thrusts into increasingly steeper positions (as displayed in Domain A). This includes the transport of these proximal thrusts, piggy-back style, onto less steeply dipping, distal thrusts below (as displayed in Domain C and modelled by Mulegeta and Koyi, 1987). In contrast, back thrusts result from the build-up of backstress during the later stages of stacking and lateral compaction. The overall pattern of progressively more ductile deformation with distance from the ice margin (toward Domain C) is presumably related to an increased preservation of folds in the distal zone where fewer, lower-angle thrusts truncate the previously folded strata. Comparable proximal to distal glaciotectonic sequences are common at former ice-margins, including the Rubjerg Knude glaciotectonic complex in northern Denmark (e.g. Pedersen, 2005), and the polydeformed Quaternary stratigraphy of East Anglia, England (e.g. Phillips et al., 2008).

Throughout Domains A-C narrow, branching networks of clastic dykes infilled with laminated sand and clay are closely associated with deformation

structures generated by ice-marginal thrusting. This stratigraphy is consistent with this setting, where overpressurized water would have been expelled preferentially along pre-existing faults, joints, and lithologic contacts toward the unconfined surface beyond. The movement of pressurized fluid along these planes of weakness would have reduced the frictional strength of the adjacent sediment, promoting displacement and thrust propagation. Blocks of buried glacial ice containing far-travelled erratics from the Precambrian Shield on the Canadian mainland also form part of the thrust sequence, and would have been thrust into position contemporaneously. It is simplest to envisage this glacial ice pre-existing at Worth Point prior to glaciotectonic event 1, rather than being sourced from the ice sheet responsible for glaciotectonic event 1 itself. Because the glaciotectonite (Domain B), glaciomarine diamict, glaciofluvial sand and gravel, and subglacial till (Domains B and C) do not form part of the piggy-back sequence, they were presumably deposited and deformed after initial ice-marginal compression.

Throughout Domains A-C, a second generation of deformation structures is imprinted onto the thrust sequence. The overprinted structures are characterized by simple shear, characteristic of subglacial deformation (McCarroll and Rijsdijk, 2003). Domain B best preserves sediments and deformation structures generated by this later event, including a ~20 m thick glaciotectonite mélange, intensely brecciated bedrock, and widespread macroscale shear structures such as boudins (e.g. Figs. 3.11d–3.11f). Thin section analysis of brecciated Kk Fm sampled from Domain B indicates that this deformation was penetrative, with sediment modification at the granular scale (Figs. 3.13b and 3.13c). This reflects

deformation within faulted rafts rather than displacement along fault planes. Sub-horizontal strain banding and intense ductile deformation within the glaciotectonite mélange (Domain B1) provide further support for high cumulative strains, probably within a ductile subglacial shear zone (McCarroll and Rijsdijk, 2003). Collectively, this deformation records the development of a subglacial shear zone when a later ice advance overrode Worth Point.

The southeast orientation of shear planes and shear-related foliation (mostly in Domain B) associated with subglacial shear are consistent with the southeast orientation of thrust-faulted rafts developed during previous ice-marginal compression (throughout Domains A-C). The simplest interpretation of the uniform orientation of the deformed strata during both ice-marginal and subglacial deformation is that they relate to the same stress field from the same ice sheet advancing from the southeast, possibly oscillatory in nature. Subglacial deformation resulted in the development of recumbent and overturned folds superimposed on the pre-existing structures, creating complex fold interference and boudinage (Figs. 3.6a-3.6d). Large clastic dykes are also widely associated with the sheared deformation sequence throughout Domains A-C (Figs. 3.8b and 3.8c), recording hydrofracturing in a subglacial environment.

Two marine transgressions and regressions are recorded in the sequence associated with glaciotectonic event 1. Glaciomarine diamict forms part of the sheared deformation sequence in Domains B and C and is a key component of the glaciotectonite at Sub-Domain B1, but is not observed within the piggy-back thrust sequence. The incorporation of glaciomarine diamict into the sheared

sequence indicates that a marine transgression occurred during initial ice-marginal deformation and ice loading, prior to ensuing overriding and subglacial reworking. A following marine regression to below modern sea level is recorded by the incision of glaciofluvial gullies into the compressed and sheared strata. A postglacial transgression, which commonly characterizes relative sea level histories of the western CAA (e.g. Andrews, 1970; Lakeman and England, 2013; Nixon et al., 2013) and/or an abundant sediment supply would explain the aggradation of glaciofluvial sand and gravel infilling the gullies to ~ 30 m asl. OSL dating of two sand samples associated with the aggradation of the glaciofluvial sand and gravel provide minimum burial ages of 247+-17 ka and 407+-33 ka (Sheffield Centre for International Drylands Research, UK, 2012), constraining aggradation to the Mid-Pleistocene (*sensu-lato*). Consequently, glaciotectonic event 1 must be broadly penecontemporaneous with and/or older than glaciofluvial aggradation, and glaciotectonic event 2 must be broadly penecontemporaneous and/or younger. A second marine regression following glaciofluvial aggradation is required to account for modern sea level that is currently ~30 m below the top of the infilled gullies.

3.1.2. Glaciotectonic event 2

A final and subtle set of deformation structures characterized by compressional deformation orientated to the east is superimposed on the preceding compressional and shear deformation structures orientated to the southeast. This final deformation is best observed in Domain C, where ice-marginally compressed and subglacially sheared strata (orientated to the

southeast) are consistently cross-cut by low-angle, thrust-faulted glaciofluvial sand and gravel, Kk Fm, and glaciomarine diamict (orientated to the east). The thrust-faulted glaciofluvial sand and gravel preserve what was originally sub-horizontal bedding, suggesting that they were thrust as frozen rafts. A clast macrofabric measured within the overlying till is orientated east-west providing further evidence for an ice advance from the east, overriding Worth Point. The lack of shear in the eastward-dipping deformation sequence suggests that glaciotectonic disturbance was initiated predominantly proglacially.

A significant interval of non-deformation is inferred to have separated glaciotectonic events 1 and 2 based on the time required to incise and infill the glaciofluvial gullies that are OSL dated to the Mid-Pleistocene (*sensu lato*, Domain C). Also, modified permafrost characteristics may have influenced the change to dominantly brittle deformation during glaciotectonic event 2. For example, if permafrost had thickened (i.e. refreezing patches) and/or become colder (i.e. inhibiting the existence of water) prior to glaciotectonic event 2, then the strata would have been more susceptible to brittle failure.

3.2 Glaciotectonic model

Collectively, two glaciotectonic events and two marine transgressions and regressions have been reconstructed from the polydeformed Worth Point section (Fig. 14). These are summarized below:

1) *Glaciotectonism by a Mid-Pleistocene ice sheet*. Initial ice sheet advance from the southeast produced a hill-hole pair and deformed the strata ice-marginally under compression, creating a distinct proximal to distal thrust

sequence (Fig. 3.14, Boxes, 1-2). A marine transgression, facilitated by glacial loading, reworked the deformed strata and deposited a glaciomarine diamict (Fig. 3.14, Boxes 3-4). A readvance or ongoing advance of the ice sheet then overrode and redeformed the strata, imprinting shear deformation structures and depositing a thick glaciotectonite mélange, likely in a subglacial shear zone (Fig. 3.14, Boxes 4-5). As ice retreated from Worth Point, initial emergence resulted in a regression to below modern sea level, allowing incision of outwash gullies into Domain C. Subsequent postglacial submergence and/or an abundant sediment supply led to the aggradation of glaciofluvial sand and gravel in these gullies (Fig. 3.14, Box 6), which entrapped sediments until the ice sheet retreated beyond the regional drainage divide ~200 km inland occasioning renewed emergence. No subsequent drainage has re-excavated these gullies but rather it has remained confined to the Lennie and Kellett river valleys. The OSL burial dating of glaciofluvial sand to 247 ± 17 ka or alternatively 407 ± 33 ka supports an extensive ice sheet crossing Banks Island during the Mid-Pleistocene (*sensu lato*).

2) *Glaciotectonism by the Laurentide Ice Sheet (LIS)*. During the Late Wisconsinan the LIS is recognized to have overridden north and central Banks Island (England et al., 2009; Lakeman and England, 2012) as well as Worth Point (This thesis, Chapter 2). This advance is the most likely candidate for redeforming the strata proglacially and depositing a capping till. (glaciotectonic event 2, Fig. 3.14, Box 7).

Tentative age control is provided by OSL analyses and the relative timing of glaciotectonic events is derived from cross-cutting relationships and

superimposed deformation styles. Based on these relationships, deformation by an oscillatory Mid-Pleistocene ice sheet (ancestral LIS) followed by the Late Wisconsinan LIS is the simplest explanation of the glaciotectonic sequence at Worth Point.

4. DISCUSSION AND CONCLUSIONS

The evolution of the polydeformed stratigraphic sequence at Worth Point has implications for: a) characterizing process-form relationships of hill-hole pairs; b) understanding the nature of deformation in diverse permafrozen lithologic units imposed by glacial stress; c) constraining regional glacial and sea level histories, and; c) testing the validity of a formerly-proposed environmental framework of Banks Island extending back to the Early Pleistocene (Vincent, 1982, 1983, 1984, 1990; Barendregt et al., 1998).

The mechanisms that govern the formation of hill-hole pairs in permafrost terrain remain uncertain (Aber and Ber, 2007). High porewater pressures generated in the proglacial foreland by glacier surging have been proposed for the establishment of hill-hole pairs in Scotland (Evans and Wilson, 2006), and glaciotectonic deformation in Iceland, Svalbard, and the Canadian High Arctic (e.g. Croot, 1988; Kalin, 1971; Copland et al., 2003). At Worth Point, the role of past ice-marginal surging is difficult to constrain; however, the thin lobes of ice invoked for the valleys of western Banks Island seem more suited for cold-based ice glaciologically and climatologically. Consequently, the operation/interplay of other factors are inferred to facilitate hill-hole construction at Worth Point,

including: a) high porewater pressures developed in taliks occupying otherwise impermeable and permafrozen sediment (Kk Fm) like the modern Mackenzie Delta (Mackay, 1959, 1989); b) a basal décollement plane (shallow permafrost) above which deformation is initiated as characterized adjacent to modern glaciers that have advanced into recently emergent valleys of the Canadian High Arctic (Evans and England 1991); c) effective ice-bed coupling between cold-based ice and permafrost terrain (Waller et al., 2012); and d) diverse lithologic units that permit effective transmission of stress by failure along unit contacts (décollement planes; Benn and Evans, 2010). At a regional scale, the spatial distribution of hill-hole pairs across Banks Island can help to elucidate the primary factors controlling glaciotectonism. Here, hill-hole pairs are clustered in a belt ~200 km long and < 20 km wide flanking the island's west coast. The former extent of this belt is unknown because ongoing coastal erosion (submergence) throughout most or all of the Holocene has removed an unidentifiable volume of sediment. Nonetheless, glaciotectonized strata on Robillard and Phillips island (~10 km off the northwest coast of Banks Island) suggest that glaciotectonic disturbance extended at least this far offshore (T. Lakeman, pers comm. 2010). The hill-hole belt broadly coincides with the margin of outcropping Kk Fm and may also coincide with the zone of former marine submergence that would have occasioned permafrost degradation. Therefore, the development of high porewater pressures in impermeable sediment (Kk Fm) and the existence of a basal décollement surface (thinner permafrost) are proposed to have been the primary factors

governing hill-hole construction on Banks Island. The influence of these process-form relationships in other permafrost terrains requires further investigation.

Initial construction of the Worth Point hill-hole pair is tentatively constrained to the Mid-Pleistocene, and as such constitutes the oldest hill-hole pair currently reported in Canada. Herschel Island, offshore from the Yukon Coastal Plain, constitutes another large-scale hill-hole pair that was formed during the last glacial maximum (LGM) on the exposed (emergent) Beaufort Sea Shelf where thin permafrost likely aggraded in the path of the advancing northwest LIS (Mackay, 1959; Fritz et al. 2012). Hershel Island is the largest ice-pushed hill currently recognized in the Canadian Arctic and locally demarcates the maximum extent of the northwest LIS adjacent to mainland Canada. Elsewhere on western Banks Island, a similar Late Wisconsinan age for the hill-hole belt is supported by Mid-Wisconsinan ice-transported shells lying distal to it, and by meltwater channels associated with the hill-hole pairs that grade to Late Wisconsinan marine limit (Lakeman and England, 2013; This thesis, Chapter 2). This Late Wisconsinan signature may be superimposed over the Mid-Pleistocene record with the assumption that other hill-hole pairs across Banks Island are polydeformed, as exemplified at Worth Point. The investigation and absolute dating of additional stratigraphic sequences across west Banks Island is required to address and clarify the long-term evolution of its glaciotectonic landforms and sediments.

The deformation of lithologically-variable permafrozen sediment in ice-marginal and subglacial environments remains poorly understood (Waller et al.,

2012). This is because the most investigated glaciotectonized stratigraphic sequences are located in mid-latitudes, where their original structures have been disturbed or lost as ice cores (initially permafrost) degraded (Dyke and Savelle, 2000). Worth Point provides an exceptional opportunity to document and understand the deformation of permafrozen sediments because: a) permafrost likely has existed continuously on Banks Island since the Mid-Pleistocene *(sensu lato)* or earlier, permitting exceptional preservation of detailed deformation structures and styles imparted during multiple episodes of glaciotectonism; b) a wide range of litholigic units are present at Worth Point, providing diverse opportunities to observe lithologically-specific responses (from brittle to ductile) to glacially-imposed stress (from compression to shear).

At Worth Point, ground ice and debris-rich glacial ice dating to the Mid-Pleistocene (*sensu lato*) or earlier (emplaced during or prior to glaciotectonic event 1) have been preserved for at least two intervening glacial-interglacial cycles, persisting through multiple glaciotectonic events. The preservation of buried glacial ice and ground ice in permafrost is a common and well-documented phenomenon throughout the western Canadian Arctic (e.g. Mackay, 1959; Mackay et al., 1972; O'Cofaigh et al., 2003; Murton et al., 2004; Harris and Murton, 2005; Fritz et al., 2012). Early investigations of these buried ice bodies in the western Canadian Arctic inferred them to be *in situ* (epigenetic permafrost) and formed by ice segregation or ice injection (Mackay, 1971, 1989). However, a growing consensus now recognizes that much of the buried ice became detached from former ice sheets and was then buried and incorporated into the permafrost.

This phenomenon has been observed on Banks Island (French and Harry, 1988; Lakeman and England, 2013), Victoria Island (Lorrain and Demeur, 1985; Dyke and Savelle, 2000), the Canadian Arctic mainland (e.g. Mackay et al., 1972; French and Harry, 1990; Dyke and Evans, 2003; Murton, 2005), Russian Arctic (e.g. Astakhov and Isayeve, 1988; Svendsen et al., 2004), Svalbard (e.g. Brandt et al., 2007) and Antarctica (e.g. Sugden et al., 1995; Marchant et al., 2002). Furthermore, reported buried ice preserved in permafrost can be ancient. For example, buried glacial ice reported from the southern Kara Sea coast of Russia and from Bylot Island in the CAA is thought to date from the Mid-Pleistocene (Ingolfsson and Lokrantz, 2003; Fortier et al., 2009), whereas buried glacial ice reported from southern Victoria Land in Antarctica is thought to date from the Miocene (Marchant et al., 2002). In unglaciated terrain, ice-rich permafrost > 700 ka has also been reported from the Yukon (Froese et al., 2008). The preservation of buried glacial ice tentatively dated to the Mid-Pleistocene or earlier at Worth Point accords with widespread evidence that ancient glacial ice can survive multiple glacial and interglacial cycles when incorporated into permafrost, and also serves to highlight the antiquity of permafrost in the CAA. Such thermal inertia exhibited by permafrost on Banks Island has important implications for our understanding of modern climate change (IPCC AR5, 2013), especially if this long-established buried ice begins to degrade.

The revised glaciotectonic model for Worth Point reported here replaces the purportedly *in situ*, horizontally-bedded stratigraphic sequence that formed an elaborate, long-standing and widely cited environmental framework for the

western CAA, spanning the Neogene and Quaternary (Vincent 1982, 1983, 1984, 1989, 1990, 1992; Vincent et al., 1984; Matthews et al., 1986; Barendregt et al., 1998). The current reinterpretation of glaciations and glacioisostatically forced marine transgressions and regressions at Worth Point help to constrain the extent and style of glaciation along the polar continental shelf of the Arctic Ocean where increasing interest is being placed on the age and origin of deep scouring of the circumpolar seafloor (Polyak et al. 2001; Jakobsson et al. 2008, 2010, 2013). This record from the westernmost CAA also contributes to an improved understanding of the relationship between the northwest margin of the LIS and the adjoining Ice Age refugium of Beringia that had incorrectly included Banks Island during the LGM (England et al., 2009).

5. REFERENCES

Aber, J.S. 1985. The nature of glaciotectonism. Geologie en Mijnbouw. 64, 389-395.

Andews, J.T. 1970. A Geomorphological Study of Post-glacial Uplift with Particular Reference to Arctic Canada. Institute of British Geographers, Alden Press, Oxford.

Astakhov, V.I., Isayeva, L.L. 1988. The 'Ice Hill'; an example of 'retarded deglaciation' in Siberia. Quaternary Science Reviews. 7, 29-40.

Aber, J.S., Ber, A. 2007. Glaciotectonism. Developments in Quaternary Science, 6. Elsevier, Amsterdam.

Barendregt, R.W., Vincent, J-S., Irving, E., Baker, J. 1998. Magnetostratigraphy of Quaternary and late Tertiary sediments on Banks Island, Canadian Arctic Archipelago. Canadian Journal of Earth Sciences. 35, 147-161.

Benn, D.I., Evans, D.J.A. 2010. Glaciers and Glaciation. Second Edition, Hodder Education, London.

Blasco, S., Bartlett, J., Bennett, R., Hughes-Clark, J., Maclean, B., Scott, S., Sonnichsen, G. 2005. Northwest Passage marine sediments: a record of Quaternary history and climate change. Arctic Workshop abstract, March 9th-12th, University of Alberta, Edmonton, Canada.

Boulton, G.S. 1999. The sedimentary and structural evolution of a recent push moraine complex: Holstrømbreen, Spitsbergen. Quaternary Science Reviews. 18, 339-371.

Brandt, O., Langley, K., Kohler, J., Hamran, S-E. 2007. Detection of buried ice and sediment layers in permafrost using multi-frequency Ground Penetrating Radar: A case examination on Svalbard. Remote Sensing of Environment. 111, 212-217.

Clark, D.L., Vincent, J-S, Jones, G.A., Morris, W.A. 1984. Correlation of marine and continental glacial and interglacial events, Arctic Ocean and Banks Island. Nature. 311, 147-149.

Copland, L., Sharp, M.J., Dowdeswell, J.A. 2003. The distribution and flow characteristics of surge-type glaciers in the Canadian High Arctic. Annals of Glaciology. 36, 73-81.

Craig, B.J., Fyles, J.G. 1960. Pleistocene geology of Arctic Canada. Geological Survey of Canada. Paper 60-10, 21.

Croot, D.G. 1988. Glaciotectonics and surging glaciers: a correlation based on Vestpitsbergen, Svalbard, Norway. In: Croot, D.G. (Ed.). Glaciotectonics: Forms and Processes, Balkema, Rotterdam, 33-47.

Darby, D, A. 2003. Sources of sediment found in sea ice from the western Arctic Ocean, new insights into processes of entrainment and drift patterns. Journal of Geophysical Research. Oceans. 108, 13.1-13.8.

Dyke, A.S. 1993. Landscapes of cold-centred Late Wisconsinan ice caps, Arctic Canada. Progress in Physical Geography. 17, 223-247.

Dyke, A.S., Savelle, J. M. 2000. Major end moraines of Younger Dryas age on Wollaston Peninsula, Victoria Island, Canadian Arctic: implications for

paleoclimate and for formation of hummocky moraines. Canadian Journal of Earth Sciences. 37, 601-619.

Ehlers, J., Gibbard, P.L. (Eds). 2004. Quaternary Glaciations: extent and chronology. Part II: North America. Developments in Quaternary Science 2. Elsevier, Amsterdam.

Ehlers, J., Gibbard, P.L., Hughes, P.D. (Eds). 2011. Quaternary glaciations: extent and chronology: a closer look. Elsevier, Amsterdam.

England, J.H., Furze, M.F.A., Doupe, J.P. 2009. Revision of the NW Laurentide Ice Sheet: Implications for paleoclimate, the northeast extremity of Beringia, and Arctic Ocean Sedimentation. Quaternary Science Reviews. 28, 1573-1596.

Evans, D.J.A., England, J.H. 1991. Canadian landform examples 19: High Arctic thrust block moraines. The Canadian Geographer. 35, 93-97.

Evans, D.J.A., Rea, B.R. 1999. Geomorphology and sedimentology of surging glaciers: a landsystems approach. Annals of Glaciology. 28, 75-82.

Evans, D.J.A., Salt, K., Allen, C.S. 1999. Glacitectonized lake sediments, Barrier Lake, Kanninaskis Country, Canadian Rocky Mountains. Canadian Journal of Earth Sciences. 36, 395-407.

Evans, D.J.A., Rea, B.R. 2003. Surging glacier landsystem. In: Evans, D.J.A. (Ed.). Glacial Landsystems. Arnold, London, 259-288.

Evans, D.J.A., Wilson, S.B. 2006. A temporary exposure through the Loch Lomond Readvance end moraine/ice-contact delta complex near Drymen, Stirlingshire. Scottish Geographical Journal. 122, 344-351.

Evans, D.J.A., Twigg, D.R., Rea, B.R., Shand, M. 2007. Surficial geology and geomorphology of the Brúarjökull surging glacier landsystem. Journal of Maps. 349-367.

Evans, D.J.A., Clark, C.D., Rea, B.R. 2008. Landform and sediment imprints of fast glacier flow in the southwest Laurentide Ice Sheet. Journal of Quaternary Science. 23, 249-272.

Eyles, N., Boyce, J.I. 1998. Kinematic indicators in fault gouge: tectonic analog for soft-bedded ice sheets. Sedimentary Geology. 116, 1-12.

Fortier, F., Godin, E., Kanevskiy, M.Z., Allard, M. 2009. Middle Pleistocene (?) buried glacial ice on Bylot Island, Canadian Arctic Archipelago. EOS Transactions of the American Geophysical Union. 90, 52.

Fritz, M., Wetterich, S., Schirrmeister, L., Meyer, H., Lantuit, H., Preusser, F., Pollard, W.H. 2012. Eastern Beringia and beyond: Late Wisconsinan and Holocene landscape dynamics along the Yukon Coastal Plain, Canada. Palaeogeography, Palaeoclimatology, Palaeoecology. 319, 28-45.

French, H.M., Harry, D.G. 1988. Nature and origin of ground ice, Sandhills Moraine, southwest Banks Island, Western Canadian Arctic. Journal of Quaternary Science. 3, 19-30.

French, H.M., Harry, D.G. 1990. Observations on buried glacier ice and massive segregated ice. Western Arctic Coast, Canada. Permafrost and Periglacial Processes. 1, 31-43.

Froese, D.G., Westgate, J.A., Reyes, A, V., Enkin, R.J., Preece, S.J. 2008. Ancient Permafrost And A Future, Warmer Arctic. Science. 321, 1648.

Fyles, J.G., Hills, L.V., Matthews, J.V., Barendregt, R., Baker, J., Irving, E., Jetté, H. 1994. Ballast Brook and Beaufort Formations (Late Tertiary) on northern Banks Island, Arctic Canada. Quaternary International. 22-23, 141-171.

Harris, C., Murton, J.B. 2005. Interactions between glaciers and permafrost: an introduction. Geological Society, London. 242, 1-9.

Ingolfsson, O., Lokrantz, H. 2003. Massive Ground Ice Body of Glacial Origin at Yugorski Peninsula, Arctic Russia. Permafrost and Periglacial Processes. 14, 199-215.

International Panel on Climate Change (IPCC) Co-Chairs of Working Group 1. 2013. Working Group 1 Contribution to the IPCC Fifth Assessment Report Climate Change 2013: The Physical Science Basis. Chapter 4: Observations: Cryosphere – Final Draft Underlying Scientific-Technical Assessment.

Jakobsson, M., Polyak, L., Edwards, M., Klemen, J., Coakley, B. 2008. Glacial geomorphology of the Central Arctic Ocean: the Chukchi Borderland and the Lominosov Ridge. Earth Surface Processes and Landforms. 33, 526-545.

Jakobsson, M., Nilsson, J., O'Regan, M., Backman, J., Löwemark, L., Dowdeswell, J.A., Mayer, L., Polyak, L., Colleoni, F., Anderson, L., Björk, G., Darby, D., Eriksson, B., Hanslik, D., Hell, B., Marcussen, C., Sellén, E., Wallin, Å. 2010. An Arctic Ocean ice shelf during MIS 6 constrained by new geophysical and geological data. Quaternary Science Reviews. 29, 3505-3517

Jakobsson, M., Andreassen, K., Bjarnadóttir, L.R., Dove, D., Dowdeswell, J.A., England, J.H., Funder, S., Hogan, K., Ingólfsson, O., Jennings, A., Krog-

Larsen, N., Kirchner, N., Landvik, J.Y., Mayer, L., Moller, P., Niessen, F., Nilsson, J., O'Regan, M., Polyak, L., Petersen, N.N., Stein, R. Arctic Ocean Glacial History. In press.

Kalin, M. 1971. The active push moraine of the Thompson Glacier. Montreal McGill University, Axel Heiberg Island Research, Reports Glaciology. 4, 68.

Kneier, F., Langer, M., Froeb, K., Overduin, P.P. 2012. Modelling subsurface heat flow during a marine transgression in the Western Laptev Sea. Tenth International Conference on Permafrost extended abstract. 270-271.

Lakeman, T.R., England, J.H. 2012. Paleoglaciological insights from the age and morphology of the Jesse moraine belt, western Canadian Arctic. Quaternary Science Reviews. 47, 82-100.

Lakeman, T.R., England, J.H. 2013. Late Wisconsinan glaciation and postglacial relative sea level change on western Banks Island, Canadian Arctic Archipelago. Quaternary Research. 80, 99-112.

Le Heron, D.P., Etienne, J.L. 2005. A complex subglacial clastic dyke swarm, Solheimajökull, southern Iceland. Sedimentary Geology. 181, 25-37.

Lorrain, R.D., Demeur, P. 1985. Isotopic evidence for relict Pleistocene glacier ice on Victoria Island, Canadian Arctic Archipelago. Arctic and Alpine Research. 17, 89-98.

Mackay, J.R., 1956. Deformation by glacier ice at Nicholson Peninsula, N.W.T Arctic. 9, 218-228.

Mackay, J.R., 1959. Glacier ice-thrust features of the Yukon Coast. Geographical Bulletin of Canada. 13, 5-21.

Mackay, J.R. 1971. The origin of massive icy beds in permafrost, western Arctic Coast, Canada. Canadian Journal of Earth Sciences. 8, 397-422.

Mackay, J.R. 1989. Massive ice: some field criteria for the identification of ice types. Geological Survey of Canada. Paper 89-1G, 5-11.

Mackay, J.R., Matthews, W.H. 1964. The role of permafrost in ice-thrusting. Journal of Geology. 72, 378-380.

Mackay. J.R., Rampton, V.N., Fyles, J.G. 1972. Relict Pleistocene permafrost, Western Arctic, Canada. Science. 176, 1321-1323.

MacLean, B., Blasco, S., Bennett, R., Lakeman, T., Hughes-Clarke, J., Kuus, P., Patton, E. 2012. Marine evidence for a glacial ice stream in Amundsen Gulf, Canadian Arctic Archipelago. 42nd Annual Arctic Workshop abstract, March 7th-9th, University of Colorado, US.

Marchant, D.R., Lewis, A.R., Phillips, W.M., Moore, E.J., Souchez, R.A., Denton, G.H., Sugden, D.E., Potter, N., Landis, G.P. 2002. Formation of patterned ground and sublimation till over Miocene glacier ice in Beacon Valley, southern Victoria Land, Antarctica. Geological Society of America Bulletin. 114, 718-730.

Matthews, J.V., Mott, R.J., Vincent, J-S. 1986. Preglacial and interglacial environments on Banks Island: pollen and macrofossils from Duck Hawk Bluffs and related sites. Geographie physique et Quaternaire. 3, 279-298.

Mathews, W.H., Mackay, J.R. 1960. Deformation of soils by glacier ice and the influence of pore pressures and permafrost. Transactions of the Royal Society of Canada. 54, 27-36.

McCarroll, D., Rijsdijk, K.F. 2003. Deformation styles as a key for interpreting glacial depositional environments. Journal of Quaternary Science. 18, 473-489.

Miall, A. D. 1976. Sedimentary structures and paleocurrents in a Tertiary deltaic succession, northern Banks Island, Arctic Canada. Canadian Journal of Earth Sciences. 13, 1422-1432.

Mooers, H.D. 1990. Ice-marginal thrusting of drift and bedrock: thermal regime, subglacial aquifers, and glacial surges. Canadian Journal of Earth Sciences. 27, 849-862.

Mulugeta, G., Koyi, H. 1987. Three-dimensional geometry and kinematics of experimental piggyback thrusting. Geology. 15, 1052-1056.

Murton, J.B. 2005. Ground-ice stratigraphy and formation at North Head, Tuktoyaktuk Coastlands, western Arctic Canada: a product of glacier-permafrost interactions. Permafrost and Periglacial Processes. 16, 31-50.

Murton, J.B., Waller, R.I., Hart, J.K., Whiteman, C.A., Pollard, W.H., Clark, I.D. 2004. Stratigraphy and glaciotectonic structures of a relict deformable bed of permafrost at the northwestern margin of the Laurentide Ice Sheet, Tuktoyaktuk Coastlands, Canada. Journal of Glaciology. 50, 399-412.

Nixon, C.F., England, J.H., Lajeunesse, P., Hanson, M.A. Deciphering patterns of postglacial sea level at the junction of the Laurentide and Innuitian Ice Sheets, western Canadian Arctic. Quaternary Science Reviews. In press.

Núñez-Betelu, L.K., Hills, L.V., Krause, F.F. 1994. Upper Cretaceous paleoshorelines of the northeastern Sverdrup Basin, Ellesmere Island, Canadian Arctic Archipelago. ICAM-94 Proceedings, Stratigraphy and Paleogeography. 43-49.

O'Cofaigh, C., Evans, D.J.A., England, J. 2003. Ice-marginal terrestrial landsystems: sub-polar glacier margins of the Canadian and Greenland high arctic. In: Evans, D.J.A. (Ed.). Glacial Landsystems. Arnold, London, 44-64.

Pedersen, S.A.S. 1989. Glacitectonite: brecciated sediments and cataclastic sedimentary rocks formed subglacially. In: Goldthwaite, R.P., Matsch, C.L. (Eds.). Genetic Classification of Glacigenic Deposits, Balkema, Rotterdam, 89-91.

Pedersen, S.A.S. 2005. Structural analysis of the Rubjerg Knude Glaciotectonic Complex, Vendsyssel, northern Denmark. Geological survey of Denmark and Greenland, Bulletin 8.

Phillips, E., Merritt, J. 2008. Evidence for multiphase water-escape during rafting of shelly marine sediments at Clava, Inverness-shire, NE Scotland. Quaternary Science Reviews. 27, 988-1011.

Phillips, E.R., Lee, J.R., Burke, H.F. 2008. Progressive proglacial to subglacial deformation and syntectonic sedimentation at the margins of the Mid-

Pleistocene British ice sheet: evidence from north Norfolk, UK. Quaternary Science Reviews. 27, 1848-1871.

Phillips, E., Lee, J.R., Evans, H.M. (Eds). 2011. Glacitectonics - field guide. Quaternary Research Association.

Piotrowski, J.A. 2006. Groundwater under ice sheets and glaciers. In: Knight, P.G. (Ed.). Glacier Science and Environmental Change. Blackwell Publishing, Oxford. 50-59.

Polyak, L., Bischof, J., Ortiz, J., Darby, D., Chappell, J., Xuan, C., Kaufman, D., Loylie, R., Schneider, D., Adler, R. 2009. Late Quaternary stratigraphy and sedimentation patterns in the western Arctic Ocean. Global Planetary Change. 68, 5-17.

Rampton, V.N. 1982. Quaternary Geology of the Yukon Coastal Plain. Geological Survey of Canada. Bulletin 317.

Rijsdijk, K.F., Owen, G., Warren, W.P., McCarroll, D., van der Meer, J.J.M. 1999. Clastic dykes in over-consolidated tills: evidence for subglacial hydrofracturing at Killiney Bay, eastern Ireland. Sedimentary Geology. 129, 111-126.

Rotniki, K. 1976. The theoretical basis for and a model of glaciotectonic deformations. Quaestiones Geographicae. 3, 103-139.

Sharp, M.J. 1985. Sedimentation and stratigraphy at Eyjabakkajökull: an Icelandic surging glacier. Quaternary Research. 24, 268-284.

Sharp, M.J. 1988. Surging glaciers: behaviour and mechanisms. Progress in Physical Geography. 12, 349-370.

Sugden, D.E., Marchant, D.R., Potter, N., Jr, Souchez, R.A., Denton, G.H., Swisher, C.C., Tison, J.L. 1995. Preservation of Miocene glacier ice in East Antarctica. Nature. 376, 412-414.

Svendsen, J.I., Alexanderson, H., Astakhov, V.I. 2004. Late Quaternary ice sheet history of Northern Eurasia. Quaternary Science Reviews. 23, 1229-1271.

Taylor, A.E., Dallimore, S.R., Outcalt, S.I. 1996. Late Quaternary history of the Mackenzie-Beaufort region, Arctic Canada, from modeling of permafrost temperatures: the onshore-offshore transition. Canadian Journal of Earth Sciences. 33, 52-61.

Tozer, E.T. 1956. Geological reconnaissance of Prince Patrick Island, Eglinton and western Melville Islands, Arctic Archipelago, Northwest Territories. Geological Survey of Canada Paper. 55-5, 1-32.

Tsytovich, N.A. 1975. The mechanics of frozen ground. McGraw-Hill, New York.

Twiss, R. J., Moores, E.M. 1992. Structural Geology. Freeman and Co., New York.

van der Meer, J.J.M., Kjaer, K.H., Kruger, J., Rabassa, J., Kilfeather, A.A. 2009. Under pressure: clastic dykes in glacial settings. Quaternary Science Reviews. 28, 708-720.

Van der Wateren, F.M., 1995. Structural geology and sedimentology of push moraines. Mededelingen Rijks Geologische Dienst. 54.

Vincent, J-S. 1982. The Quaternary History of Banks Island, Northwest Territories, Canada. Geographie Physique et Quaternaire. 36, 209-232.

Vincent, J-S. 1983. La geologie du quaternaire et la geomorphologie de L'ile Banks, arctique Canadien. In: Commission Geologique du Canada Memoir 405.

Vincent, J-S. 1984. Quaternary stratigraphy of the western Canadian Arctic Archipelago. In: Fulton, R.J. (Ed.). Quaternary Stratigraphy of Canada – A Canadian Contribution to IGCP Project 24. Geological Survey of Canada. 87-100.

Vincent, J-S. 1989. Quaternary geology of the northern Canadian Interior Plains. In: Fulton, R. J. (Ed.). Quaternary geology of Canada and Greenland: Geological Survey of Canada, Geology of Canada. 1, 100-137.

Vincent, J-S. 1990. Late Tertiary and Early Pleistocene Deposits and History of Banks Island, southwestern Canadian Arctic Archipelago. Arctic. 43, 339-363.

Vincent, J-S. 1992. The Sangamonian and early Wisconsinan glacial record in the western Canadian Arctic. In: Clark, P. U. and Lea, P. D. (Eds.) The Last Glacial-Interglacial Transition in North America. Geological Society of America, Special Paper. 270, 233-252.

Vincent, J.S., Occhietti, S., Rutter, N., Lortie, G., Guilbault, J-P., De Boutray, B. 1983. The Late Tertiary-Quaternary record of the Duck Hawk Bluffs, Banks Island, Canadian Arctic Archipelago. Canadian Journal of Earth Science. 20, 1694-1712.

Vincent, J-S., Morris, W.A. & Occhietti, S. 1984. Glacial and non-glacial sediments of Matuyama paleomagnetic age on Banks Island, Canadian Arctic Archipelago. Geology. 12, 139-142.

Waller, R.I., Murton, J., Whiteman, C. 2009. Geological evidence for subglacial deformation of Pleistocene permafrost. Proceedings of the Geologists Association. 120, 155-162.

Waller, R.I., Murton, J.B., Kristensen, L. 2012. Glacier-permafrost interactions: Processes, products and glaciological implications. Sedimentary Geology. 255-256, 1-28.

Wintle, A.G. 2010. Future directions of luminescence dating of quartz. Geochronometria. 37, 1-7.

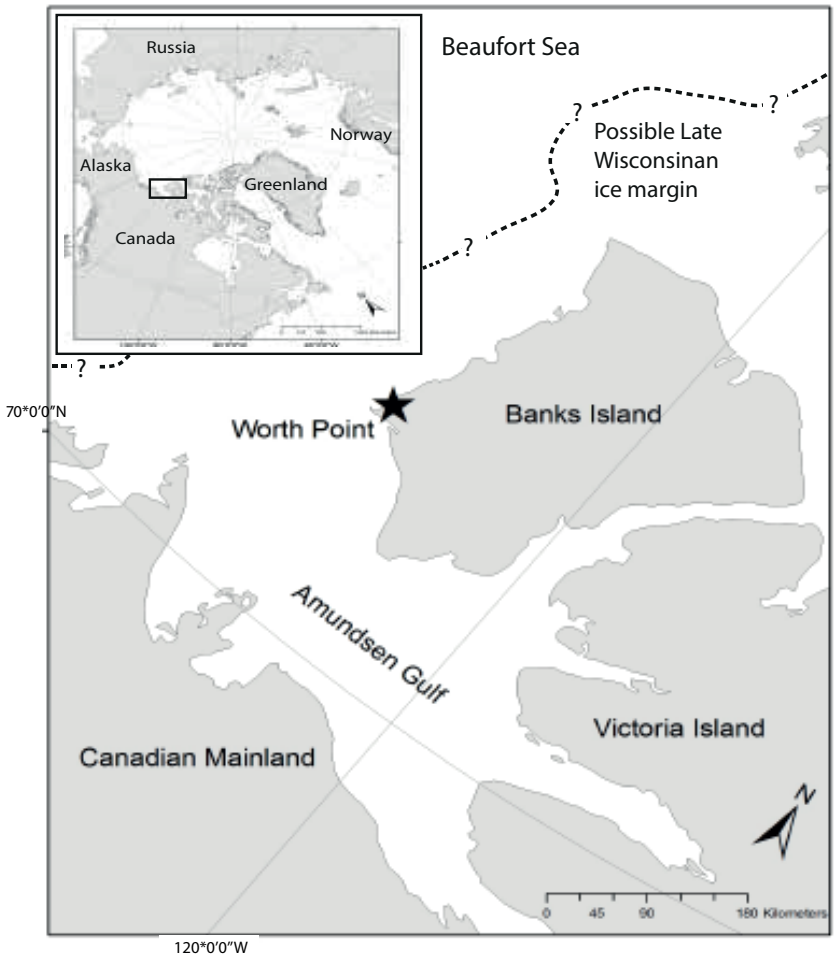

Fig. 3.1. Location map of Worth Point, Banks Island, showing possible Late Wisconsinan ice margin after England et al (2009), Lakeman and England (2012, 2013) and This thesis, Chapter 2.

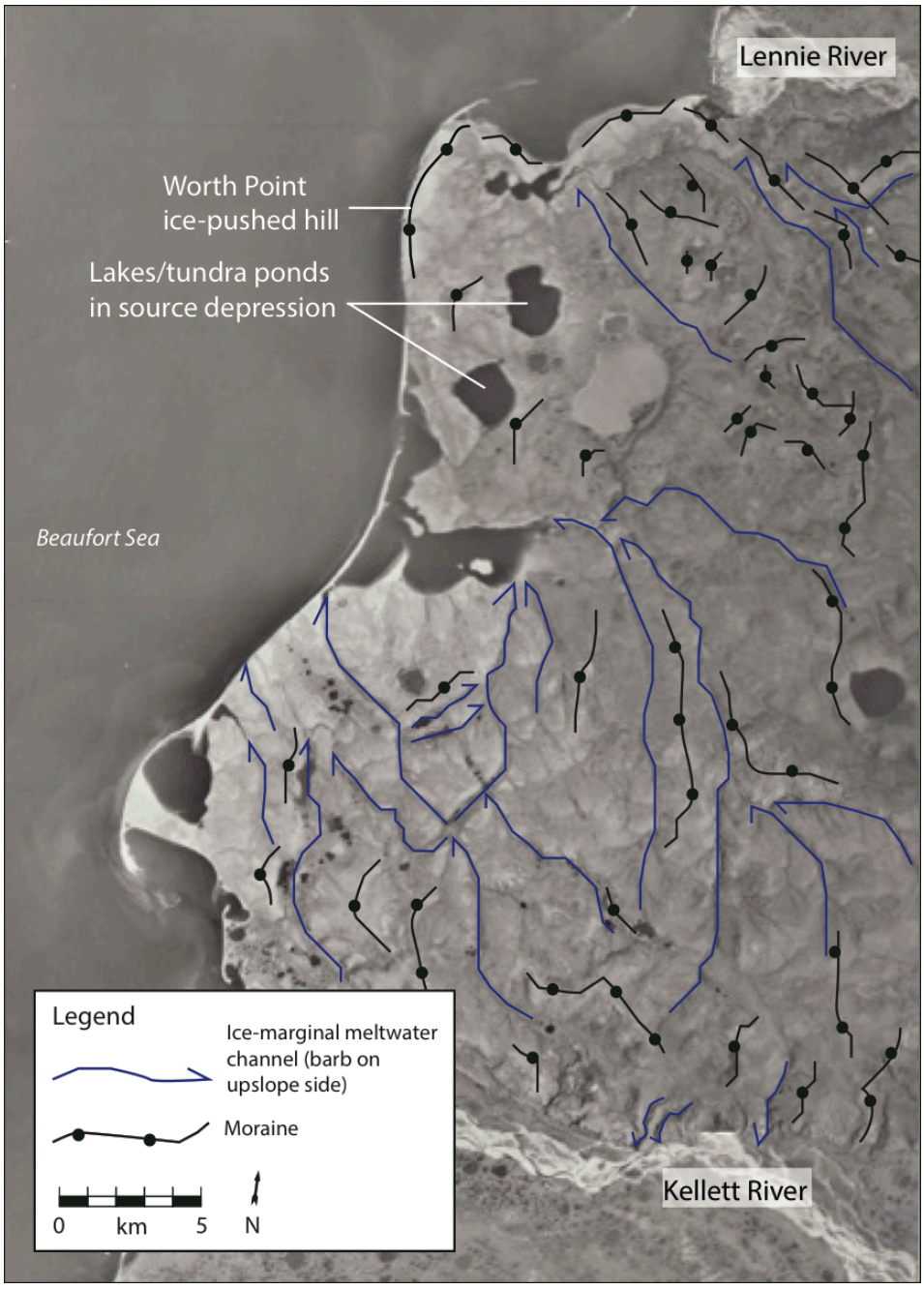

Fig. 3.2. Annotated aerial photograph of Worth Point showing primary meltwater channels, moraines, and bounding river valleys.

Fig. 3.3a

Fig. 3.3b

Fig. 3.3c

Fig. 3.3d

Fig. 3.3e

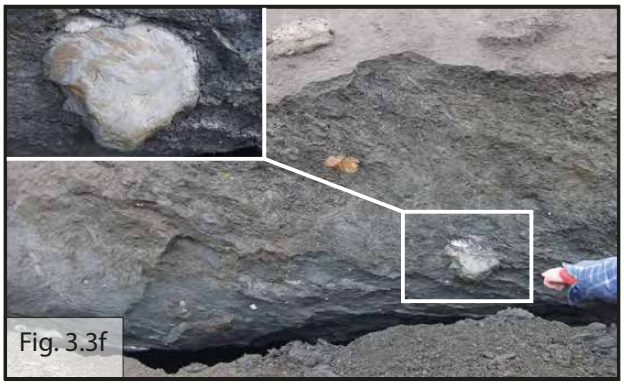

Fig. 3.3f

(previous page)

Fig. 3.3a. Photograph showing thermal erosion and undercutting of Worth Point bluffs, resulting in the frequent detachment of sediment blocks.

Fig. 3.3b. Photograph showing the melt-out of buried glacial ice and ground ice causing widespread slumping and slope failure.

Fig. 3.3c. Photograph showing a heavily brecciated raft of Kanguk Fm (distal marine mudstone).

Fig. 3.3d. Photograph showing a thrust-faulted raft of Eureka Sound Fm sandstone. Note the typical green and red banding.

Fig. 3.3e. Photograph showing a thrust-faulted raft of Beaufort Fm composed of well-sorted sand and gravel.

Fig. 3.3f. Photograph of glaciomarine diamict displaying crude bedding and containing striated clasts (inset).

Fig. 3.3g

Fig. 3.3h

Fig. 3.3i

Fig. 3.3j

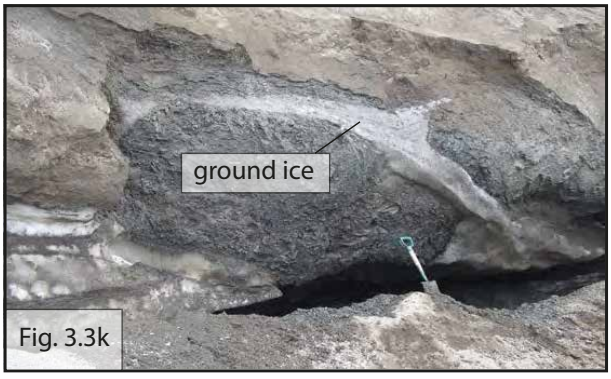

Fig. 3.3k

(previous page)

Fig. 3.3g. Photograph showing sub-horizontally bedded and unlithified glaciofluvial sand and gravel.

Fig. 3.3h. Photograph showing heterogeneous and compacted diamict (site for clast fabric analyses).

Fig. 3.3i. Photograph showing glaciotectonite mélange. Note the large-scale organics, including logs, within a deformed fine-grained matrix.

Fig. 3.3j. Photograph showing a raft of buried glacial ice displaying crude bedding with small inclusions.

Fig. 3.3k. Photograph showing a sheet of ground ice occupying a fault/plane of weakness within brecciated Kanguk Fm.

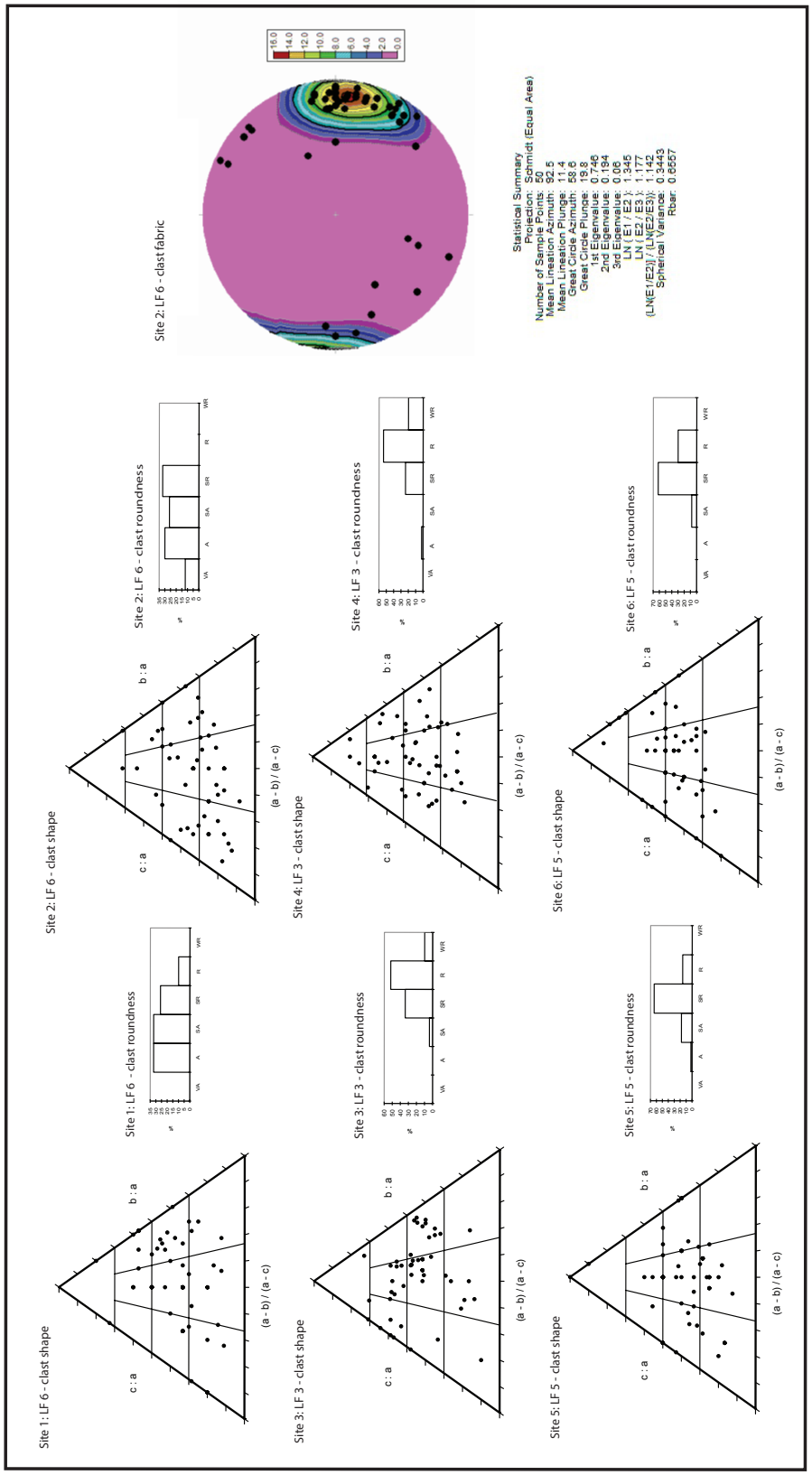
Site 1: LF 6 - clast shape
Site 2: LF 6 - clast shape
Site 3: LF 3 - clast shape
Site 4: LF 3 - clast shape
Site 5: LF 5 - clast shape
Site 6: LF 5 - clast shape
Site 1: LF 6 - clast roundness
Site 2: LF 6 - clast roundness
Site 3: LF 3 - clast roundness
Site 4: LF 3 - clast roundness
Site 5: LF 5 - clast roundness
Site 6: LF 5 - clast roundness
Site 2: LF 6 - clast fabric
Statistical Summary
Projection: Schmidt (Equal Area)
Number of Sample Points: 50
Mean Lineation Azimuth: 92.5
Mean Lineation Plunge: 11.4
Great Circle Azimuth: 58.8
Great Circle Plunge: 19.8
1st Eigenvalue: 0.746
2nd Eigenvalue: 0.184
3rd Eigenvalue: 0.069
LN (E1 / E2): 1.345
LN (E2 / E3): 1.177
(LNE1/E2)) / (LNE2/E3)): 1.142
Spherical Variance: 0.3443
Rbar: 0.6667
c : a
b : a
(a - b) / (a - c)
VA
A
SA
SR
R
VR

Fig. 3.4.

Fig. 3.4. (previous page). Clast form analyses based on data collected from two separate and representative sites for LF3, LF5 and LF6. Clast fabric analyses shown for site 2 for LF 6.

Fig. 3.5.

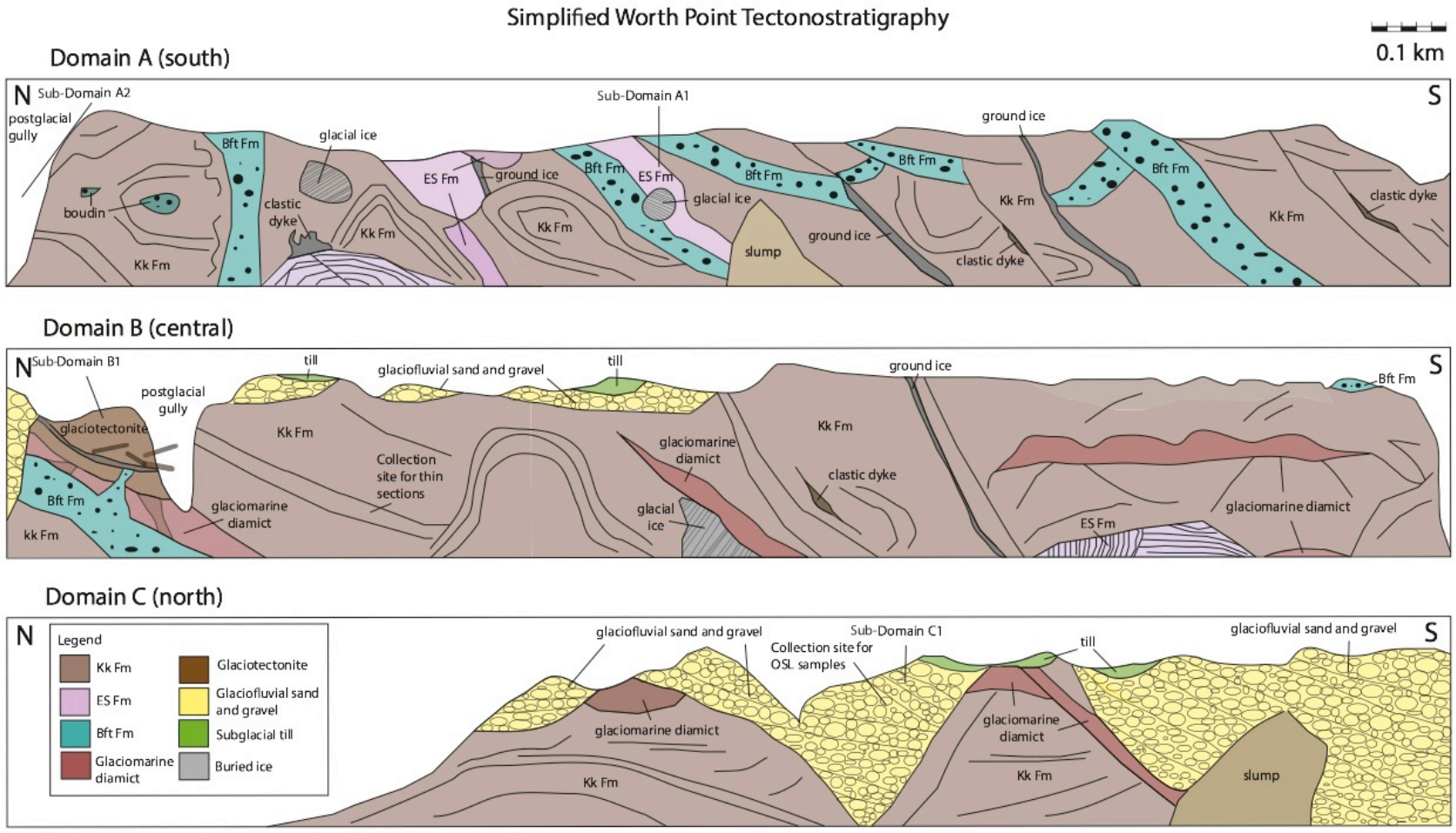
Simplified Worth Point Tectonostratigraphy
0.1 km
Domain A (south)
N
S
Sub-Domain A2
postglacial gully
boudin
Kk Fm
Bft Fm
clastic dyke
glacial ice
ES Fm
ground ice
Kk Fm
Sub-Domain A1
Bft Fm
ES Fm
glacial ice
slump
ground ice
clastic dyke
Bft Fm
ground ice
Kk Fm
Bft Fm
Kk Fm
clastic dyke
Domain B (central)
N
S
Sub-Domain B1
postglacial gully
glaciotectonite
Bft Fm
kk Fm
till
glaciofluvial sand and gravel
Kk Fm
Collection site for thin sections
glaciomarine diamict
till
glaciomarine diamict
glacial ice
ground ice
Kk Fm
clastic dyke
Bft Fm
glaciomarine diamict
ES Fm
Domain C (north)
N
S
Legend
Kk Fm
ES Fm
Bft Fm
Glaciomarine diamict
Glaciotectonite
Glaciofluvial sand and gravel
Subglacial till
Buried ice
glaciofluvial sand and gravel
Collection site for OSL samples
Sub-Domain C1
glaciomarine diamict
Kk Fm
till
glaciomarine diamict
Kk Fm
glaciofluvial sand and gravel
slump

Fig. 3.5. (previous page). Simplified tectonostratigraphy of Worth Point along a north-south transect (as observed from the coast) approximately 6 km in length. Domain A forms the southernmost 2 km, Domain B forms the central 2.2 km, and Domain C forms the northernmost 1.8 km of the coastal section.

Detailed deformation structures and styles are not shown as they are too numerous and complex to include at this scale. Readers should use the figure as a reference to orient themselves throughout the chapter and to note the primary locations of lithofacies and their dominant tectonostratigraphic settings. Section locations described in this chapter are identified, along with sample location sites for OSL dating and thin section analyses.

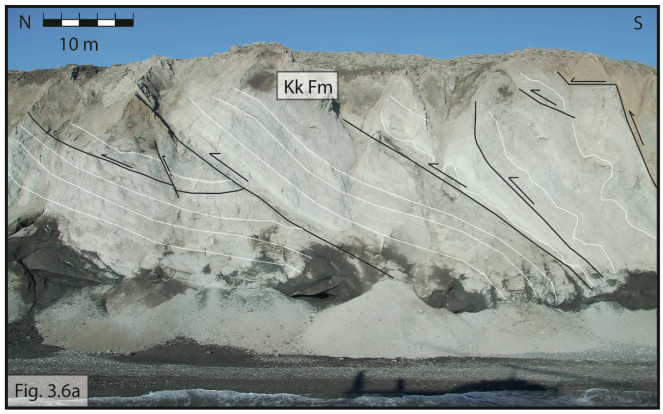
N
10 m
S
Kk Fm
Fig. 3.6a

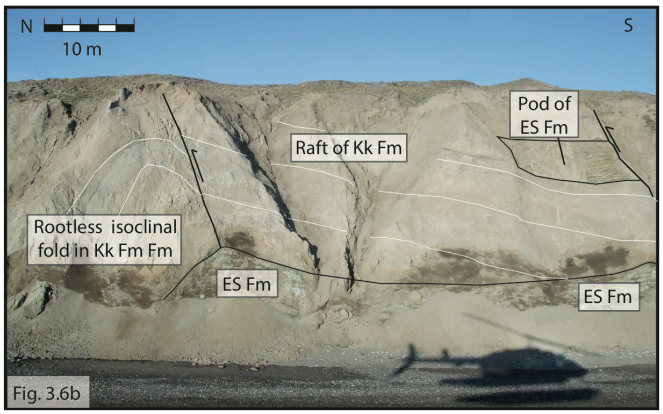
N
10 m
S
Pod of ES Fm
Raft of Kk Fm
Rootless isoclinal fold in Kk Fm Fm
ES Fm
ES Fm
Fig. 3.6b

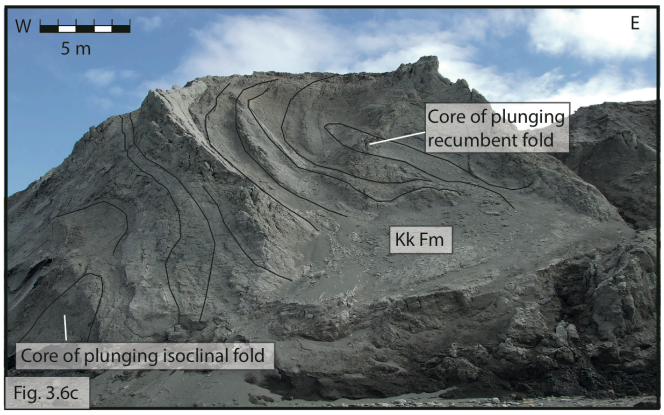
W
5 m
E
Core of plunging recumbent fold
Kk Fm
Core of plunging isoclinal fold
Fig. 3.6c

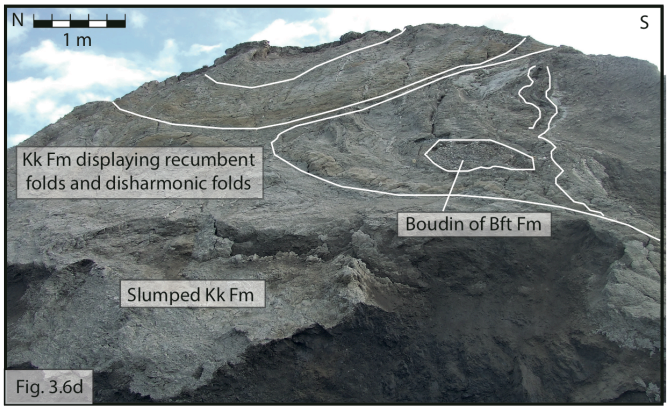
N
1 m
S
Kk Fm displaying recumbent folds and disharmonic folds
Boudin of Bft Fm
Slumped Kk Fm
Fig. 3.6d

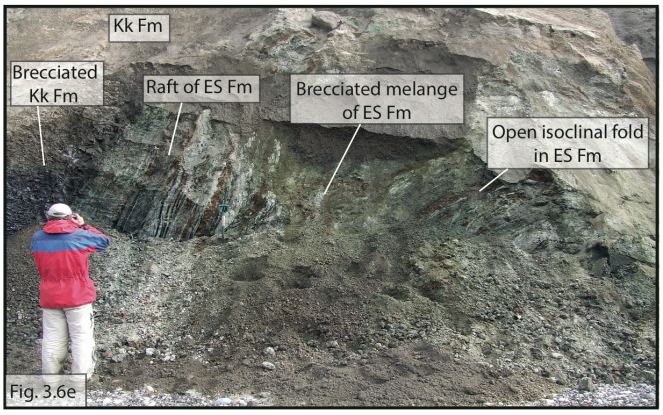
Kk Fm
Brecciated Kk Fm
Raft of ES Fm
Brecciated melange of ES Fm
Open isoclinal fold in ES Fm
Fig. 3.6e

(previous page)

Fig. 3.6a. Photograph showing an imbricated thrust-faulted raft of Kanguk Fm oriented to the southeast (toward the source basin) truncated by low-angle thrust faults near the modern surface.

Fig. 3.6b. Photograph showing thrust-faulted Kanguk Fm with a rootless isoclinal fold and a coherent pod of Eureka Sound Fm. A thrust-faulted raft of Eureka Sound Fm can be observed at the base.

Fig. 3.6c. Photograph showing the core of a recumbent fold and a plunging isoclinal fold in Kanguk Fm.

Fig. 3.6d. Photograph showing fold interference in Kanguk Fm with a boudin of Beaufort Fm at the core of a recumbent fold.

Fig. 3.6e. Photograph showing brittle and ductile deformation of Eureka Sound Fm. Note the open isoclinal fold in Eureka Sound Fm (right) truncated by a back-thrusted high angle raft of Eureka Sound Fm with brecciated shear zones either side of the raft (left).

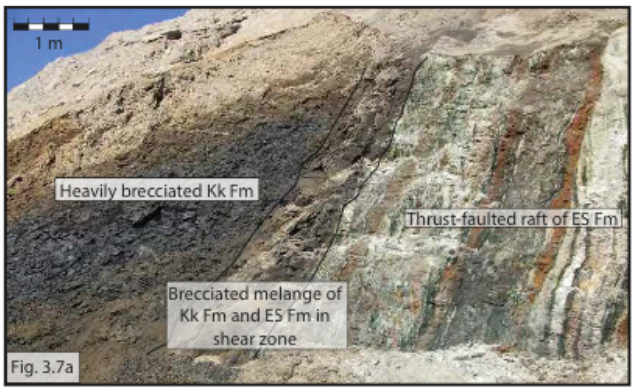
1 m
Heavily brecciated Kk Fm
Thrust-faulted raft of ES Fm
Brecciated melange of Kk Fm and ES Fm in shear zone
Fig. 3.7a

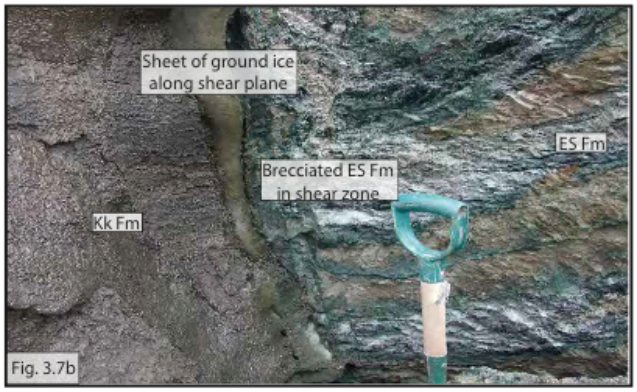
Sheet of ground ice along shear plane
ES Fm
Brecciated ES Fm in shear zone
Kk Fm
Fig. 3.7b

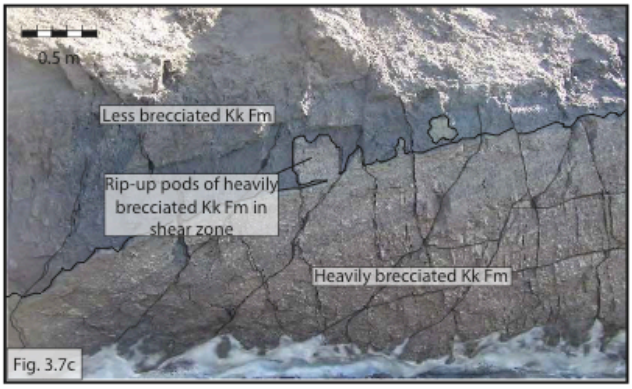
0.5 m
Less brecciated Kk Fm
Rip-up pods of heavily brecciated Kk Fm in shear zone
Heavily brecciated Kk Fm
Fig. 3.7c

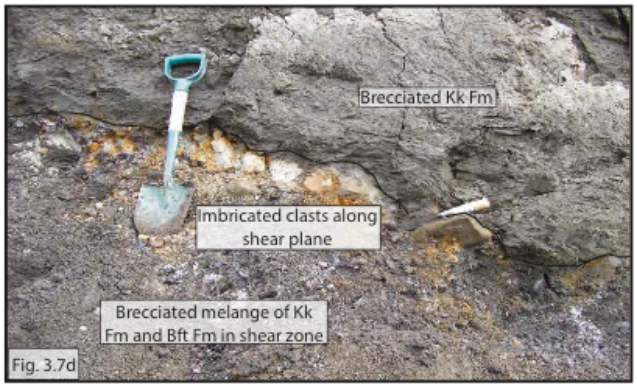
Brecciated Kk Fm
Imbricated clasts along shear plane
Brecciated melange of Kk Fm and Bft Fm in shear zone
Fig. 3.7d

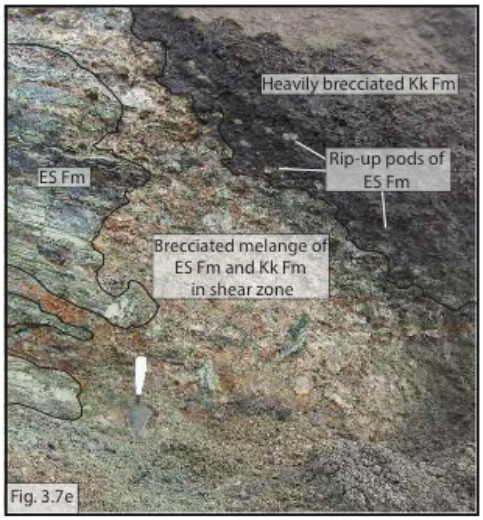
Heavily brecciated Kk Fm
Rip-up pods of ES Fm
ES Fm
Brecciated melange of ES Fm and Kk Fm in shear zone
Fig. 3.7e

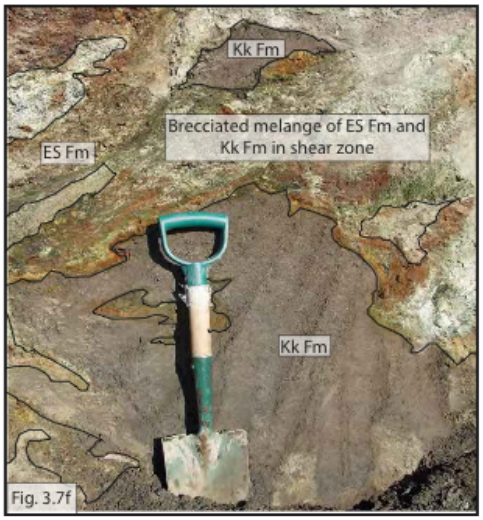
Kk Fm
ES Fm
Brecciated melange of ES Fm and Kk Fm in shear zone
Kk Fm
Fig. 3.7f

(previous page)

Fig. 3.7a. Photograph showing a brecciated mélange in a shear zone between thrust-faulted rafts of Eureka Sound Fm (right) and brecciated Kanguk Fm (left).

Fig. 3.7.b. Photograph showing a brecciated shear zone between Eureka Sound Fm (right) and Kanguk Fm (left) with ground ice occupying shear plane.

Fig. 3.7c. Photograph showing rip-up at a shear zone between two differentially brecciated rafts of Kanguk Fm.

Fig. 3.7d. Photograph showing imbricated clasts along a shear plane between Kanguk Fm (above) and a brecciated mélange of Kanguk Fm and Beaufort Fm (below).

Fig. 3.7e. Photograph showing intensely brecciated Eureka Sound Fm (left) and Kanguk Fm (right) in a shear zone between thrust rafts of Eureka Sound Fm and Kanguk Fm.

Fig. 3.7f. Photograph showing rip-up pods of Kanguk Fm and Eureka Sound Fm (mélange) in a shear zone between Kanguk Fm and Eureka Sound Fm.

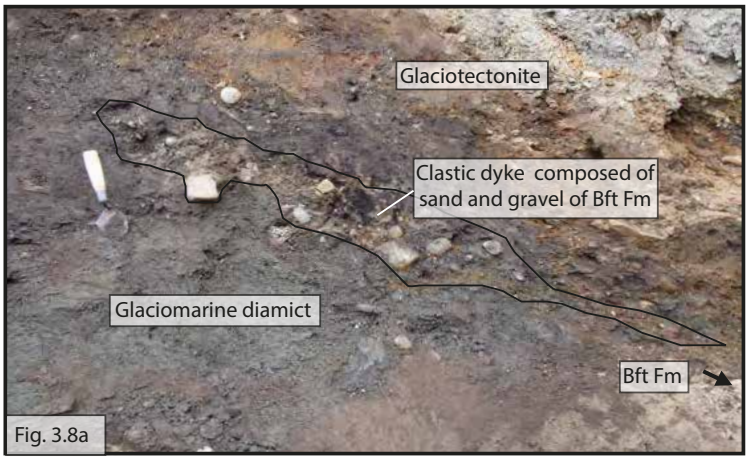
Glaciotectonite
Clastic dyke composed of sand and gravel of Bft Fm
Glaciomarine diamict
Bft Fm
Fig. 3.8a

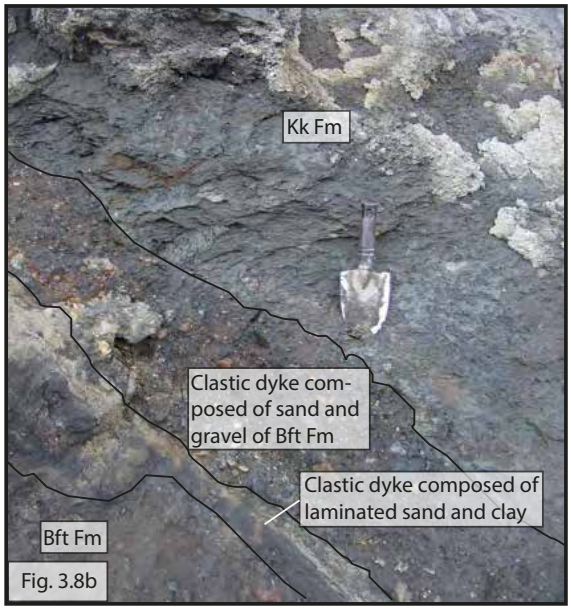
Kk Fm
Clastic dyke composed of sand and gravel of Bft Fm
Clastic dyke composed of laminated sand and clay
Bft Fm
Fig. 3.8b

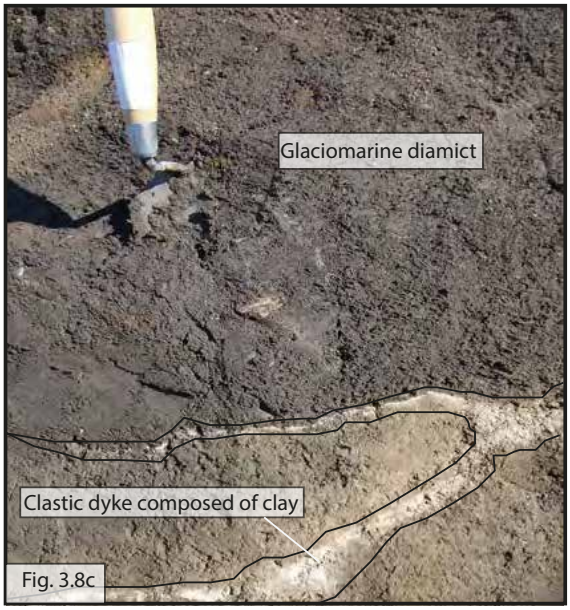
Glaciomarine diamict
Clastic dyke composed of clay
Fig. 3.8c

(previous page)

Fig. 3.8a. Photograph showing a clastic dyke composed of massive sand and gravel sourced from an underlying raft of Beaufort Fm. The clastic dyke has been injected under high hydraulic pressure along a shear plane separating glaciomarine diamict and glaciotectonite.

Fig. 3.8b. Photograph showing a multi-phase clastic dyke. The lower clastic dyke is composed of laminated sand and clay (sourced from the underlying Beaufort Fm and Kanguk Fm) and records a period of lower, more variable hydraulic pressures. The upper dyke is composed of massive sand and gravel (sourced from the underlying Beaufort Fm) and clearly cross-cuts the lower dyke. The upper dyke records a subsequent period of higher hydraulic pressures. The same shear plane has been utilized twice for hydrofracturing.

Fig. 3.8c. Photograph showing a forking clastic dyke composed of massive and laminated clay injected into glaciomarine diamict under lower hydraulic pressures.

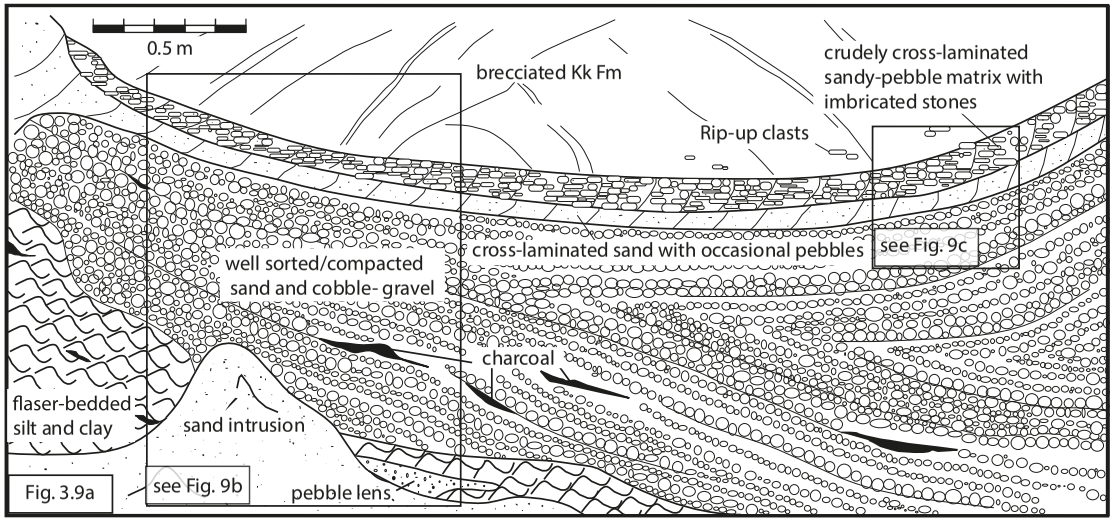
0.5 m
brecciated Kk Fm
crudely cross-laminated
sandy-pebble matrix with
imbricated stones
Rip-up clasts
see Fig. 9c
cross-laminated sand with occasional pebbles
well sorted/compacted
sand and cobble- gravel
charcoal
flaser-bedded
silt and clay
sand intrusion
see Fig. 9b
pebble lens
Fig. 3.9a

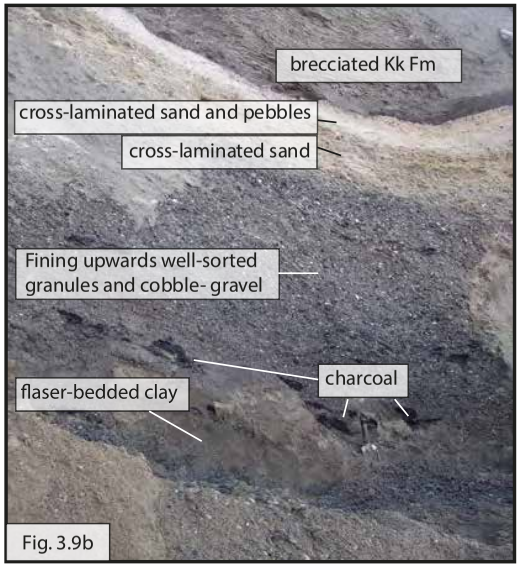
brecciated Kk Fm
cross-laminated sand and pebbles
cross-laminated sand
Fining upwards well-sorted
granules and cobble- gravel
charcoal
flaser-bedded clay
Fig. 3.9b

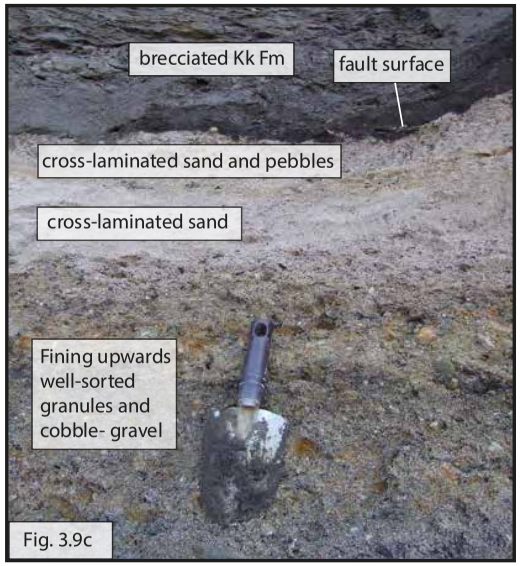
brecciated Kk Fm
fault surface
cross-laminated sand and pebbles
cross-laminated sand
Fining upwards
well-sorted
granules and
cobble- gravel
Fig. 3.9c

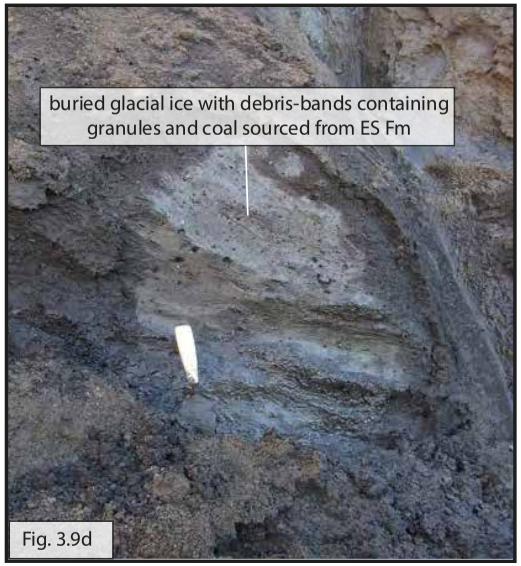
buried glacial ice with debris-bands containing
granules and coal sourced from ES Fm
Fig. 3.9d

(previous page)

Fig. 3.9a. Scaled log of Sub-Domain A1 showing a reverse-faulted raft of Eureka Sound Fm comprising flaser-bedded silt and clay, well-sorted and crudely bedded cobble-gravel with charcoal inclusions, and cross-laminated sandy-pebbles with imbricated stones. The Eureka Sound Fm raft is overlain by a brecciated raft of Kanguk Fm.

Fig. 3.9b. Photograph showing excellent preservation of depositional structures within the raft of Eureka Sound Fm.

Fig. 3.9c. Photograph showing a close-up of the sharp fault surface separating the raft of Eureka Sound Fm from the overlying raft of Brecciated Kanguk Fm.

Fig. 3.9d. Photograph showing buried glacial ice with debris-rich bands currently melting out of the base of the section where it comprises isolated bodies at the contact between the raft of Eureka Sound Fm and an underlying raft of Beaufort Fm. Debris melting out of glacial ice includes granules and coal directly sourced from the overlying Eureka Sound Fm.

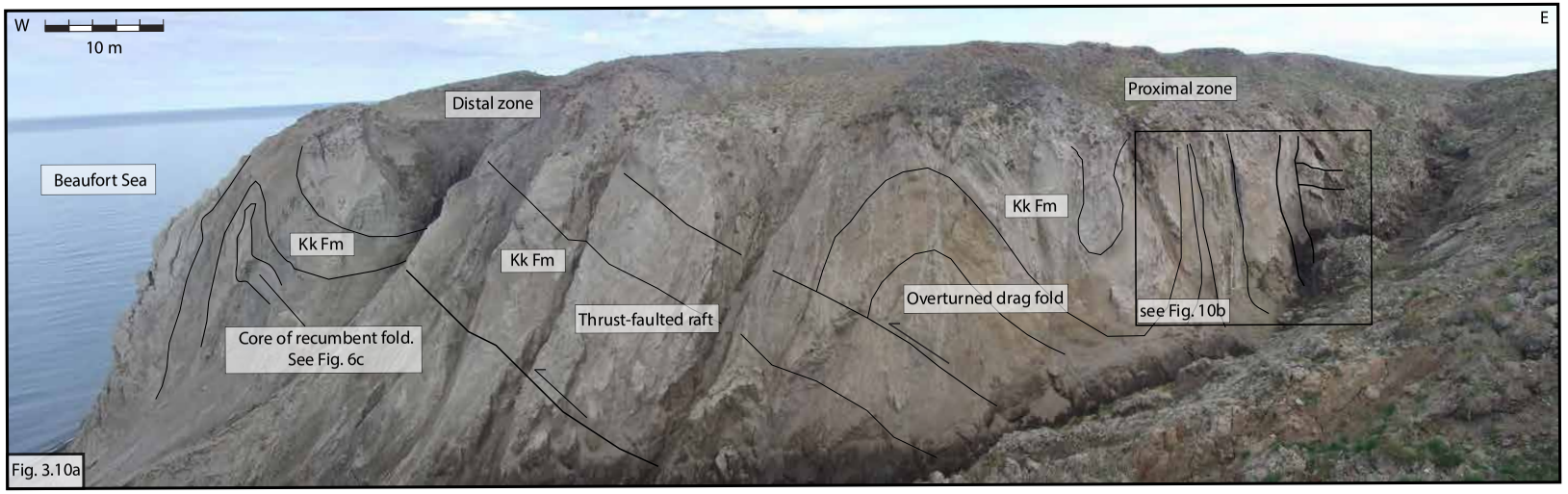
W
10 m
E
Distal zone
Proximal zone
Beaufort Sea
Kk Fm
Kk Fm
Kk Fm
Overturned drag fold
Thrust-faulted raft
see Fig. 10b
Core of recumbent fold.
See Fig. 6c
Fig. 3.10a

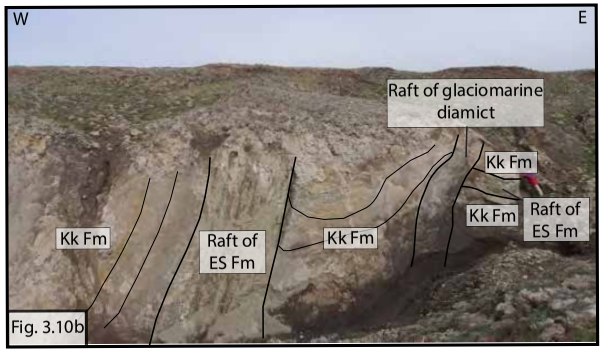
W
E
Raft of glaciomarine
diamict
Kk Fm
Kk Fm
Raft of
ES Fm
Kk Fm
Raft of
ES Fm
Kk Fm
Fig. 3.10b

(previous page)

Fig. 3.10a. Annotated photomosaic showing an east-west exposure (across-strike) of Sub-Domain A2, dominated by Kanguk Fm. A distinct change in deformation can be observed from east (back-thrusted and thrust faulted bedrock rafts) to west (large-scale recumbent fold).

Fig. 3.10b. Photograph showing a close-up of the easternmost stratigraphy. Note the low angle thrust-faulted rafts of Kanguk Fm and Eureka Sound Fm that have been truncated by imbricately stacked back-thrusted rafts of glaciomarine diamict, Kanguk Fm, and Eureka Sound Fm.

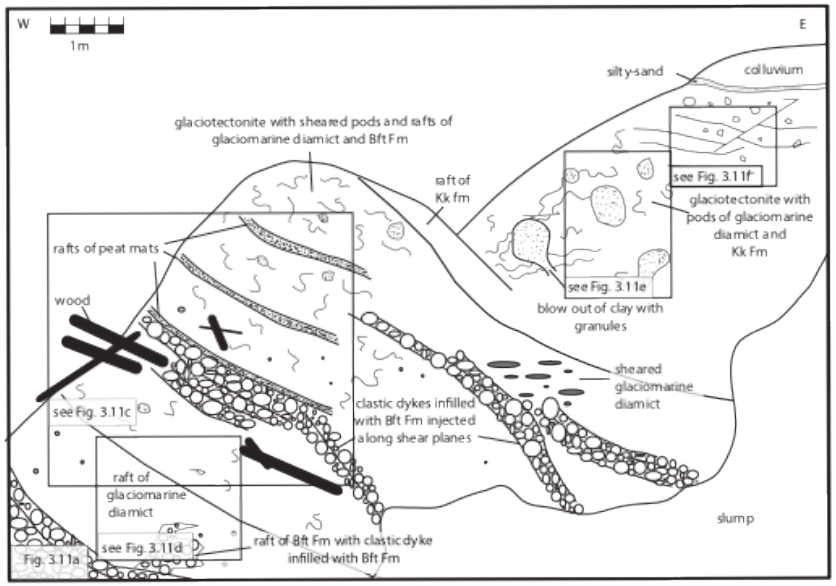
W
E
1m
silty-sand
colluvium
glaciotectonite with sheared pods and rafts of glaciomarine diamict and Bft Fm
raft of Kk fm
see Fig. 3.11f
glaciotectonite with pods of glaciomarine diamict and Kk Fm
rafts of peat mats
wood
see Fig. 3.11e
blow out of clay with granules
sheared glaciomarine diamict
see Fig. 3.11c
clastic dykes infilled with Bft Fm injected along shear planes
raft of glaciomarine diamict
see Fig. 3.11d
slump
raft of Bft Fm with clastic dyke infilled with Bft Fm
Fig. 3.11a

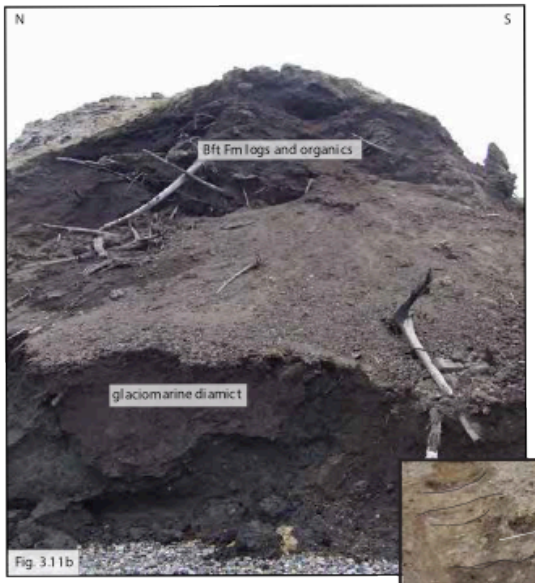
N
S
Bft Fm logs and organics
glaciomarine diamict
Fig. 3.11b

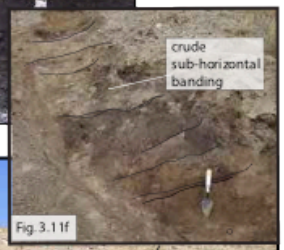
crude sub-horizontal banding
Fig. 3.11f


W
E
Fig. 3.11c

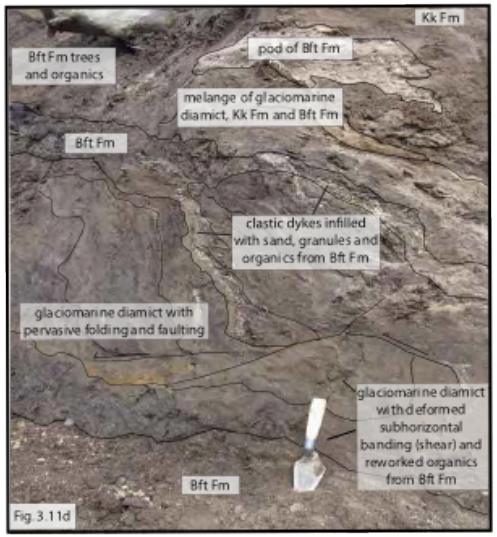
Kk Fm
Bft Fm trees and organics
pod of Bft Fm
melange of glaciomarine diamict, Kk Fm and Bft Fm
Bft Fm
clastic dykes infilled with sand, granules and organics from Bft Fm
glaciomarine diamict with pervasive folding and faulting
glaciomarine diamict with deformed subhorizontal banding (shear) and reworked organics from Bft Fm
Bft Fm
Fig. 3.11d

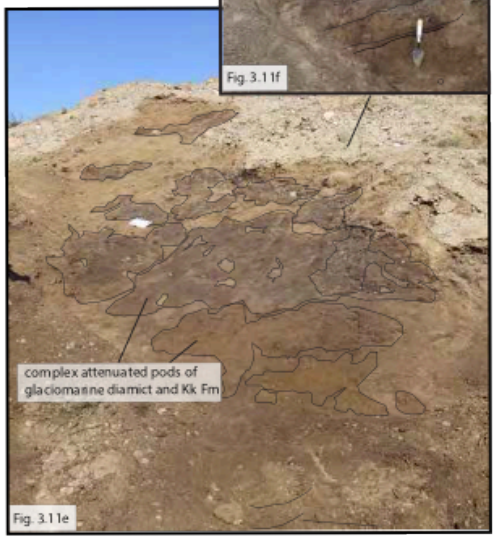
complex attenuated pods of glaciomarine diamict and Kk Fm
Fig. 3.11e

(previous page)

Fig. 3.11a. Scaled log of Sub-Domain B1 (west-east) showing a basal raft of Beaufort Fm overlain by a raft of glaciomarine diamict, in turn overlain by a complex glaciotectonite mélange. From the base upward, the mélange comprises three organic rafts sourced from the Beaufort Fm that have been sheared and deformed along with the rafts of glaciomarine diamict and Kanguk Fm. The glaciotectonite becomes increasingly homogeneous up-section as Beaufort Fm organics become absent and glaciomarine diamict dominates. The deformed Kanguk Fm and glaciotectonite display progressively more distinct strain banding with distance up-section.

Fig. 3.11b. Photograph of Sub-Domain B1 as it appears from the coast (north-south). Note the conspicuous logs and peat eroding from the basal organic raft.

Fig. 3.11c. Photograph showing the base of the glaciotectonite mélange. Note the logs eroding from the basal organic raft.

Fig. 3.11d. Photograph showing a close-up of the glaciotectonite mélange at base of sequence. Note the pervasive folding, small-scale faults, detached pods of Beaufort Fm, and large-scale organics.

Fig. 3.11e. Photograph showing a close-up of the glaciotectonite mélange further up-section. Note the absence of large-scale organics, and complex attenuation of glaciomarine diamict and Kanguk Fm.

Fig. 3.11f. Photograph showing a close-up of the glaciotectonite mélange at top of the section. Note the crude sub-horizontal banding.

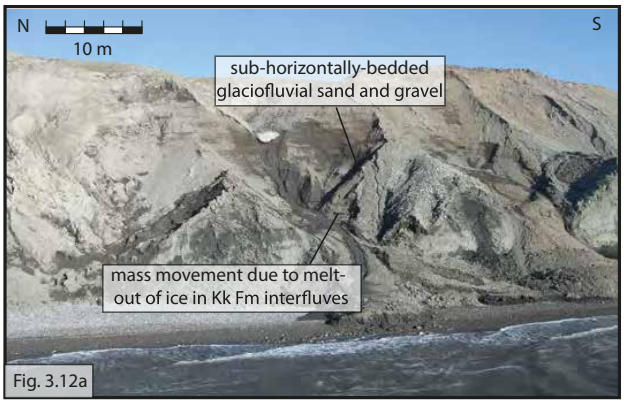
N
10 m
S
sub-horizontally-bedded glaciofluvial sand and gravel
mass movement due to melt-out of ice in Kk Fm interfluves
Fig. 3.12a


granite
Fig. 3.12b


polished surface with slickensides
Fig 3.13a

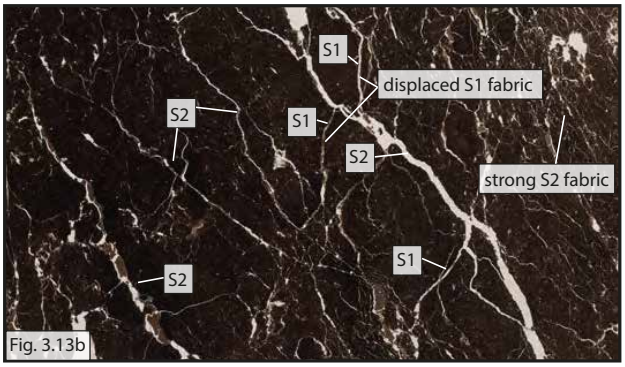
S1
displaced S1 fabric
S2
S1
S2
strong S2 fabric
S1
S2
Fig. 3.13b

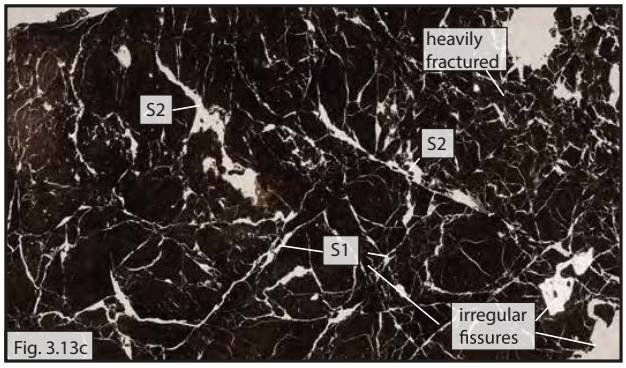
heavily fractured
S2
S2
S1
irregular fissures
Fig. 3.13c

(previous page)

Fig. 3.12a. Annotated photograph showing sub-horizontally bedded glaciofluvial sand and gravel incising Kanguk Fm (interfluves currently slumping).

Fig. 3.12b. Close-up of coarse glaciofluvial sand and gravel displaying sub-horizontal bedding and containing occasional granite clasts (inset).

Fig. 3.13a. Close-up of brecciated Kanguk Fm where sediment samples were collected for thin section production. Kanguk Fm displays polished surfaces and slickensides.

Fig. 3.13b. Thin section of sample 1 of brecciated Kanguk Fm

Fig. 3.13c. Thin section of sample 2 of brecciated Kanguk Fm

Glaciotectonic Model for the Worth Point stratigraphic sequence

Glaciotectonic event 1: Ice-marginal deformation, glaciomarine reworking, and subglacial deformation

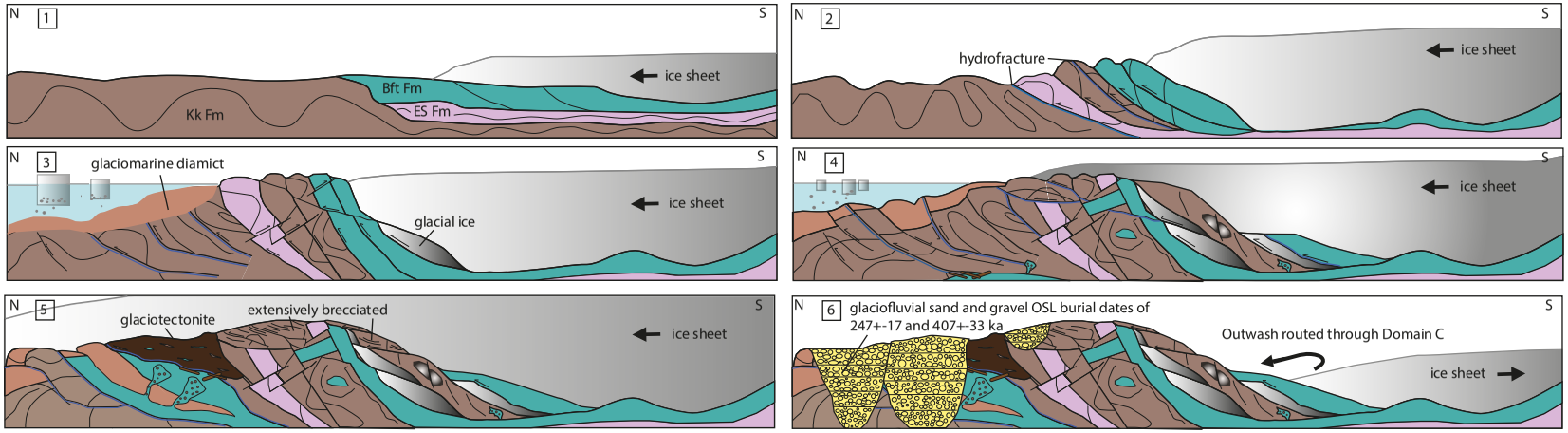

Glaciotectonic event 2: Subglacial deformation

Postglacial erosion to produce modern bluffs

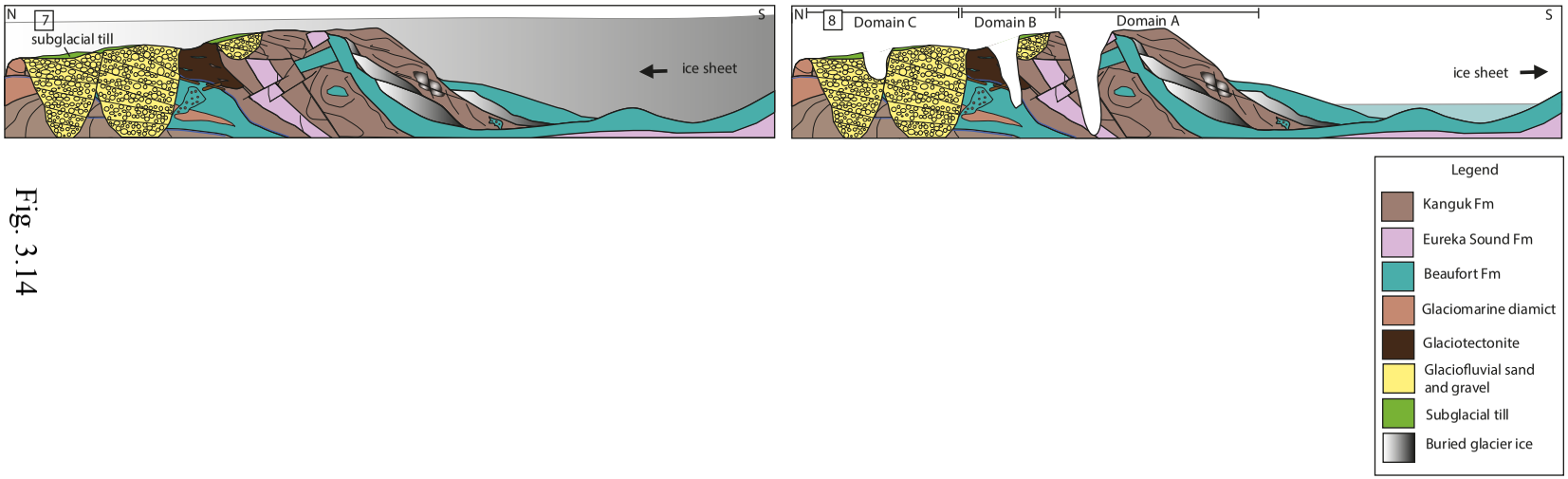

Fig. 3.14

Fig. 3.14. (previous page). Simplified, schematic two-dimensional glaciotectonic model showing the progressive evolution of the Worth Point stratigraphic sequence. The model shows the evolution of the stratigraphic sequence during two distinct glaciotectonic events. Each glaciotectonic event is broken into blocks (1-8) that represent key snapshots in time when the stratigraphic sequence underwent major modification. Block 8 shows a simplified diagram of the sequence as it looks today, with the approximate locations of Domains A-C. The model shows strata oriented south-north (i.e. observed from the coast) with ice advance from the southeast during glaciotectonic event 1, and ice advance from the east during glaciotectonic event 2. As a result, deformational patterns and structures shown for glaciotectonic event 1 are the result of glacially-imposed compression and shear oriented oblique to the viewer, and during glaciotectonic event 2 perpendicular to the viewer.

Glaciotectonic event 1 is represented by blocks 1-6. Blocks 1-2 show initial compressional deformation of the Early Cretaceous and Late Tertiary bedrock by progressive ice-marginal advance, while block 3 shows the concurrent reworking of strata by a glaciomarine transgression and the deposition of a glaciomarine diamict. Compressional deformation was most intense proximal to the ice-margin and best represented in Domain A. Blocks 4-5 show a readvance or sustained advance of the ice sheet and the overriding of the previously deformed strata. This overriding led to the overprinting of shear deformation structures and the deposition of a glaciotectonite that are best represented in Domain B. Block 6 shows subsequent ice sheet retreat, and the incision and aggradation (dated to

approximately 247 ka BP and 407 ka BP) of outwash gullies in Domain C. A deglacial marine regression (to facilitate incision) and a postglacial transgression and/or abundant sediment supply (to facilitate aggradation) are inferred.

Glaciotectonic event 2 is represented by block 7. Block 7 shows the overriding of strata by an ice sheet that produced minimal deformation and deposited a capping till. The till and deformed strata are best preserved and characterized in Domain C.

The model shows how each glaciotectonic event affected the entire stratigraphic sequence, with the final tectonostratigraphy (block 8) resulting from polydeformation. However, the model also highlights how Domains A-C- display deformational patterns and structures resulting from each glaciotectonic event to varying extents. Ice-marginal deformation during glaciotectonic event 1 is best displayed in Domain A, subglacial deformation during glaciotectonic event 1 is best displayed in Domain B, and subglacial deformation during glaciotectonic event 2 is best displayed in Domain C.

CHAPTER 4

A REVISED PLEISTOCENE GLACIAL HISTORY FOR BANKS ISLAND, NT: INSIGHTS FROM THE POLYDEFORMED WORTH POINT STRATIGRAPHIC SEQUENCE.

1. INTRODUCTION

Banks Island, western Canadian Arctic Archipelago (CAA; Fig 4.1), has long been recognized for its outstanding record of Quaternary landforms and sediments (e.g. Hobbs, 1945; Washburn, 1947; Porsild, 1950; Jenness, 1952; Manning, 1956; Craig and Fyles, 1960; Fyles, 1962). An earlier series of Quaternary papers from Banks Island documented an elaborate record of Neogene and Quaternary environmental change (Vincent, 1982, 1983, 1984, 1990; Vincent et al., 1983, 1984) that was widely used for long-distance correlations of Quaternary events around the circumpolar world (e.g. Clark et al., 1984; Matthews and Ovenden, 1990; Darby, 2003; Ehlers and Gibbard, 2004; Ehlers et al., 2011). The model was based on the identification of glacial, nonglacial, and interglacial deposits mantling Banks Island and exposed in expansive coastal sections up to 50 m thick (Vincent, 1983, 1990). Magnetostratigraphic analyses of key subsurface units provided a chronologic framework used to correlate widely separated subsurface sections across the island, prompting the identification of eight continental glaciations and five interglaciations extending back beyond one

million years (1 Ma; Fig. 4.2; Vincent, 1990; Vincent and Barendregt, 1990; Barendregt et al., 1998).

Notably, the interpretation of subsurface units built upon the preceding synthesis of the island's surficial Quaternary geology, which described three separate continental glaciations primarily expressed by lithologically distinct till sheets and a suite of attendant moraines, proglacial lakes and raised marine sediments (Vincent, 1982, 1983). Collectively, these Quaternary deposits were assigned over 50 formal lithostratigraphic names that, for almost three decades, outlined the most detailed record of glacial and sea level change throughout the CAA (Vincent, 1982, 1983, 1984, 1990; Vincent et al., 1983, 1984; Barendregt et al., 1998).

Vaughan et al (in press) have reinvestigated the stratigraphy and sedimentology at Worth Point, southwest Banks Island, which served as one of the type localities in the Quaternary model for Banks Island (Fig. 4.1; Vincent, 1982, 1983, 1984, 1990, 1992; Vincent et al., 1983, 1984). Previous investigations of Worth Point proposed a sequence of undisturbed, horizontally-bedded Quaternary units overlying Cretaceous and Pliocene bedrock (Fig. 4.3; Vincent, 1982, 1983, 1984, 1990). Most notably, till assigned to the earliest island-wide glaciation was reported to directly overly an organic-rich unit ascribed to the preglacial Worth Point Fm, thereby preserving the contact between preglacial and glacial environments on Banks Island (Fig 4.3; Vincent, 1990). In contrast, the revised model of Vaughan et al (in press) documents eight lithofacies at Worth Point, including five previously unreported glaciogenic units that display deep-

seated glaciotectonic disturbance. Vaughan et al (in press) emphasize the description and interpretation of the lithofacies along with evidence for their sequence of deformation. In particular, the nature and style of deformation is discussed and placed in the context of the interaction between cold-based ice and permafrost terrain. This chapter builds upon Vaughan et al (in press) by evaluating further the revised depositional and deformational record at Worth Point in the context of local and regional implications, including the source and timing of deep seafloor scouring throughout the Arctic Ocean that, in part, have been attributed to the northwest Laurentide Ice Sheet (LIS; Kristoffersen et al., 2004; Engels et al., 2007; Jakobsson et al., 2008, 2010, in press; Polyak et al., 2009, 2011; Stein et al., 2010).

1.1. BACKGROUND

Early investigations at Worth Point focused on the 'Worth Point Fm type-site', where conspicuous 'forest beds' were observed eroding from a ~50 m wide valley fill incised into Cretaceous and Pliocene bedrock (Fig. 4.3; Kuc, 1974; Vincent, 1982, 1983, 1990). The 'forest beds' were reputed to contain whole logs and contiguous peat mats of possible interglacial age yielding a rich macrofloral and macrofuanal assemblage symptomatic of an open larch-dominated tundra environment (Kuc, 1974). This floristic signature was interpreted to be distinct from both the underlying bedrock (Pliocene Beaufort Fm) and subsequent interglacial environments identified in the subsurface across Banks Island (Matthews et al., 1986; Fyles et al., 1994). Consequently, the 'forest beds' were assigned to a separate preglacial unit termed the Worth Point Fm (Fig. 4.3;

Vincent, 1990). Two additional Quaternary units were proposed to overly the Worth Point Fm in a horizontally-bedded, 'layer-cake' sequence (Vincent, 1990). These units were assigned to Bernard Till from the earliest glaciation on Banks Island (> 0.78 Ma), overlain by Big Sea sediments from a glacioisostatically forced marine transgression following a Mid-Pleistocene glaciation (0.78 – 0.12 Ma; Fig. 4.3; Vincent, 1990).

Magnetostratigraphic analyses of over 50 sediment samples collected at the Worth Point Fm type-site provide chronologic control on the timing of deposition (Fig. 4.3; Barendregt et al., 1998). Paleomagnetic readings were integrated with the pre-existing Quaternary framework for Banks Island and interpreted to record deposition of the lower Worth Point Fm during the Matuyama Chron (> 1.95 Ma), deposition of the upper Worth Point Fm during the Olduvai subzone within the Matuyama Chron (1.95 – 1.77 Ma), and deposition of Bernard Till and Big Sea sediments during the Brunhes Chron (< 0.78 Ma, Barendregt et al., 1998). Bernard Till was later re-assigned to the Matuyama Chron, prior to the Jaramillo subzone (> 0.99 - 1.07 Ma), based on correlation with the proposed stratigraphy at Morgan Bluffs, eastern Banks Island, where magnetically reversed sediments assigned to the Jaramillo subzone were identified in an organic unit ascribed to a subsequent interglacial (Fig. 4.3; Vincent, 1990; Barendregt et al., 1998). Consequently, the Worth Point Fm type-site was interpreted to record an apparently *in situ* depositional sequence spanning the past 2 million years (Barendregt et al., 1998).

The reinvestigation of Worth Point fundamentally revises the former environmental interpretation (Fig. 4.4; Vaughan et al., in press). Eight lithofacies are now recognized within the stratigraphic sequence, including three bedrock units and five previously unreported glaciogenic units. Bedrock units are interpreted to be mudstone of the Late Cretaceous Kanguk Fm, deltaic sand and gravel of the Eocene-Miocene Eureka Sound Fm, and fluvial sand and gravel of the Pliocene Beaufort Fm (Fig. 4.4; Vaughan et al., in press). Glaciogenic units are interpreted to be buried glacial ice and ground ice, glaciomarine diamict, glaciofluvial sand and gravel, subglacial till, and a glaciotectonite mélange (Fig. 4.4). All eight units have been pervasively glaciotectonized and display complex overprinting of deformation structures indicative of polydeformation (Fig. 4.4; Vaughan et al., in press). Based on the analyses of cross-cutting patterns and the application of optically stimulated luminescence (OSL) dating to sand within glaciofluvial deposits, two separate glaciotectonic events are identified (Vaughan et al., 2013).

A fundamental revision of the Worth Point stratigraphic sequence is consistent with similarly major revisions of subsurface records at Morgan Bluffs and Duck Hawk Bluffs, eastern and southwestern Banks Island, respectively (Fig. 4.1; Lakeman, 2012; Evans et al., in press). Collectively, these stratigraphic sections document at least three Pleistocene glaciations spanning the Bruhnes-Matuyama Chrons (~1 Ma – 0.02 Ma), replacing the previous proposal for up to eight glaciations and five interglaciations (Vincent, 1990). Similarly, widespread resurveys of the surficial glacial geology of Banks Island demonstrate island-wide

glaciation by the northwest LIS during the Late Wisconsinan (England et al., 2009; Lakeman and England, 2012, 2013; This thesis, Chapter 2), supplanting the former surficial model outlining a series of three Quaternary glaciations (Vincent, 1982, 1983).

Revisions of the surface and subsurface glacial records on Banks Island warrant a reassessment of former regional correlations (Vincent, 1982, 1983, 1984, 1990; Barendregt et al., 1998). This chapter reintroduces and expands upon key lithological and chronological data from Worth Point that form a foundation for this assessment.

2. KEY DATA FROM WORTH POINT

2.1. Timing of glaciation

Analysis of cross-cutting and superimposed deformation structures within the Worth Point stratigraphic sequence support glaciotectonism by two separate ice sheets (Vaughan et al., in press). Regional geomorphology indicates that Banks Island was most recently glaciated by the northwest LIS during Late Wisconsinan (England et al., 2009; Lakeman and England, 2013; This thesis, Chapter 2). At Worth Point, meltwater channels grade to marine limit (11-15 m asl) that is fully compatible with the previously published, island-wide gradient (England et al., 2009; Lakeman and England 2012, 2013; This thesis, Chapter 2). These meltwater channels form a single deglacial sequence extending eastwards across Banks Island where widespread shell-bearing marine limit deposits constrain their age to an interval predating ~13,750 cal yr BP (England et al., 2009; Lakeman and England, 2012; This thesis, Chapter 2). Moreover, reworked

shells mantling marine limit across western Banks Island consistently date to marine isotope stage (MIS) 3, supporting redeposition by Late Wisconsinan ice (McNeely and Jorgensen, 1992; Lakeman and England, 2013; This thesis, Chapter 2). This Late Wisconsinan advance is the most likely candidate for the superimposed (youngest) glaciotectonic deformation identified at Worth Point.

Two minimum OSL burial ages of 247 ± 17 ka and 407 ± 33 ka obtained on glaciofluvial sand that aggraded in gullies following initial glaciotectonism at Worth Point currently provide the best minimum limiting ages for the timing of the earliest identified ice advance (Vaughan et al., in press). OSL ages were determined using the single-aliquot regenerative (SAR) technique for quartz at the Sheffield Centre for International Drylands Research, UK. OSL dating was utilized at Worth Point as it has been shown to produce more consistent results than infrared stimulated luminescence (IRSL) and thermoluminescence (TL) dating for pre-Late Wisconsinan Arctic sediments (e.g. Buylaert et al., 2012; Alexanderson and Håkansson, in press). Furthermore, quartz was selected over feldspar for OSL dating as it bleaches more readily – a particularly important factor in high-latitude glaciofluvial environments where suspended sediment limits summer sunlight (Bateman, 2008). Despite the advantages of OSL quartz dating, replicate data for both OSL ages produced significant scatter. Several aliquots of the sample yielding the oldest age (407 ± 33 ka) were also saturated, possibly reflecting the incorporation of sediment from multiple ages (Alexanderson et al., in press). The age discrepancy between the two dates also renders one incorrect.

Additional chronological control is provided by over 50 paleomagnetic readings previously obtained from the Worth Point Fm type-site (Fig. 4.3; Barendregt et al., 1998). The Worth Point Fm type-site has been reinterpreted by Vaughan et al (in press) as a glaciotectonite mélange, comprising thrust and sheared rafts of Cretaceous Kanguk Fm, Pliocene Beaufort Fm, and Mid-Pleistocene (*sensu lato*) glaciomarine diamict (Fig. 4.4). Placed within a glaciotectonic context, the presence of both reversed and normal polarity readings likely reflects the stacking of these units (Fig. 4.3). Reversed polarity readings reported on organic rafts previously assigned to the Worth Point Fm (Barendregt et al., 1998) support their origin as Pliocene Beaufort Fm deposited during the Early Matuyama Chron (> 0.78 Ma). The inclusion of coniferous trunks and peat mats also corroborate a Beaufort Fm origin. Similarly, the occurrence of normal polarity readings in deposits overlying the Beaufort Fm rafts support their origin as largely reworked glaciomarine diamict deposited during the Bruhnes normal Chron (< 0.78 Ma). The orderly pattern of polarity readings up-section is interpreted to document the thrusting of lithologic units as discrete frozen rafts that escaped significant mixing with surrounding sediment (Fig. 4.3).

2.2. Source of glaciation

Far-travelled erratics have been identified in buried glacial ice, glaciomarine diamict, glaciofluvial sand and gravel, and subglacial till at Worth Point (Vaughan et al., in press). Notably, these erratics include granite erratics indicative of northwestward transport from the Precambrian Shield on mainland Canada, and sandstone, siltstone, and quartzite erratics indicative of westward

transport from Neoproterozoic and Cambrian-Devonian bedrock on Victoria Island (Vaughan et al., in press). In accordance with the depositional and deformational sequence outlined by Vaughan et al (in press), buried glacial ice is inferred to have been deposited during or prior to a Mid-Pleistocene (*sensu lato*) glaciation, glaciomarine diamict and glaciofluvial sand and gravel during a Mid-Pleistocene (*sensu lato*) glaciation, and subglacial till during a Late Wisconsinan glaciation.

The similarity of erratic lithologies observed in glaciogenic units inferred to be of widely separate ages is most simply explained by deposition from ice sheets with comparable configurations. Because the primary configuration of the Late Wisconsinan LIS on southern Banks Island has been documented (This thesis, Chapter 2), this configuration may be used to broadly infer that of the Mid-Pleistocene (*sensu lato*) ice sheet. Notably, Late Wisconsinan Laurentide ice that crossed southern Banks Island dispersed from ice divides within the Keewatin Ice Dome and advanced beyond Banks Island onto the polar continental shelf (This thesis, Chapter 2). Ice dispersal was predominantly from the north-south trending M'Clintock Ice Divide bisecting Victoria Island to the east (Dyke and Prest, 1987), which fed a westward flowing ice stream in Amundsen Gulf that was coalescent with cold-based ice advancing westward across the island's interior (Stokes et al., 2005, 2006, 2009; This thesis, Chapter 2). Prior to the establishment of the Amundsen Gulf Ice Stream, the east-west trending Ancestral Keewatin Ice Divide bisecting mainland Canada to the south (Dyke and Prest, 1987) likely dispersed ice northwards into the western CAA (Doornbos et al., 2009; This

thesis, Chapter 2). If advance of the Mid-Pleistocene (*sensu lato*) ice sheet followed a similar trajectory – as supported by erratic lithologies – then early glaciation by the ancestral northwest LIS, rather than by localized ice caps, is implicit. Evidence for the overriding of Worth Point by the Mid-Pleistocene (*sensu lato*) ice sheet (imparting shear deformation in a subglacial setting) also supports its extension onto the adjacent polar continental shelf (Vaughan et al., in press).

3. DISCUSSION

3.1. Former correlations

3.1.1. Chukchi-Alpha Ridge

The previous Neogene and Quaternary record on Banks Island was the first in the CAA to extend beyond the Bruhnes-Matuyama polarity reversal at 0.78 Ma (Vincent et al., 1983; Barendregt and Vincent, 1990; Barendregt et al., 1998). The identification of this polarity reversal provided a prominent marker horizon that permitted correlation between the Banks Island record and magnetically constrained sediments of the Chukchi-Alpha ridge in the Arctic Ocean, over 1000 km away (Clark et al., 1984). Accordingly, till deposits on Banks Island formerly ascribed to three progressively less extensive continental glaciations were assumed to correlate with layers in Arctic Ocean cores composed of correspondingly less coarse ice-rafted debris (IRD; Clark et al., 1984). Conversely, interglacial deposits identified in the subsurface record on Banks Island were correlated with intervening layers of fine-grained, IRD-free sediment in the Arctic Ocean cores (Clark et al., 1984). Collectively, these correlations

extended back to marine isotope stage (MIS) 22 (> 1 Ma) and constituted the first attempt to link long-term and long-distance terrestrial and marine records in the Canadian Arctic (Vincent, 1982; Clark et al., 1984).

This correlation has been fundamentally challenged by the recently revised Banks Island record documenting the advance of an extensive northwest LIS across Banks Island during the Late Wisconsinan and Mid-Pleistocene (*sensu lato*), with an additional advance reaching at least eastern Banks Island during the Early Pleistocene ((England et al., 2009; Lakeman, 2012; Lakeman and England, 2012, 2013; This thesis, Chapter 2). This revised record contrasts with the former model proposing widespread ice-free terrain during the Mid to Late Pleistocene that was used to interpret earlier records of IRD in the Arctic Ocean cores of the Chukchi-Alpha ridge (Vincent, 1982, 1983, 1984; Clark et al., 1984). Consequently, the previously proposed correlations between the Late Quaternary record of the CAA and the Arctic Ocean need to be revisited.

3.1.2. Horton Plateau

The former long-term glacial record of Banks Island continues to be correlated with the glacial record of the Horton Plateau, NT, where an independent ice cap is proposed during the Early Pleistocene (Fig. 4.5; Barendregt and Duk-Rodkin, 2004; Duk-Rodkin et al., 2004: Duk-Rodkin and Barendregt, 2011). This proposal is based on a single section in the Smoking Hills area where four till sheets are reported to overlie preglacial sand and gravel (Duk-Rodkin et al., 2004). Paleomagnetic measurements of the till sheets indicate that the lowest three were deposited during the magnetically reversed Matuyama Chron (> 0.78

Ma, Early Pleistocene) whereas the uppermost till sheet was deposited during the magnetically normal Bruhnes Chron (< 0.78 Ma, Mid to Late-Pleistocene; Duk-Rodkin et al., 2004). The identification of shield clasts within and directly mantling the uppermost till sheet led to its assignment to the Late Wisconsinan when the LIS subsumed the region (Duk-Rodkin et al., 2004; Dyke, 2004). In contrast, the three underlying till sheets contain clasts that are entirely local in origin, ostensibly supporting the hypothesis that they were deposited by an independent ice cap centered over the Horton Plateau (Fig. 4.5; Duk-Rodkin and Barendregt, 2011).

The Smoking Hills record is correlated with the former Banks Island record, where multiple magnetically reversed diamictons, interpreted as till sheets, were ascribed to Early Pleistocene glaciations (Vincent, 1982, 1983, 1984, 1990; Vincent et al., 1983, 1984; Vincent and Barendregt, 1990; Barendregt et al., 1998). At Worth Point, till purportedly deposited during the earliest Banks Glaciation (prior to the Jaramillo subzone of the Matuyama Chron, > 1.99 – 1.07 Ma) forms a central component of this correlation (Vincent, 1990; Barendregt et al., 1998). Based on paleomagnetic affinity, the Horton Plateau Ice Cap is proposed to have dispersed northwards and glaciated Banks Island up to three times during the Early Pleistocene (Duk-Rodkin and Barendregt, 2011). However, why the glaciation of Banks Island would have originated in the Smoking Hills is glaciologically perplexing. Firstly, the proposed accumulation area would have been very small (assuming ice could not have formed on the adjacent Precambrian Shield) and all of southeast Banks Island has comparably high topography to the

Smoking Hills and hence would be expected to form its own ice cap farther north. Secondly, the advance of ice from localized uplands like the Smoking Hills would have had considerable difficulty in overcoming calving throughout Amundsen Gulf (500 m deep) south of Banks Island (Fig. 4.5).

It follows that any till deposits at Worth Point associated with glaciation by the Horton Plateau Ice Cap should be: a) devoid of granite clasts, and; b) magnetically reversed. Buried glacier ice, glaciomarine diamict, and glaciofluvial sand and gravel emplaced during the *earliest* recorded glaciation *all* contain granite erratics that require an ice sheet trajectory from the Precambrian Shield, ~200 km east of the Horton Plateau. Moreover, the reinterpretation of polarity readings at the Worth Point Fm type-site indicates that thrust rafts of Beaufort Fm are the only sediments that are magnetically reversed. Consequently, it is proposed that correlation between the Smoking Hills record on the Horton Plateau and subsurface sections on Banks Island be abandoned (Barendregt and Duk-Rodkin, 2004; Duk-Rodkin et al., 2004; Duk-Rodkin and Barendregt, 2011). Moreover, because the northwest LIS is known to have reached at least eastern Banks Island during the Early Pleistocene (Lakeman, 2012), it is suggested that this ice margin was also able to reach the Horton Plateau and deposit the magnetically reversed till sheets identified there (Duk-Rodkin and Barendregt, 2011). Alternatively, ice that reached the Horton Plateau might have been sourced from the Mackenzie Valley, transporting non-shield lithologies during earlier ice advances (e.g. Hidy et al., 2013).

3.2. Alternative hypotheses

Correlation with the revised glaciotectonic model of Worth Point (Vaughan et al., in press) remains untenable until a more robust chronology is established. However, an assessment of regional evidence in support of glaciation coincident with each OSL date, and with an inferred Late Wisconsinan glaciation, will provide an improved insight into the most likely timing of glaciotectonic events identified at Worth Point. Despite limitations associated with the OSL ages (section 3.1), in the absence of additional chronological control, these ages currently provide the best indication of the broad timing of early glaciotectonism, and as such warrant further assessment.

3.2.1. Regional glaciation during MIS 12

The oldest OSL date of 407 ± 33 ka BP may reflect glaciation during MIS 12. MIS 12 has been identified as a period of northwest LIS expansion based on the provenance and age of IRD in sediment cores obtained from the Mendeleev Ridge, western Arctic Ocean (Stein et al., 2010). Terrestrial evidence supporting this expansion, however, is absent. West of former LIS limits, raised marine shorelines up to 23 m above sea level (asl) across the Arctic Coastal Plain on the opposing Alaskan mainland may relate to an MIS 12 highstand that was forced glacioisostatically (Kauffman and Brigham-Grette, 1993). This highstand, termed the Wainwrightian transgression, has been constrained by amino acid racemization dates to 0.47-0.54 Ma, though an incomplete knowledge of environmental factors that impacted protein degradation within the dated fossils renders their ages tentative (Kauffman and Brigham-Grette, 1993). The

Wainwrightian transgression has been correlated with the Anvillian Transgression on the Seaward Peninsula of western Alaska and with a period of glaciation in the Brooks Range of northwestern Alaska (Kauffman and Hopkins, 1986; Kauffman and Brigham-Grette, 1993). Beyond the Alaskan Arctic extensive MIS 12 glaciation has been recorded in Europe, where ice sheets advanced across the lowlands of Europe and into the North Sea Basin farther than during any previous Quaternary glaciation (Sejrup et al., 2005; Böse et al., 2012).

3.2.2. Regional glaciation during MIS 6

The youngest OSL date of 247 ± 17 ka may alternatively record glaciation during MIS 6. An extensive MIS 6 ice margin in the western CAA has been proposed based on the provenance of IRD in widespread Arctic Ocean sediment cores (Bischof and Darby, 1997; Phillips and Grantz, 2001; Jakobsson et al., 2008, in press; Stein et al., 2010). Beyond the western CAA, the depth of MIS 6 glaciogenic scouring observed throughout the Arctic Ocean basin is deeper and more pervasive than during any other Quaternary glaciation, including the last glacial maximum (LGM; Jakobsson et al., in press). Specifically, deep draft glacial erosion has also been documented on the Lominosov Ridge, Yermak Plateau, and Morris Jessup Rise, reflecting expansive circumpolar ice sheets fringing the Arctic Ocean and extending onto and beyond the polar continental shelf as ice shelves (Jakobsson et al., 2001, in press; Polyak et al., 2001; Kristoffersen et al., 2004; Svendsen et al., 2004; Dowdeswell et al., 2010; Gebhardt et al., 2011). Collectively, this expansive marine ice sheet complex supports conceptual oceanographic models proposing reduced and deeper inflow

of Atlantic water into the western Arctic Ocean during MIS 6, precluding basal melting and promoting ice shelf stability (Jakobsson et al., 2010).

Terrestrial evidence within the western CAA for the source of formerly thick ice shelves grounded in the adjacent Arctic Ocean remains enigmatic (Jakobsson et al., 2010). However, high-resolution seismic bathymetric profiles of the marine channels encircling Banks Island have been interpreted to record at least nine Quaternary ice advances, all of which terminate on the continental shelf edge at a trough mouth fan containing a minimum of 10,000 km^3 of glaciogenic debris (Blasco et al., 1990, 2005; Batchelor et al., in press). Despite the questionable assumption that only one till sheet is deposited per glacial cycle (i.e. precluding stacked or complex facies associations), the volume of sediment deposited in the terminal trough mouth fan does support the likelihood of multiple Pleistocene LIS advances, but leaves their chronology undocumented with regard to MIS 6 or other pre-Late Wisconsinan glaciations (Batchelor et al., in press).

Additional terrestrial evidence for MIS 6 ice sheets encircling the Arctic Ocean is widespread, including in the East Siberian Islands (Basilyan et al., 2010), Barents and Kara Seas (e.g. Svendsen et al., 2004; Möller et al., 2006; Jakobsson et al., in press), northern Europe and the British Isles (e.g. Ehlers et al., 2011; Böse et al., 2012), North Sea (e.g. Böse et al., 2012), and Midcontinent North America (e.g. Jennings et al., 2007). Within northwestern North America, MIS 6 expansion of the Cordilleran Ice Sheet is recorded in central Yukon (Demuro et al., 2012) and southern Yukon (Ward, 2012), and localized upland glaciations are recorded in central Alaska (Béget et al., 2003), and northeastern

Russia (Brigham-Grette et al., 2003; Stauch and Gualtieri, 2008; Nürnberg et al., 2011; Barr and Clark, 2012). Colleoni et al (2011) attribute such extensive global glaciation to an MIS 6 orbital configuration that resulted in less solar energy reaching polar regions than during the LGM.

Based on terrestrial and marine evidence for Mid-Pleistocene glaciation, the younger OSL date of 247 ± 17 ka (MIS 6) is currently the preferred age estimate for initial glaciotectonism documented at Worth Point. Consequently, the older OSL date (407±33 ka BP) should be dismissed. It is noted that other, pre-Late Wisconsinan advances cannot be discounted. For example, during MIS 4 consistently oriented glaciogenic bedforms observed at depths of 450 - 1000 m below sea level (bsl) on the Northwind Ridge and Chukchi Plateau are proposed to record the vigorous delivery of deep draft ice from the northwest LIS to the western Arctic Ocean (Polyak et al., 2001, 2007; Jakobsson et al., 2008, 2010). East-west oriented bedforms on the Alaska-Beaufort Margin also dated to MIS 4 corroborate that the Early Wisconsinan was an interval of energetic ice evacuation from the western CAA (Engels et al., 2008).

3.2.3. Regional glaciation during the Late Wisconsinan

In addition to a Mid-Pleistocene (MIS 6?) glaciation, the revised Worth Point model supports a later glaciation, most likely during the Late Wisconsinan (Vaughan et al., in press). This interpretation supports the revised surficial model on Banks Island documenting island-wide glaciation by the northwest LIS (England et al., 2009; Lakeman and England, 2012, 2013; This thesis, Chapter 2). An expansive northwest LIS is also compatible with evidence for an LGM ice

sheet complex occupying the CAA, including the coalescent margins of the northwest LIS and southwest Innuitian Ice Sheet (IIS), which collectively nourished multiple ice streams that debouched into the Arctic Ocean (Stokes et al., 2005, 2006, 2009; England et al., 2009; Scott et al., 2009; Lakeman and England, 2012, 2013; Maclean et al., 2010, 2012; Nixon et al., in press). These ice streams included the Massey Sound Ice Stream (> 440 m thick), and Nares Strait Ice Stream (> 1000 m thick) debouching from the IIS, along with the M'Clure Strait Ice Stream (> 635 m thick), and Amundsen Gulf Ice Stream (> 1000 m thick) debouching from the northwest LIS (Stokes et al., 2005, 2006, 2009; England et al., 2006, 2009; Scott et al., 2009; MacLean et al., 2010, 2012; This thesis, Chapter 2). To the south of Banks Island, ice streams in the Mackenzie and Anderson river valleys advanced toward the Beaufort Sea shelf and were flanked to the west by Laurentide ice that entered the Richardson Mountains and Peel Plateau (impounding Glacial Lake Old Crow) and subsumed the Mackenzie Delta and Yukon Coastal Plain (Mackay, 1959; Hughes, 1972; Rampton, 1982; Morlan et al., 1990; Duk-Rodkin and Hughes, 1991; Zazula et al., 2004; Kennedy et al., 2010; Fritz et al., 2012). Stability of these former ice streams was likely favoured by landfast 'paleocrystic' sea ice and/or ice shelves throughout the Arctic Ocean, hampering ocean sedimentation and circulation patterns (Bradley and England, 2008; Polyak et al., 2009). An absence of biogenic matter and extremely low sedimentation rates in the western Arctic Ocean between 13,000 – 20,000 ^{14}C yr BP also support pervasive ice cover at this time (Polyak et al., 2004). Notably, keel scour marks at depths of < 350 – 400 m bsl on the Northwind Ridge and

Chukchi Plateau in the western Arctic Ocean have been linked to the passage of icebergs and/or ice shelves nourished by ice streams draining the northwest LIS during the LGM (e.g. Polyak et al., 2001; Engels et al., 2008; Hill and Driscoll, 2010). Collectively, this data supports the advance of the northwest LIS across Worth Point and onto the polar continental shelf during the Late Wisconsinan.

3.3. Implications for the ancestral Laurentide Ice Sheet

The provenance of far-travelled erratics in glaciogenic deposits identified at Worth Point provide new insights into the configuration of the ancestral LIS. Notably, erratic lithologies in Mid-Pleistocene (MIS 6?) glaciogenic deposits are similar to those inferred to have been deposited during the Late Wisconsinan, indicating that the paleotopography of the northwest LIS was broadly similar during widely separated glaciations. This may reflect the dominant role of topographic troughs in the western CAA, such as Amundsen Gulf, for governing former ice sheet flow patterns (Batchelor et al., in press). Evidence for glacial overriding at Worth Point during initial glaciotectonism also confirms that the ancestral LIS extended onto the polar continental shelf, placing new constraints on its extent. Evidence for an expansive northwest LIS during the Mid-Pleistocene (MIS 6?) builds upon evidence from eastern Banks Island documenting an Early Pleistocene advance of the northwest LIS (Lakeman, 2012). Collectively, these studies contribute to a major gap in our understanding of Quaternary events (the ancestral activity of the LIS) that has long remained enigmatic, reflecting the fragmented nature of subsurface records in the western CAA and the large-scale obliteration of surficial geomorphic evidence by the Late

Wisconsinan LIS (Polyak et al., 2007; Stein et al., 2010; Jakobsson et al., in press).

The chronology discussed in this chapter is provisional, and should be utilized to prompt future research into the history of the ancestral LIS. To facilitate meaningful correlation between Worth Point and other circumpolar records, additional chronologic control is required. Possible future research could focus on comprehensive OSL dating at Worth Point to constrain the timing of glaciation, combined with seismic surveys on the adjacent polar continental shelf to identify ancestral LIS margins (Blasco et al., 1990, 2005; MacLean et al., 2012; Batchelor et al., in press).

4. CONCLUSIONS

The revised glaciotectonic model for Worth Point identifies two glaciations that have been tentatively constrained to the Mid-Pleistocene (*sensu lato*) and Late Wisconsinan (Vaughan et al., in press). This chapter assesses key lithological data from Worth Point that support glaciation by similarly configured ice sheets that dispersed from the Keewatin Ice Dome and terminated on the polar continental shelf distal to Banks Island. These findings negate former proposals for early glaciation by a localized ice cap on the Horton Plateau, mainland Canada (Barendregt and Duk-Rodkin, 2004; Duk-Rodkin et al., 2004; Duk-Rodkin and Barendregt, 2011). An assessment of chronological data highlights regional evidence in support of early glaciation during MIS 6 when the largest Quaternary marine ice sheet complex occupied the Arctic Ocean (e.g. Svendesen et al., 2004;

Jakobsson et al., 2010; Böse et al., 2012). A later glaciation during the Late Wisconsinan is consistent with evidence for the complete inundation of Banks Island by the northwest LIS during the LGM (e.g. England et al., 2009; Lakeman and England, 2012, 2013; This Thesis, Chapter 2). This revised chronology challenges former environmental correlations, including the Chukchi-Alpha Ridge record in the Arctic Ocean (Clark et al., 1984).

Notably, this chapter identifies the revised glacial record at Worth Point as an important foundation for future investigations of the ancestral LIS. Instructive areas of future research include the establishment of a robust chronology for Worth Point and the identification of ancestral LIS margins on the adjacent polar continental shelf. Constraining this history bears upon the flux of ice and sediment to the Arctic Ocean where ancient seabed scouring is documented (e.g. Jakobsson et al., 2010) and on the evolution of circumpolar paleoclimate during glacial/interglacial cycles (e.g. Abe-Ouchi and Otto-Bliesner, 2009).

5. REFERENCES

Abe-Ouchi, A., Otto-Bliesner, B. 2009. Ice sheet-climate interactions during the ice age cycle. PAGES news. 17, 73-74.

Alexanderson, H., Backman, J., Cronin, T.M., Funder, S., Ingólffson, O., Jakobsson, M., Landvik, J.Y., Lowemark, L., Mangerud, J., Marz, C., Möller, P., O'Regan, M., Spielhagen, R.F. An Arctic perspective on dating Mid-Late Pleistocene environmental history. Quaternary Science Reviews. In press.

Alexanderson, H., Hákansson, L. Coastal glaciers advanced onto Jameson Land, east Greenland during the late glacial-early Holocene Milne Land Stade. Polar Research. In press.

Barendregt, R.W., Vincent, J-S., Irving, E., Baker, J. 1998. Magnetostratigraphy of Quaternary and Late Tertiary sediments on Banks Island, Canadian Arctic Archipelago. Canadian Journal of Earth Sciences. 35, 147-161.

Barendregt, R.W., Duk-Rodkin. 2004. Chronology and extent of Late Cenozoic ice sheets in North America: a magnetostratigraphic assessment. In: Ehlers, J., Gibbard, P. (Eds.). Quaternary Glaciations – Extent and Chronology. Part II: North America. Amsterdam. Elsevier.

Barr, I.D**.,** Clark, C.D. 2012. Late Quaternary glaciations in Far NE Russia; combining moraines, topography and chronology to assess regional and global glaciation synchrony. *Quaternary Science Reviews.* 53, 72-87.

Basilyan, A.E., Nikol'skyi, P.A., Maksimov, F.E., Kuznetsov, V.Y. 2010. Age of cover glaciation of the New Siberian islands based on 230Th/U-dating of mollusk shells, Structure and development of the lithosphere. Paulse, Moscow. 506-514.

Batchelor, C.L., Dowdeswell, J.A., Pietras, J.T. Evidence for multiple Quaternary ice advances and fan development from the Amundsen Gulf cross-shelf trough and slope, Canadian Beaufort Sea Margin. Marine and Petroleum Geology. In press.

Bateman, M.D. 2008. Luminescence dating of periglacial sediments and structures. Boreas. 37, 574-588.

Berger, G.W., Polyak, L. 2012. Testing the use of quartz 'micro-hole' photon-stimulated luminescence for dating sediments of the central Lominosov Ridge, Arctic Ocean. Quaternary Geochronology. 11, 42-51.

Béget, J.E., Layer, P., Keskinen, M. 2003. Interactions between volcanism, permafrost, Milankovitch cycles, and climate change on the Seward Peninsula. Abstracts with Programs, Geological Society of America 2003 Annual Meeting. 35, 546.

Bischof, J.F., Darby, D.A. 1997. Mid- to Late Pleistocene Ice Drift in the western Arctic Ocean: Evidence for a Different Circulation in the Past. Science. 277, 74-78.

Blasco, S. M., Fortin, G., Hill, P.R., O'Connor, M.J., and Brigham-Grette, J. 1990. The late Neogene and Quaternary stratigraphy of the Canadian Beaufort continental shelf. In: Grantz, A., Johnson, L., Sweeney, J. F. (Eds). The Arctic Ocean Region. The Geology of North America, Vol. L. Geological Society of America: Boulder, Colorado. 491–502.

Blasco, S.M., Bennett, R., Hughes-Clarke, J., Bartlett, J., Shearer, J.M. 2005. 3-D Multibeam Mapping Reveals Geological Processes Associated With

Fluted Seabed, Slump Feature, Pockmarks, Mud Volcanoes and Deep Water Ice Scours in the Beaufort Sea–Amundsen Gulf: Geological Association of Canada – Mineralogical Association of Canada.

Böse, M., Lüthgens, C., Lee, J.R., Rose, J. 2012. Quaternary glaciations of northern Europe. Quaternary Science Reviews. 44, 1-25.

Bradley, R.S., England, J.H. 2008. The Younger Dryas and the Sea of Ancient Ice. Quaternary Research. 70, 1-10.

Brigham-Grette, J., Gualtieri, L.M., Glushkova, O.Y., Hamilton, T.D., Mostoller, D., Kotov, A. 2003. Chlorine-36 and ^{14}C chronology support a limited last glacial maximum across central Chukotka, northeastern Siberia, and no Beringian ice sheet. Quaternary Research. 59, 386-398.

Buylaert, J.P., Jain, M., Murray, A.S., Thomsen, K.J., Thiel, C., Sohbati, R. 2012. A robust feldspar luminescence dating method for Middle and Late Pleistocene sediments. Boreas. 41, 534-451.

Clark, D.L., Vincent, J-S., Jones, G.A., Morris, W.A. 1984. Correlation of marine and continental glacial and interglacial events, Arctic Ocean and Banks Island. Nature. 311, 147-149.

Clark, P.U., Mix, A.C. 2002. Ice sheets and sea level of the Last Glacial Maximum. Quaternary Science Reviews. 21, 1-7.

Craig, B.J., Fyles, J.G. 1960. Pleistocene geology of Arctic Canada. Geological Survey of Canada. Paper 60-10, 21.

Colleoni, F., Krinner, G., Jakobsson, M., Peyaud, V., Ritz, C., 2009. Influence of regional parameters on the surface mass balance of the Eurasian ice

sheet during the peak Saalian (140 kya). Global and Planetary Change. 68, 132-148.

Darby, D, A. 2003. Sources of sediment found in sea ice from the western Arctic Ocean, new insights into processes of entrainment and drift patterns. Journal of Geophysical Research. Oceans. 108, 13.1-13.8.

Demuro, M., Froese, D., Arnold, L.J., Roberts, R.G. 2012. Single-grain OSL dating of glaciofluvial quartz constrains Reid Glaciation in NW Canada to MIS 6. Quaternary Research. 77, 305-316.

Doornbos, C., Heaman,L., Doupé, J. P., England, J. H., Simonetti, A., Lajeunesse. P. 2009. The first integrated use of in situ U-Pb geochronology and geochemical analyses to determine long-distance transport of erratics, from mainland Canada to the western Canadian Arctic Archipelago. Canadian Journal of Earth Sciences. 46, 101-122.

Dowdeswell, J.A., Jakobsson, M., Hogan, K.A., O'Regan, M., Antony, D., Backman, J., Darby, D., Eriksson, B., Evans, D.J.A., Hell, B., Janzen, T., Löwemark, L., Marcussen, C., Noormets, R., Ó Cofaig, C., Polyak, L., Sellén, E., Sölvsten, M. 2010. High-resolution geophysical observations from the Yermak Plateau and northern Svalbard margin: implications for ice-sheet grounding and deep-keeled icebergs. Quaternary Science Reviews. 29, 3518-3531.

Duk-Rodkin, A., Hughes, O. L. 1991. Age relationships of Laurentide and montane glaciations, Mackenzie Mountains, Northwest Territories. Géographie physique et Quaternaire. 45, 79-90.

Duk-Rodkin, A., Barendregt, R.W., Froese, G.D., Weber, F., Enkin, R., Smith, R. 2004. Timing and extent of Plio-Pleistocene glaciations in north-western Canada and east-central Alaska. In: Ehlers, J., Gibbard, P.L. (Eds), Quaternary Glaciations – Extent and Chronology, Part II, Elsevier North America, Amsterdam. 313-345.

Duk-Rodkin, A., Barendregt, R.W. 2011. Stratigraphical Records of Glacials/Interglacials in Northwest Canada. The Glacial History of Northwestern Canada. In: Ehlers, J., Gibbard, P.L. & Hughes, P,D. (Eds.), Quaternary Glaciations -- Extent and Chronology. Part IV: A Closer Look, Amsterdam, Elsevier. Ch. 49, p 661-698.

Dyke, A.S. 2004. An outline of the deglaciation of North America with emphasis on central and northern Canada. In: Ehlers, J., Gibbard, P.L (Eds). Quaternary Glaciations, Extent and Chronology. Part II. North America. Developments in Quaternary Science, vol 2b. Elsevier, Amsterdam.

Ehlers, J., Gibbard, P.L. (Eds). 2004. Quaternary Glaciations: extent and chronology. Part II: North America. Developments in Quaternary Science 2. Elsevier, Amsterdam.

Ehlers, J., Gibbard, P.L., Hughes, P.D. (Eds). 2011. Quaternary glaciations: extent and chronology: a closer look. Elsevier, Amsterdam.

Engels, J.L., Edwards, M.H., Polyak, L., Johnson, P.D. 2008. Seafloor evidence for ice shelf flow across the Alaska-Beaufort margin of the Arctic Ocean. Earth Surface Processes and Landforms. 33, 1047-1063.

England, J., Atkinson, N., Bednarski, J., Dyke, A. S., Hodgson, D. A., Ó Cofaigh C. 2006. The Innuitian Ice Sheet: configuration, dynamics and chronology. Quaternary Science Reviews. 25, 689-703.

England, J.H., Furze, M.F.A., Doupe, J.P. 2009. Revision of the NW Laurentide Ice Sheet: implications for the paleoclimate, the northeast extremity of Beringia, and Arctic Ocean sedimentation. Quaternary Science Reviews. 28, 1573-1596.

Evans, D.J.A., England, J.H., LaFarge. C., Coulthard, R., Lakeman, T. Quaternary geology of the Duck Hawk Bluffs, southwest Banks Island, Arctic Canada: a re-investigation of a critical terrestrial type locality for glacial and interglacial events around the Arctic Ocean. In press.

Fritz, M., Wetterich, S., Schirrmeister, L., Meyer, H., Lantuit, H., Preusser, F., Pollard, W.H. 2012. Eastern Beringia and beyond: Late Wisconsinan and Holocene landscape dynamics along the Yukon Coastal Plain, Canada. Palaeogeography Palaeoclimatology Palaeoecology. 319, 28-45.

Fyles, J.G. 1962. Physiography. In: Thorsteinsson R., Tozer, E.T. (Eds.). Banks, Victoria, and Steffansson Island, Arctic Archipelago. Geological Survey of Canada. Memoir 330, 8-17.

Fyles, J.G; Hills, L.V., Matthews, J.V., Barendregt, R., Baker, J., Irving, E., Jetté, H. 1994. Ballast Brook and Beaufort Formations (Late Tertiary) on northern Banks Island, Arctic Canada. Quaternary International. 22, 141-171.

Gebhardt, A.C., Jokat, W., Niessen, F., Matthiessen, J., Geissler, W.H., Schenke, H.W. 2011. Ice sheet grounding and iceberg plow marks on the northern

and central Yermak Plateau revealed by geophysical data. Quaternary Science Reviews. 30, 1726-1738.

Hidy, A.J., Gosse, J.C., Froese, D.G., Bond, J.D., Rood, D.H. 2013. A latest Pliocene age for the earliest and most extensive Cordilleran Ice Sheet in northwestern Canada. Quaternary Science Reviews. 61, 77-84.

Hill, J.C., Driscoll, N.W. 2010. Iceberg discharge to the Chukchi Shelf during the Younger Dryas. Quaternary Research. 22, 18-30.

Hobbs, W.H. 1945. The boundary of the latest glaciation in Arctic Canada. Science. 101, 549-551.

Hughes, O.L. 1972. Surficial geology of northern Yukon Territory and northwestern District of Mackenzie. Northwest Territories. Geological Survey of Canada. Paper 69-36, 11.

Jakobsson, M., Polyak, L., Edwards, M., Klemen, J., Coakley, B. 2008. Glacial geomorphology of the Central Arctic Ocean: the Chukchi Borderland and the Lominosov Ridge. Earth Surface Processes and Landforms. 33, 526-545.

Jakobsson, M., Nilsson, J., O'Regan, M., Backman, J., Löwemark, L., Dowdeswell, J.A., Mayer, L., Polyak, L., Colleoni, F., Anderson, L., Björk, G., Darby, D., Eriksson, B., Hanslik, D., Hell, B., Marcussen, C., Sellén, E., Wallin, Å. 2010. An Arctic Ocean ice shelf during MIS 6 constrained by new geophysical and geological data. Quaternary Science Reviews. 29, 3505-3517.

Jakobsson, M., Andreassen, K., Bjarnadóttir, L.R., Dove, D., Dowdeswell, J.A., England, J.H., Funder, S., Hogan, K., Ingólfsson, O., Jennings, A., Krog-Larsen, N., Kirchner, N., Landvik, J.Y., Mayer, L., Moller, P., Niessen, F.,

Nilsson, J., O'Regan, M., Polyak, L., Petersen, N.N., Stein, R. Arctic Ocean Glacial History. Quaternary Science Reviews. In press.

Jenness, J.L. 1952. Problem of glaciation in the western islands of Arctic Canada. Bulletin of Geological Society of America. 63, 939-952.

Jennings, C.E., Aber, J.S., Balco, G., Barendregt, R., Bierman, P.R., Rovey II, C.W., Roy, M., Thorleifson, L.H., Mason, J.A. 2007. Glaciations: Mid-Quaternary in North America. Encyclopedia of Quaternary Science. 1044-1051.

Kauffman, D.S., Hopkins, D.M. 1986. Glacial History of the Seaward Peninsula. In: Hamilton, T.D., Reed, K.M., Thorson, R.M. (Eds.). Glaciation of Alaska: The Geologic Record. Alaska Geological Society, Anchorage. 51-78.

Kauffman, D.S., Brigham-Grette, J. 1993. Aminostratigraphic correlations and paleotemperature implications, Pliocene-Pleistocene high sea level deposits, northwestern Alaska. Quaternary Science Reviews. 12, 21-33.

Kennedy, K.E., Froese, D.G., Zazula, G.D., Lauriol, B. 2010. Last Glacial Maximum age for the northwest Laurentide maximum from the Eagle River spillway and delta complex, northern Yukon. Quaternary Science Reviews. 29, 1288-1300.

Kristoffersen, Y., Sorokin, M.Y., Jokat, W., Svendsen, O. 2004. A submarine fan in the Amundsen Basin, Arctic Ocean. Marine Geology. 204, 317-324.

Kuc, M. 1974. The interglacial flora of Worth Point, western Banks Island. Report of activities, Part B, Geological Survey of Canada. Paper 74-1B, 227-231.

Lakeman, T.R. 2012. Revision of the Early Quaternary stratigraphy at Morgan Bluffs, Banks Island, western Canadian Arctic. PhD Thesis, University of Alberta, Edmonton, Canada.

Lakeman, T.R., England, J.H. 2012. Paleoglaciological insights from the age and morphology of the Jesse moraine belt, western Canadian Arctic. Quaternary Science Reviews. 47, 82-100.

Lakeman, T.R., England, J.H. 2013. Late Wisconsinan glaciation and postglacial relative sea level change on western Banks Island, Canadian Arctic Archipelago. Quaternary Research. 80, 99-112.

Mackay, J.R. 1959. Glacier ice-thrust features of the Yukon Coast. Geographical Bulletin of Canada. 13, 5-21.

MacLean, B., Blasco, S., Bennett, R., England, J., Rainey, W., Hughes-Clarke, J., Beaudoin, J. 2010. Ice keel seabed features in marine channels of the central Canadian Arctic Archipelago: evidence for former ice streams and iceberg scouring. Quaternary Science Reviews. 29, 2280-2301.

MacLean, B., Blasco, S., Bennett, R., Lakeman, T., Hughes-Clarke, J., Kuus, P., Patton, E. 2012. Marine evidence for a glacial ice stream in Amundsen Gulf, Canadian Arctic Archipelago. 42nd Annual Arctic Workshop abstract, March 7th-9th, University of Colorado, US.

Manning, T.H. 1956. Narrative of a second Defence Research Board expedition to Banks Island, with notes on the country and its history. Arctic. 9, 2-77.

Matthews, J.V., Mott, R.J., Vincent, J-S. 1986. Preglacial and interglacial environments on Banks Island: pollen and macrofossils from Duck Hawk Bluffs and related sites. Geographie physique et Quaternaire. 3, 279-298.

Matthews, J.V., Jr., Ovenden, L.E. 1990. Late Tertiary plant macrofossils from localities in Arctic/Subarctic North America: a review of the data. Arctic. 43, 364-392.

Möller, P., Lubinski, D.J., Ingólfsson, O., Forman, S.L., Seidenkrantz, M.S., Bolshiyanov, D.Y., Lokrantz, H., Antonov, O., Pavlov, M., Ljung, K., Zeeberg, J., Andreev, A. 2006. Severnaya Zemlya, Arctic Russia: a nucleation area for Kara Sea ice sheets during the Middle to Late Quaternary. Quaternary Science Reviews. 25, 2894-2936.

Morlan, R.E., Nelson, D.E., Brown, T.A., Vogel, J.S., Southon, J.R. 1990. Accelerator mass spectrometry dates on bones from Old Crow, northern Yukon Territory. Canadian Journal of Archaeology. 14, 75-92.

Nixon, C.F., England, J.H., Lajeunesse, P., Hanson, M.A. Deciphering patterns of postglacial sea level at the junction of the Laurentide and Innuitian Ice Sheets, western Canadian Arctic. Quaternary Science Reviews. In Press.

Nürnberg, D., Dethleff, D., Tiedemann, R., Kaiser, A., Gorbarenko, A.A. 2011. Okhotsk Sea ice coverage and Kamchatka glaciation over the last 350 ka – Evidence from ice-rafted debris and planktonic $\partial^{18}O$. Palaeogeography Paleoclimatology Palaeoecology. 310, 191-205.

Peltier, W.R. 2004. Global Glacial Isostasy and the Surface of the Ice-Age Earth: The ICE-5G (VM2) Model and GRACE. Annual Reviews of Earth and Planetary Sciences. 32, 111-149.

Phillips, R.L., Grantz, A. 2001. Regional variations in provenance and abundance of ice-rafted clasts in Arctic Ocean sediments: implications for the configuration of late Quaternary oceanic and atmospheric circulation in the Arctic. Marine Geology. 172.

Polyak, L., Edwards, M.H., Coackley, B.J., Jakobsson, M. 2001. Ice shelves in the Pleistocene Arctic Ocean inferred from glaciogenic deep-sea bedforms. Nature. 410, 453-547.

Polyak, L., Curry, W.B., Darby, D.A., Bischof, J., Cronin, T.M. 2004. Contrasting glacial/interglacial regimes in the western Arctic Ocean as exemplified by a sedimentary record from the Mendeleev Ridge. Palaeogeography Palaeoclimatology Palaeoecology. 203, 73-93.

Polyak, L., Darby, D., Bischof, J., Jakobsson, M. 2007. Stratigraphic constraints on Late Pleistocene glacial erosion and deglaciation of the Chukchi margin, Arctic Ocean. Quaternary Research. 67, 234-245.

Polyak, L., Bischof, J., Ortiz, J., Darby, D., Chappell, J., Xuan, C., Kaufman, D., Loylie, R., Schneider, D., Adler, R. 2009. Late Quaternary stratigraphy and sedimentation patterns in the western Arctic Ocean. Global Planetary Change. 68, 5-17.

Polyak, L., Jakobsson, M. 2011. Quaternary sedimentation in the Arctic Ocean: Recent advances and further challenges. Oceanography. 24, 52-64.

Porsild, A.E. 1950. A biological exploration of Banks Island and Victoria Island. Arctic. 3, 45-54.

Rampton, V.N. 1982. Quaternary Geology of the Yukon Coastal Plain. Geological Survey of Canada, Bulletin 317.

Scott, D.B., Schell, T., St-Onge, G., Rochon, A., Blasco, S. 2009. Foraminiferal assemblage changes over the last 15,000 years on the Mackenzie Beaufort Sea Slope and Amundsen Gulf, Canada: Implications for past sea ice conditions. Paleoceanography. 24, 1-20.

Sejrup, H.P., Hjelstuen, B.O., Dahlgren, K.I.T., Haflidason, H., Kuijpers, A., Nygård, A., Praeg, D., Stoker, M.S., Vorren, T.O. 2005. Pleistocene glacial history of the NW European continental margin. Marine and Petroleum Geology. 22, 1111-1129.

Serreze, M.C., Barrett, A.P., Slater, A.G., Steele, M., Zhang, J., Trenberth, K.E. 2007. The large-scale energy budget of the Arctic. Journal of Geophysical Research. 112.

Stauch, G., Gualtieri, L. 2008. Late Quaternary glaciations in northeastern Russia. Journal of Quaternary Science. 23, 545-558.

Stein, R., Matthiessen, J., Niessen, F., Krylov, R., Nam, S., Bazhenova, E. 2010. Towards a better litho-stratigraphy and reconstruction of Quaternary palaeoenvironment in the Amerasian Basin (Arctic Ocean). Polarforschung. 79, 97-121.

Stokes, C.R., Clark, C.D., Darby, D.A., Hodgson, D.A. 2005. Late Pleistocene ice export events into the Arctic Ocean from the M'Clure Strait Ice

Stream, Canadian Arctic Archipelago. Global and Planetary Change. 49, 139–162.

Stokes, C.R., Clark, C., Winsborrow, M. 2006. Subglacial bedform evidence for a major paleo-ice stream in Amundsen Gulf and its retreat phases, Canadian Arctic Archipelago. Journal of Quaternary Science. 21, 300–412.

Stokes, C.R., Clark, C.D., Storrar, R. 2009. Major changes in ice stream dynamics during deglaciation of the north-western margin of the Laurentide Ice Sheet. Quaternary Science Reviews. 28, 721-738.

Svendsen, J.I., Alexanderson, H., Astakhov, V.I. 2004. Late Quaternary ice sheet history of Northern Eurasia. Quaternary Science Reviews. 23, 1229-1271.

Vaughan, J.M, England, J.H, Evans, D.J.A. Glaciotectonic deformation and reinterpretation of the Worth Point stratigraphic sequence: Banks Island, NT, Canada. Quaternary Science Reviews. In Press.

Vincent, J-S. 1982. The Quaternary History of Banks Island, Northwest Territories, Canada. Geographie Physique et Quaternaire. 36, 209-232.

Vincent, J-S. 1983. La geologie du quaternaire et la geomorphologie de L'ile Banks, arctique Canadien. In: Commission Geologique du Canada Memoir 405.

Vincent, J-S. 1984. Quaternary stratigraphy of the western Canadian Arctic Archipelago. In: Fulton, R.J. (Ed.). Quaternary Stratigraphy of Canada – A Canadian Contribution to IGCP Project 24. Geological Survey of Canada. 84-10, 87-100.

Vincent, J-S. 1990. Late Tertiary and Early Pleistocene Deposits and History of Banks Island, southwestern Canadian Arctic Archipelago. Arctic. 43, 339-363.

Vincent, J-S. 1992. The Sangamonian and Early Wisconsinan glacial record in the western Canadian Arctic. In: Clark, P. U. and Lea, P. D. (Eds.). The Last Glacial-Interglacial Transition in North America. Geological Society of America, Special Paper. 270, 233-252.

Vincent, J-S., Occhietti, S., Rutter, N., Lortie, G., Guilbault, J-P., De Boutray, B. 1983. The Late Tertiary-Quaternary record of the Duck Hawk Bluffs, Banks Island, Canadian Arctic Archipelago. Canadian Journal of Earth Science. 20, 1694-1712.

Vincent, J-S., Morris, W.A. & Occhietti, S. 1984. Glacial and non-glacial sediments of Matuyama paleomagnetic age on Banks Island, Canadian Arctic Archipelago. Geology. 12, 139-142.

Ward, B. 2012. Comparison of MIS 4 and 6 Glaciations, Yukon Territory, Canada. Quaternary International. 279-280, 528.

Washburn, A.L. 1947. Reconnaissance geology of portions of Victoria Island and adjacent regions, Arctic Canada. Geological Society of America. Memoir 22, 142.

Zazula, G.D., Duk-Rodkin, A., Schweger, C.E., Morlan, R.E. 2004. Late Pleistocene chronology of glacial lake Old Crow and the northwest margin of the Laurentide Ice Sheet. In: Ehlers, J., Gibbard, P.I (Eds.). Quaternary Glaciations – Extent and Chronology, Part II. Elsevier, 347-362.

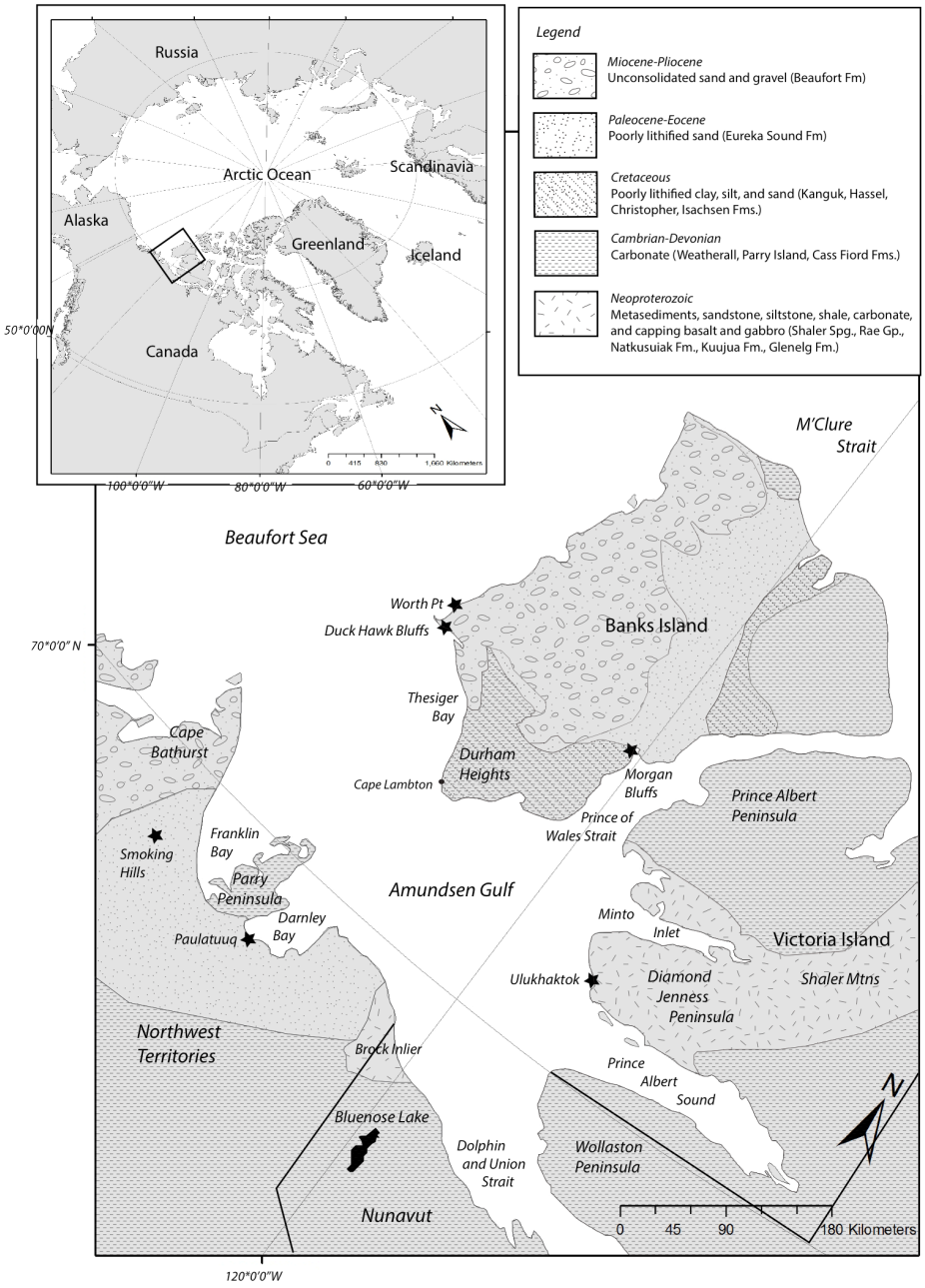

Figure 4.1. Location map of Banks Island showing generalized bedrock and place names mentioned in Chapter 4.

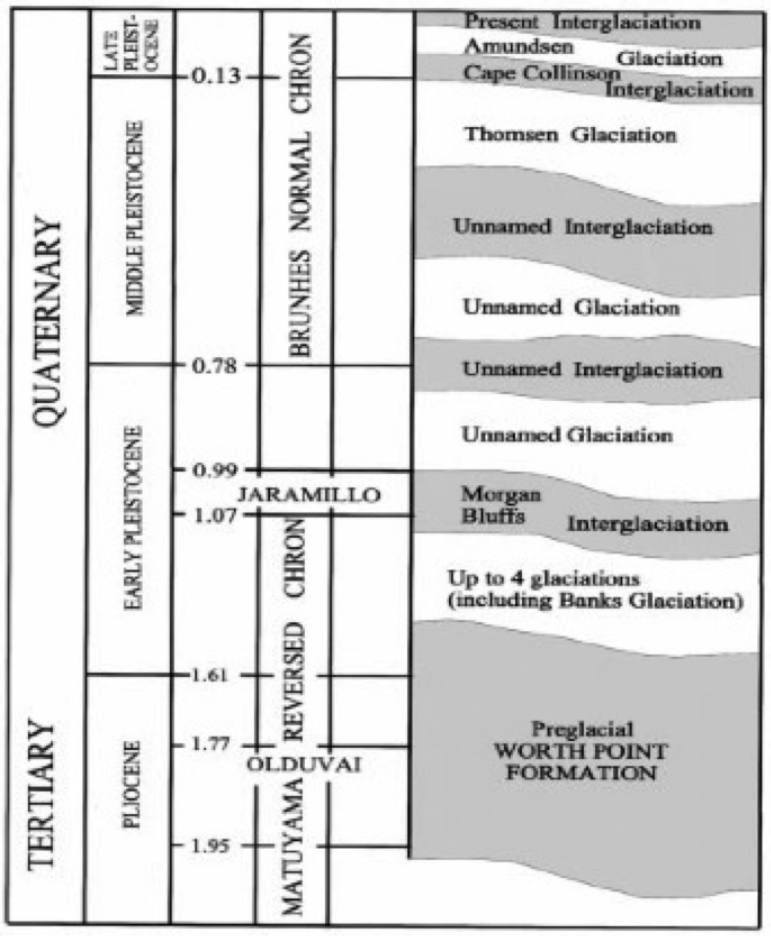

Figure 4.2. Magnetostratigraphic framework for Banks Island from Barendregt et al (1998). Note the proposed eight glaciations and five interglaciations extending back over one million years. Also note the preglacial Worth Point Fm (bottom right) that has been reinterpreted as reworked Beaufort Fm (Vaughan et al., in press).

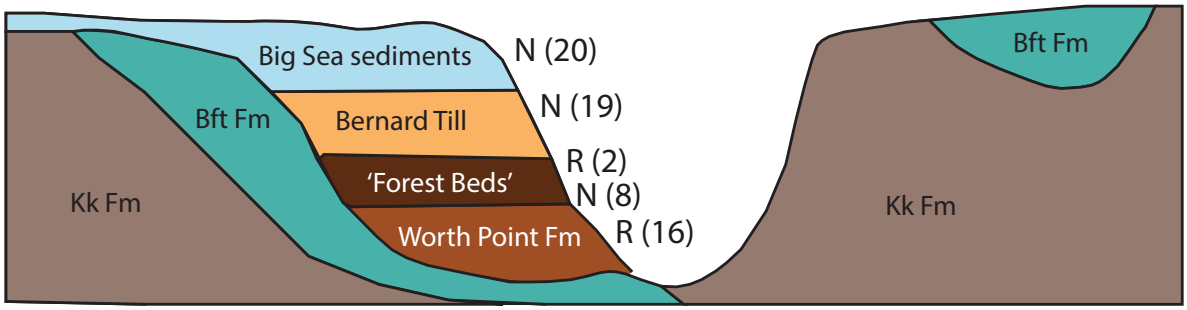

Figure 4.3. Simplified diagram showing the stratigraphic sequence for the Worth Point Fm type-site as proposed by Vincent (1990).

Kk Fm = Kanguk Fm, Bft Fm = Beaufort Fm.

R = Reversed polarity, N = Normal polarity. Number in brackets represents number of polarity readings. From Barendregt et al (1998).

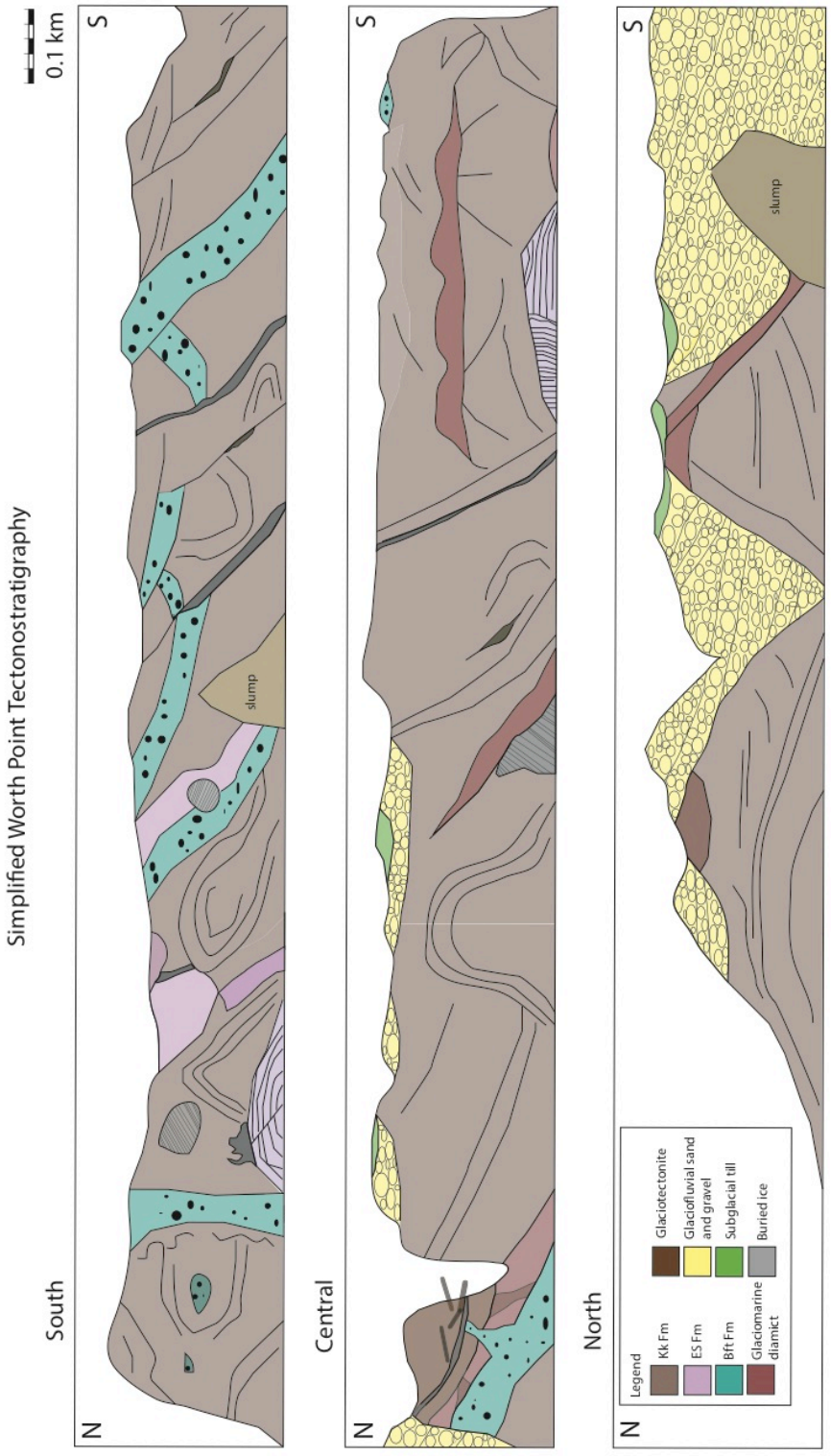
Simplified Worth Point Tectonostratigraphy
0.1 km
South
Central
North
N
S
slump
Legend
Kk Fm
ES Fm
Bft Fm
Glaciomarine diamict
Glaciotectonite
Glaciofluvial sand and gravel
Subglacial till
Buried ice

Fig. 4.4

Figure 4.4. (previous page). Simplified tectonostratigraphy of Worth Point along a north-south transect (viewed from the coast) approximately 6 km long. Kk Fm = Kanguk Fm, ES Fm = Eureka Sound Fm, Bft Fm = Beaufort Fm. From Vaughan et al (in press).

Note the pervasive deformation (folding, faulting and stacking) of bedrock and newly identified glaciogenic units. Also note the localized outcrop of logs and organics (middle box, far left) that formed the focus of earlier investigations (the Worth Point Fm type-site of Vincent, 1990).

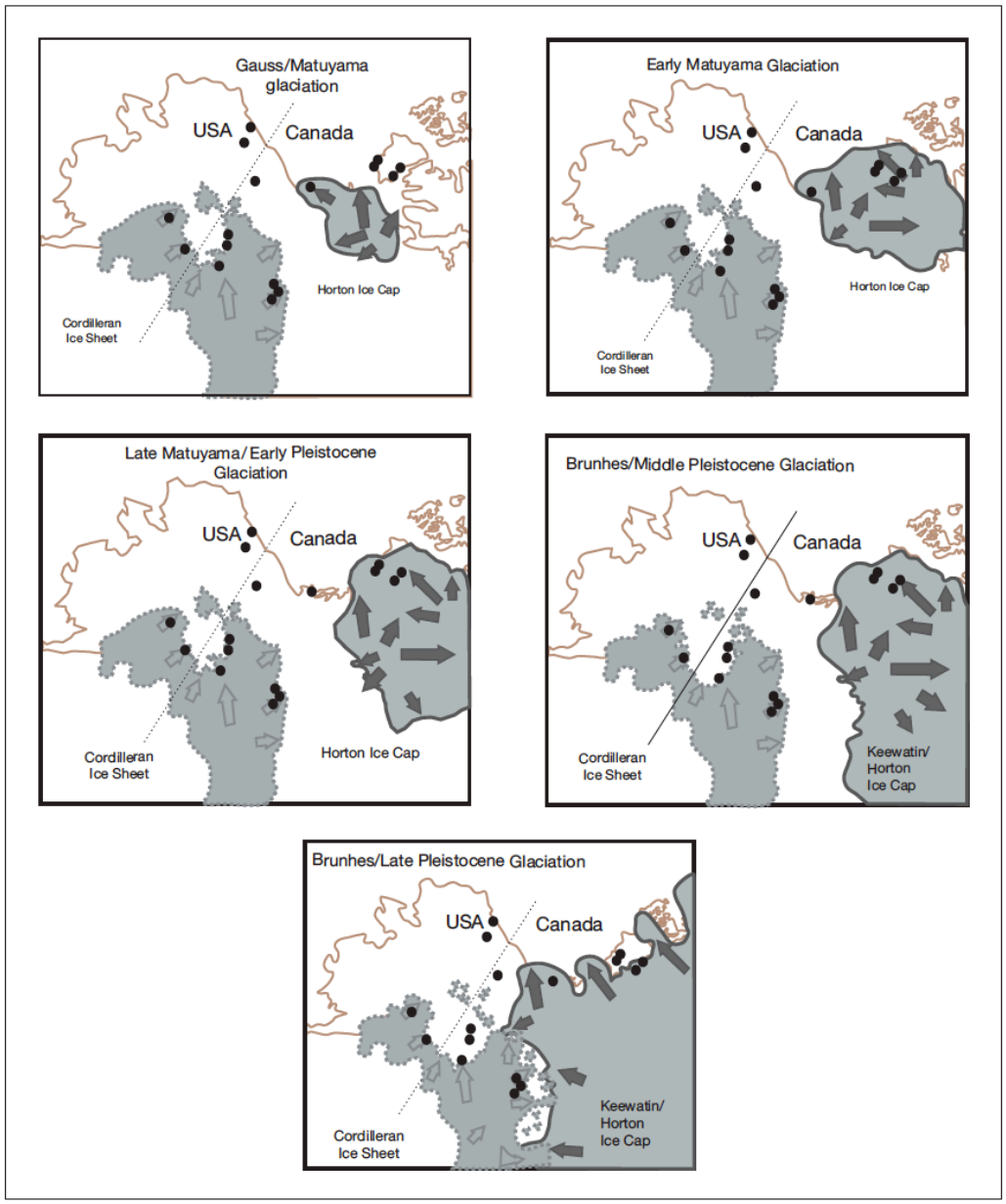
Gauss/Matuyama glaciation
USA
Canada
Horton Ice Cap
Cordilleran Ice Sheet
Early Matuyama Glaciation
USA
Canada
Horton Ice Cap
Cordilleran Ice Sheet
Late Matuyama/Early Pleistocene Glaciation
USA
Canada
Cordilleran Ice Sheet
Horton Ice Cap
Brunhes/Middle Pleistocene Glaciation
USA
Canada
Cordilleran Ice Sheet
Keewatin/ Horton Ice Cap
Brunhes/Late Pleistocene Glaciation
USA
Canada
Keewatin/ Horton Ice Cap
Cordilleran Ice Sheet

Fig. 4.5.

Fig. 4.5. (previous page). Proposed extent and timing of Bruhnes-Matuyama glaciations in northwestern Canada and Alaska from Jennings et al (2013), based on Barendregt and Duk-Rodkin (2004). Note how the earliest glaciation to reach Banks Island originated from the Horton Plateau (Early Matuyama Glaciation, top right box) and how the Horton Plateau Ice Cap was subsequently subsumed by the Keewatin Ice Dome during the Mid to Late-Pleistocene (middle right and bottom boxes).

CHAPTER 5

CONCLUSIONS

1. MAJOR DISCOVERIES

This dissertation contributes new findings on the nature of Pleistocene paleoenvironmental change based on three summers of fieldwork (2008-2010) that extended across southern Banks Island from Prince of Wales Strait in the east to the Beaufort Sea in the west (~200 km of coastline and up to ~100 km inland). This transect set out to test the previous model of past glaciation and relative sea level change summarized in several widely cited, seminal papers conducted primarily under the leadership of J-S Vincent, Geological Survey of Canada (Vincent 1982, 1983, 1984, 1990; Vincent et al., 1983, 1984; Barendregt et al., 1998). This dissertation was designed to complement adjoining transects concerning the Quaternary geology across central and northern Banks Island, as well as those conducted farther north across M'Clure Strait as part of the decade-long NSERC Northern Research Chair Program at the University of Alberta (*Environmental Change across the western Canadian Arctic Archipelago: Ice Age to present*, *2002-2012*; England et al. 2009; Lakeman and England 2012, 2013; Nixon et al., in press).

The primary findings are summarized in three chapters (2-4) that outline new perspectives on: 1) the dynamics of the northwest Laurentide Ice Sheet (LIS) during the last glacial maximum (LGM); 2) the nature of ice retreat, especially the transition from a former ice stream to an ice shelf in Amundsen Gulf that underwent episodic readvances; 3) the magnitude and pattern of postglacial

rebound across southern Banks Island occasioned by Laurentide ice retreat; 4) the sedimentary and glaciotectonic record of an expansive coastal section (30 m thick and 6 km long) at Worth Point, SW Banks Island, that includes the ancestral activity of the LIS extending back to the Mid-Pleistocene (*sensu lato*); and 5) the mechanisms of glaciotectonic landform generation in permafrost terrain at Worth Point, including the deformation of permafrozen lithologic units under variable glacial stress regimes. Collectively, this new data not only contributes to our understanding of high-latitude landscape evolution and paleoglaciological processes, but also revises widely adopted models of Neogene and Quaternary paleoenvironmental change (Vincent, 1982, 1983, 1984; Barendregt et al., 1998).

This dissertation revises the long-standing, glacial history of southern Banks Island proposing ice-free conditions during the LGM (Vincent, 1982, 1983, 1984). Instead, glacial mapping and dating demonstrate that terrestrial and marine-based ice of the northwest LIS subsumed southern Banks Island and extended onto the polar continental shelf during the LGM. New constraints on the thickness of trunk ice in western Amundsen Gulf indicate that it was at least 1 km thick adjacent to the polar continental shelf, reinforcing its importance for discharging deep-draft icebergs and sediments into the Arctic Ocean. Keel marks (< 450 m below sea level) recorded in the western Arctic Ocean, notably on the Chukchi shelf and rise, as well as the Northwind Ridge, have been attributed to the grounding of icebergs calved from a former Laurentide and/or Innuitian ice sheet margin (Polyak et al., 2007; Hill and Driscoll, 2010). Following the LGM, initial Laurentide retreat left widespread marine limit shorelines across the full

length of southern Banks Island (~200 km) that are distinguished by a conspicuous absence of shells in growth position. The barren nature of deglacial marine limit requires that the Amundsen Gulf Ice Stream retreated to southeast Banks Island prior to the re-entry of Pacific fauna ~13,750 cal yr BP (England and Furze, 2008). This early retreat involved the loss of ~60,000 km^2 of ice, constituting the most significant mass loss from the LIS during an interval that coincides with Meltwater Pulse 1A (MWP-1A; Carlson, 2009). Drawdown from ice divides occasioned by ice stream retreat likely led to the reorganization of ice flow from the northwest LIS, prompting coeval retreat across interior Banks Island for which geomorphic evidence is widespread (Lakeman and England, 2012, 2013; this study). Regional scale retreat is also recorded on the Canadian Mainland (e.g. Murton et al., 2007; Zazula et al, 2009) and throughout M'Clure Strait (England et al., 2009). This study provides new chronologic constraints on the timing of abrupt deglaciation of southeastern Banks Island (~12,600 cal yr BP), signalling final break up of the Amundsen Gulf Ice Stream and the adjoining LIS margin occupying Prince of Wales Strait. Importantly, these findings demonstrate that the Amundsen Gulf Ice Stream – during thinning and retreat – evolved into an ice shelf, highlighting the role of calving in governing ice sheet mass loss (e.g. Fastook and Schmidt, 1982; Benn et al., 2007).

The past activity of the northwest LIS during the LGM is substantially diversified by detailed observations at the coastal section of Worth Point, southwest Banks Island. New observations there provide a fundamental revision of the Worth Point stratigraphic sequence that was originally proposed to be

undeformed and to contain the type section of the preglacial Worth Point Formation (Vincent, 1990; Barendregt et al., 1998). Widespread glaciotectonism of this section provides an opportunity to determine how cold-based ice interacts with permafrost terrain – a glaciological scenario that characterizes much of western Banks Island where numerous hill-hole pairs occupy the landscape. The stratigraphic sequence of Worth Point is interpreted to expose the internal architecture of a polydeformed ice-pushed hill. Prior studies of ice-pushed hill formation have emphasized the role of glacier surging for generating the high porewater pressures required for substrate deformation (Croot, 1988; Kalin, 1971; Copland et al., 2003; Evans and Wilson, 2006). New insights into the mechanisms of hill-hole formation at Worth Point confirm the importance of high porewater pressures, and suggest that surging is not required. Instead, it is proposed that high porewater pressures can be developed in taliks occupying otherwise impermeable and permafrozen sediment (Mackay, 1959, 1989), and that deformation can be promoted by a basal décollement surface, such as thinner permafrost fringing formerly submerged coastlines (Evans and England, 1991). These findings have significant implications for our understanding of glaciotectonic landform evolution. Research from this dissertation also improves our understanding of the deformation of lithologically-variable permafrozen sediment in ice-marginal and subglacial environments (Waller et al., 2012). These deformation processes remain poorly understood, largely because research efforts have focused on glaciotectonized stratigraphies in the mid-latitudes where the subsequent removal of permafrost has degraded the original internal architecture (Dyke and Savelle,

2000). In contrast, the persistence of permafrost at Worth Point provides an exceptional opportunity to observe and reconstruct lithologically-specific responses (from brittle to ductile) to glacially-imposed stress (from compression to shear). Notably, these observations confirm the operation of ductile deformation in fine-grained sediments at sub-zero temperatures (i.e. 'warm permafrost', Waller et al., 2012) and highlight the dynamic and erosive capabilities of cold-based ice. The antiquity of permafrost at Worth Point (patchy to continuous) is demonstrated by the survival of ancient buried ice through at least two glacial-interglacial cycles. This finding affirms the longevity of circumpolar permafrost (e.g. Marchant et al., 2002; Ingolfsson and Lokrantz, 2003; Froese et al., 2008; Fortier et al., 2009) and contributes to a growing body of evidence recognizing the ability of permafrost to incorporate and preserve buried glacial ice (e.g. Mackay, 1959; Mackay et al., 1972; O'Cofaigh et al., 2003; Murton et al., 2004; Harris and Murton, 2005; Fritz et al., 2012).

This dissertation also presents a glaciotectonic model for the Worth Point stratigraphic sequence that challenges the long-standing and widely cited Neogene and Quaternary environmental framework for the western CAA (Vincent 1982, 1983, 1984, 1989, 1990, 1992; Vincent et al., 1983, 1984; Matthews et al., 1986; Barendregt et al., 1998). Notably, the Worth Point glaciotectonic model outlines an initial pre-Late Wisconsinan advance of the ancestral LIS and a final advance of the LIS during the Late Wisconsinan. Tentative chronologic control for the pre-Late Wisconsinan advance suggests a Mid-Pleistocene age, possibly during marine isotope stage (MIS) 6 when ice shelves in the adjacent Arctic Ocean

attained their Pleistocene maximum thickness (e.g. Dowdeswell et al., 2010; Jakobsson et al., 2010, in press). The Worth Point glaciotectonic model raises new, important questions about the history of the ancestral LIS, the evolution of circumpolar ice sheets, and the long-term flux of ice and glacial debris to the Arctic Ocean.

Collectively, this dissertation contributes to a broad understanding of Quaternary Arctic environmental change. Clarifying this natural history is particularly relevant for contextualizing current environmental change. For example, ongoing Arctic amplification (a series of positive feedbacks perpetuating warming) is driving unprecedented rates of observed surface-air warming leading to permafrost thaw and sea ice loss across the western CAA (Serreze et al., 2009; Serreze and Barry, 2011). Placing these changes into a long-term context is essential for a meaningful assessment of their significance and for forecasting future change.

2. FUTURE RESEARCH

Future research is warranted to address new questions raised by this dissertation, including the need to clarify details that remain unresolved. The largest need identified is to clarify the chronology of the Late Wisconsinan advance and retreat and to better constrain the subsurface chronology at Worth Point. In order to improve the age of the last advance of the northwest LIS, terrestrial cosmogenic nuclide (TCN) dating will need to be applied to high elevation erratics. During the NSERC Northern Research Chair Program the

erratics best suited for measurement (large erratics on stable bedrock surfaces) were exclusively mafic on southern Banks Island, whereas the emphasis for analyses was placed on other lithologies with an abundant quartz content (e.g. granite and sandstone) that were common farther north on Banks Island and in the western CAA. Advances in TCN dating now routinely include the analyses of mafic erratics (^{36}Cl) and this could be applied to erratics across southern Banks Island (e.g. Schaefer and Lifton, 2013). Additional AMS radiocarbon dating of ice-transported shells collected across southern Banks Island would also help to confirm their MIS 3 age and to provide additional maximum limiting dates for ice advance. The application of OSL dating to lacustrine sediments adjacent to the Sachs Moraine and Sand Hills Moraine belt could also constrain the timing of late-glacial readvances of the Amundsen Gulf Ice Stream. Additional U-Pb zircon dating could also be applied to both mafic and granitic erratics across southern Banks Island to determine their provenance.

Because ice retreat occurred in what is widely regarded to have been a barren Arctic Ocean, at least on the polar continental shelf of the western CAA (Kaufman et al, 2004; Polyak et al., 2004; England and Furze, 2008; England et al., 2009), both OSL and cosmogenic burial dating could provide independent age estimates on the deglacial shorelines deposited between initial ice retreat from western Banks Island and the re-entry of molluscs ~13,750 cal yr BP. Moreover, the relative sea level history on southern Banks Island - characterized by a postglacial regression from marine limit to an unknown lowstand offshore, followed by submergence to present sea level – raises the possibility that drowned

lakes fringe the coastline. Freshwater lakes currently being transgressed on southwest Banks Island host thick accumulations of mirabilite beneath hypersaline brines (Grasby et al., 2013). The brines form in winter when freezing not only increases lake salinity but also isolates the basins by blocking shallow sills connecting them to the ocean (Grasby et al., 2013). Based on this unique phenomenon, future coring of former lake basins may be able to identify and date similar hypersaline transitions, providing new insights into the timing and nature of relative sea level change unavailable from surficial records. More detailed seismic surveys and sediment sampling in western Amundsen Gulf would also add new, important opportunities to refine the depositional record of ice retreat (Blasco et al., 1990, 2005; Scott et al., 2008, 2009; Batchelor et al., in press). Specifically, the dating of benthic and planktonic foraminifera (Scott et al., 2008, 2009) and dinoflagellate cysts (Richerol et al., 2008) that entered the western CAA prior to molluscs would help to bolster chronological control. Collectively, an improved glacial chronology for western Amundsen Gulf and western and southern Banks Island will help to determine the interplay between ice stream retreat and MWP-1A. This relationship will bear upon our understanding of ice stream stability thresholds in response to future eustatic sea level rise (e.g. Weertman, 1975; Hollin and Barry, 1979; Oppenheimer, 1998). An established chronology of retreat for the Amundsen Gulf Ice Stream would also help to elucidate far-reaching paleoceanographic and/or paleoclimatic impacts associated with its significant mass loss (e.g. Darby et al., 2002; Tarasov and Peltier, 2006; Stein et al., 2010). For example, as documented for the Hudson Strait Ice Stream

(Heinrich, 1988; Bond et al., 1992; Broecker et al., 1992), did the Amundsen Gulf Ice Stream trigger millennial-scale climate change during iceberg calving events (i.e. 'Heinrich Events')?

Another promising direction for future research concerns the history of the LIS recorded by the sedimentary record on the polar continental shelf distal to Banks Island. Seismic surveys and sediment sampling of the adjacent Beaufort Sea margin will help to constrain the total number of LIS advances and to identify bedforms indicative of former ice sheet limits and dynamics (Blasco et al., 1990, 2005; MacLean et al., 2012; Batchelor et al., in press; Pienkowski et al., in press). Evidence for the offshore grounding of an ancestral LIS would be particularly important for clarifying long-term glacial histories independently inferred from subsurface stratigraphies (Lakeman, 2012; Vaughan et al., in press).

Determining the absolute timing of pre-Late Wisconsinan glaciation at Worth Point is a compelling area of future research. However, the accurate dating of pre-Late Wisconsinan permafrozen sediment remains challenging (Alexanderson et al., in press). For example, while OSL dating of quartz grains using the single aliquot regenerative technique (utilized at Worth Point) has produced consistent results in other Arctic settings (e.g. Berger and Polyak, 2012), age overestimation remains a problem. This can result from incomplete bleaching due to limited sunlight restricted to summer (Bateman, 2008) and in the case of glaciofluvial environments, from suspended sediment that becomes increasingly problematic with ice-marginal proximity (Alexanderson and Hákansson, in press). Permafrost and ground ice have also been shown to influence the dose rate from

surrounding sediments, occasionally resulting in apparent age under-estimates (Alexanderson et al., in press). The absence of stable erratics overlying Worth Point, and of suitable organics within the stratigraphic sequence, further limit the use of alternative dating methods such as TCN and electron spin resonance dating. Consequently, additional OSL dating at Worth Point combined with seismic surveys and sediment sampling on the adjacent polar continental shelf appear to offer the best opportunities for improved age control. U-Pb dating of granite erratics deposited by the ancestral LIS would also help to clarify former ice flow trajectories and configurations. A robust chronology for Worth Point is essential for meaningful correlation with other circumpolar terrestrial and marine records.

The antiquity of permafrost demonstrated at Worth Point raises important questions about future permafrost stability. For example, if permafrost at Worth Point survived multiple periods of interglacial warming, including warmer than present temperatures during the last interglacial (Sangamonian), can it survive future warming (e.g. Reyes et al., 2010)? Such questions are even more pertinent when considering potential carbon output from thawing peatlands, which characterize vast areas of the circumpolar north (Tarnocai, 2006). Studies of permafrost degradation during the last interglacial highlight the resilience of deep permafrost, even within discontinuous zones (Froese et al., 2008), but demonstrate the prevalence of shallow thaw (Reyes et al., 2010). This trend has been forecasted during future warming, with a modelled loss of up to 80% of near surface permafrost by the end of the 21st century (Lawrence et al., 2008). If warming exceeds predicted rates (IPCC AR5, 2013), and long-established

permafrost begins to degrade, this could have unprecedented impacts on high-latitude landscapes. The concurrent degradation of buried glacial ice and ground ice enclosed within permafrost throughout the Arctic would also have significant implications for landscape change, including an expansion of thermokarst terrain (e.g. (e.g. Mackay, 1959; Mackay et al., 1972; O'Cofaigh et al., 2003; Murton et al., 2004; Harris and Murton, 2005; Dyke and Savelle, 2000; Fritz et al., 2012). Observations across southern Banks Island confirm widespread buried glacier ice that is now being exposed by retrogressive thaw flow slides, particularly on the Sand Hills Moraine belt and Jesse moraine belt. Understanding and mapping these glacial landscapes is critical for predicting how ongoing global warming will impact and destabilize these vulnerable (shallow-buried) ice masses.

3. REFERENCES

Alexanderson, H., Backman, J., Cronin, T.M., Funder, S., Ingólffson, O., Jakobsson, M., Landvik, J.Y., Lowemark, L., Mangerud, J., Marz, C., Möller, P., O'Regan, M., Spielhagen, R.F. 2013. An Arctic perspective on dating Mid-Late Pleistocene environmental history. Quaternary Science Reviews. In press.

Alexanderson, H., Hákansson, L. Coastal glaciers advanced onto Jameson Land, east Greenland during the late glacial-early Holocene Milne Land Stade. Polar Research. In press.

Andrews, J.T., MacLean, B. 2003. Hudson Strait Ice Streams: a review of stratigraphy, chronology and links with North Atlantic Heinrich events. Boreas. 32, 4-17.

Barendregt, R.W., Vincent, J-S., Irving, E., Baker, J. 1998. Magnetostratigraphy of Quaternary and Late Tertiary sediments on Banks Island, Canadian Arctic Archipelago. Canadian Journal of Earth Sciences. 35, 147-161.

Bateman, M.D. 2008. Luminescence dating of periglacial sediments and structures. Boreas. 37, 574-588.

Batchelor, C.L., Dowdeswell, J.A., Pietras, J.T. Evidence for multiple Quaternary ice advances and fan development from the Amundsen Gulf cross-shelf trough and slope, Canadian Beaufort Sea Margin. Marine and Petroleum Geology. In Press.

Benn, D.I., Warren, C.R., Mottram, R.H. 2007. Calving processes and the dynamics of calving glaciers. Earth-Science Reviews. 82, 143-179.

Berger, G.W., Polyak, L. 2012. Testing the use of quartz 'micro-hole' photon-stimulated luminescence for dating sediments of the central Lominosov Ridge, Arctic Ocean. Quaternary Geochronology. 11, 42-51.

Blasco, S. M., Fortin, G., Hill, P.R., O'Connor, M.J., and Brigham- Grette, J., 1990. The late Neogene and Quaternary stratigraphy of the Canadian Beaufort continental shelf. In: Grantz, A., Johnson, L., Sweeney, J. F., (Eds). The Arctic Ocean Region. The Geology of North America Geological Society of America, Boulder, Colorado. 491–502.

Blasco, S.M., Bennett, R., Hughes-Clarke, J., Bartlett, J., Shearer, J.M. 2005. 3-D Multibeam Mapping Reveals Geological Processes Associated With Fluted Seabed, Slump Feature, Pockmarks, Mud Volcanoes and Deep Water Ice Scours in the Beaufort Sea–Amundsen Gulf. Geological Association of Canada – Mineralogical Association of Canada.

Bradley, R.S., England, J.H. 2008. The Younger Dryas and the Sea of Ancient Ice. Quaternary Research. 70, 1-10.

Bond, G., Heinrich, H., Broecker, W., Labeyrie, L., McManus, J., Andrews, J., Huon, S. 1992. Evidence for massive discharges of icebergs into the North Atlantic Ocean during the last glacial period. Nature. 365, 143-147.

Broecker, W., Bond, G., Klas, M., Clark, E., McManus, J. 1992. Origin of the northern Atlantic's Heinrich events. Climate Dynamics. 6, 265-273.

Clark, D.L., Vincent, J-S., Jones, G.A., Morris, W.A. 1984. Correlation of marine and continental glacial and interglacial events, Arctic Ocean and Banks Island. Nature. 311, 147-149.

Conway, H., Cantania, G., Raymond, C.F., Gades, A.M., Scambos, T.A., Engelhardt, H. 2002. Switch of flow direction in an Antarctic ice stream. Nature. 419, 465-467.

Copland, L., Sharp, M.J., Dowdeswell, J.A. 2003. The distribution and flow characteristics of surge-type glaciers in the Canadian High Arctic. Annals of Glaciology. 36, 73-81.

Croot, D.G. 1988. Glaciotectonics and surging glaciers: a correlation based on Vestpitsbergen, Svalbard, Norway. In: Croot, D.G. (Ed.). Glaciotectonics: Forms and Processes, Balkema, Rotterdam, 33-47.

Darby, D.A., Bischof, J.F., Speilhagen, R.F., Marshall, S.A., Herman, S.W. 2002. Arctic ice export events and their potential impact on global climate during the late Pleistocene. Paleoceanography. 17, 1-17.

Dowdeswell, J.A., Jakobsson, M., Hogan, K.A., O'Regan, M., Antony, D., Backman, J., Darby, D., Eriksson, B., Evans, D.J.A., Hell, B., Janzen, T., Löwemark, L., Marcussen, C., Noormets, R., O'Cofaigh, C., Polyak, L., Sellén, E., Sölvsten, M. 2010. High-resolution geophysical observations from the Yermak Plateau and northern Svalbard margin: implications for ice-sheet grounding and deep-keeled icebergs. Quaternary Science Reviews. 29, 3518-3531.

Dyke, A.S., Savelle, J.M. 2000. Major end moraines of Younger Dryas age on Wollaston Peninsula, Victoria Island, Canadian Arctic: implications for paleoclimate and for formation of hummocky moraine. Canadian Journal of Earth Sciences. 37, 601-619.

Dyke, A.S., Moore, A., Robertson, L. 2003. Deglaciation of North America. In: Geological Survey of Canada. Open File 1574.

England, J.H., Furze, M.F.A. 2008. New evidence from the western Canadian Arctic Archipelago for the resubmergence of Bering Strait. Quaternary Research. 70, 60-67.

England, J.H., Furze, M.F.A., Doupe, J.P. 2009. Revision of the NW Laurentide Ice Sheet: implications for the paleoclimate, the northeast extremity of Beringia, and Arctic Ocean sedimentation. Quaternary Science Reviews. 28, 1573-1596.

Evans, D.J.A., England, J. 1991. Canadian landform examples 19, high arctic thrust block moraines. Canadian Geographer. 35, 93-97.

Evans, D.J.A., Wilson, S.B. 2006. A temporary exposure through the Loch Lomond Readvance end moraine/ice-contact delta complex near Drymen, Stirlingshire. Scottish Geographical Journal. 122, 344-351.

Fastook, J.L., Schmidt, W.F. 1982. Finite element analysis of calving from ice fronts. Annals Of Glaciology. 3, 103-106.

Fortier, F., Godin, E., Kanevskiy, M.Z., Allard, M. 2009. Middle Pleistocene (?) buried glacial ice on Bylot Island, Canadian Arctic Archipelago. EOS Transactions of the American Geophysical Union. 90, 52.

Fritz, M., Wetterich, S., Schirrmeister, L., Meyer, H., Lantuit, H., Preusser, F., Pollard, W.H. 2012. Eastern Beringia and beyond: Late Wisconsinan and Holocene landscape dynamics along the Yukon Coastal Plain, Canada. Palaeogeography Palaeoclimatology Palaeoecology. 319, 28-45.

Froese, D.G., Westgate, J.A., Reyes, A, V., Enkin, R.J., Preece, S.J. 2008. Ancient Permafrost and a Future, Warmer Arctic. Science. 321, 1648.

Grasby, S.E., Smith, R.I., Bell, T., Forbes, D.L. 2013. Cryogenic formation of brine and sedimentary mirabilite in submergent coastal lake basins, Canadian Arctic. Geochimica et Cosmochimica Acta. 13-28.

Harris, C., Murton, J.B. 2005. Interactions between glaciers and permafrost: an introduction. Geological Society, London. 242, 1-9.

Heinrich, H. 1988. Origin and consequences of cyclic ice rafting in the Northeast Atlantic Ocean during the past 130,000 years. Quaternary Research. 29, 142-152.

Hill, J.C., Driscoll, N.W. 2010. Iceberg discharge to the Chukchi shelf during the Younger Dryas. Quaternary Research. 74, 57-62.

Hollin, J.T., Barry, R.G. 1979. Empirical and theoretical evidence concerning the response of the Earth's ice and snow cover to a global temperature increase. Environmental International. 2, 437-444.

Ingólfsson, O., Lokrantz, H. 2003. Massive Ground Ice Body of Glacial Origin at Yugorski Peninsula, Arctic Russia. Permafrost and Periglacial Processes. 14, 199-215.

International Panel on Climate Change (IPCC) Co-Chairs of Working Group 1. 2013. Working Group 1 Contribution to the IPCC Fifth Assessment Report Climate Change 2013: The Physical Science Basis. Chapter 4: Observations: Cryosphere – Final Draft Underlying Scientific-Technical Assessment.

Jakobsson, M., Nilsson, J., O'Regan, M., Backman, J., Löwemark, L., Dowdeswell, J.A., Mayer, L., Polyak, L., Colleoni, F., Anderson, L., Björk, G., Darby, D., Eriksson, B., Hanslik, D., Hell, B., Marcussen, C., Sellén, E., Wallin, Å. 2010. An Arctic Ocean ice shelf during MIS 6 constrained by new geophysical and geological data. Quaternary Science Reviews. 29, 3505-3517.

Kalin, M. 1971. The active push moraine of the Thompson Glacier. Montreal McGill University, Axel Heiberg Island Research, Reports Glaciology. 4, 68.

Kauffman, D.S., Ager, T.A., Anderson, P.M., Andrews, J.T., Bartlein, P.J., Brubaker, L.B., Coats, L.B., Cwynar, L.C., Duvall, M.L., Dyke, A.S., Edwards, M.E., Eisner, W.R., Gakewski, K., Gerisdottir, A., Hu, F.S., Jennings, A.E., Kaplan, M.R., Kerwin, M.W., Lozhkin, A.V., MacDonald, G.M., Miller, G.H., Mock, J.J., Oswald, W.W., Otto-Bleisner, B.L., Porinchu, D.F., Ruhland, K., Smol, J.P., Steig, E.J., Wolfe, B,B. 2004. Holocene thermal maximum in the western Arctic (0-180W). Quaternary Science Reviews. 23, 529-560.

Lakeman, T.R. 2012. Revision of the Early Quaternary stratigraphy at Morgan Bluffs, Banks Island, western Canadian Arctic. PhD Thesis, University of Alberta, Edmonton, Canada.

Lakeman, T.R., England, J.H. 2012. Paleoglaciological insights from the age and morphology of the Jesse moraine belt, western Canadian Arctic. Quaternary Science Reviews. 47, 82-100.

Lakeman, T.R., England, J.H. 2013. Late Wisconsinan glaciation and postglacial relative sea level change on western Banks Island, Canadian Arctic Archipelago. Quaternary Research. 80, 99-112.

Lawrence, D.M., Slater, A.G., Romanovsky, V.E., Nicolsky, D.J. 2008. Sensitivity of a model projection of near-surface permafrost degradation to soil column depth and representation of soil organic matter. Journal of Geophysical Research. 113.

MacAyeal, D.R. 1993. Binge/Purge oscillations of the Laurentide Ice Sheet as a cause of the north Atlantic's Heinrich events. Paleocoeanography. 8, 775-784.

Mackay, J.R. 1959. Glacier ice-thrust features of the Yukon Coast. Geographical Bulletin of Canada. 13, 5-21.

Mackay. J.R., Rampton, V.N., Fyles, J.G. 1972. Relict Pleistocene permafrost, Western Arctic, Canada. Science. 176, 1321-1323.

Mackay, J.R. 1989. Massive ice: some field criteria for the identification of ice types. Geological Survey of Canada. Paper 89-1G, 5-11.

MacLean, B., Blasco, S., Bennett, R., Lakeman, T., Hughes-Clarke, J., Kuus, P., Patton, E. 2012. Marine evidence for a glacial ice stream in Amundsen Gulf, Canadian Arctic Archipelago. 42nd Annual Arctic Workshop abstract, March 7th-9th, University of Colorado, US.

Marchant, D.R., Lewis, A.R., Phillips, W.M., Moore, E.J., Souchez, R.A., Denton, G.H., Sugden, D.E., Potter, N., Landis, G.P. 2002. Formation of patterned ground and sublimation till over Miocene glacier ice in Beacon Valley,

southern Victoria Land, Antarctica. Geological Society of America Bulletin. 114, 718-730.

Matthews, J.V., Mott, R.J., Vincent, J-S. 1986. Preglacial and interglacial environments on Banks Island: pollen and macrofossils from Duck Hawk Bluffs and related sites. Geographie physique et Quaternaire. 3, 279-298.

Murton, J.B., Waller, R.I., Hart, J.K., Whiteman, C.A., Pollard, W.H., Clark, I.D. 2004. Stratigraphy and glaciotectonic structures of a relict deformable bed of permafrost at the northwestern margin of the Laurentide Ice Sheet, Tuktoyaktuk Coastlands, Canada. Journal of Glaciology. 50, 399-412.

Murton, J.B., Frechen, M., Maddy, D. 2007. Luminescence dating of mid- to Late-Wisconsinan aeolian sand as a constraint on the last advance of the Laurentide Ice Sheet across the Tuktoyaktuk Coastlands, western Arctic Canada. Canadian Journal of Earth Sciences. 44, 857-863.

Nixon, C.F., England, J.H., Lajeunesse, P., Hanson, M.A. Deciphering patterns of postglacial sea level at the junction of the Laurentide and Innuitian Ice Sheets, western Canadian Arctic. Quaternary Science Reviews. In press.

O'Cofaigh, C., Evans, D.J.A., England, J. 2003. Ice-marginal terrestrial landsystems: sub-polar glacier margins of the Canadian and Greenland high arctic. In: Evans, D.J.A. (Ed.). Glacial Landsystems. Arnold, London, 44-64.

Oppenheimer, M. 1998. Global warming and the stability of the West Antarctic Ice Sheet. Nature. 393, 325-332.

Pienkowski, A.J., England, J.H., Furze, M.F.A., MacLean, B., Blasco, S. 2013. The late Quaternary environmental evolution of marine Arctic Canada: Barrow Strait to Lancaster Sound. Quaternary Science Reviews. In press.

Polyak, L., Curry, W.B., Darby, D.A., Biscof, J., Cronin, T.M. 2004. Contrasting glacial/interglacial regimes in the western Arctic Ocean as exemplified by a sedimentary record from the Mendeleev Ridge. Paleoceanography Paleoclimatology Paleoecology. 203, 73-93.

Polyak, L., Darby, D., Bischof, J., Jakobsson, M. 2007. Stratigraphic constraints on Late Pleistocene glacial erosion and deglaciation of the Chukchi margin, Arctic Ocean. Quaternary Research. 67, 234-245.

Polyak, L., Bischof, J., Ortiz, J., Darby, D., Chappell, J., Xuan, C., Kaufman, D., Loylie, R., Schneider, D., Adler, R. 2009. Late Quaternary stratigraphy and sedimentation patterns in the western Arctic Ocean. Global Planetary Change. 68, 5-17.

Reyes, A.V., Froese, D.G., Jensen, B.J.L. 2010. Permafrost response to last interglacial warming: field evidence from non-glaciated Yukon and Alaska. Quaternary Science Reviews. 29, 3256-3274.

Richerol, T., Rochon, A., Blasco, S., Scott, D.B, Schell, T.M., Bennett, R.J. 2008. Distribution of dinoflagellate cysts in surface sediments of the Mackenzie Shelf and Amundsen gulf, Beaufort Sea (Canada). Journal of Marine Systems. 74, 825-839.

Schaefer, J.M., Lifton, N. 2013. Cosmogenic Nuclide Dating: Methods. Encyclopedia of Quaternary Science (second edition). 410 – 417.

Scott, D.B., Schell, T., Rochon, A., Blasco, S. 2008. Benthic foraminifera in the surface sediments of the Beaufort Shelf and slope, Beaufort Sea, Caada: Applications and implications for past sea-ice conditions. Journal of Marine Systems. 74, 840-863.

Scott, D.B., Schell, T., St-Onge, G., Rochon, A., Blasco, S. 2009. Foraminiferal assemblage changes over the last 15,000 years on the Mackenzie Beaufort Sea Slope and Amundsen Gulf, Canada: Implications for past sea ice conditions. Paleoceanography. 24, 1-20.

Serreze, M.C., Barry, R.G. 2011. Processes and impacts of Arctic Amplification: A research synthesis. Global and Planetary Change. 77, 85-96.

Serreze, M.C., Barret, A.P., Stroeve, J.C., Kindig, D.M., Holland, M.M. 2009. The emergence of surface-based Arctic amplification. Cryosphere. 3, 11-19.

Stein, R., Matthiessen, J., Niessen, F., Krylov, R., Nam, S., Bazhenova, E. 2010. Towards a better litho-stratigraphy and reconstruction of Quaternary palaeoenvironment in the Amerasian Basin (Arctic Ocean). Polarforschung. 79, 97-121.

Stokes, C.R., Clark, C.D., Darby, D.A., Hodgson, D.A. 2005. Late Pleistocene ice export events into the Arctic Ocean from the M'Clure Strait Ice Stream, Canadian Arctic Archipelago. Global and Planetary Change. 49, 139–162.

Stokes, C.R., Clark, C., Winsborrow, M. 2006. Subglacial bedform evidence for a major paleo-ice stream in Amundsen Gulf and its retreat phases, Canadian Arctic Archipelago. Journal of Quaternary Science. 21, 300–412.

Stokes, C.R., Clark, C.D., Storrar, R. 2009. Major changes in ice stream dynamics during deglaciation of the north-western margin of the Laurentide Ice Sheet. Quaternary Science Reviews. 28, 721-738.

St-Onge, D.A., McMartin, I. 1995. Quaternary Geology of the Inman River Area, Northwest Territories. In: Geological Survey of Canada. Bulletin 446.

St-Onge, D.A., McMartin, I. 1999. La moraine du Lac Bluenose (Territories du nordouest), une moraine a noyau de glace de glacier. Geographie Physique et Quaternaire. 53, 287-295.

Svendsen, J.I., Alexanderson, H., Astakhov, V.I. 2004. Late Quaternary ice sheet history of Northern Eurasia. Quaternary Science Reviews. 23, 1229-1271.

Tarasov, L., Peltier, R.W. 2006. A calibrated deglacial drainage chronology for the North American continent: evidence for an Arctic trigger for the Younger Dryas. Quaternary Science Reviews. 25, 659-668.

Tornocai, C. 2006. The effect of climate change on carbon in Canadian peatlands. Global and Planetary Change. 53, 222-232.

Vaughan, J.M, England, J.H, Evans, D.J.A. Glaciotectonic deformation and reinterpretation of the Worth Point stratigraphic sequence: Banks Island, NT, Canada. Quaternary Science Reviews. In Press.

Vincent, J-S. 1982. The Quaternary History of Banks Island, Northwest Territories, Canada. Geographie Physique et Quaternaire. 36, 209-232.

Vincent, J-S. 1983. La geologie du quaternaire et la geomorphologie de L'ile Banks, arctique Canadien. In: Commission Geologique du Canada Memoir 405.

Vincent, J-S. 1984. Quaternary stratigraphy of the western Canadian Arctic Archipelago. In: Fulton, R.J. (Ed.). Quaternary Stratigraphy of Canada – A Canadian Contribution to IGCP Project 24. Geological Survey of Canada. 87-100.

Vincent, J-S. 1990. Late Tertiary and Early Pleistocene Deposits and History of Banks Island, southwestern Canadian Arctic Archipelago. Arctic. 43, 339-363.

Vincent, J.S., Occhietti, S., Rutter, N., Lortie, G., Guilbault, J-P., De Boutray, B. 1983. The Late Tertiary-Quaternary record of the Duck Hawk Bluffs, Banks Island, Canadian Arctic Archipelago. Canadian Journal of Earth Science. 20, 1694-1712.

Vincent, J-S., Morris, W.A. & Occhietti, S. 1984. Glacial and non-glacial sediments of Matuyama paleomagnetic age on Banks Island, Canadian Arctic Archipelago. Geology. 12, 139-142.

Waller, R.I., Murton, J., Whiteman, C. 2009. Geological evidence for subglacial deformation of Pleistocene permafrost. Proceedings of the Geologists Association. 120, 155-162.

Waller, R.I., Murton, J.B., Kristensen, L. 2012. Glacier-permafrost interactions: Processes, products and glaciological implications. Sedimentary Geology. 255-256, 1-28.

Weertman, J. 1975. Stability of Antarctic Ice. Nature. 253, 159.

Zazula, G.D., MacKay, G., Andrews, T.D., Shapiro, B., Letts, B., Brock, F. 2009. A late Pleistocene steppe bison (*Bison priscus*) partial carcass from Tsiigehtchic, Northwest Territories, Canada. Quaternary Science Reviews. 28, 2734-2742.